EVALUATION OF FORWARD OSMOSIS TECHNOLOGY FOR THE TREATMENT OF SELECTED CONCENTRATED BRINES

Namadzavho Enos Sitabule
MSc Chemistry (Wits University)
BSc Honours Water Utilisation (Pretoria University)

Submitted in fulfilment of the academic requirements for the PhD degree in Chemical Engineering in the School of Engineering at the University of KwaZulu-Natal.

June 2021

DECLARATION 1 - PLAGIARISM

I, …Namadzavho Enos Sitabule…….……., declare that:

1. The research reported in this dissertation, except where otherwise indicated, is my original research.
2. This dissertation has not been submitted for any degree or examination at any other university.
3. This dissertation does not contain other persons' data, pictures, graphs or other information, unless specifically acknowledged as being sourced from other persons.
4. This dissertation does not contain other persons' writing, unless specifically acknowledged as being sourced from other researchers. Where other written sources have been quoted, then:
   a. Their words have been re-written, but the general information attributed to them has been referenced
   b. Where their exact words have been used, then their writing has been placed in italics and inside quotation marks and referenced.
5. This dissertation does not contain text, graphics or tables copied and pasted from the Internet, unless specifically acknowledged, and the source being detailed in the dissertation and in the References sections.

Signed… … …

……

As the candidate's Supervisor I have approved this dissertation for submission

1) …….. ……. ……

Name Signature Date

2) …….. ……. ……..

Name Signature Date

DECLARATION 2 - PUBLICATIONS

DETAILS OF CONTRIBUTION TO PUBLICATIONS that form part and/or include research presented in this thesis (include publications in preparation, submitted, *in press* and published and give details of the contributions of each author to the experimental work and writing of each publication)

Publication 1

EN Sitabule[*], C Buckley**, 2020. Forward Osmosis Treatment of Thermal Evaporator Brine Stream. Paper in Preparation

[*]Group Technology

** University of KwaZulu Natal

Publication 2

EN Sitabule[*], C Buckley**, 2020. Forward Osmosis Treatment of Ion Exchange Regeneration Effluent Streams. Paper in Preparation

[*]Group Technology

** University of KwaZulu Natal

Signed:

ACKNOWLEDGEMENT

The following people and institutions are acknowledged for their contributions in the successful execution of this study:

- The Almighty for guiding me during this journey
- My family for supporting and encouraging me during the completion of this study. Dad, I wish you were here to witness this achievement. To my Wife & Kids & my Mom, Thank You.
- My Supervisor, Prof Chris Buckley for the guidance he gave during the execution of the work and write up of the dissertation
- Chris Brouckaert for guidance he gave me when addressing the corrections from the examiners
- Science Research (Water & Waste) management team for supporting the development of forward osmosis (FO) technology
- WRC for supporting the development of FO technology
- Sarushen Pillay for supporting the collaboration study and the development of FO technology from the Technology Management
- Haasbroek Hasie (R&T) for ensuring that the construction of the FO unit is done according to scope.
- Neil Paton and Natasja Raijmakers (R&T) for their efforts during the execution of the experiments (execution of the runs, solution preparation and sampling)
- Robert Doubell (R&T) for technical support during the commissioning of the FO unit
- Lynette Baratta (R&T) for technical guidance as well as reviewing of the work
- Lucille Naidoo (Secunda Technical Support) for engineering support during the construction of the FO Unit
- Lawrence Tsatsi, Sibongile Tshangela and Teboho Segele (SS Lab Sol) for IC analyses
- Antonio Baratta (R&T Analytics) for the ICP analyses
- Alisa Govender, Werner Barnard and Esna du Plessis (R&T Analytics) for analysing/characterizing flat sheet membranes using SEM, EDX, Raman Spectroscopy and XRD.
- Gerhard Koekemoer (PD, R&T) for technical support on data analysis (Statistics)

Operation Support, R&T department for the contributions during the construction of the FO unit, specifically with the DELTA V System to control the FO experiments and data logging

WRC Reference Group (Steering Committee)

Dr Lynette Baratta	Mr Willem van Krimpen Ir.
Senior Scientist Gr I	Engineer
Sasol Technology	Sunflower Scientific

Associate Prof EP Jacobs
Institute for Polymer Science
University of Stellenbosch

Prof Alison Lewis
Crystallization and Precipitation Unit,
Dept. of Chemical Engineering
University of Cape Town

Mr Jeeten Nathoo
Director: Research and Development
NUWATER (HEAD OFFICE)

Dr Gerhard Offringa Pr Eng
Go Water Management
Prof PGL Baker
Chemistry Department
University of the Western Cape

Mr Rachi Rajagopaul
Senior Scientist
Umgeni Water

Prof Lingam Pillay
University of Stellenbosch
Department of Process Engineering

Prof Joe Modise
Vaal University of Technology

Mr Gerhard Gericke
Eskom
John Ngoni Zvimba, PhD, MWISA, MIWA
Research Manager: Wastewater Treatment
and Management
Water Research Commission

ABSTRACT

The cost of disposing of the residual brines has limited the use of thermal and membrane desalination technologies, especially for inland industries. To avoid expensive brine disposal costs, increasing attention is being given to brine concentration (Minimum Liquid Discharge (MLD)) and zero liquid discharge (ZLD) practices, in which waste is disposed of in a solid form. A combination of membrane and thermal processes are often used to achieve ZLD for saline wastewaters. These thermal processes, however, are energy and cost-intensive. Membrane-based alternatives such as Membrane Distillation (MD), Ultra High-Pressure Reverse Osmosis (UHPRO) and Osmotically Assisted Reverse Osmosis (OARO) are also being advanced as potential options to process brine streams with TDS above 70 000 mg/L. These options, however, still require a significant amount of energy to treat high salinity brines.

One of the emerging membrane technologies that are currently being considered in the desalination market to minimise the cost associated with brine disposal is forward osmosis. Unlike with other membrane desalination technologies, this technology relies on the osmotic pressure differential between the concentrated draw solution and feedwater with a lower concentration to drive the water through the semipermeable membrane using natural osmosis phenomena. Forward osmosis process requires minimal external energy input, mainly for liquid circulation and draw solution regeneration. Also, as a result of low or, no hydraulic pressure applied, forward osmosis will have a low propensity for fouling which could reduce the capital and operating cost of the plant. The lack of industrial track record has been identified as a significant hindrance to mass adoption of forward osmosis technology. Some of the reasons for the poor uptake are the challenges relating to an ideal membrane, ideal draw solution and membrane fouling. Full scale application of forward osmosis technology for reclamation and reuse of high salinity streams could contribute to addressing water scarcity challenges experienced worldwide due to the inherent advantages associated with the technology. Despite advances made over the years on forward osmosis technology, fundamental understanding of critical parameters that governs the performance of this technology with respect to water flux, salt flux and fouling remains a challenge, especially the role of reverse solute diffusion phenomenon (interaction of scaling precursors in the feed with the draw solution) on forward osmosis technology fouling tendency. Although numerous bench-scale and pilot-scale evaluations have been completed over the years in support of continuous development of an FO process, studies on the impact of the concentration of scaling precursors in the feed water on draw solution enhanced fouling remains a gap. The default has always been the inclusion of the pre-treatment step in the flow scheme to ensure complete removal of these precursors through chemical or membrane softening which add to the Capex and Opex of the plant.

In this study, forward osmosis technology was evaluated on bench-scale for the concentration of selected concentrated brine streams from a petrochemical and power generating industry using ammonium bicarbonate as a draw solution.

The brine streams considered for this study were high salinity brine streams from reverse osmosis, thermal evaporation and ion-exchange plants. Studies conducted to gain a fundamental understanding of various parameters that influences FO process showed that the key phenomena affected by the various experimental factors and therefore greatly influenced the FO performance was internal concentration polarization (ICP) as reported extensively in the literature. This phase of the study enabled the selection of the membrane orientation, draw solution type, draw solution concentration, membrane type and operating conditions (pH, temperature, cross-flow velocity) to be used for the batch experiments.

Batch experiments were conducted to gain an appreciation of the potential of using forward osmosis technology to desalinate high salinity brine streams and limitations using synthetic pure-component analogues of the selected concentrated brine streams as feed solution; ammonium bicarbonate (3 M) as a draw solution and TFC-FO membrane. Critical performance parameters such as water flux, reverse salt diffusion, water recovery and membrane fouling were monitored and evaluated.

The results from the batch studies conducted using synthetic High Rinse Portion (ion-exchange regeneration effluent (ca. 15 000 mg/L TDS)), TRO/SRO Brine (RO Brine, (ca. 10 500 mg/L TDS)), Combined Ion-Exchange Regeneration Effluent (ca. 30 000 mg/L TDS) and Mother Liquor (thermal evaporator blowdown (ca. 60 000 mg/L TDS)) solutions showed that the High Rinse Portion, TRO/SRO Brine and Mother Liquor streams have high fouling propensity when compared to the Combined Regeneration Effluent. The Combined Regeneration Effluent solution had the lowest Ca^{+2} concentration (~100 mg/L) when compared to that of the other three brine streams [High Rinse Portion (~860 mg/L), TRO/SRO Brine (~500 mg/L) and Mother Liquor (~545 mg/L)]. Membrane surface characterisation conducted on the used membrane coupons showed that the membrane surface was fouled with aragonite and calcite. Formation of the aragonite and calcium carbonate was found to be due to the interaction between the calcium ions that exist in the feed solution with carbonate ions from the draw solution. The specific reverse salt flux for the membrane coupons used ranged from 6 to 7.4 g/L. Furthermore, the experiments conducted to evaluate the impact of hardness removal on FO process performance using Mother Liquor brine stream as feed showed that, in the absence of some hardness (complete or partial removal of calcium and magnesium), water fluxes and water recoveries of between 4-6 L. $m^{-2}.h^{-1}$ and 45-60%, respectively could be achieved. It was concluded in this study that the concentration of the calcium ions in the feed does have an impact on the formation of calcium carbonate scale implying that some hardness can be tolerated in the feed to the forward osmosis process. The study provided valuable fundamental understanding on the application of FO technology for treating high salinity brines from the petrochemical and power generation industry

PREFACE

This dissertation entitled "Evaluation of forward osmosis technology for the treatment of selected concentrated brines" was prepared by the candidate Mr Namadzavho Enos Sitabule, under the supervision of Professor Chris Buckley. This dissertation was solely prepared by the candidate. Some parts of the dissertation refer to research work of others, and references for these sources have been provided to the best of the candidate's efforts.

This preface also intends to highlight that some of the parts of this dissertation form part of a scientific report entitled "Evaluation of forward osmosis technology for the treatment of selected concentrated brines" (K5/2101) prepared for and submitted to the Water Research Commission (WRC) in South Africa who funded the research. The candidate was the principal author of the scientific report submitted to the WRC.

COPYRIGHT PERMISSION

Permission to reprint some of the figures cited in the dissertation was requested and approval is listed below:

1. We hereby grant you permission to reproduce the material detailed below in print and electronic format at no charge (Journal (1168885) [210518-015842])-Article title: A comprehensive review of hybrid forward osmosis systems: Performance, applications and future prospects (Elsevier e-mail correspondence-19-05-2021)
2. We hereby grant you permission to reproduce the material detailed below in print and electronic format at no charge (Journal (1168868) [210518-015435])- Article title: Calcium carbonate scaling in seawater desalination by ammonia–carbon dioxide forward osmosis: Mechanism and implications (Elsevier e-mail correspondence-19-05-2021)
3. We hereby grant you permission to reproduce the material detailed below in print and electronic format at no charge (Journal (1168866) [210518-014915])- Article title: The sweet spot of forward osmosis: Treatment of produced water, drilling wastewater, and other complex and difficult liquid streams (Elsevier e-mail correspondence-19-05-2021)
4. We hereby grant you permission to reprint the material below at no charge in your thesis (Journal (1168898) [210518-017158])- Article title: A novel low energy fertilizer driven forward osmosis desalination for direct fertigation: Evaluating the performance of fertilizer draw solutions ((Elsevier e-mail correspondence-19-05-2021)
5. For the first paper, D&WT – Going Big with Forward Osmosis, Oasys purchased the rights to the paper from the publisher, so that we could use it freely. When Oasys went under, the parent of our Chinese partner purchased assets of the company and the IP. But, I am not sure if they own these rights or not. I am sure they were not specifically called out in any listing of assets. I would say the paper is free to use in your published work (John Tracy (Authors) e-mail correspondence-13-05-2021). This is an Open Access Article.

TABLE OF CONTENTS

LIST OF FIGURES

LIST OF TABLES

LIST OF ABBREVIATIONS

AQ	Aqueous model
AS-DI	Active layer (side) facing deionised water
AS-DS	Active layer (side) facing draw solution
CA	Cellulose Acetate
CEOP	Cake Enhanced Osmotic Pressure
CP	Concentration Polarization
CTA	Cellulose Triacetate
D-H	Debye-Hückel
DI	Deionised water
DS	Draw Solution
EC	Evaporative-Crystallizer
ECP	External Concentration Polarization
EDR	Electrodialysis Reversal
EDS	Energy Dispersive Spectroscopy
FO	Forward Osmosis
HRP	High Rinse Portion
HTI	Hydration Technology Inc.
IC	Ion Chromatography
ICP	Inductive Coupled Plasma
ICP	Internal Concentration Polarization
IEX	Ion Exchange
LEA	Local Equilibrium Assumption
MBC	Membrane Brine Concentrator
MOD	Manipulated Osmosis Desalination
MSE	Mixed Solvent Electrolyte model
NF	Nanofiltration
O&G	Oil and Gas
PA	Polyamide
PRO	Pressure Retarded Osmosis
R&D	Research & Development
RO	Reverse Osmosis
RSF	Reverse Solute Flux
SCADA	Supervisory Control and Data Acquisition
SEM	Scanning Electron Microscopy

SRO	Spiral Wound Reverse Osmosis
SRSF	Specific Reverse Solute Flux
SWRO	Sea Water Reverse Osmosis
TDS	Total Dissolved Solids
TFC	Thin Film Composite
TOC	Total Organic Carbon
TRO	Tubular Reverse Osmosis
WAC	Weak Acid Cation
WDR	Water Desalination Report
XRD	X-Ray Diffraction
ZLD	Zero Liquid Discharge
ZLED	Zero Liquid Effluent Discharge

NOMENCLATURE OR SYMBOLS

A – Pure water permeability coefficient (m/s·atm)

Am – effective membrane area (cm^2)

B – Salt permeability coefficient of the active layer (m/s)

D – Diffusion coefficient (m^2/s)

$e^{(Jw/k)}$ – represent the amplification factor of feed solution osmotic pressure as a results concentrative external concentration polarisation

$e^{(-JwK)}$ – represent the reduction factor of draw solution osmotic pressure as a result of dilutive internal concentration polarisation

J_s = Reverse solute flux

Jw – Water flux (L m^{-2} h^{-1})

Jw, sp – Specific water flux (L m^{-2} h^{-1} bar^{-1})

k – Boltzmann's constant (1.38x10-3 J/K)

k – Mass transfer coefficient (m/s)

K – Solute diffusion resistance (s/m)

M – Solute molar concentration (mol/L)

n – Moles of solute (mol)

NA – Avogadro's number

ppm – parts per million (mg/l)

R – Gas constant (0.08314 L bar mol-1 K^{-1})

t – Thickness (μm)

t – Thickness of the membrane (m)

ΔC = concentration gradient of solute across the membrane

ΔP - differential applied hydraulic pressure across the membrane (~0 for FO)

Δt – change in time (min)

ΔV – change in volume (ml)

π – Osmotic pressure (bar)

$\pi_{Draw,b}$ – represent the bulk osmotic pressure of the draw solution facing the porous support layer of the FO membrane

$\pi_{Draw,m}$ – represent the osmotic pressure of the draw solution on the porous support layer of the FO membrane

$\pi_{Feed,b}$ – represent the bulk osmotic pressure of the feedwater solution facing the active layer of the FO membrane

$\pi_{Feed,m}$ – represent the osmotic pressure of the feedwater solution facing the active layer of the FO membrane

φ – Osmotic pressure coefficient

CHAPTER 1 : INTRODUCTION AND BACKGROUND

1.1 Problem statement and research needs

Desalination processes such as reverse osmosis, thermal evaporators, ion exchange and electrodialysis produce brine streams that require disposal more sustainably (Nathoo, Jivanji and Lewis, 2009; Menon et al., 2020; Chen and Yip, 2018). For landlocked plants, a serious challenge is posed, as ocean disposal of brine is not available as an option (Ahmed et al., 2002; Rioyo et al., 2017)). As a result, effective brine minimisation technologies towards achieving Zero Liquid Effluent Discharge (ZLED) are required to reduce the water treatment costs and environmental impact. Brine management for inland industries include discharge to the surface, deep well injection, land disposal or treatment through reverse osmosis (RO), electrodialysis reversal (EDR), evaporation ponds, and thermal evaporation (Morillo et al., 2014, Muftah, 2011; Ahmed et al, 2002; Rioyo et al., 2017; Blandin et al., 2019; Li, Shi and Yu, 2019). Brine disposal to evaporation ponds holds the danger of ground and surface water contamination. Treatment of brines using RO and EDR generates large quantities of brines as water recovery in these processes is restricted by scaling, fouling and salinity of the water. Mechanical/thermal evaporation technologies for brine treatment are very expensive, and scaling is a big challenge (Menon et al., 2020; Chen and Yip, 2018). Deep well injection is an attractive option for disposing of brines, but this option is not always available (Morillo et al., 2014, Muftah, 2011; Ahmed et al, 2002; Rioyo et al., 2017).

Sasol (petrochemical) (Sasol.com, 2019) and Eskom (power generation) (Eskom, co.za, 2019) coal processing facilities are located inland in water-sensitive catchment areas where water re-use and recycling is a requirement. These two coal processing companies produce, and landfill large quantities of boiler fly ash. Apart from the fly ash generated in the coal-fired power stations, the treatment of wastewaters with the aim of recovering water for reuse using technologies such a RO, EDR, vapour compression (VC) and other methods results in the production of hyper-saline brine streams which require disposal. Sasol and Eskom face major problems in the management of brines generated by various water treatment technologies such as ion exchange and membrane desalination plants that are used to produce boiler feed water required for steam generation and cooling water for process cooling. The handling and disposal of saline effluents produced remain expensive, complex and challenging to resolve as the plants are situated inland. As a result of these challenges, Sasol and Eskom have been researching desalination technologies and brine treatment processes for many years which resulted in the installation of a number of full-scale softening, microfiltration/ultrafiltration, RO, EDR, and evaporative-crystallizer (EC) technologies to desalinate various surface water, wastewater and brines.

Current practices involve the co-disposal of saline effluents into the ash systems. Sasol uses wet ash disposal system, whereas Eskom uses dry ash disposal system.

These systems act as salt sinks and evaporation (with and without crystallisation) as a means of managing excess saline effluents (Petrik et al., 2008; Gitari et al., 2009, de Bod, 2012, Nyamhingura, 2009, Mahlaba et al., 2012, Ras and van Blottnitz, 2013, Rogers et al., 2013). For Sasol complexes, the water that drains from the fine ash dams is typically used to transport more ash with the excess water being upgraded to boiler feed water using thermal evaporators and membrane technologies. In the Eskom case, no water drained from the ash dumps that require further treatment.

Figures 1-1 and 1-2 shows a typical Sasol & Eskom Complexes Water Treatment System showing installed technologies and brine streams produced

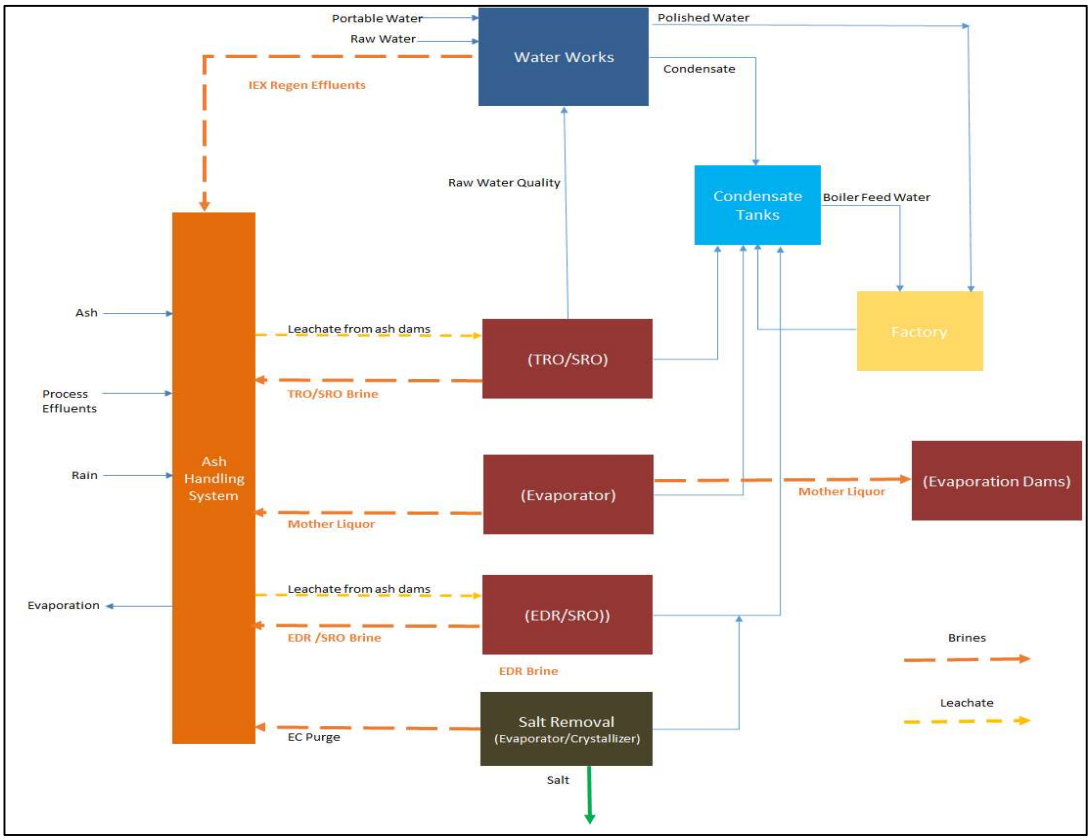

Figure 1-1: Typical Sasol Complexes Water Treatment System

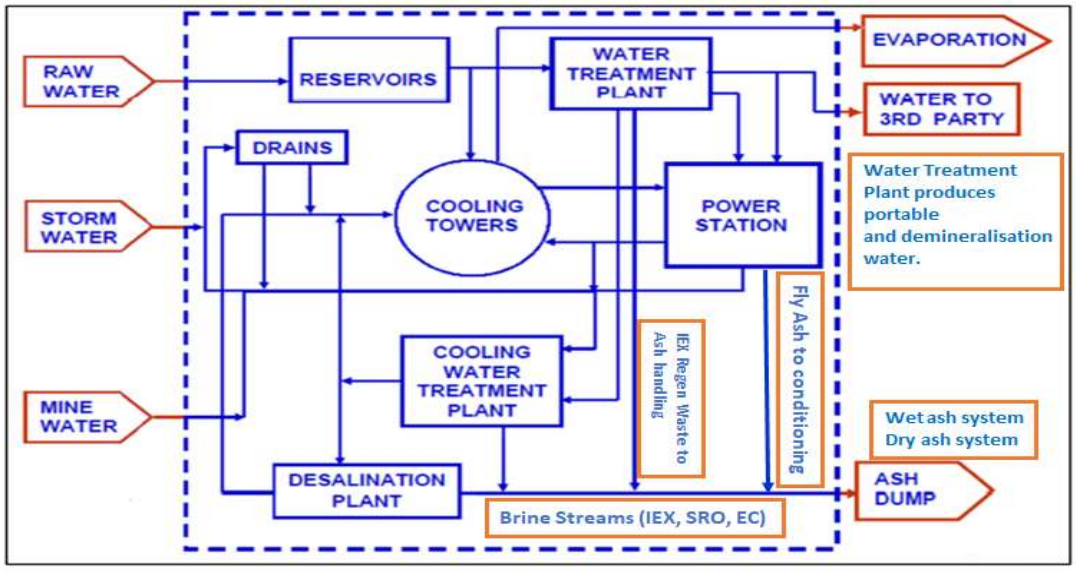

Figure 1-2: Typical Eskom Complex Water Treatment System

Although well established, the processes depicted in Figure 1-1 and Figure 1-2 are unable to reach higher water recoveries due to an increase in fouling and scaling potential as recovery increases.

Pre-treatment of the feedwater is usually applied to achieve higher water recoveries. It is also evident from Figure 1-1 and Figure 1-2 that several brine streams are produced, namely, ion exchange regeneration effluent (combined regeneration effluent), reverse osmosis brines (tubular reverse osmosis -TRO and spiral wound reverse osmosis -SRO, brine), evaporator blowdown (mother liquor) and purge from evaporator crystallizer.

These streams are characterised by high concentrations of total dissolved solids and organic compounds. Some of these brines (e.g. TRO/SRO brines, evaporator crystalliser and combined regeneration effluents) are used for fine ash transportation to fine ash dams where salt is also retained in the fine ash particles through water retention. The brine from the evaporator is disposed of via the evaporation pond (salt water dams). Unfortunately, the evaporation, ponds and evaporator crystallizer, which are additional salt sinks, have limited capacity to process the large volumes of brines produced within the complex which could subsequently lead to volume and salt imbalance.

Due to the limitations associated with existing membrane and thermal desalination technologies briefly discussed above, alternative technologies are required in order to improve water recovery (Menon et al, 2020). In order to achieve zero liquid effluent discharge (ZLED) or near ZLED, thermal desalination technologies (e.g. evaporators, crystallisers) are traditionally considered due to their ability to treat brines to a slurry or final product that is easy to handle or sell while achieving water recoveries up to 99% (Ahmed et al., 2002; Rioyo et al, 2017). Despite these benefits, these technologies are both CAPEX and OPEX intensive due to equipment cost and energy cost, respectively (Menon et al., 2020; Morillo et al., 2014; Blandin et al., 2020; Semiat, 2008; Goh et al., 2017; Li, Shi and Yu, 2019). The high cost for brine treatment/management together with strict environmental legislation (pending Waste Discharge Charges) provides an incentive to find additional technologies to treat brines from inland industries.

Forward Osmosis (FO) has emerged as a potential technology that could be used to further concentrate brines (High Saline Streams) and subsequently reduce the cost of a brine disposal (Khan, Shon and Nghiem, 2019; Chen and Yip, 2018; Haupt and Lerch, 2018; Li, Shi and Yu, 2019; Blandin et al., 2020). This technology has been identified as having potential incremental and breakthrough opportunities for brine treatment/desalination options (Khan, Shon and Nghiem, 2019; Chen and Yip, 2018; Blandin et al., 2020; Li, Shi and Yu, 2019). The attractiveness of the FO process revolves around potentially its low power consumption and high-water recovery. Unlike with other membrane desalination technologies, this technology relies on the osmotic pressure differential between the concentrated draw solution and feedwater with a lower concentration to drive the water through the semipermeable membrane using natural osmosis phenomena.

During this process, a diluted draw solution is produced, and further treatment is usually required to recover the draw solution, and in the process, clean water is produced. Below are some of the distinct advantages associated with FO technology (Zhao et al., 2012; Khan, Shon and Nghiem, 2019; Haupt and Lerch 2018; Li, Shi and Yu, 2019; Blandin et al., 2020):

- Unlike pressure and thermal driven processes, in FO, the energy requirement is for maintaining flowrates on both sides of the membrane and draw solution recovery, resulting in reduced OPEX.
    - using thermal energy from waste heat or renewables to vaporize draw solution ions (in cases where volatile draw solution is used)
- Reduced capital cost because it is membrane-based and as a result, exotic materials of construction (e.g. Titanium, duplex stainless steel) is not required
- Low fouling when compared to competing membrane and thermal systems
- The ability to handle higher salinity solutions compared to RO (FO can handle five times the salinity of seawater)
- Reduced crystalliser size due to lower brine volume generated as a result of higher water recoveries achievable
- Can be implemented in a modular fashion resulting in a wider turndown capability than thermal concentrators to handle feed water quality/flow variations

Figure 1-2 shows an energy comparison of forward osmosis technology (membrane brine concentrator (MBC)) with conventional desalination technologies such as RO and thermal technologies.

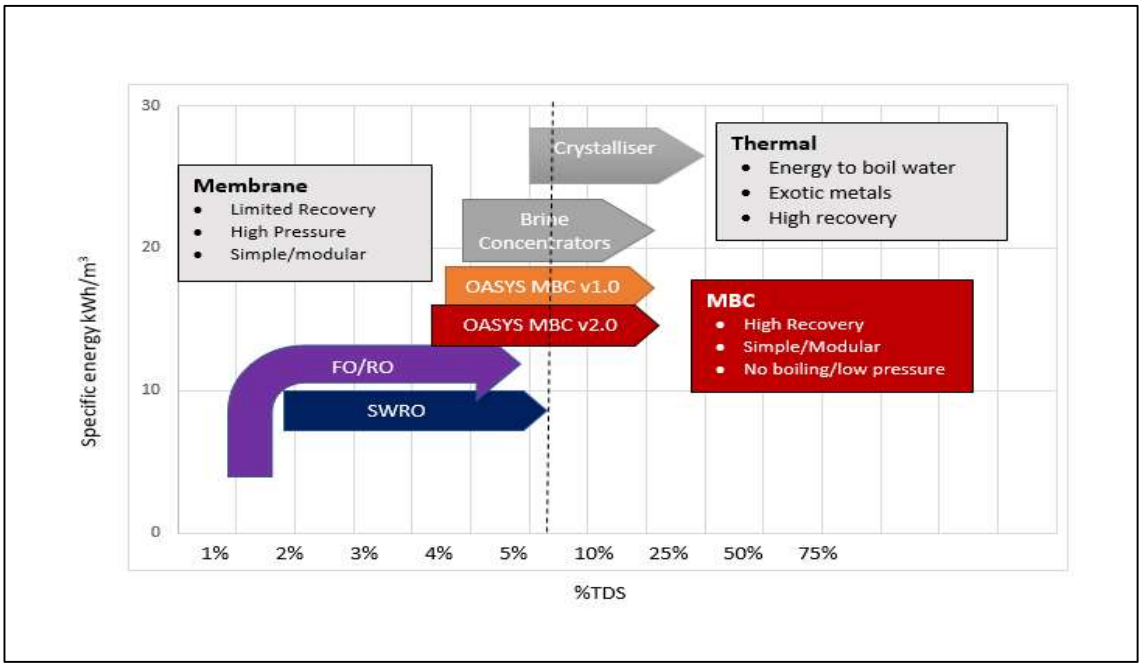

Figure 1-3: Energy Consumption in Forward Osmosis Desalination (MBC) Compared to other Desalination Techniques. (adapted from Hancock, 2013, redrawn).

It is evident from Figure 1-3 that FO technology can be used to concentrate brines from technologies such as RO to high total dissolved solids at lower specific energy when compared to traditional thermal processes. The high concentration factor (i.e. water recovery) achievable using FO technology results in reduced size of a crystallizer or an evaporation pond which subsequently reduce the capital cost.

Forward Osmosis systems have been successfully built on an industrial scale by companies such as Oasys Water Inc. for global customers. Some examples of commercial operating FO plants include Changxing Flue Gas Desulphurisation ZLED Project, Yangmei Taihua Coal-to-Chemical ZLED project and Zhongtian Hechang Energy Ordos ZLED Project (Oasys, 2014; Haupt and Lerch, 2018; Blandin et al., 2020; Li, Shi and Yu, 2019). Furthermore, Modern Water has successfully commercialised FO technology for seawater desalination in Oman (Modernwater.com, 2011; Haupt and Lerch, 2018; Blandin et al., 2020; Li, Shi and Yu, 2019).

Despite advances made over the years on forward osmosis technology, few studies have been conducted on the fundamental understanding of critical parameters that governs the performance of this technology with respect to water flux, salt flux and fouling, especially the role of reverse solute diffusion phenomenon (interaction of scaling precursors in the feed with the draw solution) on forward osmosis technology fouling tendency.

Although numerous bench-scale and pilot-scale evaluations have been conducted over the years in support of continuous development of an FO process, studies on the impact of the concentration of scaling precursors in the feed water on draw solution enhanced fouling remains a gap that requires addressing. For full scale application, in order to deal with scaling precursors in the feed, the default has always been the inclusion of the pre-treatment step in the flow scheme to ensure complete removal of these scaling precursors through chemical or membrane softening which add to the Capex and Opex of the plant. The approach of complete removal of the scaling precursors in the feed water is well documented for RO applications to ensure high water recoveries. The driving force for the RO process is hydraulic pressure whereas FO process uses osmotic pressure and as a result the fouling mechanisms of the two processes is not the same. In order to advance the FO process into a viable and competitive alternative for concentrating high salinity streams, a thorough and extensive studies on the impact of high salinity feed water chemistry and identification of critical operational parameters that must be considered for the treatment of these streams is required for the better understanding of the feasibility of using FO process to treat high salinity streams. Furthermore, fundamental understanding on the fouling tendencies of the FO process treating high salinity streams when employing specific set of operational parameters is also required for further advancement of this technology. The lack of industrial track record has been identified as a significant hindrance to mass adoption of forward osmosis technology. Some of the reasons for the poor uptake are the challenges relating to an ideal membrane, ideal draw solution and membrane fouling. Full scale application of forward osmosis technology for reclamation and reuse of high salinity streams could contribute to addressing water scarcity challenges experienced worldwide due to the inherent advantages associated with the technology.

1.2 Objectives and Scope of the study

The high salinity streams produced by the petroleum and power generating industry include ion exchange regeneration effluents, RO brine and evaporator mother liquor. The handling of these streams remains a challenge as most of these plants are situated inlands and handling of these streams through conventional technologies is capital intensive. The main objective of this study was to explore the potential of FO technology for the treatment of selected concentrated brines to reduce brine volumes and recover water for reuse in industry such as Sasol and Eskom. In order to achieve this primary objective, the following scope of work was developed:

- To conduct comprehensive literature review on FO technology in order to identify opportunities and challenges associated with this technology

- To conduct chemical speciation of the brine streams identified and draw solution using OLI Stream Analyzer software to understand the speciation of the brine streams as well as to calculate the thermo-physicochemical properties such as osmotic pressure of the solution. Chemical speciation information was essential when designing the FO experiment with respect to choosing appropriate operating conditions, i.e. temperature, pH and providing an indication of possible mineral phases that could form
- To validate the FO experiment experimental set-up and methods by repeating some of the experiments cited in the literature. Furthermore, the effects of various factors on the FO performance, a mechanistic study on the transport phenomena in the FO membrane were evaluated. Factors evaluated were temperature, membrane type, feed and draw solution concentration, cross-flow velocity, draw solution type, membrane orientation, reverse salt diffusion
- To propose the FO transport phenomena and mechanistic explanation on how the various factors evaluated affect the FO performance.
- To study the feasibility of using FO technology to further concentrate high salinity brine streams.
- To identify critical parameters that must be considered for the treatment of high salinity streams using FO technology and recommend areas that requires further exploration.
- Furthermore, fundamental understanding on the fouling tendencies of the FO process treating high salinity streams when employing specific set of operational parameters is also required for further advancement of this technology.

1.3 Structure of the Dissertation

This dissertation presents important contributions in the field of desalination using forward osmosis technology. The dissertation presents the study on the feasibility of using FO process for the treatment of selected concentrated brine streams from inland industries using a laboratory-scale FO setup. To achieve the objectives outlined above (section 1.2), this dissertation is divided into six (6) chapters.

The background information on the need for energy-efficient desalination technologies, review of conventional desalination techniques and their drawbacks, introduction to forward osmosis and its theory are presented in Chapter One. Chapter Two provide an extensive literature review on the principles of FO process, development of the technology, challenges facing the technology and its successful demonstration for various applications. Recent developments in FO membrane development, system configurations and osmotic draw solutions were also thoroughly reviewed.

Furthermore, chemical speciation, OLI thermodynamic framework and concept of precipitation, dissolution and saturation were also reviewed in support of the overall objectives of the study.

Chapter Three focuses on the survey conducted on selected concentrated brine streams using OLI software. OLI Stream Analyzer software (Olisystem.com, 2011) was acquired, and its application on high ionic strength inorganic solutions were evaluated. In this chapter, the OLI Stream Analyzer software was used to understand the speciation of the selected brine streams and draw solution as well as to calculate the thermo-physicochemical properties such as bulk osmotic pressure of the solutions. This information was useful when designing the FO experiment in terms of choosing appropriate operating conditions, i.e. temperature and providing an indication of possible mineral phases that could form. Sequential precipitation of various minerals as water is removed from the selected brine streams was studied to identify potential limitations for FO studies. Furthermore, an indication of potential water recoveries achievable for selected brine streams is presented in this chapter.

Chapter Four focuses on the establishment of appropriate operating conditions with respect to membrane type, membrane orientation, draw solution concentration, feed solution concentration, temperature and cross-flow velocity to be used in the main experiments described in Chapter 5. Experiments were undertaken to achieve these objectives by evaluating the effects of various factors that are known to impact FO process performance (a mechanistic study on the transport phenomena in the FO membrane) using sodium chloride. In this chapter, the justification for choosing experimental conditions, membrane and draw solution subsequently used for the evaluation of feasibility of using FO process for treating high salinity brine streams is presented.

In Chapter Five, FO process was studied for the treatment of the selected concentrated brine streams from power generating industry. Synthetic solutions of selected concentrated brines were prepared and used as feed solutions for the FO process. A TFC-FO membrane provided by Hydration Technologies Inc. (HTI) was used in this study. Ammonium bicarbonate was used as a draw solution based on the results presented and discussed in Chapter Three and Four. Details of the results from the experiments conducted to evaluate the feasibility of treating selected concentrated brine streams from industry such as Sasol and Eskom using TFC-FO and ammonium bicarbonate as a membrane and draw solution, respectively, are presented and discussed. Fundamental understanding on the fouling tendencies of the FO process treating high salinity streams when employing specific set of operational parameters for further advancement of this technology is presented.

In Chapter Six, the reflections of the results (summary of the results) obtained in this dissertation on the treatment of selected concentrated brine streams are presented. Future outlook of the technology following the results from this study is presented and this is followed by recommendations for future work to advance the technology further based on the findings from this study.

CHAPTER 2 : LITERATURE REVIEW

In this chapter, a brief description of forward osmosis technology, challenges and applications is given. This is followed by chemical speciation literature review.

2.1 Forward Osmosis Technology

In Forward Osmosis (FO), a solution consisting of specially selected solutes (often called the "draw solution or osmotic agent") is used to provide a solution with a lower chemical potential energy of water than the feed stream to be treated. A semipermeable membrane is used to induce this difference in potential energy (osmotic pressure gradient differential) to spontaneously dewater the feedwater stream through permeation of water through the semi-permeable forward osmosis membrane, into the draw solution, which results in the dilution of the draw solution. During the process, all suspended constituents and the majority of all dissolved ions are rejected (Cath et al., 2006). A secondary step is, however, used to recover the draw solution for reuse in the FO process. This could be achieved by using RO/NF or distillation as a reconcentration step, producing water with low total dissolved solids. The energy requirements of the secondary process may be less than those of conventional desalination technologies (i.e. membrane and thermal-based). The fouling and scaling propensity of the FO membrane may be reduced because low hydraulic pressure is applied to the membrane. Forward Osmosis technology can, however, be used without the need for draw solution recovery step and one such example is in fertigation application (Phuntsho, 2012).

During the FO process, the feedwater stream is concentrated while the draw solution is diluted. The driving force in the forward osmosis process can theoretically be much higher than that in RO process, potentially resulting in higher water fluxes, recovery and subsequently, the reduction in cost associated with brine handling. In Pressure Retarded Osmosis (PRO) process, some hydraulic pressure is applied on the draw solution side of the semipermeable membrane. The direction of the water flow is, however, still in the direction of the draw solution, and the PRO process is therefore regarded as an intermediate between the RO and FO processes. The general equation that is used to describe the water transport in FO, PRO and RO is given by the equation below:

Equation 2-1

$$J_w = A_m(\Delta P - \Delta\pi) \rightarrow A_m\left(\pi_{DS} - \pi_{feed}\right)$$

J_w = Water flux

A_m = Membrane water permeability coefficient

ΔP = differential applied hydraulic pressure across the membrane (~0 for FO)

$\Delta\pi$ = osmotic pressure differential

π_{Draw} and π_{Feed} are the osmotic pressure of the draw and feed solutions, respectively.

For FO, ΔP is zero; water diffuses to the more concentrated side of the membrane (draw solution)

For RO, ΔP> Δπ, water diffuses to the less concentrated side due to hydraulic pressure (permeate)

For PRO, Δπ> ΔP, water diffuses to the more concentrated side under positive pressure (draw solutions)

Figure 2-1 below shows direction of water flow in FO, PRO and RO processes.

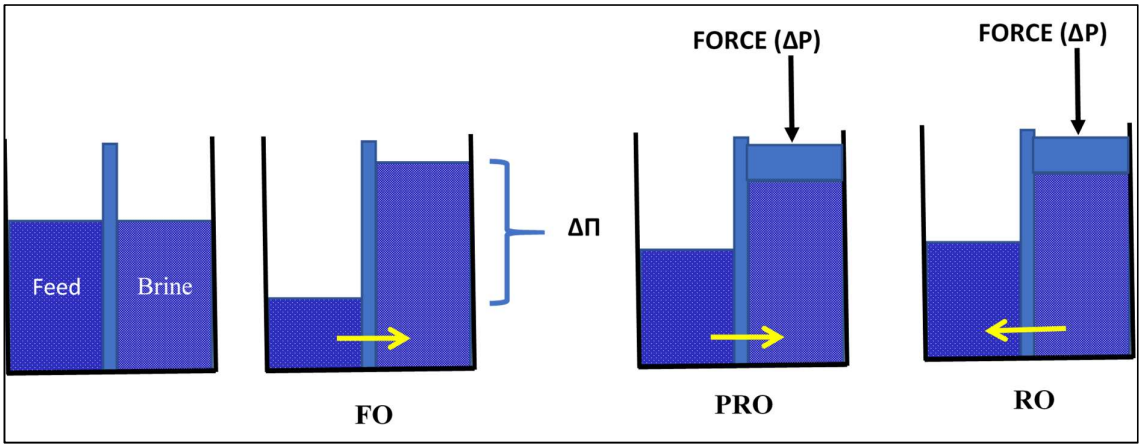

Figure 2-1: Direction of water flow in FO, PRO, and RO [adapted from Cath et al., 2006]

Since the FO process takes advantage of the natural phenomenon (osmosis), low operating and capital cost could be achieved as compared to traditional technologies such as RO or thermal evaporators. The main advantage of Forward Osmosis is that it operates at a low hydraulic pressure and therefore cheap materials of construction (MOC) could be used to construct the FO plant.

Schematic diagrams of a typical RO and FO systems are shown in Figure 2-2 and 2-3, respectively [Cath et al., 2006; Elimelech and McGinnis, 2007].

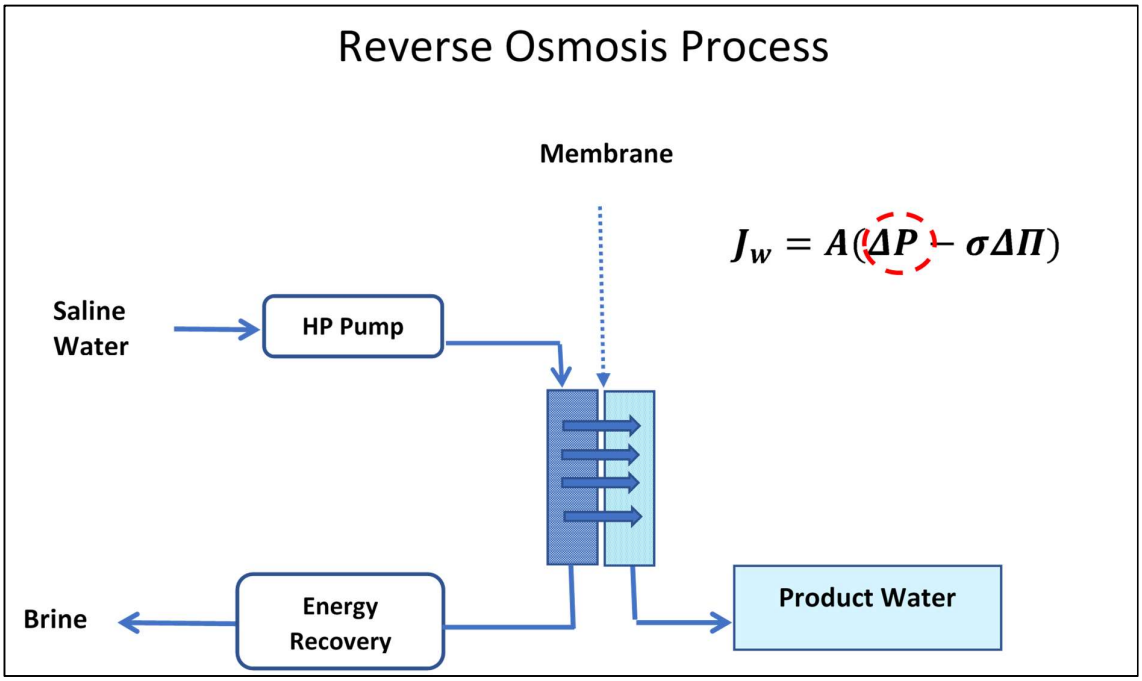

Figure 2-2: Schematic of RO desalination process [adapted from Cath et al., 2006]

J_w is the water flux, A is the water permeability coefficient of the membranes, σ is the reflection coefficient, ΔP is the trans-membrane hydraulic pressure, Δπ is the osmotic pressure gradient across the RO membrane.

For RO, ΔP must be greater than σΔπ in order to generate enough hydraulic pressure differential for the transfer of clean water through the RO membrane.

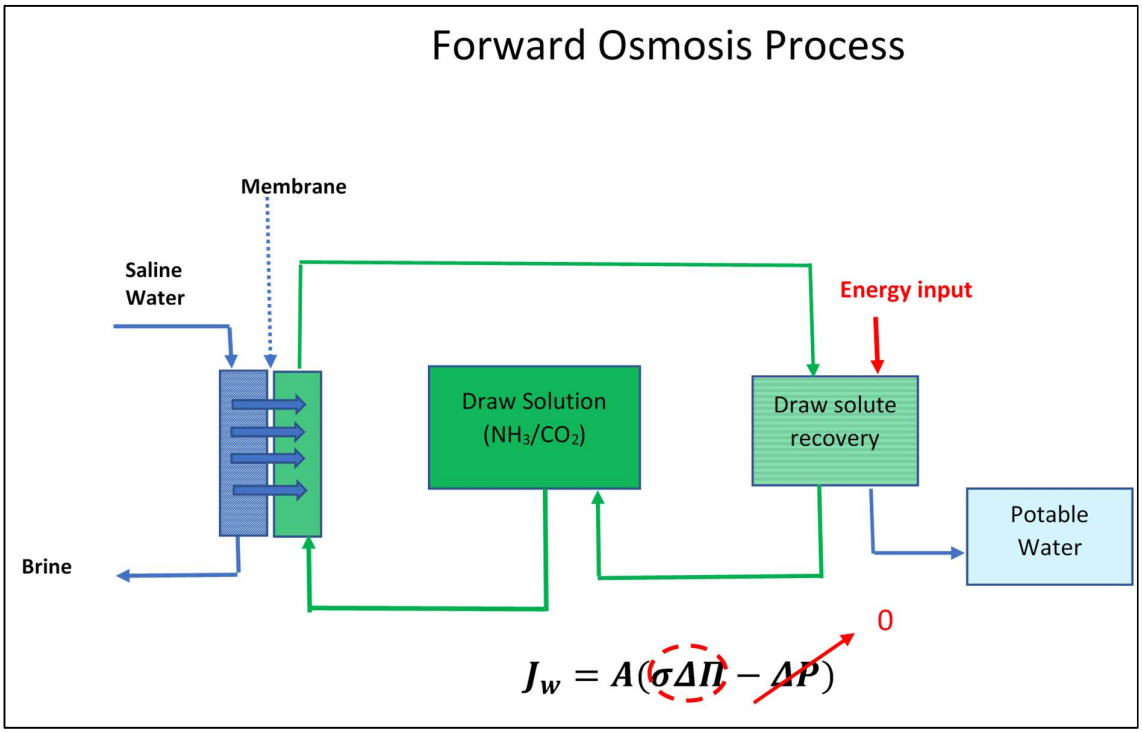

Figure 2-3: Schematic of FO desalination process [adapted from Cath et al., 2006]

J_w is water flux, A is the water permeability coefficient of the membranes, σ is the reflection coefficient, ΔP is the trans-membrane hydraulic pressure, Δπ is the osmotic pressure gradient across the FO membrane between the draw and a feed solution.

For FO, ΔP is zero

Forward osmosis systems exist as either stand-alone or hybrid systems. Figure 2-4 shows a typical diagram of a standalone FO system.

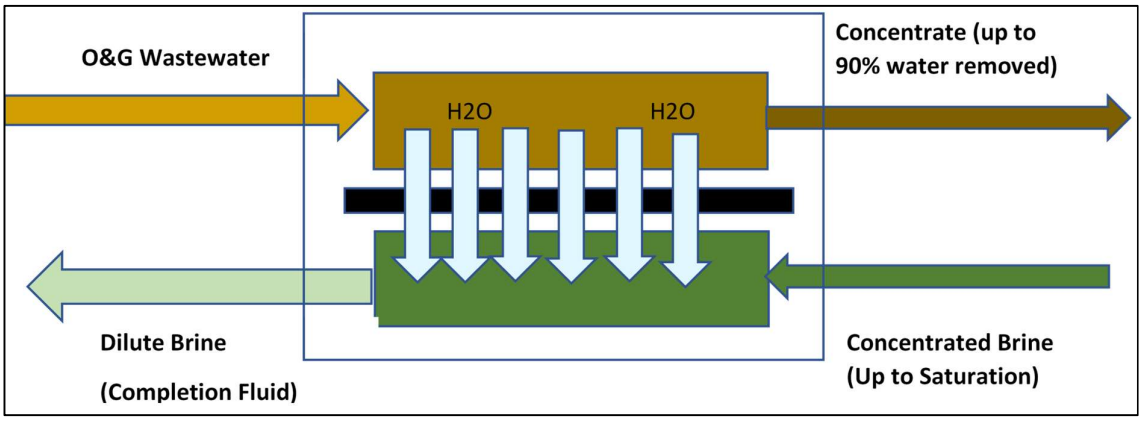

Figure 2-4: Typical diagram of a standalone FO system treating Oil & Gas (O&G) Wastewater (adapted from ForwardOsmosisTech's Forward Osmosis Guide, 2016).

In this case, the FO process allows for the use of the osmotic energy to filter and recycle drilling wastewater that would be otherwise destined for disposal. Another typical example of a standalone FO system is where the feed and draw solutions represent wastewater streams, which become cheaper to dispose of once they are concentrated and diluted, respectively.

Figure 2-5 shows a typical diagram of a hybrid FO system.

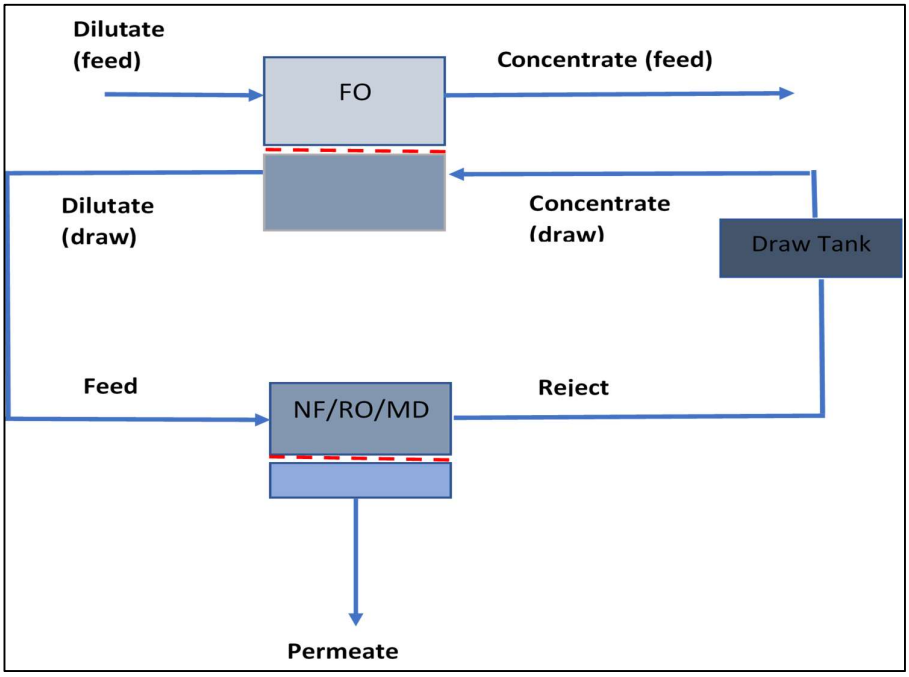

Figure 2-5: Typical diagram of a hybrid FO system using membrane technology to recover the draw solution (adapted from ForwardOsmosisTech's Forward Osmosis Guide, 2016).

In the hybrid FO system, the two streams produced are the concentrate and permeate streams. The permeate stream can either be reused or discharged and the concentrate can be further processed using thermal desalination technologies. In this case, membrane technologies (NF/RO/MD) were being used to separate the clean water from the feed stream from the draw solution.

Figure 2-6 shows another configuration of a hybrid FO system, but in this case a thermolytic draw solution was used as a draw solution and it was separated from the treated water using thermal desalination technology.

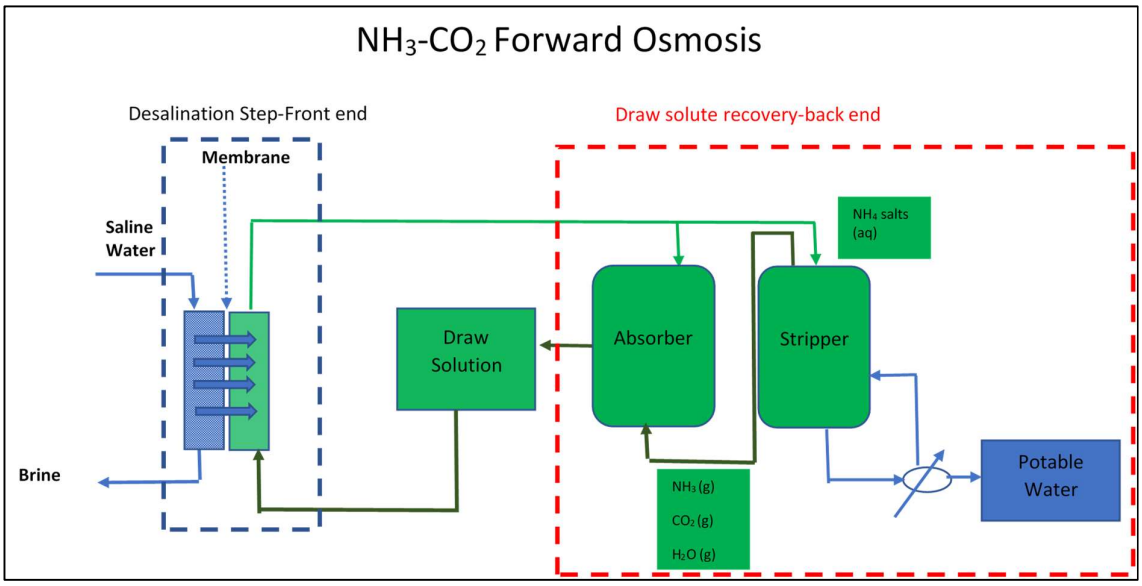

Figure 2-6: A hybrid FO system, using thermolytic draw solution [adapted from Cath et al., 2006]

2.1.1 Challenges in Forward Osmosis

Despite numerous studies conducted on FO technology, some difficulties need to be resolved in order to increase the rate of commercialisation. Internal and external concentration polarisation, fouling, specific reverse salt diffusion, lack of a fit for purpose membrane and lack of draw solution that generates higher osmotic pressure and is easy to regenerate, are some of the challenges that require attention (Zhao et al., 2012).

These factors are briefly discussed in the sections below.

2.1.1.1 Concentration Polarization

The build-up of salt concentration gradients on both sides of the forward osmosis membrane results in concentration polarisation. The concentration gradient results in the reduction of the effective driving force available for the FO process, thus reducing theoretical achievable water flux and water recoveries. Concentration polarization is typical for both pressure-driven and osmotically driven processes. External concentration polarisation (ECP) and internal concentration polarization (ICP) are the two types of concentration polarisation prominent in forward osmosis. Depending on the orientation of the FO membrane, concentration polarisation can further be classified as either dilutive or concentrative (ForwardOsmosisTech's Forward Osmosis Guide, 2016).

The membranes used in forward osmosis are asymmetric (i.e. they are comprised of dense contaminants rejection layer and porous supporting layer). External and internal concentration polarisation occurs on the rejection and porous supporting layer, respectively (Gray et al., 2006; Elimelech and McCutcheon, 2006; Mehta and Loeb, 1978; Lee et al., 1981; McCutcheon and Elimelech, 2007; Khan, Shon and Nghiem, 2019):

- When the rejection layer of the forward osmosis membrane is on the feed solution side, in a configuration defined as AL-FS, the clean water entering the porous support layer from the feed side results in dilutive ICP as a result of draw solution dilution. Concentrative ECP occurs on the feed solution side, similar to the phenomena experienced in conventional reverse osmosis.

- Conversely, when the rejection layer of the forward osmosis membrane is on the draw solution side, in a configuration defined as AL-DS, the clean water entering the rejection layer from the feed side results in dilutive ECP as a result of draw solution dilution. Concentrative ICP occurs on the feed solution side.

The ECP and ICP are responsible for the lower than theoretically expected water fluxes observed empirically when evaluating forward osmosis technology.

The concept of ICP (dilutive and concentrative) is depicted in Figure 2-7 below.

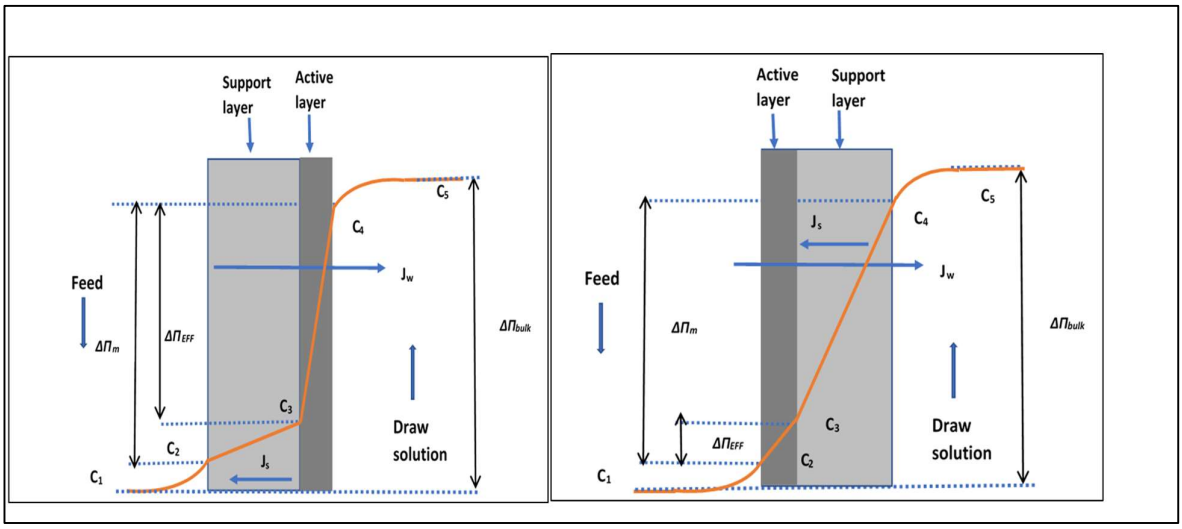

a b

Figure 2-7: Concentrative and dilutive ICP concept in forward osmosis [adapted from Cath et al., 2006]

Concentrative ICP occurs when the rejection layer of the forward osmosis membrane is on the draw solution side, in a configuration defined as AL-DS. As depicted in Figure 2-7 (a), bulk feed water concentration (C_1), is lower than the concentration on the membrane wall (C_3). The formation of C3 result in the lowering of driving force available, resulting in reduced water flux and potentially higher CAPEX and OPEX.

Dilutive ICP occurs when the rejection layer of the forward osmosis membrane is on the feed solution side, in a configuration defined as AL-FS, the clean water entering the porous support layer from the feed side result in the dilution of the draw solution. As depicted in Figure 2-7 (b), the bulk draw solution concentration decreases from C5 to C4. The dilutive ICP also result in increased CAPEX and OPEX.

In the scenario where the active layer of the FO membrane is facing feed water (AL-FS) orientation which is a configuration of choice for the FO process; dilutive ICP occurs within the membrane support layer as water penetrates through the active layer of the membrane resulting in the dilution of the draw solution. A decline in solute concentration happens from C5 to C4, as illustrated in Figure 2-7 (b). The decrease in concentration results in a reduced effective osmotic pressure differential and thus yields a lower than expected water flux and consequently increasing the size of the plant.

The equation representing effective osmotic pressure differential in the presence of concentration polarisation is shown below (McCutcheon et al., 2006):

In a situation where the active layer (AL) of the semipermeable FO membrane is facing the feedwater solution, dilutive ICP and concentrative ECP are more prevalent.

Equation 2-2

$$\Delta\pi_{effective} = \pi_{Draw,m} - \pi_{Feed,m} = \pi_{Draw,b} * e^{(-JwK)} - \pi_{Feed,b} * e^{\left(\frac{Jw}{k}\right)}$$

$\pi_{Draw,m}$ represent the osmotic pressure of the draw solution on the porous support layer of the FO membrane

$\pi_{Feed,m}$ represent the osmotic pressure of the feedwater solution facing the active layer of the FO membrane

$\pi_{Feed,b}$ represent the bulk osmotic pressure of the feedwater solution facing the active layer of the FO membrane

$\pi_{Draw,b}$ represent the bulk osmotic pressure of the draw solution facing the porous support layer of the FO membrane

Jw represent the permeate water flux

K represent the solute resistivity for diffusion

k represent the mass transfer coefficient

$e^{(-JwK)}$ represent the reduction factor of draw solution osmotic pressure as a result of dilutive internal concentration polarisation

$e^{(Jw/k)}$ represent the amplification factor of feed solution osmotic pressure as a results concentrative external concentration polarisation

In AL-FS configuration, water flux reduction is mainly governed by dilutive ICP in cases were the feedwater solution has low bulk osmotic pressure.

In a situation where the active layer (AL) of the semipermeable FO membrane is facing the draw solution, concentrative ICP and dilutive ECP are more prevalent.

Equation 2-3

$$\Delta\pi_{e} = \pi_{draw,m} - \pi_{Feed,m} = \pi_{draw,b} * e^{\left(-\frac{Jw}{k}\right)} - \pi_{Feed,b} * e^{JwK}$$

Conversely, in an AL-DS configuration, the reduction in water flux is governed by dilutive external concentration polarisation in cases where the feedwater solutions has low osmotic pressure.

The mass transfer coefficient, k, is a function of cross-flow velocity across the FO membrane surface, and this parameter can be controlled by playing around the cross-flow velocity. The solute resistivity for diffusion impacts the solute diffusion within the porous support layer. Generally, the smaller the K, the higher is the rate of solute diffusion within the support layer, which minimises ICP. As a result, several studies are being undertaken to modify the K value in order to address challenges associated with ICP, as ICP contributes significantly to the low fluxes experienced in the FO process (ForwardOsmosisTech's Forward Osmosis Guide, 2016).

2.1.1.2 Membrane Fouling

There are, in general, four types of membrane fouling, namely, colloidal, scaling, organic and biofouling. Membrane fouling is common to all membrane-based processes such as ultrafiltration, reverse osmosis, electrodialysis and forward osmosis. Membrane fouling is influenced by feedwater quality components such as the presence of scaling precursors, microorganisms, suspended solids and organic compounds (Klaysom et al., 2013. Mecha, 2017; Khan, Shon and Nghiem, 2019).
Like concentration polarisation and reverse salt diffusion (to be discussed later), membrane fouling is also a challenge in the FO process.

Lower membrane fouling results in a reduction in operational (increased membrane life) and capital costs (small footprint). The low hydraulic pressure in the FO process, however, results in different fouling mechanism when compared to that of the pressure-driven process such as RO. Figure 2-8 below shows the comparison of fouling behaviour in FO and RO. Figure 2-8b shows that although there was a decline in water flux for FO when treating water containing alginate, the fouling was less compact and could easily be removed by hydrodynamic shear force. For RO, which is operating under hydraulic pressure, the fouling is more compact and cohesive and could not be removed by physical cleaning.

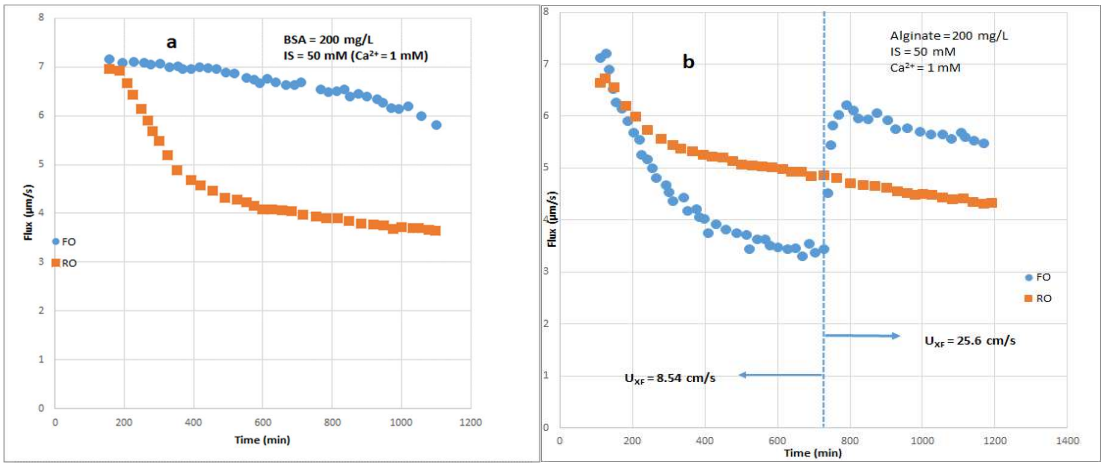

Figure 2-8: Comparison of fouling behaviour in FO and RO (adapted from Lee et al., 2010)

The impact of membrane orientation on fouling is depicted in Figure 2-9 below.

In AL-FS configuration, the deposition of fouling material is on the rejection layer as the rejection layer is facing the feedwater. Conversely, in AL-DS configuration, deposition of the fouling material occurs on and within the support layer of the FO membrane as a result of the feedwater facing the support layer of the FO membrane. Standard practices available for dealing with external fouling in FO processes include adjustment of cross-flow velocity, osmotic backwash and the use of appropriate feed spacer.

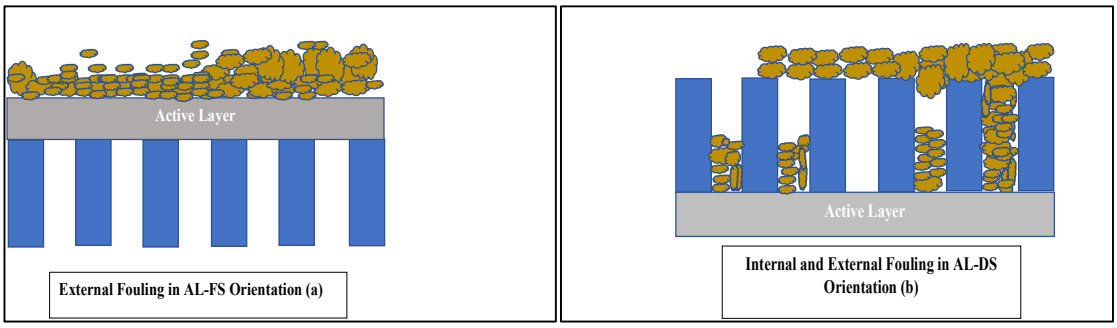

Figure 2-9: Impact of membrane orientation on fouling in Forward Osmosis process (adapted from She et al., 2016)

Due to the difficulties associated with the removal of internal fouling, most of the industry recommended configuration is AL-FS. The degree of compaction of the fouling layer (as a result of external fouling) is low when compared to that observed in the conventional RO process due to low hydraulic pressure experienced in the FO process. Internal fouling occurs within the porous support layer and cannot be dealt with by adjusting operating conditions such as cross-flow velocity. Internal fouling is less reversible than external fouling.

Several authors have conducted extensive research on the FO process membrane fouling, and their findings are discussed briefly in the section below.

Holloway et al. (2007) conducted a study to evaluate the differences in fouling behaviour between FO and RO processes when treating anaerobic digester wastewater, and their results showed a lower propensity (indicated by reduced loss in membrane permeability) for fouling in FO than in RO. Holloway et al., (2007) also demonstrated that osmotic backwash could successfully be employed in the FO process to control fouling. Chemical cleaning in general removes the cake layer only and cannot effectively remove foulants within the membrane pores. Martinetti et al. (2009) also demonstrated the effective use of osmotic backwash when investigating the potential recovery of concentrated RO brines using FO process.

Mi et al. (2008) investigated the impact of the foulant-foulant interaction (between organic and inorganic foulants) on the formation of fouling layer on the FO membrane surface. Results from this study showed that the binding of calcium to the organic matter, rate of permeation at the beginning, membrane configuration and operating parameters plays a significant role in controlling FO membrane fouling. Lee et al. (2010) compared the fouling behaviours of the FO and RO process using organic and particulate foulants.

The results from this study showed that the organic fouling layer formed could be controlled by adjusting the cross-flow velocity as the permeability on the FO membrane was recovered when compared to that of the RO membrane. The results from this study presents an opportunity for reducing the high operating cost associated with conventional clean in place (CIP).

Mi et al. (2010) investigated the gypsum scaling and cleaning behaviour in the FO process. The results from this study showed that gypsum scaling in the FO process was almost fully reversible following a water rinse without the addition of chemicals. A study was also done to compare FO membrane fouling behaviour between cellulose acetate and polyamide membrane. The result of this study showed that the polyamide membrane was susceptible to more compact fouling due to enhanced surface crystallisation (gypsum scaling). On the other hand, the flux decline observed on cellulose acetate membrane surface was not severe, primarily because its scaling mechanism involved bulk crystallisation which was followed by deposition of crystals onto the membrane surface.

A study by Li et al. (2015) showed a draw solution induced scaling of the FO membrane using ammonium bicarbonate as a draw solution. The scaling on the membrane surface at the feed side was caused by the interaction between anions that diffused from the draw solution (HCO_3^- (bicarbonate)) and a cation present in the feed solution (calcium and magnesium), causing a significant decline in the water flux. The authors indicated that the scaling occurred even at a low solute concentration and at an early stage of the FO process. This observation provides a necessary inference regarding the importance of the selection of a fit for purpose draw solution and the development of new membranes for the FO process.

Chun et al. (2017) published a review paper on membrane fouling focusing on organic, inorganic and biological fouling. The authors also provided insight into membrane fouling monitoring and mitigation strategies available.

She et al. (2016) identified factors that play a role when it comes to membrane fouling in the FO process. The identified factors were operating conditions (initial water flux, feed and draw solution cross-flow velocity, spacer geometry, aeration, and feed and draw solution temperature), Feedwater characteristics, such as foulant concentration, pH, ionic strength, and ionic composition (fouling precursors in the feed water such as calcium, magnesium, sulphates etc.), Draw solution composition (i.e. draw solution type and draw solution concentration), Membrane properties (i.e. such as membrane separation and structural properties) and Membrane Orientation (i.e. AL-DS or AL-FS).

Approaches that have been cited in the literature to manage fouling challenges include pre-treatment of the feed water (e.g. filtration, softening, antiscalant addition, coagulation-flocculation etc.), proper selection of draw solution (e.g. draw solution should not enhance fouling of the membrane) and optimization of operating parameters (e.g. temperature, cross flow velocity etc.) (She et al., 2016; Coday et al., 2014; Zhao et al., 2012, Mecha, 2017)

2.1.1.3 Reverse Salt Diffusion

Unlike in the RO process, the mass transfer in the FO process occurs in both the forward and reverse direction as a result of the concentration gradient between the draw solution and the feedwater. In the FO process, the osmotic pressure of the feedwater is lower than that of the draw solution, which results in water permeation from the feedwater solution to the draw solution. Regarding the solute diffusion, the diffusion of salt is bidirectional (i.e. from feed to draw solution and from draw solution to the feed). Although the forward diffusion (from the feed to the draw solution) is similar to that observed in the RO, process, the reverse salt diffusion (from the draw to feed solution) only occurs in the FO process [Phuntsho, 2012, Khan, Shon and Nghiem, 2019].

Reverse salt diffusion is an essential parameter to the FO process because it brings complexity when it comes to the feed water concentrate management and could potentially contribute to the decrease in the net osmotic potential or driving force leading to reduced water fluxes. Furthermore, reverse salt diffusion could also increase the fouling potential of the feed solution due to the formation of scaling compounds with the feed constituents. Several studies conducted by various researchers have shown a strong correlation between reverse diffusion of draw solute to membrane fouling [Zhao et al., 2012]. Reverse salt diffusion also results in draw solution loss which could require replenishment. Table 2-1 presents a list of draw solutions generally used in the FO process. A vital column to take note of is the scale precursor ions in these draw solutes.

Table 2-1: Compounds commonly used as draw solution for the FO process (Phuntsho, 2012)

Draw Solution tested	Osmotic Pressure at 2.0 M (atm)[a]	pH at 2.0 M	Max. solubility[a]	Scale Precursor Ions
CaCl2	217.6	6.29	7.4	Yes (Ca^{+2})
KBr	89.7	6.92	4.5	No
$KHCO_3$	79.3	7.84	2	Yes (CO_3^{2-})
K_2SO_4	32.4	32.4	0.6	Yes (SO_4^{2-})
MgCl2	256.5	5.64	4.9	Yes (Mg^{+2})
$MgSO_4$	54.8	6.7	2.8	Yes (Mg^{+2})
NaCl	100.4	6.98	5.4	No
$NaHCO_3$	46.7	7.74	1.2	Yes (CO_3^{2-})
Na_2SO_4	95.2	7.44	1.8	Yes (SO_4^{2-})
NH_4HCO_3	66.8	7.69	2.9	Yes (CO_3^{2-})
$(NH_4)SO_4$	92.1	5.46	5.7	Yes (SO_4^{2-})
NH_4Cl	87.7	4.76	7.4	No
$Ca(NO_3)_2$	108.5	4.68	7.9	Yes (Ca^{+2})
KCl	89.3	6.8	4.6	No

[a] OLI Stream Analyzer was used to derive parameters in the Table.

The reverse solute flux (RSF) (J_s) is used in the FO process to track the movement of draw solutes from the draw solution to the feed solution. This parameter shows the rate at which draw solutes are leaving the draw solution in the reverse direction to the water flux.

Equation 2-4

$$J_s = B\Delta C = B(C_{DS} - C_{FS})$$

J_s = Reverse solute flux

B = Membrane solute permeability coefficient

ΔC = concentration gradient of solute across the membrane.

Reverse solute flux is also a measure of the mass (measured in either mg or g) of draw solution salt lost to the feed solution per unit area of membrane per unit time (hour). The RSF however, does not provide any relationship with water flux.

The specific reverse salt flux (SRSF), a ratio of the reverse solute flux to the water flux (Js/Jw) is preferably used as it gives an accurate measure of FO membrane selectivity. A higher SRSF indicates a high rate of draw solute diffusion (poor membrane selectivity) in the opposite direction to the water flux, which could alter the chemistry of the feed solution (potential for fouling and scaling), increase in the rate ICP (CAPEX impact-low water flux) and increase in the amount of draw solution required (OPEX impact-draw solution make-up).

Studies conducted by Lay et al.; Li et al.; Zhao et al. and Lee et al. (Lay et al., 2010; Li et al., 2015; Zhao et al., 2012; Lee et al., 2010]) have shown that reverse diffusion of draw solution solute can aggravate FO fouling which leads to flux reduction, a critical Achilles heel for FO processes. Furthermore, reverse solute diffusion could lead to the contamination of the feed, and this might impact on the disposal of the generated brine stream. Figure 2-10 is a representation of the role of reverse diffusion on membrane fouling in the FO process (She et al., 2016).

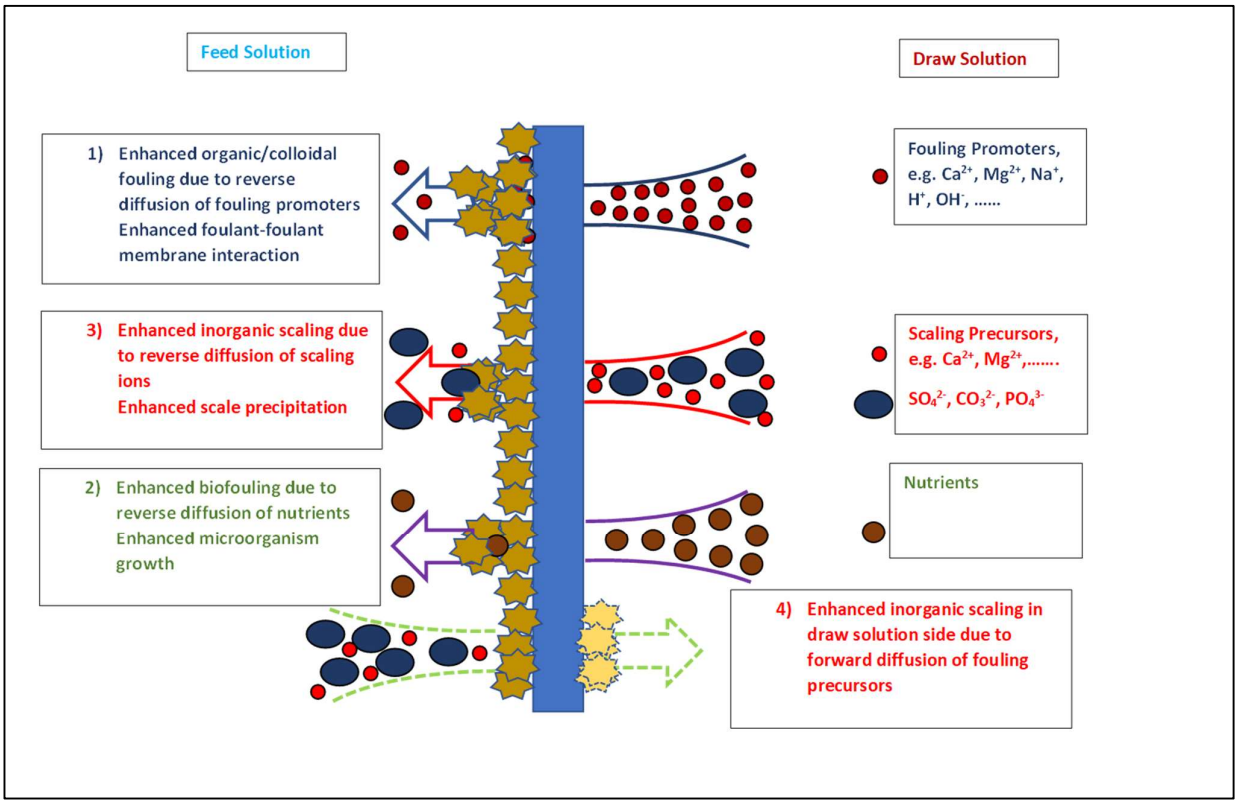

Figure 2-10: Representation of the role of reverse diffusion on membrane fouling in the FO process (adapted from She et al., 2016)

Figure 2-11 below illustrate the fouling mechanism as observed by Li et al. (2016) when ammonium bicarbonate draw solution was used as draw solution for seawater desalination.

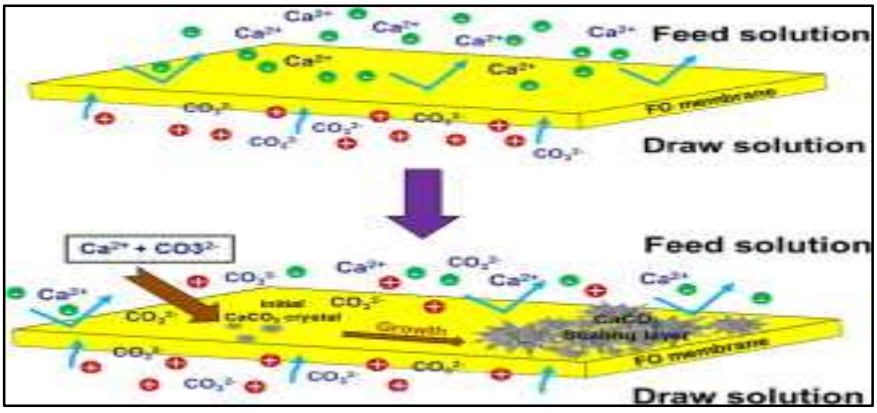

Figure 2-11: Reverse Salt diffusion enhanced membrane fouling in FO process (Li et al., 2016) (reprinted with permission from Elsevier)

As discussed in this section, reverse solute diffusion is one of the challenges facing FO membrane processes, and it should, therefore, be fully understood and minimised in the development of fit for purpose membrane and draw solution

2.1.1.4 Draw Solution Development

In the FO process, the driving force is provided by the osmotic pressure differential between the concentrated solution on the support side of the membrane and the feedwater solution on the rejection side of the membrane. Researchers have used terms such as osmotic agent, osmotic media, driving solution to describe the draw solution. The details around the evolution of the draw solution are presented in the section below.

2.1.1.4.1 History of draw solution development

For desalination of seawater, the development of draw solution is the significant development that has been extensively researched. Batchelder (1965) suggested the use of volatile solutes like sulphur dioxide by dissolving it in water. The recovery of this draw solution was to be achieved by first heating the draw solution to a specific temperature, and the draw solution recovery was achieved in a stripping column where the warm air was running counter-current to the heated draw solution (Batchelder, 1965). Batchelder's idea of using removable gases as a draw solution was further expanded by Glew, who suggested that either gases or liquids are used as osmotic solutes for draw solutions (Glew, 1965). In 1972, Frank used aluminium sulphate as a draw solute to evaluate FO process. The attempt to recover this draw solution was made by reacting the diluted draw solution with lime ($Ca(OH)_2$) to form aluminium hydroxide and calcium sulphate which were then separated from the solution by sedimentation amongst other methods (Frank, 1972). The drawback with this method was that none of the precipitates could be reused as a draw solution. Solutions of carbohydrates have also been proposed for the draw solutions for desalination of seawater.

Kravath and Davis (1975) created a flux of water from seawater to a concentrated glucose solution in a dialysis cell. The possible use of this cell is in emergency lifeboats where dialysis bag can be immersed into seawater. A water flux from seawater over a cellulose acetate membrane dilutes the salt or glucose solution to a level where ingestion is possible (Kravath and Davis, 1975). Though the osmotic agent is consumed, the method does not demand the removal of the osmotic agent and the method is therefore not suited for large scale application.

McGinnis proposed the utilisation of potassium nitrate (KNO_3) and sulphur dioxide (SO_2) as draw solutes in 2002. Two stages were proposed for these draw solutes. The first stage entailed the use of osmosis process to dewater seawater (pre-heated to between 60 and 100 ^{0}C) with a concentrated solution of KNO_3 as a draw solution. During the osmosis process, the KNO_3 becomes diluted with water permeating from the feedwater. By cooling the diluted KNO_3 in a heat exchanger using incoming seawater, precipitation of KNO_3 occurs. The second stage involved the use of diluted KNO_3 as the feedwater with pressurised SO_2 solution as a draw solution.

Through osmosis process water from the diluted KNO_3 solution (which now serves as a feedwater solution) permeate to the draw solution side, leading to the dilution of SO_2. The recovery of SO_2 draw solution was achieved through thermal evaporation (McGinnis, 2002).
In the process discussed above, KNO_3 and SO_2 are recycled back to the process. The option of using sulphur dioxide as the only draw solution is not preferred, primarily due to its low osmotic pressure at saturation when compared to potassium nitrate. The studies discussed above demonstrate that one of the primary challenges to a feasible FO process in the early days of technology development is the lack of an appropriate draw solution.

Some breakthrough when it comes to draw solution development was achieved by McGinnis and co-workers when they utilised ammonia and carbon dioxide gases (McCutcheon et al., 2005; McCutcheon et al., 2006; McGinnis and Elimelech, 2007) at various molar ratios. The resultant mixture was a draw solution with high osmotic pressure, and this draw solution could be thermally recovered at moderate temperatures. Hancock et al. (2009) studied the reverse diffusion of various draw solution in the FO process, namely, sodium chloride, magnesium chloride and ammonium bicarbonate.

Achill et al. (2009) have evaluated more than 500 inorganic compounds for potential use in the FO process as draw solutions. When it came to performance as a criterion, Achill et al. (2009) found that $CaCl_2$, $KHCO_3$, $MgCl_2$, $MgSO_4$, and $NaHCO_3$ were the most favourable draw solutions. Draw solutions such as $KHCO_3$, $MgSO_4$, NaCl, $NaHCO_3$, and Na_2SO_4 were found to be favourable when it comes to replenishment cost.
The draw solutions that satisfied both criteria (performance and replenishment cost) were ($KHCO_3$, $MgSO_4$, and $NaHCO_3$). The main finding from this study was that there is a need for rigorous evaluation of draw solutions before a suitable draw solution is selected. Specific application and the type of the membrane to be used are essential in selecting a fit for purpose draw solution.

A summary of draw solution development over the years is shown in Table 2-2

Table 2-2: Historical development of draw solutions used in FO process (including how they were recovered and challenges) (adapted from Ge et al., 2013)

Year	Researchers	Draw solute	Method of recovery	Drawbacks
1964	Neff	Ammonia and carbon dioxide	Heating	Energy-intensive
1965	Batchelder	Volatile solutes (e.g. SO_2)	Heating or air stripping	Energy-intensive, toxic
1965	Glew	A mixture of water and another gas (SO_2) or liquid (aliphatic alcohols)	Distillation	Energy-intensive
1970	Hough	Organic acids and inorganic salts	Temperature variation or chemical reaction	Complicated and many corrosive chemicals are involved
1972	Franks	Al_2SO_4	Precipitation by doping lime	Toxic byproducts
1975	Kravath and Davis	Glucose	None	Not pure water
1976	Kessler and Moody	Glucose-Fructose	None	Not pure water
1989	Stache	Fructose	None	Not pure water
1992	Yaeli	Glucose	Low pressure RO	Energy-intensive
1997	Loeb et al.	$MgCl_2$	None	Not pure water
2002	McGinnis	KNO_3 & SO_2	SO_2 was recycled through standard means	Energy-intensive, toxic
2005-2007	McCutcheon et al.	NH_3 & CO_2 (NH_4HCO_3)	Moderate heating (60°C	High reverse draw solute flux, insufficient removal of ammonia
2007	Adham et al.	Magnetic nanoparticles	Captured by canister separator	Poor performance, agglomeration
2007	Adham et al.	Dendrimers	Adjusting pH or UF	Not feasible
2007	Adham et al.	Albumin	Denatured and solidified by heating	Not feasible
2008	McCormick et al.	Salt and ethanol	Pervaporation based separations	High reverse draw solute flux and low water flux
2010	Yen et al.	2-methyl imidazole-based solutes	Membrane distillation	Materials costly
2010-2011	Ling et al & Ge et al.	Magnetic nanoparticles	Recycled by an external magnetic field	agglomeration
2011	Li et al.	Stimulus-responsive polymeric hydrogels	Desweling of polymeric hydrogels	Energy-intensive and poor water flux

Year	Researchers	Draw solute	Method of recovery	Drawbacks
2011	Ling and Cheng	Hydrophilic nanoparticles	UF	Poor water flux
2011	Phuntsho et al.	Fertilizers	None	Only applicable for agriculture
2011	Lyer and Linda	Fatty acid-polyethylene glycol	Thermal methods	Poor water flux
2012	Su et al.	Sucrose	NF	Relatively low water flux
2012	Ge et al.	Polyelectrolytes	UF	Relatively high viscosity
2012	Noh et al.	Thermo-sensitive solute	Not studied	Poor water flux
2012	Yong et al.	Urea, ethylene glycol, glucose	Not studied	Low water flux and high draw solute flux
2012	Bowden et al.	Organic salts	RO	Low water flux, energy-intensive
2012	Carmignani et al.	Polyglycol polymers	NF	High viscosity, severe ICP
2012	Stone et al.	Hexavalent Phosphazene	Not studied	Not economical and practical

Characteristics of ideal draw solutions are (Ge et al., 2013):

- The draw solution must have the ability to generate high osmotic pressure.
- Reverse salt diffusion must be minimal, as discussed in section 2.1.1.3.
- Must offer lower energy consumption and overall operational costs.
- The draw solute must have low molecular weight as molecular weight influences diffusion coefficient.
- Other criterion includes high recoverability, non-toxic compatibility with FO membranes and low cost.

A comprehensive review of draw solutes in Forward Osmosis was done by Shon et al. (2015) providing information on how to select an ideal draw solution, the study of various draw solution parameters affecting FO performance. The review also addresses the commercialisation of draw solution for multiple applications.

It is apparent from the discussion above that draw solution selection is critical to ensure optimal performance of an FO process.

2.1.1.5 FO Membrane Development

In the FO process, any dense, nonporous, selective and permeable material can be utilised to manufacture FO membrane. FO membranes were tested in the 1970s in a flat sheet and capillary configurations (Kravath, 1975; Mehta, 1979). Further development came in the 1990s when the then Omotek Inc successfully manufactured a special FO membrane. Cellulose Acetate (CTA) and polyamide thin-film composite (TFC) membranes are the most prominent commercially applied FO membranes. The CTA membrane was produced and sold by the then Hydration Technology Innovations (HTI) and this membrane at some point was the only commercially proven FO membrane. Numerous studies on the FO process for different research focus discussed in this dissertation have been undertaken using the CTA membrane (Hancock and Cath, 2009; NG et al., 2006; Tang, 2009; Achilli et al., 2010). The CTA FO membrane is proprietary; unlike the conventional RO membrane, this membrane does not have a thick porous support layer for mechanical support. Instead, polyester mesh embedded in the membrane offers mechanical support. Advantages that come with cellulose-based membranes are hydrophilicity, robustness and readily availability of the material. The CTA polymers, however, have inherent drawbacks such as narrow pH and temperature of operation range which could limit their applications. The optimum pH and temperature of operation is pH 4-6 and temperature not more than 35°C, respectively. Outside these ranges, the integrity of the membrane can be compromised. The CTA membrane has the potential to degrade when exposed to draw solutions such as NH_4HCO_3. Also, the CTA membranes have in general low water permeability and low salt rejection, and therefore, their application in the desalination industry could be limited.

The thin-film composite membranes used in conventional RO process; however, possess properties required in the RO process, namely, high rejection and stability (chemically and mechanically). The TFC-RO membranes fail in FO operation mainly because of the thick and dense support layers, essential for mechanical strength at high pressures, resulting in internal CP.

The primary distinguishing factor between thin-film composite FO and thin-film composite RO membrane is the support structure of the membrane. The support structure for the FO membrane is comprised of more porous, hydrophilic and thinner structure. For the RO membrane, the support structure is thicker because it must support the membrane during pressurisation.

In the FO, the use of thin-film composite FO membrane provides the following advantages over the CTA membrane:

- Operation at higher temperatures (over 60°C)
- Operation at wider pH band (pH 2-11)
- Highly permeable

The drawback for the thin-film membrane is its high cost of production when compared to the CTA.

Elimelech and co-workers demonstrated the successful manufacturing of the TFC membrane for the FO process. The manufactured membrane exhibited fluxes and salt rejection over 18 L/m^2.hr and 97%, respectively when tested using sodium chloride (1.5 M) as draw solution and deionised water as feedwater. The integrity of the membrane was not compromised after long exposure of the membrane to NH_4HCO_3 draw solution (Yip et al., 2010; Elimelech et al., 2011).

Comparison of water flux and salt rejection between different membranes studied by Elimelech and co-workers is shown in Figure 2-12 below.

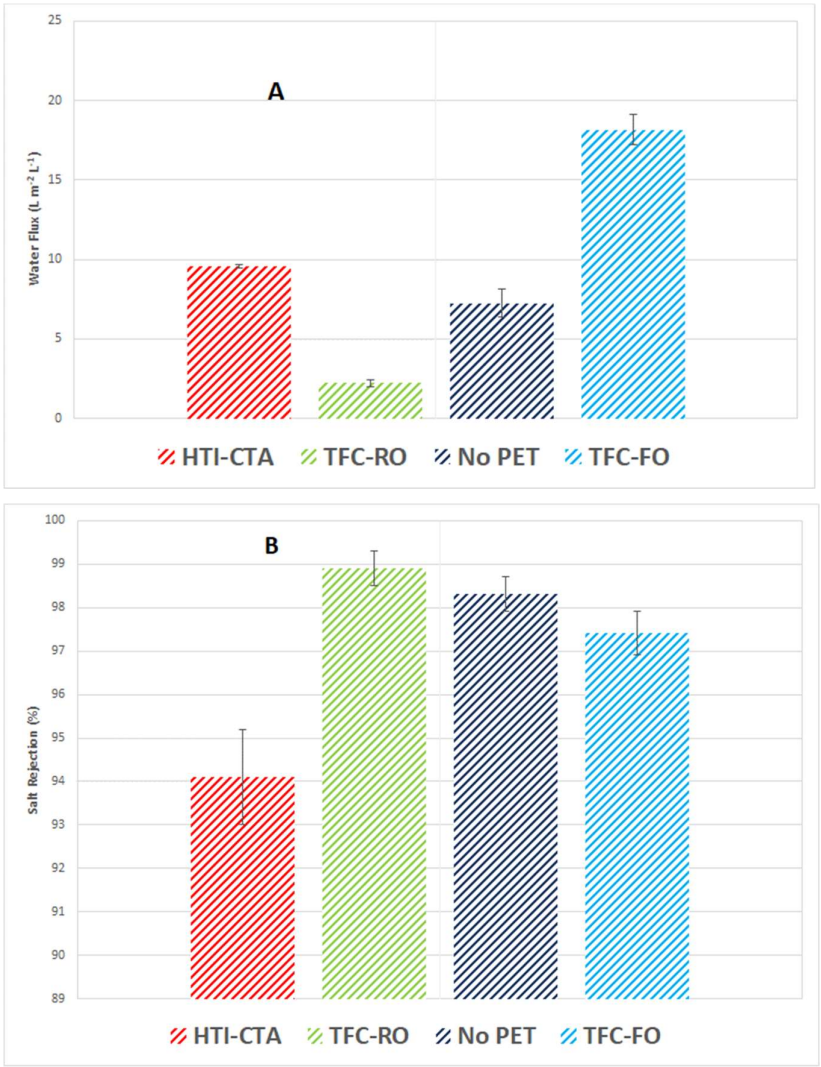

Figure 2-12: Performance comparison of (a) water flux and (b) salt rejection between TFC-FO, HTI-CTA, TFC-RO, and TCF-RO (No PET) [adapted from Yip et al., 2010].

The TFC-FO membrane was patented by OASYS Water, Inc. [Water desalination report, 2010]. This membrane was used in the full-scale application, together with ammonium bicarbonate draw solution by Oasys water (Pendergast et al., 2015; Pendergast et al., 2016). Hydration Technology Innovations developed an 8-inch diameter spiral-wound TFC membrane, and this membrane has been commercially available in the market since 2012. Coday et al. (2013 and 2014) and Ren et al. (2014) have tested HTI-TFC membrane for various applications, with the membrane performance showing higher water fluxes when compared to the HTI-CTA membrane.

Table 2-3 shows membrane physical and chemical properties for CTA & TFC FO membrane

Table 2-3: Physical and chemical properties of the membrane (adapted from Coday et al. (2013 and 2014) and Ren et al. (2014).

Membrane Parameter	**unit**	**CTA**	**TFC1**	**TFC2**
Pure water permeability coefficient (*A*)	L. $m^{-2}.h^{-1}bar^{-1}$	0.55	4.72	1.63
Salt Permeability coefficient (*B*)	m/s	$4.8x10^{-8}$	$1.2x10^{-7}$	$8.3x10^{-8}$
Structural Parameter (*S*)	µm	463	365	690
Zeta Potential, Rejecting/Active layer	mV	-34.9	-42.5	-38.6
Zeta Potential, Support layer	mV	-39.5	-3.0	-9.5
Contact Angle	º	63.7±6.8	67.8±	27.7
Average water flux	L m^{-2} h^{-1}	9.9±0.1[a] 8.4±0.1[b]	31.9±3.3	9.8±0.6[a] 10.4±0.3[b]
Average reverse NaCl flux	mmol m^{-2} h^{-1}	88.2±8.5[a] 63.9±1.1[b]	344.7±26.7	143.4±14.2[a] 113.6±2.5[b]

[a] virgin membrane utilized during tests with NaCl draw solution

[b] Virgin membrane utilized tests with sea salt draw solution

[c] Virgin membrane at 20ºC, 1M NaCl draw solution, and deionised feed water

[d] at pH 7.0

CTA-HTI; TFC1-Oasys Water; TFC2-HTI

Zhao et al. (2012); Alsvik et al. (2013); Linares et al. (2017) and Klaysom et al. (2013) have conducted comprehensive reviews on the progress of FO membrane development.

The FO membrane manufacturers and commercial status of manufactured membranes are summarised in Table 2-4 below.

Table 2-4: The FO membrane manufacturers and commercial status of manufactured membranes (adapted from Coday et al., 2014)

Manufacturer	Membrane Type	System supply	Application	Commercial Status
Aquaporin A/S	Aquaporin	No	FO	Pre-commercial
Fuji	NA	No	NA	Development
GKSS	Polymeric	No	NA	Development
GreenCentre Canada	NA	No	SWFO	Development
HTI	CA, TFC	Yes	Various	Commercial
Idaho National Lab	NA	No	NA	Development
IDE Technologies	NA	Yes	PRO	Pre-commercial
Modern Water	Undefined	Yes	SWFO	Commercial
Oasys Water	TFC	Yes	Brine concentration	Commercial
Porifera	TFC	Yes	Various	Pre-commercial
Samsung	NA	No	NA	Development
Trevi Systems	NA	Yes	SWFO	Development

NA (information not available)

**HTI was acquired by Fluid Technology Solutions (FTS)*

**Oasys Water are no longer in operation.*

Companies listed above have developed various configurations between them, which include spiral wound, tubular, hollow fibre, plate and frame. The detail description, including the advantages and disadvantages of these modules, has been covered by Cath et al. (2006).

2.1.1.6 Relationships between the FO challenges

Zhao et al (2012) summarized the relationships between the key FO challenges discussed in section 2.1.1.1-2.1.1.5. Figure 2-13 summarizes the relationships.

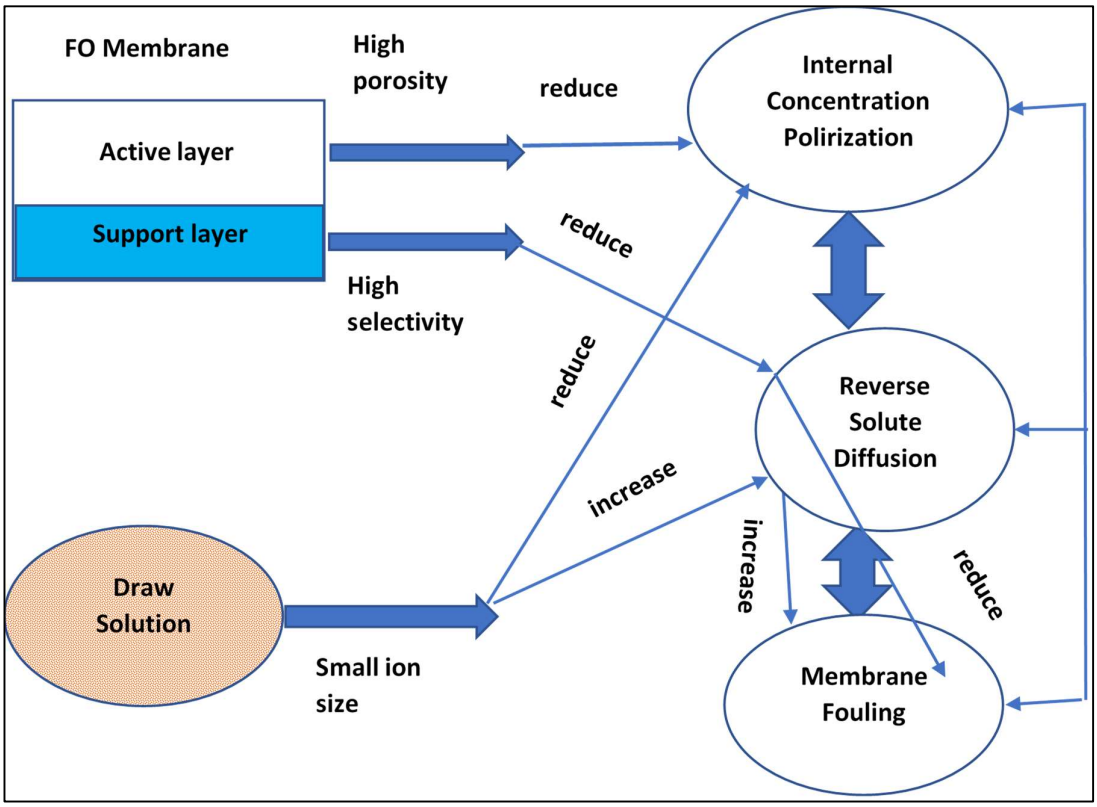

Figure 2-13: Relationships between FO key challenges (adapted from Zhao et al (2012)).

The following can be deduced from the above diagram to have an optimum FO process:

- Internal Concentration Polarization phenomenon could be reduced by increasing the porosity of the FO membrane support layer.
- Reverse solute diffusion could be minimised by improving the selectivity of the FO membrane rejection layer.
- Lower molecular weight draw solute could reduce ICP, but on the contrary, it could also lead to increased reverse solute diffusion and membrane fouling
- An increase in reverse solute diffusion also influences membrane fouling.
- Characteristics of the membrane as well as draw solute properties influences reverse solute diffusion, membrane fouling and ICP.

2.1.2 Application of Forward Osmosis Technology (Commercial & Potential Applications)

The FO process has been applied in various applications such as fertigation, seawater desalination, treatment of fracking wastewater, the concentration of RO brines, treatment of landfill leachates, emergency water supply and osmotic dilution before RO. Commercial applications, though still limited, have emerged for desalination and high salinity brine treatment (Haupt and Lerch, 2018). The following section summarises some applications that have been demonstrated either on a bench scale, pilot scale or commercial scale.

2.1.2.1 Forward Osmosis Treatment of Landfill Leachate

Organic compounds (chemical oxygen demand), heavy metals, nutrients (nitrogen) and total dissolved solids (cation and anion) are the primary pollutants found in landfill leachate. Landfill leachate water quality is very variable and hence present a challenge to any treatment technology.

Wastewater treatment facilities (e.g. activated sludge, anaerobic processes, and coagulation-flocculation) are utilised to process landfill leachate wastewater. These processes are however focused on removing COD, metals and nutrients. The lack of removal of TDS components renders this wastewater unsuitable for discharge into the sewers. Beaudry et al. (1999) evaluation of desalination processes (thermal and membrane-based) showed that these processes could be a potential solution to address the high TDS in the landfill leachate. Furthermore, the evaluation showed that the FO process could also play a significant role when it comes to treating TDS in the landfill leachate (Beaudry, Thiel and York, 1999).

Subsequently, Osmotek Inc. piloted an FO system for three months to evaluate the feasibility of treating landfill leachate using FO process. This evaluation was for landfill leachate at the Coffin Butte Landfill in Corvallis, Oregon (Beaudry, Thiel and York, 1999, Cath et al., 2006)

Approximately 20 000 to 40 000 m^3 of leachate was generated annually and the leachate required to be treated to a TDS of lower than 100 mg/L for disposal/discharge or reuse within the treatment facility.

The pilot-scale studies showed that recoveries of between 94 and 96% were achievable with high contaminant rejection. After the success of the pilot plant, a full-scale plant (150 m^3/d) was designed and constructed.

Figure 2-14 shows the process flow scheme of the full-scale FO leachate treatment process (Beaudry, Thiel and York, 1999)

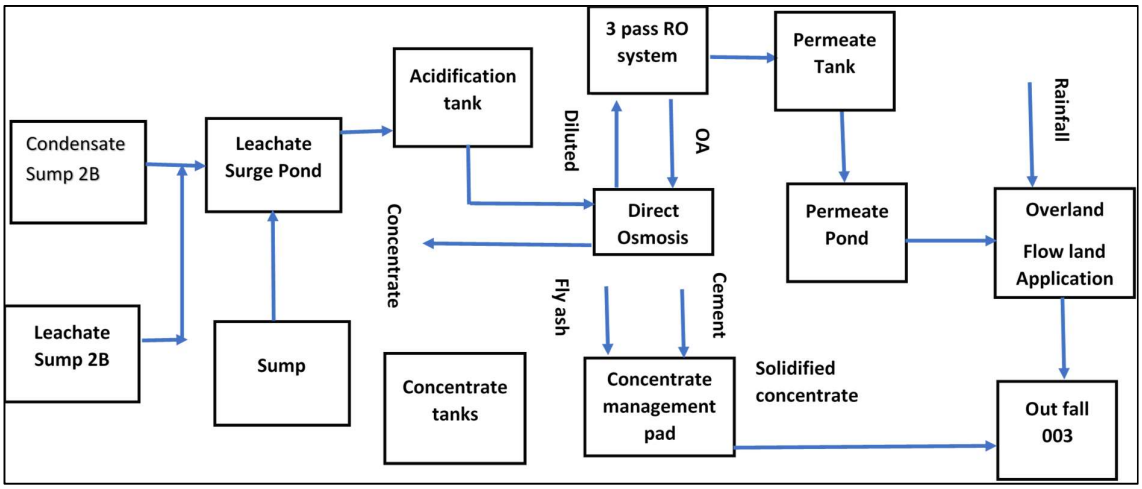

Figure 2-14: A process flow scheme of full-scale FO leachate treatment process (adapted from Beaudry, Thiel and York, 1999)

The raw leachate was pre-treated (pH correction and 100-µm bag filters to remove particulates) before water it was treated in six stages of the FO process. A three-pass polishing RO system produced water suitable for land application and a reconcentrated stream of draw solution at ca. 75 g/L NaCl which was then reused in the FO process. The brine stream from the FO process was solidified before disposal. During its operation, the full-scale plant achieved an average recovery of ca. 92% and an average RO product water conductivity of approximately 35 µS/cm. The final effluent concentrations were within specification for land application (Cath et al., 2006). The plant is no longer in operation as it was designed specifically for the rehabilitation of the landfill site.

2.1.2.2 Treatment of Seawater using FO process

Seawater desalination using FO process is one of the most exciting and challenging applications of the FO process. Although many of the earlier studies on the draw solution, including those described in this dissertation were aimed at seawater desalination, very few of those studies matured to commercial application.

McCutcheon et al. (2005 and 2006) and McGinnis (2002) have demonstrated that when using a suitable FO CTA membrane and a strong draw solution, seawater could be efficiently desalinated. A schematic diagram of this novel ammonia-carbon dioxide is shown in Figure 2-15.

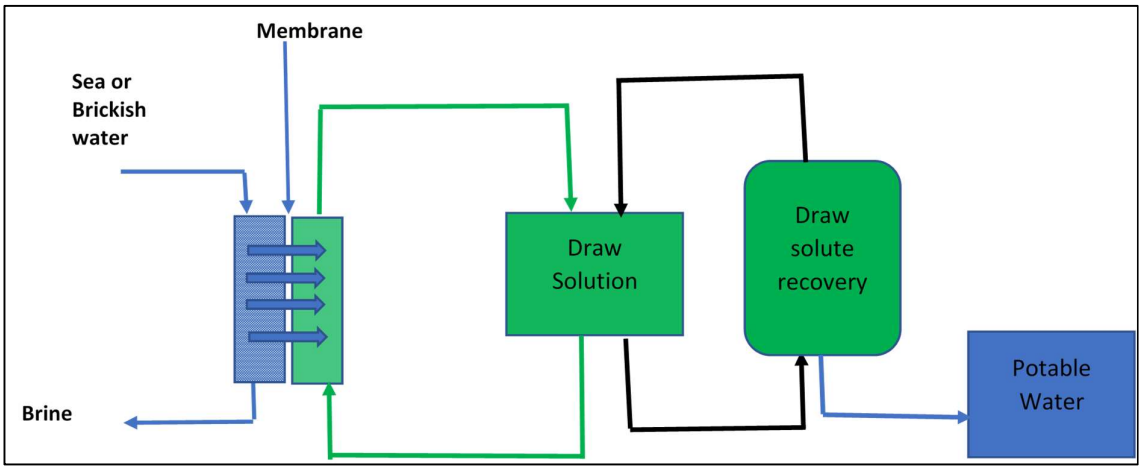

Figure 2-15: A novel ammonia-carbon dioxide FO process (adapted from McCutcheon et al., 2005; McCutcheon et al., 2006; McGinnis, 2002).

This process involves the counter-current flow of the impaired water and draw solution in the FO system chambers separated by the semi-permeable FO membrane. The ammonia-carbon dioxide draw solution can have osmotic pressure up to 250 atm. As discussed previously, the draw solution becomes diluted during the FO process, primarily due to the flow of water from the impaired chamber to the draw solution chamber. The draw solution recovery in this process involves the heating of the diluted draw solution to 60°C which leads to the decomposition of draw solution into ammonia and carbon dioxide, and the clean water was recovered in the process (McGinnis and Elimelech, 2007).

A second application for seawater desalination was by Modern Water who used FO process for direct treatment of seawater as an alternative to RO based process. Modern Water commissioned its first commercial-scale seawater desalination plant, with a capacity of 18 m^3/d, in Gibraltar in 2008, with water going into the public supply after extensive independent testing on the 1st of May 2009 (Modernwater.com, 2011).

The Gibraltar plant was followed by a larger plant, with a capacity of 100 m^3/day. The plant was located at the Public Authority for Electricity and Water's site at Al Khaluf in Oman and was commissioned in November 2009.

Due to the successes of the plants built in 2008 and 2009, the company was awarded a turnkey contract to build a 200 m^3/day capacity forward osmosis-based desalination plant at Al Naghdah. The plant was commissioned in 2012.

The high-quality freshwater produced by these plants was supplied to the local communities. The technology (patented Manipulated Osmosis Process) used had already been successfully piloted by Modern Water plc at Oman. The pilot plant (100 m^3/d) operated alongside a conventional SWRO system owned by PAEW for comparison purposes. The results from the piloting study showed less frequent membrane cleaning for the FO plant when compared to the traditional SWRO.

Figure 2-16 shows the simplified diagram of MOD technology.

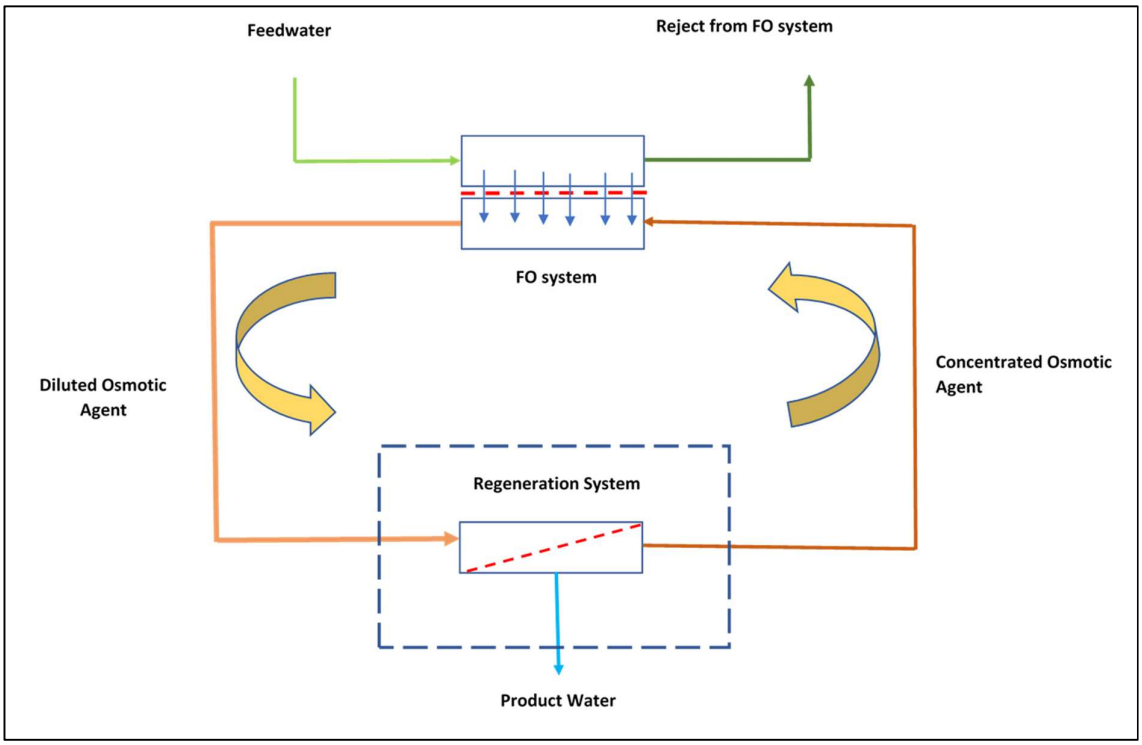

Figure 2-166: Seawater Manipulated Osmosis Desalination [adapted from Water desalination report, 2010]

Modern Water uses a membrane separation (RO or NF) process, similar to the RO to extract freshwater. Osmotic agents listed for the MOD process include, $MgSO_4.6H_2O$, $MgSO_4.7H_2O$, $MgCl_2.6H_2O$, $Na_2SO_4.10H_2O$, $CaCl_2.2H_2O$, $CaCl_2.6H_2O$, potassium alum.$24H_2O$, KCl, NaCl, $Na_2HPO_4.12H_2O$ in water (Al-Mayahi and Sharif, 2004)

2.1.2.3 Treatment of Challenging Feed Streams using FO Process

As part of the continuous establishment of the niche market for FO technology, the feasibility of using FO technology to address the waste streams generated during exploration activities in the Oil and Gas (O&G) industry has been extensively researched, from bench scale to commercial demonstration. This section will highlight some of the FO applications in the O&G industry.

2.1.2.3.1 The green machine

Hickenbottom et al. (2013) investigated the performance of FO for the treatment of O&G effluents using Green Machine (second generation). Hydration Technology Innovations (HTI) started the concept of the Green Machine, which was aimed at onsite treatment of O&G industry waste streams to produce reusable water.

Green Machine was HTI's mobile system that used HTI's custom made FO CTA membrane and a sodium chloride draw solution. Piloting was conducted using Green Machine whereby 6% w/w (ca. 60 000 mg/L) NaCl draw solution was diluted to a 4.5% w/w (ca. 45 000 mg/L). The diluted draw solution was reconcentrated using a conventional RO system, producing a high-quality product water stream fit for re-use. The Green Machine was tested at Haynesville shale gas for a week as a demonstration; the system showed that it could recover 85% of O&G drilling wastewater (ca. 3 500 mg/L TDS) while concentrating the wastewater by a factor of five (ca, 16 000 mg/L TDS). Product water from the reconcentrating step (RO) was fit for reuse. The FO system was operated for the duration of piloting without any membrane cleaning. At the end of the piloting, the membrane permeability decline was 18%. The major contributor to the decline in water was attributed to the decrease in osmotic pressure differential as a result of the increased osmotic pressure of the concentrated feed rather than membrane fouling (Coday et al., 2014).

Figures 2-17 and 2-18 below shows the schematic for FO treatment using 1st generation and 2nd generation Green Machine. Figures adapted from Coday et al. (2014)

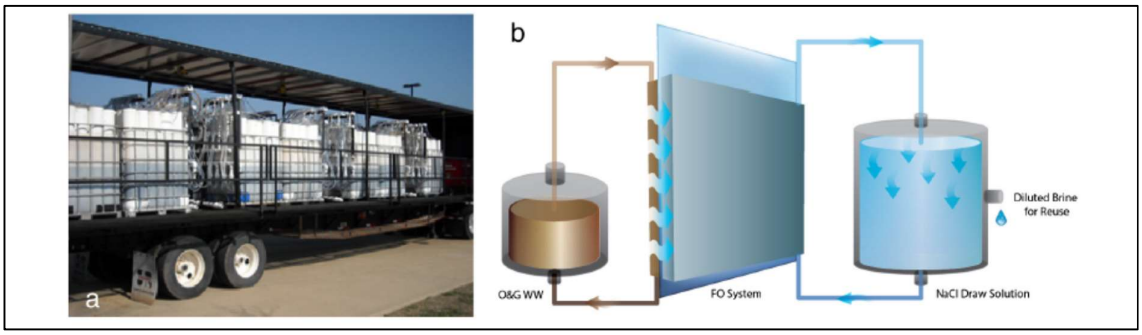

Figure 2-17: The HTI's first generation Green Machine FO treatment process (Coday et al., 2014) (reprinted with permission from Elsevier)

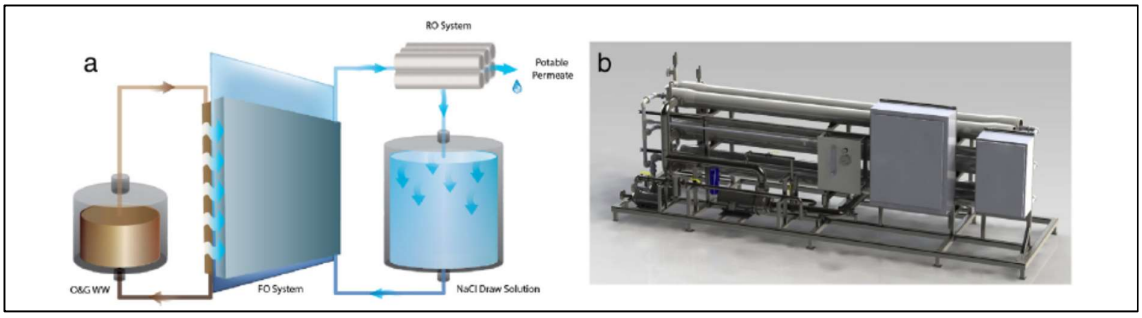

Figure 2-18: The HTI's second generation Green Machine FO treatment process (Coday et al., 2014) (reprinted with permission from Elsevier)

2.1.2.3.2 The FO technology as a membrane-based brine concentrator (MBC)

The first membrane-based brine concentrator was developed and commercialised by Oasys Water. The MBC process developed utilised thermolytic draw solution (ammonia and carbon dioxide), and TFC-FO membrane developed at Yale University. The MBC process was intended to treat challenging brines such as those from the O&G industry and flue gas desulphurisation (FGD) processes (Coday et al., 2014).

The Oasys Water MBC system consisted of a pre-treatment, MBC, and RO process to achieve the required treated water specifications. Feedwater was pre-treated in a chemical reactor in which chemical oxidiser, sodium hydroxide, and sodium carbonate are added to precipitate sparingly soluble minerals and COD. The resulting slurry was dewatered to separate sludge from the treated feedwater. The residual suspended solids and iron was then further removed from the filtrate using a green sand media filter and the cartridge filter. Pre-treated feedwater was then be concentrated up to 250 000 mg/L (TDS) using the MBC process (Coday et al., 2014). The patented draw solution was a mixture of ammonium bicarbonate and ammonium hydroxide dissolved in water at a specific ratio to generate high osmotic pressure. The draw solution facilitates the permeation of water through the TFC membrane to the draw solution. The diluted draw solution was then heated to evaporate (decompose) the draw solution solutes into gases (ammonia and carbon dioxide), which have lower vapour pressure than water. This recovery method is said to require less energy and waste heat can also be utilised. The ammonia and carbon dioxide gases are then condensed, and reconcentrated draw solution was produced for reuse in the MBC system (Coday et al., 2014).

The MBC process was demonstrated on a commercial scale for treating O&G wastewater from Marcellus Shale and Permian Basin to provide a solution for volume minimisation and reuse (Coday et al., 2014). For the Marcellus Shale testing, about 230 m3 of feedwater was processed using the MBC system and the testing was for 800 h. The commercial demonstration was sustained for six months and included seven weeks of continuous run. Averaged water fluxes achieved during the testing was between 2 and 3 $L/m^2.h$, and these fluxes were highly dependent on operating conditions. It is, however, essential to indicate that water flux under these testing conditions (feed TDS concentration up to 75 000 mg/L) with the conventional membrane-based process (RO) would be impossible due to operating limits associated with the RO technology (i.e. pressure). Marcellus demonstration test achieved averaged water recovery of 65%.

The Permian Basin demonstration unit treated feedwater of, approximately 150 m^3 during 400 h of testing. The averaged MBC feedwater total dissolved solid for the Permian Basin case was 103 000 mg/L. System water flux and water recovery averaged 3 $L/m^2.h$ and 60%, respectively. The averaged TDS of the brine and product water was 241 000 mg/L and 737 mg/L, respectively.
Figures 2-19 shows Oasys Water's MBC schematic diagram (Figure adapted from Coday et al. (2014).

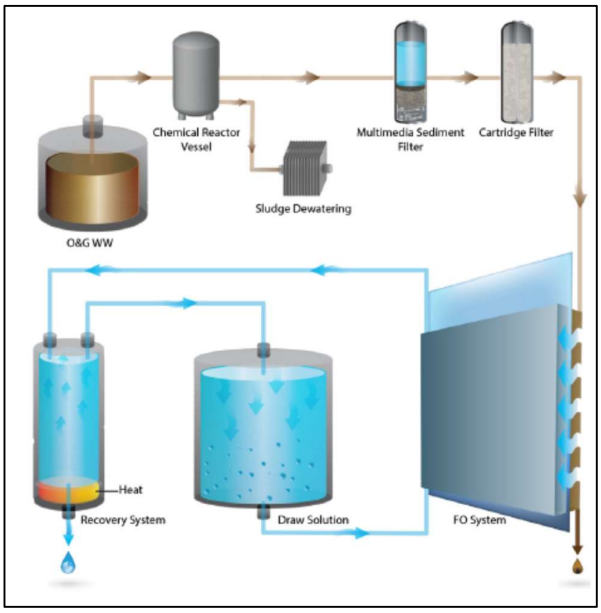

Figure 2-19: Oasys Water's MBC treatment system (Coday et al. (2014)) (reprinted with permission from Elsevier)

The first full-scale MBC plant contract was awarded to Oasys Water in 2014. This plant was the first commercial zero liquid discharge (ZLD) system to utilise an osmotically driven technology membrane process to treat challenging wastewater.

The MBC system was designed to treat 650 m^3/d of flue gas desulfurization (FGD) wastewater from the 2 x 660 MW Changxing Power Plant in China. Oasys Water offered its MBC system, which included the pre-concentrating reverse osmosis (RO) while Beijing Woteer supplied physical-chemical, filtration and ion exchange pre-treatment steps required for meeting the project objectives.

The overall process flow diagram of the Changxing FGD wastewater treatment system is configured like most other ZLD systems: chemical softening, granular media filtration, ion exchange, RO pre-concentration, brine concentration and crystallisation. However, rather than using a conventional mechanical vapour compression evaporator for brine concentration, the plant employs an MBC system incorporating forward osmosis process to concentrate RO brine further from a TDS of 60 000 mg/L to approximately 280 000 mg/L (Water desalination report, 2014).

Although Oasys Water had demonstrated its FO process in the concentration of O&G industry wastewater (Marcellus and Permian demonstration trials), this was the first commercial power plant application of the technology in a ZLD project.

The design requirements imposed by the end-user were that the plant should be robust enough to cover an expected wide range of water quality and flow rates. As a result, OASYS Water had to make critical design adjustments to accommodate these wide ranges and ensure stable performance (Pendergast et al., 2016):

- Chemical and ion exchange softening of the FGD wastewater to enable high water recovery on the MBC system and due to the high concentration factor required to achieve ZLD. This was done to minimise possibilities for scaling in pre-concentrating RO system and for sequential precipitation of minerals of interest in the final brine handling step (crystallizer).
    - A weak acid cation (WAC) unit process was also included in the flow scheme as a polishing step for hardness removal.
- Robust flow scheme that enables the processing of variable flowrates and feedwater quality.
- Optimisation of the turndown ratio by splitting the MBC system into trains. This was to enable the system to treat feedwater flowrates from 60% to 110% of the design maximum.

Figure 2-20 below is a schematic of the Changxing Power Plant FGD Treatment Process (Water online, 2015; Pendergast et al., 2016)

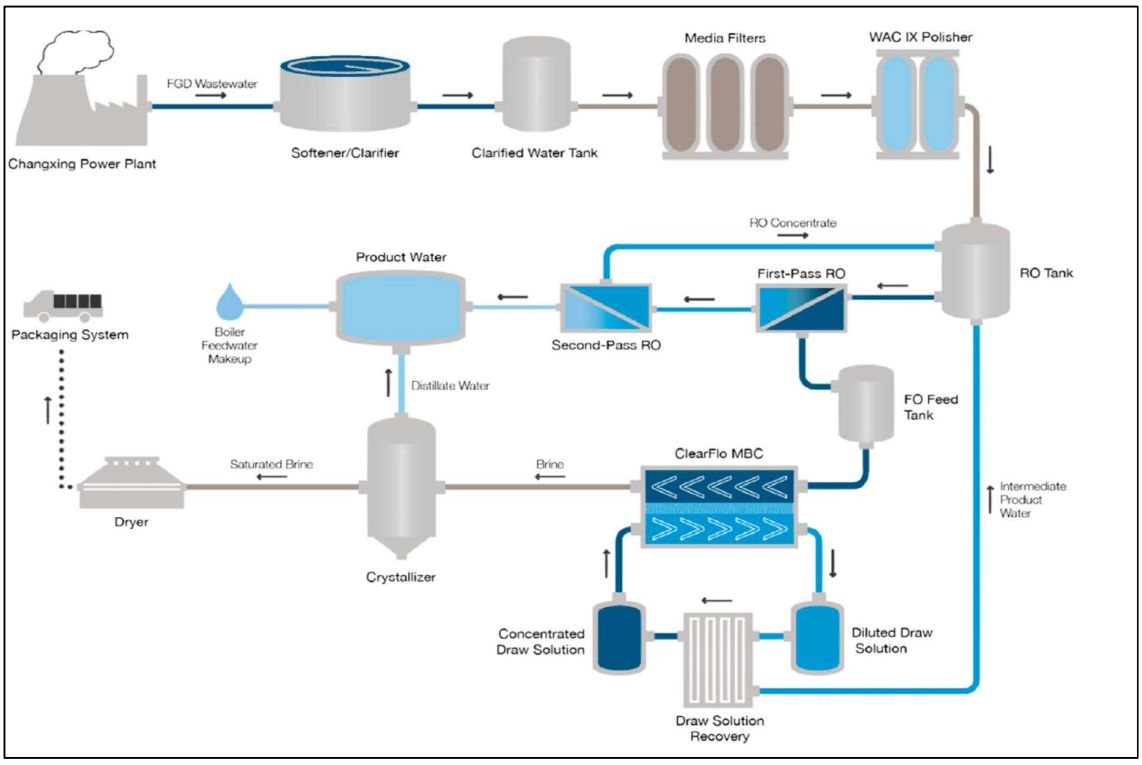

Figure 2-20: Changxing Power Plant FGD Treatment Process (Water online, 2015; Pendergast et al., 2016) (reprinted with permission from the author. Open Access article)

The freshwater stream from the MBC draw solution recovery system is co-treated with the pre-treated wastewater stream using the RO (two-pass RO) and the second pass RO permeate has a TDS of <100 mg/L. The plant was designed to have the permeate recycled back to the power plant for reuse as boiler feedwater. The MBC system was designed to achieve feedwater recovery of up to 87%.

The brine from the MBC system is further concentrated in the crystalliser to produce a mixed salt of sodium chloride and sodium sulphate. The mixed salt produced is then sold to chemical manufacturers.

2.1.2.4 Fertigation

The process whereby fertilisers are applied through the irrigation system is called fertigation. In the context of the FO process, the system involves the use of impaired wastewater (e.g. brines, seawater and brackish water) as the feedwater and the fertiliser of interest as a draw solution. The diluted draw solution is then applied at a required concentration as fertiliser, while at the same time, the impaired feedwater is concentrated. This process is classified as osmotic dilution because the draw solution recovery step is not required, unlike in cases discussed in section 2.1.2.1-2.1.2.3.

Figure 2-21 below shows an FO based fertigation concept as proposed by Phuntsho (Phuntsho, 2011).

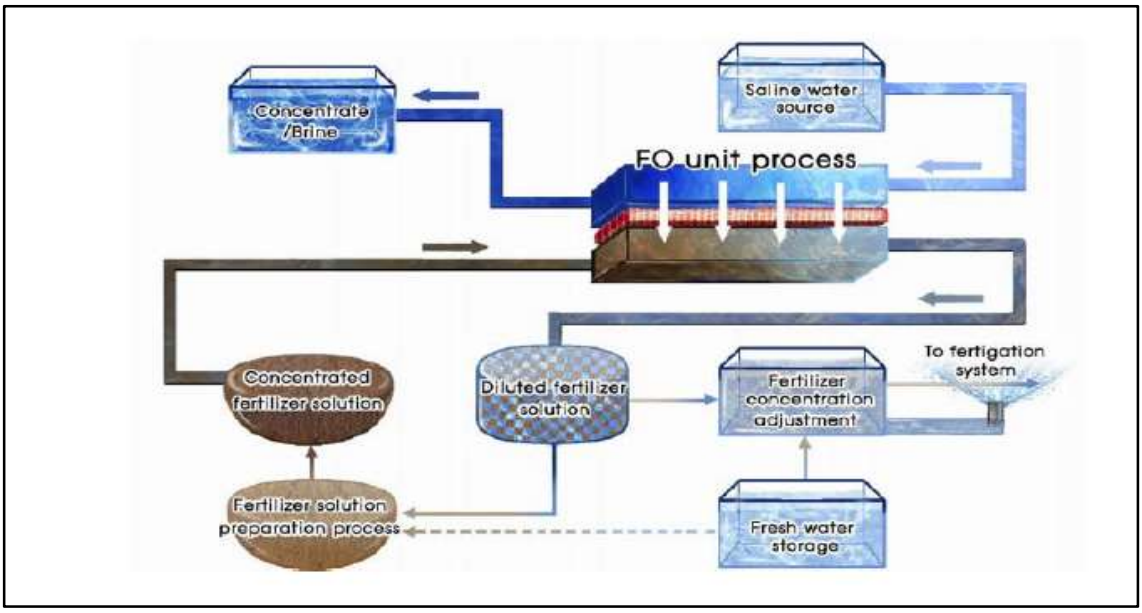

Figure 2-21: FO based fertigation concept proposed by Phuntsho (Phuntsho, 2011) (reprinted with permission from Elsevier).

Some of the challenges identified for the lack of commercialization of this concept include (ForwardOsmosisTech's Forward Osmosis Guide, 2016): transportation of intended fertiliser to the farms; impaired water might have to be pumped to the farms which will add cost if distances are long; additional dilution might be required to get to the required fertiliser concentration which adds to energy requirement of the process and FO Brine management.

The technical issue relating to the final concentration of the produced fertiliser is because FO process is based on concentration and as a result, the extent of the osmotic dilution achieved (dilution of draw solution) is dictated by the concentration or osmotic equilibrium (Chekli et al., 2016). Nanofiltration is being considered as a solution to reduce the concentration of the nutrients in the diluted draw solution to meet the fertigation specifications (Chekli et al., 2016). Pressure assisted forward osmosis (PAFO) was also considered as an alternative to Nanofiltration. Pressure assisted forward osmosis relies on additional hydraulic pressure applied to enhance water flux and subsequently dilute the draw solution beyond the osmotic equilibrium. Pressure assisted forward osmosis has been tested by Sahebi et al. (2015), and the results from this study showed that PAFO could be an option to Nanofiltration. Figure 2-22 below shows a conceptual schematic diagram of fertiliser drawn FO (FDFO)-NF and fertiliser drawn pressure-assisted FO (FDPAO).

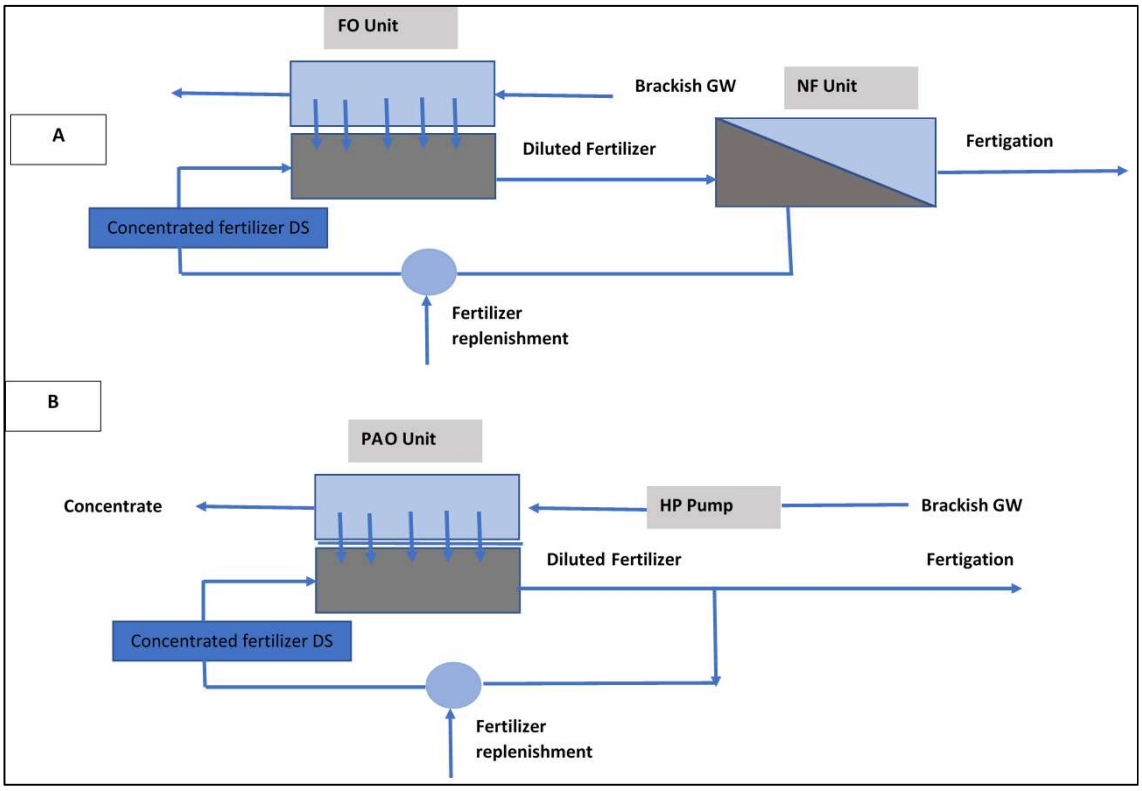

Figure 2-22: Conceptual schematic diagram for FDFO and FDPAO (adapted from Chekli et al., 2016)

2.1.2.5. Hybrid FO Systems

Although FO may not be as cost-effective as a standalone process for seawater desalination, recent studies by several authors have shown that the combination of FO and RO using FO as pre-treatment process to desalination may offer a better alternative for seawater desalination (Chung et al., 2012; Hancock et al., 2013; Bamago et al., 2011; Linares et al., 2014). The hybrid system could result in lower energy consumption and high-water recovery. The hybrid system uses high salinity seawater as a draw solute and wastewater effluent as a feed solution. By combining FO and RO processes, additional feed water is drawn from the wastewater to dilute seawater before it is treated in a seawater reverse osmosis. Due to the dilution of seawater, seawater reverse osmosis could potentially be operated at lower feed pressures which could result in overall more economical energy consumption. The performance of FO combined with low-pressure seawater reverse osmosis (LPRO) was studied by Yangali-Quintanilla et al. (2011).

Figure 2-23 shows a typical schematic diagram proposed for FO-LPRO hybrid system.

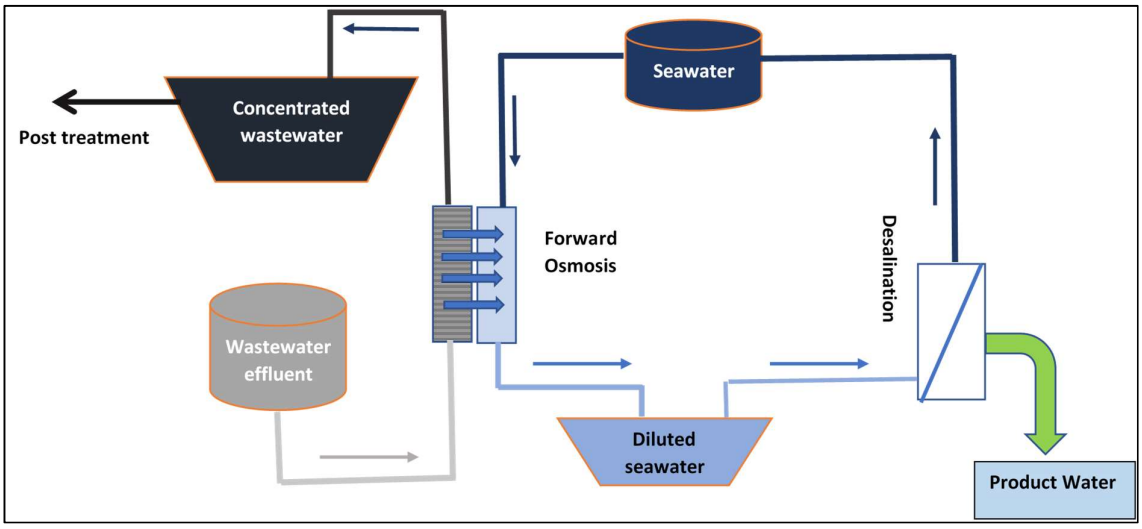

Figure 2-23: FO and RO integration for seawater desalination. Wastewater (municipal or industrial) (adapted from Linares et al., 2014)

Their studies showed that the energy consumption for the FO-LPRO hybrid system was between 1.3-1.5 kWh/m^3, which is half of the conventional standalone seawater RO (SWRO) process with typical energy consumption ranging from 2.5-4 kWh/m^3.

Figure 2-24 shows power consumption for SWRO and FO-LPRO.

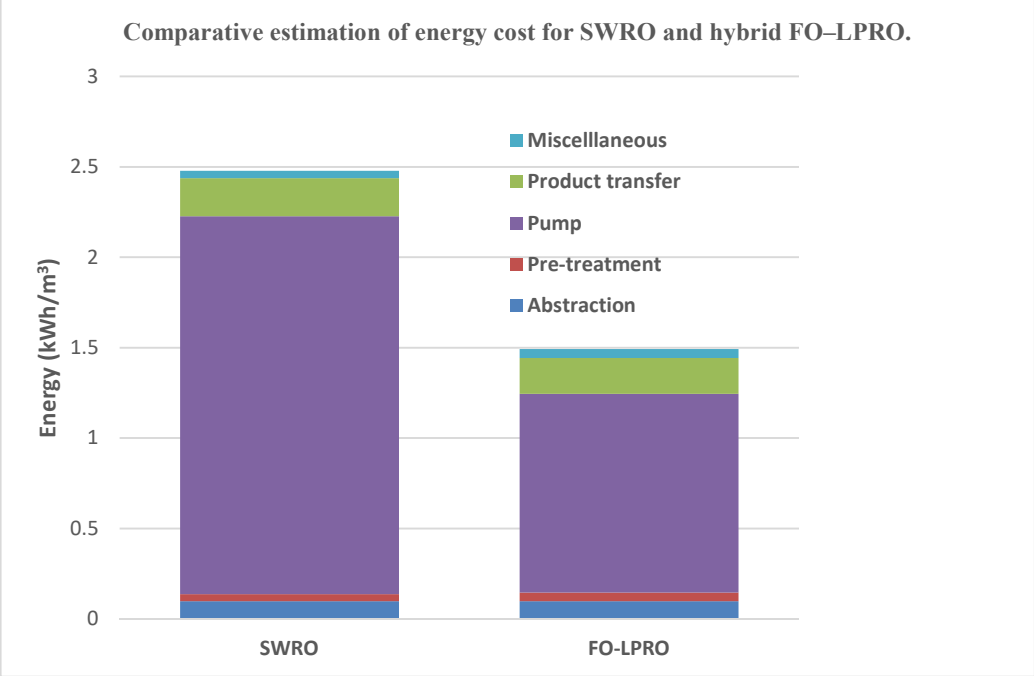

Figure 2-24: Power consumption for SWRO and FO-LPRO (adapted from Checkli et al., 2016)

Figure 2-25 shows another possible configuration for treating impaired wastewater and seawater simultaneously.

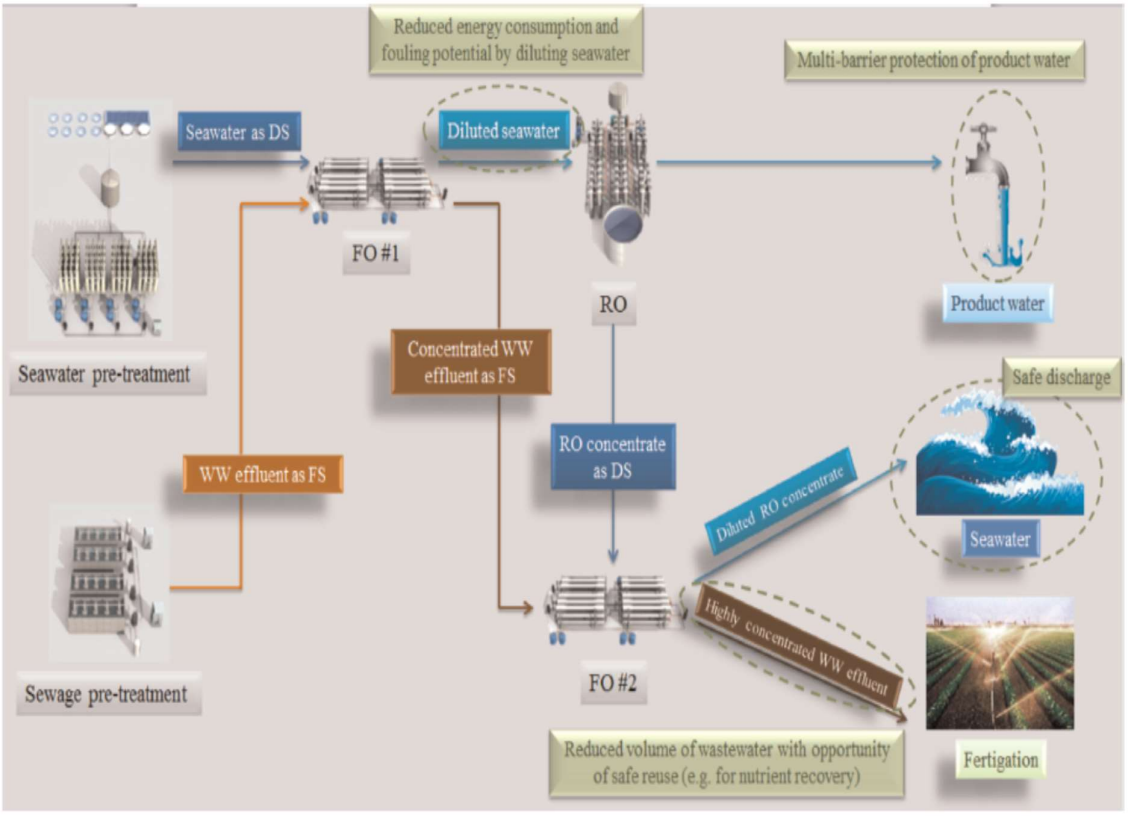

Figure 2-25: Simultaneous treatment of impaired wastewater and seawater using a combination of FO and RO technology (Checkli et al., 2016). Reprinted with permission from Elsevier)

In this system, the impaired water was used as feedwater to the first FO process, and seawater was used as a draw solution which was then diluted through osmotic dilution and become feed to SWRO which then produce potable water. The brine from the first FO was treated in the second FO process using the concentrate from the SWRO as a draw solution. The diluted SWRO brine can be reused or pumped to the sea. The concentrated wastewater can be further treated to recover nutrients for reuse as fertiliser. When compared to conventional SWRO, this hybrid system was estimated to achieve favourable economics, with recoveries as high as 63% compared to 50% for traditional SWRO.

The hybrid system's advantages include:

- Forward Osmosis step operates in the osmotic dilution mode and as a result, draw solution re-concentration step is not required, which eliminates energy associated withdraw solution re-concentration.
- Reduction in the OPEX associated with energy because of the dilution of seawater through osmotic dilution before SWRO.
- Reduction in the SWRO process fouling propensity because of the FO technology pre-treatment.
- The use of the FO and RO process guarantees treated water quality that meets the required specification.
- The hybrid system offers an opportunity for wastewater reuse, and this is important in water-scarce countries.

Checkli et al. (2016) have compiled a list of potential advantages of the researched hybrid FO systems and challenges that need to be overcome for the hybrid system to achieve commercialisation (Refer to Figure 2-26).

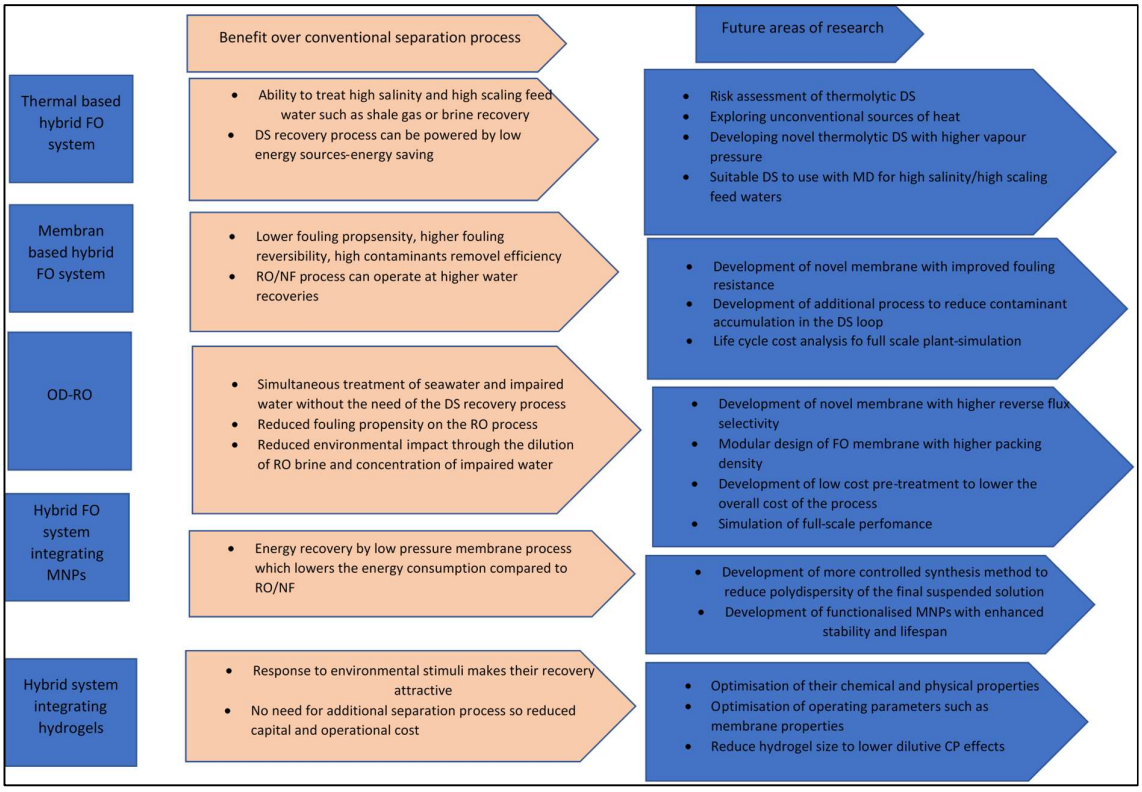

Figure 2-26: A list of potential advantages of the researched hybrid FO systems and challenges that need to be overcome for the hybrid system to achieve commercialisation (adapted from Checkli et al., 2016)

It is evident from the discussion that the FO technology has vast potential application areas which range from osmotic dilution, water reuse, fertigation, direct desalination, treatment of high salinity brines etc. Korak and Arias-Paic (2015) reviewed some of the applications discussed in this section and provided a summary of their likelihood for future implementation. According to this review, FO technology is more viable for:

- Highly fouling and scaling brines where other technologies cannot perform (e.g. technologies such as conventional RO and Thermal evaporators)
- Highly saline solutions where other desalination technologies cannot operate (e.g. standard RO)
- Applications where tight water specification for reuse is required, especially for water-scarce countries
- Applications that do not require draw solution (e.g. fertigation as discussed in this section)
- In cases where osmotic dilution of a concentrated feedwater stream with a low TDS feedwater stream for further desalination is required, as explained in this section
- Lowering the capital & operating cost of zero liquid discharge (ZLD)

2.1.3 Concluding Remarks on Forward Osmosis Literature Review

The lack of an appropriate draw solution and an appropriate membrane remains one of the Achilles heels for the advancement or broad commercialization of FO technology. As discussed in this chapter, previous studies had proposed the use of many different draw solutions; however, previous applications of the FO process were hindered by the unavailability of fit for purpose draw solution which can generate high driving force, and easy to recover. Furthermore, the specific reverse salt diffusion in FO remains a major threat to the technology as it impacts on draw solution replenishment cost. Ammonium bicarbonate, which is one of the potential draw solutions for FO processes due to its high solubility, high osmotic pressure, and recoverability (distillation), has been found to have a high specific reverse salt diffusion. The specific reverse salt flux reported in the literature for this draw solution provides a unique challenge on the sustainable use of this draw solution. As an example, one study showed that for every one litre of water that permeates through the CTA membrane to the draw solution, 2 900 mg of NH_4HCO_3 is lost from the draw solution tank. This amount of draw solution salts will transfer to the feed solution with possible negative implications for downstream processes and could require replenishment to maintain operating conditions in the FO process. In case of feed solution containing scale-forming ions (e.g. Ba^{2+}, Ca^{2+}, Sr^{2+}, Mg^{2+}, Al^{3+}) fouling occurs on the FO membrane surface because of the concentration of the feedwater beyond solubility limits sparingly soluble compounds such as calcium carbonate, calcium sulphate, strontium sulphate. It is, therefore, essential to consider the specific application before selecting an appropriate draw solution. Specific reverse salt diffusion has a significant implication on the sustainable operation of the FO process.

This literature review also reveals that another limiting feature of FO technology is an appropriate FO membrane. There is a distinct difference between the membranes used for the FO process when compared to that used for the conventional RO process, specifically with respect to the supporting layer. The majority of the studies discussed in this review were conducted using CTA-HTI membranes. Recent studies by some authors showed that a thin film composite FO membrane manufactured by Oasys Water Inc and HTI (commercialized) could be a better alternative when compared to the first-generation CTA-HTI membrane (commercialized). The TFC membranes, however, have shown high reverse salt flux when evaluated. A fit for purpose FO membrane should have high-density active layer to achieve high salt rejection or low salt passage; a thin membrane support layer to minimise ICP (leading to high achievable fluxes); membrane integrity cannot be compromised by the selected draw solution; membrane should be hydrophilic to enhance flux and reduce membrane fouling; resistance to various pH values; and high mechanical strength.

The lack of many full- scale applications could be attributed to the two challenges still facing this technology (i.e. fit for purpose draw solution and membrane). If a breakthrough on these two challenges is achieved, there will be a sudden move from FO process research to a full- scale applications.

The desirable membrane should have the characteristics of high-water permeability and selectivity (low specific reverse solute flux), minimized ICP, high mechanical strength, and stability. The ideal draw solution, on the other hand, should be able to induce high osmotic pressure, easy to regenerate (regeneration must be economical), zero toxicity and compatible with the membranes and minimal reverse diffusion across the FO membrane.

In terms of full-scale application, the most notable full-scale application is Modern Water plants in Oman treating seawater as well as Oasys Water MBC plants in China (Changxing FGD wastewater treatment). The lack of industrial track record for the emerging processes has been identified as a significant hindrance to mass adoption of these technologies (Woode, 2015). Although numerous bench-scale and pilot-scale evaluations have been completed over the years in support of continuous development of an FO process, the number of full-scale applications is still few and far between.

This literature review provided focus area for further research in support of the development of the FO technology. Despite the advances that have been made in the advancement of the FO technology which led to the commercialization of the technology as shown by case studies discussed in this literature review, there are still two key technical issues identified that need to be addressed. The lack of an ideal membrane and an ideal draw solution is hampering the development of the FO technology. The literature review also showed versatility of the FO technology as the technology can be used in various applications (fertigation, wastewater reclamation, brine concentration, seawater desalination etc.)

2.2 Chemical Speciation

This section provides an overview of chemical speciation, a review of chemical speciation modelling and practical applications of chemical speciation. Furthermore, the concepts around dissolution, precipitation and saturation are covered together with the common minerals found in water treatment systems.

2.2.1 Introduction

Chemical speciation is generally defined as the distribution of an element amongst chemical species in a system. Analytical methods solely cannot be used to determine a speciation analysis as analytical methods detect free metal and total ion concentrations (VanBriesen et al., 2010). Levels of most metals of interest cannot be measured directly using analytical methods because their concentrations in the solutions are low. Data from these analytical techniques, therefore, cannot be used to determine overall speciation (VanBriesen et al., 2010). It is, therefore, for these reasons that chemical speciation models and analytical techniques are used for chemical speciation determination.

Thermodynamic and transport properties of electrolyte solutions are essential for a variety of industrial applications (e.g. chemical process industry, petrochemical industry, etc.). Electrolyte solutions from real industrial systems are complex to understand and predict as they contain many components and the systems are operating over a wide range of concentration, pressure and temperature. Electrolyte models make it possible for engineers and scientists to improve plant design, troubleshoot and optimisation (Anderko et al., 2002).

Electrolytes solutions are involved in numerous processes, including (Anderko et al., 2002):

- Treatment of gas, treatment of wastewater or disposal of chemical waste;
- Crystallisation, distillation, desalination bio-separation etc.
- Corrosion and electrolysis

These applications require electrolyte models that cover a wide range of chemical composition (aqueous or mixed solvent, dilute or concentrated solution), conditions (ranging from ambient temperature to supercritical conditions), and as a result, continuous development of electrolyte models is therefore essential.

2.2.2 Thermodynamics during Aqueous Chemical Speciation Modelling

Thermodynamics alone is not able to provide information regarding the intermediate states of a reaction. Chemical kinetics, which predicts reaction rates and the mechanism is, however, able to provide intermediate states on the reaction.

In general, chemical kinetics predicts the type of chemicals which are present in the system, while thermodynamics only predicts the limits of distribution of those chemicals in the different phases. The design and analysis of industrial systems typically involve simulating a steady-state process which is achieved by modelling its thermodynamic equilibrium to optimise the operating conditions of the process or system of interest. Speciation models generally depend on mass balance and thermodynamics to predict the concentration of each species that contain a given component. Thermodynamics expressions are employed in predicting because reactions take place in the bulk solution and are generally quick in nature. The aqueous-based reactions are assumed to reach equilibrium because they are reversible and fast when compared to other systems, as stated in the local equilibrium assumption (LEA) (VanBriesen et al., 2010). The LEA, however, does not consider kinetics and for some system, reaction kinetics are vital in predicting chemical speciation. The LEA shortcomings are addressed by incorporating reaction kinetics into the thermodynamically based models.

Several excellent reviews of electrolyte solution models are available in the literature. Empirical and semi-empirical models were reviewed by Zematis et al. (1986), Renon (1986), Pitzer (1991) and Loehe and Donohue (1997). Theoretical fundamentals were reviewed by Friedman (1981) and Conway et al. (1983).

Speciation models predict activities, activity coefficient, and concentrations of individual species. The models rely on the input values for the total concentration of the chemical components present in the system of interest. Analytical methods such as atomic absorption (AA) and ion chromatography which are used in the characterisation of solutions provide total concentrations of the components in the solution. The analytical techniques give the total concentration of the components, and the chemical speciation models use these data as input to predict activities of individual species.

The relationship between solute activity (a) and concentration is through the single-ion activity coefficient ($\boldsymbol{\gamma}$) as shown in equation 2-5 below.

Equation 2-5

$$\boldsymbol{a_i = \gamma_i m_i \; or \; a_i = \gamma_i M_i}$$

Where a_i represent the activity of a species, m_i represent the molality of the species, and M_i represent the molarity of the species.

2.2.2.1 Prediction of Activity Coefficients

Theoretical approaches are used to describe the connection between activity and concentrations under various chemistry conditions (namely, the ion-association or the specific ion-interaction concepts). These approaches are discussed in the sections below.

2.2.2.1.1 Ion-association theory

In the ion-association theory, activity coefficients based on Debye- Hückel equations are used to relate aqueous activities to concentrations of the solution.

The underlying assumptions introduced in the development of the theory are as follows (Haghtalab, 1990):

- Anions and cations exist in the electrolyte solution
- Ions are regarded as charged hard spheres, and the solvent is replaced by a dielectric continuum with dielectric constant, D, through the whole medium.
- Long-range electrostatic interactions are considered, and short-range interactions between water molecules and ionic species are not considered for the calculation.
- The solution is considered as a collection of central ions with their respective ion cloud.
- Boltzmann distribution form is assumed for the cloud ions around the central ion.

Peter Debye and Erich Hückel developed Debye Huckel equation and the limiting law to enable the calculation of activity coefficients of the solutions. Activities are used instead of concentrations in chemical speciation calculations as the behaviour of the solutes in the solution is concentration-dependent and therefore do not always behave in an ideal manner. Activity and concentration are related to each other through a factor known as the activity coefficient (γ) and takes into consideration the energy of ions in the solution.

The Debye- Hückel limiting law enables the determination of the activity coefficient of an ion in a dilute solution of known concentration. The equation is given below:

Equation 2-6

$$\log(\gamma_i) = -AZ_i^2\sqrt{I}$$

Z_i is the charge number of ion species i

A is a constant that depend on the solvent

The Debye-Hückel limiting law is applicable to solutions with low concentration (concentration between 0.005 and 0.01 M range).

In dilute solutions (i.e. ionic strength I < 0.1 M), the activity of the ions is influenced by long-range electrostatic forces between ions. The ions are assumed to be separated enough such that only ions and the solvent interact. The effects of these forces on the activity coefficient are adequately described by extended Debye-Hückel (D-H) (Long Range Term) as shown in equation 2-7 below:

Equation 2-7

$$\boldsymbol{log\gamma_i = -AZ_i^2 \frac{\sqrt{I}}{1 + Ba\sqrt{I}}}$$

Where γ_i represents the activity coefficient, Z_i represents the charge number of the ion, A and B are the constants determined by the obsolete temperature and dielectric constant of the system, 'a' represents an adjustable size parameter corresponding crudely to the radius of the hydrated ion, and I represents the ionic strength of the solution. The ionic strength of the solution is represented by the equation below:

Equation 2-8

$$\boldsymbol{I = \frac{1}{2}\sum_i m_i z_i^2}$$

The D-H theory, however, becomes less accurate at ionic strength, greater than 0.1 molal. As it can be seen from D-H equation, activity coefficients approach unity when ionic strength near-zero (Bethke, 1996). Increasing ionic strength of the solution results in the monotonically decrease in activity coefficient as shown in Figure 2-27

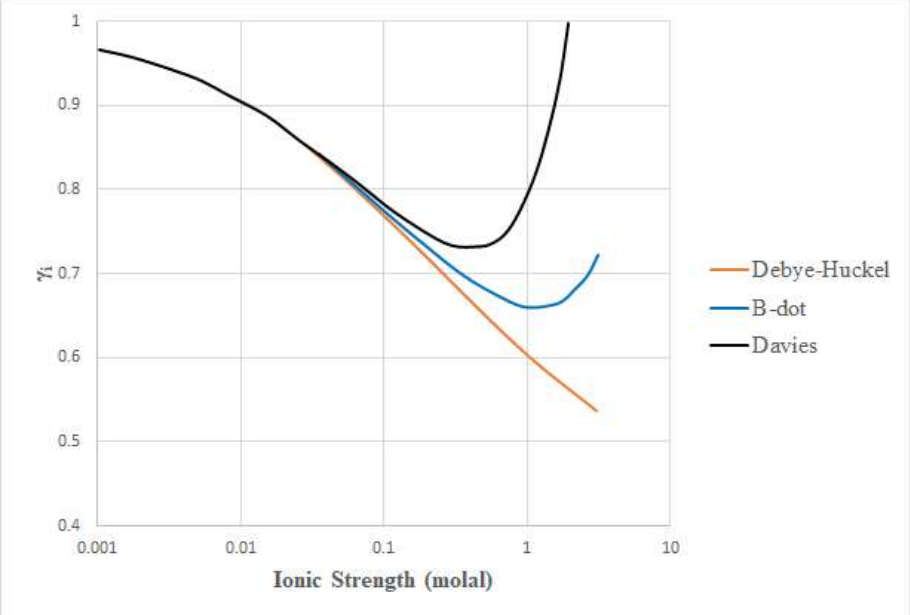

Figure 2-27: Relationship between activity coefficient and ionic strength of a solution as defined by Derby-Hückel and Davis equations (adapted from Bethke, 1996).

Dotted line shows the Davis equation evaluated with a coefficient of 0.2 instead of 0.3 (Bethke, 1996). The B-dot represent the B-dot equation developed by Helgeson for electrically charged species (Helgeson, 1969).

Various empirical and semi-empirical expressions were suggested to improve the applicability of the D-H equation to higher ionic strength solutions. This was achieved by the inclusion of the Davies equation as in the equation below:

Equation 2-9

$$log\gamma_i = -AZ_i^2\left(\frac{I^{\frac{1}{2}}}{1+I^{\frac{1}{2}}} - 0.3I\right)$$

The Davies equation can be applied to higher ionic strengths. As can be seen in Figure 2-30, there is no monotonically decrease of activity coefficient with ionic strength when the Davies equation is used, which is contrary to what was observed with D-H equation. The Davies equation is regarded as accurate to an ionic strength of about 0.5 molal.

2.2.2.1.2 Specific ion-interaction theory

Apart from the ion-association theory, specific ion-interaction theory is another model available to explain how ions interact in the aqueous solutions. According to this theory, at higher concentrations (ionic strengths), ions complexations is impacted by both the long and short-range forces.
Kenneth Pitzer expanded the Debye-Hückel equation in the 1970s and came up with Virial equations, known as Pitzer equations, to include the effect of both long and short-range forces (Pitzer, 1973, 1977, 1979).

The Pitzer equations are preferred because they can be used in solutions with high ionic strength. These equations, however, do not account for the distribution of species in solution. The equations only recognise free ions, by assuming full dissociation in the solution. The virial methods are related to the solution's excess free energy Gex (i.e. the free energy over that in an ideal solution) as shown in equation 2-10 below.

Equation 2-10

$$\frac{G_{ex}}{RT} = n_w \left[f(I) + \sum_i \sum_j \lambda_{ij}(I) m_i m_j + \sum_i \sum_j \sum_k \mu_{ijk} m_i m_j m_k \right]$$

Where:
i, j, and k = represent different components in the solution.
f = represent a function of ionic strength as it was the case in the Debye–Hückel equation
λij and μijk = represents second and third virial coefficients. These coefficients account for short-range interactions among the ions. The second virial coefficient is affected by the ionic strengths of the solutions, whereas the third virial coefficients are independent of the ionic strengths

The assumption from equation 2-11 is based on the premises that for the short-range interaction, firstly, the ions in the solutions interacts with each other in addition to interacting with the solvent. Ion activity coefficients γ_i expression is derived by differentiating Equation 2-10

Equation 2-11

$$ln\gamma_i = ln\gamma_i^{dh} + \sum_j D_{ij}(I) m_j + \sum_j \sum_k E_{ijk} m_j m_k) + \cdots$$

Equation 2-11 was named Pitzer equation as it was developed by Kenneth Pitzer (Bethke, 1996).

Where:

First term represents the Debye–Hückel activity coefficient

Xj represents molar concentration of the species j

The second virial coefficient Dij represent specific interaction among pairs of ions

The third virial coefficient represents specific interaction among three ions and so on

Empirical data is used in the ion-interaction theory to take into consideration ion pairing and complex formation. The theory achieves this by using empirically derived virial coefficients to describe the change in free-ion activity. The ion-interaction model it can, therefore, be used in calculating activity coefficients at high-ionic and low strength which makes it superior to the ion association model. The ion-interaction model can compute the activities of many electrolytes at an ionic strength of up to 20 M and temperatures up to 250°C.

The specific ion-interaction theory, however, does have some drawbacks which limit its applicability, such as the unavailability of the values required for Pitzer equation, unavailability of solubility data at high pressures and temperatures, and limited application to predict other reactions other than solubility. Equation 2-12 below shows a proposed equation for the mean ionic activity coefficient of an electrolyte that consists of cation *c* and anion *a*, which is shown in Equation 2-12

Equation 2-12

$$ln\lambda_{\mp ca} = (ln\gamma_{\mp ca})_{DH} + \frac{2\nu_+}{\nu_+ + \nu_-}\sum_{á} B_{cá} m_{á} + \frac{2\nu_-}{\nu_+ + \nu_-}\sum_{ć} B_{ća} m_{ć}$$

Where:

$B_{ca'}$ and $B_{c'a}$ are the specific ion-interaction coefficients that express the contribution of the short-range interactions

Bromley proposed an empirical model for the single strong electrolyte solutions with ionic strength up to 6 M. The model has one adjustable parameter, which is correlated to two cationic and anionic parameters with a cation-anion combination (Haghtalab, 1990). The proposed equation is in the following form:

Equation 2-13

$$log\lambda_{\mp} = (log\lambda_{\mp})_{DH} + B_{12}I$$

Where

Equation 2-14

$$B_{12} = \frac{(0.06 + 0.6B)|Z^+Z^-|}{(1 + \frac{1.5}{|Z^+Z^-|})^2} + B$$

and B is the only adjustable parameter.

Meissner and Kusik (1972) proposed a method where they defined a quantity Γ, the reduced activity coefficient as:

Equation 2-15

$$\Gamma = \lambda_{\mp}^{\frac{1}{|Z^+Z^-|}}$$

The model proposed by Meissner and Kusik is applicable for temperatures higher than 25°C and can fit the mean activity coefficient data up to the ionic strength of 6 M.

The Debye–Hückel theory presented in 1923 paved the way for modelling electrolytes by accounting for the electrostatic forces present in aqueous solutions. Many aqueous electrolyte thermodynamic models based on the Debye–Hückel theory have been developed since with most models containing adjustable interactions parameters to fine-tune their analytical approach, as demonstrated in the above discussion.

Electrolyte activity is challenging to model due to the various interaction forces present between the differently charged and differently sized molecules. Having a clear objective is essential when selecting the appropriate model to simulate the activity of electrolyte solutions. The suitable model is selected based on its validity range, interaction mode characterisation, interaction parameters availability and mathematical complexity. Also, some models can only express the activity of ionic species and do not include expressions for water or molecular species.

OLI has developed a software called OLI Stream Analyser that is used to simulate and predict electrolyte systems. The software is based on complete speciation; robust standard framework; activity coefficients for complex, high ionic strength streams; comprehensive database which covers inorganic elements, associated compounds and complexes; a database that includes extensive list of organic compounds (Scribd, 2008; support.olisystem.com, 2006; Sandler, 1994):

The OLI thermodynamic framework (OLI Stream Analyser 3.2 software) was used in this dissertation to predict the chemical speciation and osmotic pressure of the draw solution and brine streams. The advantage of this software is that the software does thermodynamic calculations based on empirically derived data and simulate thermodynamic properties over a wide range (temperature and concentration). The next section gives a brief description of the OLI thermodynamic framework.

2.3 OLI Thermodynamic Framework

It is vital to understand aqueous thermodynamics when modelling electrolyte systems. In this section, a brief discussion on aqueous solutions thermodynamic framework is given. The standard state equation is central to OLI Stream Analyser software (support.olisystem.com, 2006; scribd, 2008).

Equation 2-16

$$\Delta_R\overline{G^0} = -RTlnK$$

Where:

$\Delta_R\overline{G^0}$ represents partial molal, standard-state Gibbs free energy of reaction.

R represents Gas Constant (8.314 J/mole/K)

T represents temperature (Kelvin)

K represents equilibrium constant

The total free energy ($\Delta_R G$) is defined as:

Equation 2-17

$$\Delta_R\overline{G} = \sum_i v_i\Delta_f\overline{G_i}\ (products) - \sum_i v_i\Delta_f\overline{G_i}\ (reactants)$$

Where:

vi represents stoichiometric coefficient

$\Delta_f\overline{G_i}$ represents Gibbs Free Energy of formation for a species i

The following thermodynamics properties are essential for OLI thermodynamic framework: partial molal Gibbs free energy, partial molal enthalpy, partial molal entropy, partial molal heat capacity and lastly, partial molal volume.

There are in general two parts to each of these properties, namely, standard state part (a function of temperature and pressure), symbolised by 0 and excess part (a function of temperature, pressure and concentration), symbolised by E.

Partial Molal Gibbs free energy

Equation 2-18

$$\overline{G_i} = \overline{G_i^o} + \overline{G_i^E}$$

Partial Molal Enthalpy

Equation 2-19

$$\overline{H_i} = \overline{H_i^o} + \overline{H_i^E}$$

Partial Molal Entropy

Equation 2-20

$$\overline{S_i} = \overline{S_i^o} + \overline{S_i^E}$$

Partial Molal Heat Capacity

Equation 2-21

$$\overline{Cp_i} = \overline{Cp_i^o} + \overline{Cp_i^E}$$

Partial Molal Volume

Equation 2-22

$$\overline{V_i} = \overline{V_i^o} + \overline{V_i^E}$$

The standard state terms are based on Helgeson framework, whereas the excess terms are based on Bromley, Zemaitis, Pitzer, Debye-Hückel framework. These frameworks are incorporated into the OLI software.

The OLI model is based on the work of Harold Helgeson and co-workers. According to Helgeson et al. (1981), the standard-state thermodynamic property of any species in an aqueous solution can be expressed by an equation with seven terms which have a specific value for each species. The specific equations for the five principal standard state terms are discussed in detail elsewhere (Helgeson and Kirkham, 1974a, 1974b, 1976; Helgeson et al., 1981; Tanger, 1986; Sandler, 1994); however, a general description is shown below:

Equation 2-23

$$\boldsymbol{G^o = G(T, P, \omega, c1, c2, a1, a2, a3, a4)}$$

Equation 2-24

$$\boldsymbol{H^o = H(T, P, \omega, c1, c2, a1, a2, a3, a4)}$$

Equation 2-25

$$\boldsymbol{S^o = S(T, P, \omega, c1, c2, a1, a2, a3, a4)}$$

Equation 2-26

$$\boldsymbol{Cp^o = Cp(T, P, \omega, c1, c2, a1, a2, a3, a4)}$$

Equation 2-27

$$\boldsymbol{V^o = V(T, P, \omega, c1, c2, a1, a2, a3, a4)}$$

Parameters (a1 to a4, c1 to c2, and ω) presented in equation 2.23 to 2.27 represents the equation of state coefficients that are unique to each species, according to Helgeson et al. (1981).

° represents standard state property

a1 to a4 represents the pressure effects

c1 to c2 represents the temperature effects

Coefficients a1 to a4 are regarded as negligible unless if the pressure is above 100 bar. OLI database has values for these coefficients for any species in aqueous solution. For any constituent species in a reaction, equilibrium constants depend entirely on individual constituent species G° values. OLI software can predict these G° values, and as a result, it can predict any equilibrium constant.

This fully predictive framework for standard state properties addresses challenges associated with predicting chemical speciation using the activity coefficients.

As discussed earlier, the excess terms are based on Bromley, Zemaitis, Pitzer, Debye-Hückel framework. The activity coefficients of ions in the OLI software has the following equation:

Equation 2-28

$$\boldsymbol{\lambda = DH(I) + BZ(I,T,m)}$$

Where:
DH represents Debye- Hückel term (function of ionic strength)
BZ represents Bromley-Zemaitis term (function of ionic strength, temperature, and molality)
I represents the ionic strength of the solutions
The DH term describes the activity coefficient for very dilute systems.

The Bromley-Zemaitis activity model equation is shown below:

Equation 2-29

$$\boldsymbol{Log\lambda_{\mp} = \frac{-A|Z^{+}Z^{-}|\sqrt{I}}{1+\sqrt{I}} + \frac{(0.06+0.6B)|Z^{+}Z^{-}|\sqrt{I}}{(1+\frac{1.5}{|Z^{+}Z^{-}|\sqrt{I}})^{2}} + BI + CI^{2} + DI^{3}}$$

The B, C, and D terms shown in equation 2-29 have the following temperature functionality.

Equation 2-30

$$\boldsymbol{B = B_1 + B_2T + B_3T^2}$$

Equation 2-31

$$\boldsymbol{C = C_1 + C_2T + C_3T^2}$$

Equation 2-32

$$\boldsymbol{D = D_1 + D_2T + D_3T^2}$$

2.4 Concept of Precipitation, Dissolution and Saturation

Precipitation and dissolution concept regulate the amounts of each solid phase that are present in a given solution. A solution is deemed to be saturated with a compound (e.g. calcium sulphate, strontium sulphate, barium sulphate, magnesium hydroxide) if the solution neither precipitate the compound nor dissolve any of the solid formed if left undisturbed, under unchanging conditions, for an unlimited amount of time (Ferguson, Ferguson and Stancavage, 2011). Such a system is said to be at equilibrium for that particular compound. The amount of compound that can be dissolved in water and remain in solution is expressed by the solubility product (Ksp) (Ferguson, Ferguson and Stancavage, 2011)

For the generalised dissolution reaction:

Equation 2-33

$$M_mA_n\,(_s) = mM + nA$$

[M_mA_n (s)] = {M_mA_n (s)} = 1 by convention, assuming that M_mA_n (s) is a pure solid phase.
The *ion activity product* (IAP) is given by:

Equation 2-34

$$IAP = \{M\}_m\{A\}_n = \gamma_{M\,m}[M]_m\gamma_{An}[A]_n$$

At equilibrium IAP =Ksp

Equation 2-35

$$([M]_m[A]_n)(\gamma_{M\,m}\gamma_{An}) = K_{sp}$$

The relationship between the IAP and Ksp is defined as follows (Ferguson, Ferguson and Stancavage, 2011):

- If IAP<Ksp, the solution tends to dissolve the compound of interest and is said to be undersaturated with that compound.
- If IAP=Ksp, the solution neither precipitate nor dissolve the compound and the solution is said to be at equilibrium with a compound.
- If IAP>Ksp, the solution tends to precipitate the compound and the solution is said to be supersaturated with a compound.

The index called Saturation Level, Degree of Supersaturation, Scaling tendency (as defined in OLI) describe the degree of saturation as a ratio of ionic activity product to solubility product (Scribd, 2011; support.olisystem.com, 2006 and Ferguson, Ferguson and Stancavage, 2011).

Equation 2-36

$$Scaling\ \frac{Tendency}{Saturation}\ Level\ = \frac{IAP}{Ksp}$$

The *saturation index* (SI) is defined as below.

Equation 2-37

$$SI\ = \log\left(\frac{IAP}{Ksp}\right)$$

- When SI < 0, the solution is said to be undersaturated with respect to the compound of interest
- When SI > 0, the solution is said to be oversaturated with respect to the compound of interest
- When SI = 0, the solution is said to be at equilibrium with respect to the compound of interest

The saturation index of the solution can either be ≤ 0 at equilibrium conditions. In this situation, the mineral of interest is either not present in the solution or present but no precipitation or dissolution. On the other hand, when the saturation index is > 0, the equilibrium shifts towards the formation of the

mineral of interest. In a case where the mineral has already formed, and saturation index becomes < 0, the solution is no longer at equilibrium as the mineral already formed can dissolve.

2.4.1 Mechanism of Precipitation

Precipitation is the formation of one or more new phases of composition different from that of the original multicomponent single-phased system. From a fundamental point of view, the precipitation process follows five stages: supersaturation, nucleation, induction time, crystal growth and aging. The stages of a precipitation process are presented in Figure 2-28.

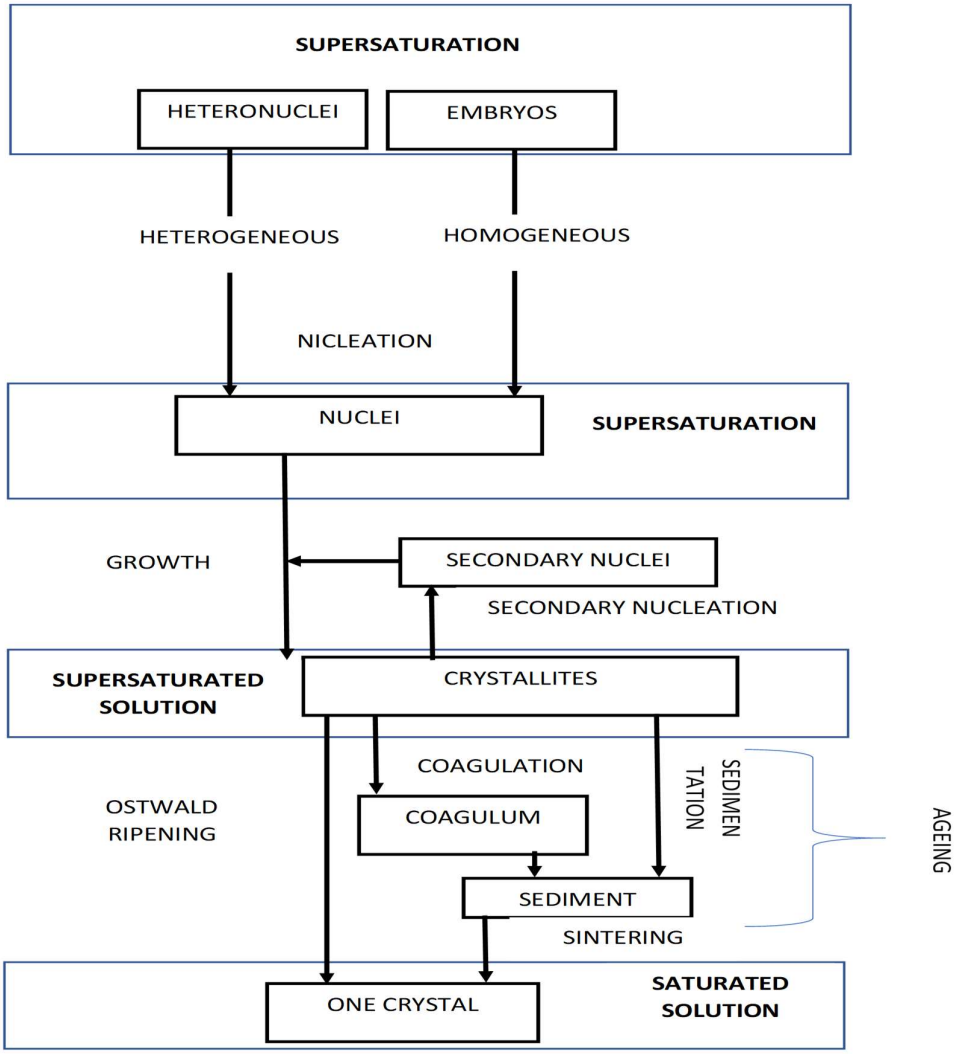

Figure 2-28: Stages of precipitation process (Adapted from Nielsen, 1970)

Precipitation starts with nucleation on impurity particles (or seeds), or with the formation of embryos. The nuclei grow into visible crystallites. Sometimes the growth process is accompanied by the formation of new (secondary) nuclei so that crystallites of two or more size groups are present. The crystallites may form a stable suspension, or they may coagulate. When the crystallites or the coagulated clusters in a liquid become larger, they tend to sediment. This is the last step of the precipitation process, and the growth of the individual particles seems to have ceased. But if the system is observed for a very long time the smaller crystallites redissolve and the larger ones grow further. Thermodynamically the system is not stable until all the solute in excess of the amount corresponding to the solubility is united into a single crystal.

2.4.1.1 Supersaturation

Precipitation is not possible unless the solution is supersaturated. A saturated solution can be made supersaturated by temperature change or by fractionation through evaporation or crystallization of the solvent. Another way of making a supersaturated solution is to mix two solutions or liquids which react chemically (e.g. electrolyte precipitation from aqueous solution) or otherwise (salting out; addition of a poor solvent to a solution in a good solvent).

Supersaturation may result from several conditions:

- Heating/Cooling-Cooling a standard solubility salt solution or heating an inverse solubility salt solution may result in supersaturation.
- Water Evaporation-The solution becomes more concentrated when water is removed through evaporation. After a sufficient period, the solution begins to be saturated and then supersaturated.
- Solution Mixing-The solubility limit may be exceeded when a soluble salt is added to a solution of another salt, which have common ion or produces a sparingly soluble salt. This supersaturation condition is reached when the ionic product becomes higher than the solubility constant.
- Mixing of saturated or near-saturated solutions due to the change of solubility with temperature, the mixing of saturated or near-saturated solutions may also result in supersaturation conditions.
- Gas/Liquid Equilibria-Equilibrium conditions of carbon dioxide dissolved from atmosphere air could influence the solubility of related ions such as calcium.

2.4.1.2 Nucleation

Nucleation is defined as the process in which the smallest stable aggregates of a crystalline phase are formed in a crystallizing system. Nucleation is the initial stage of scale formation, occurring with minimum supersaturation of the scale-forming compound established in the liquid layer adjacent to the exposed surface. There are two types of nucleation mechanisms that are recognized, namely, heterogeneous and homogeneous nucleation. Primary nucleation occurs in systems that do not contain crystalline matter. The condition for crystals to be able to grow is the existence of tiny solid particles, either being foreign bodies or crystallites spontaneously formed from solution. The former is referred to as heterogeneous nucleation and the latter is referred to as homogeneous nucleation. On the other hand, if the nuclei are generated in the vicinity of existing crystals, this is referred to as secondary nucleation. Figure 2-28 illustrates these types of nucleation.

2.4.1.3 Induction Period

Induction period is the period of time that elapses between the point supersaturation is achieved and a precipitate is first detected. It is controlled by many factors such as the degree of supersaturation, temperature, the mixing intensity, and the presence of impurities (or inhibitors). The significance of the induction time period is difficult to analyze although undoubtedly it is related to the kinetics of nucleation. A measured induction period time is comprised of three different components: the time necessary to achieve a quasi-steady-state distribution of the embryos; the time necessary to form nuclei; and the time necessary for nuclei to grow to experimentally detectable dimensions (Melia, 1965). Induction time is controlled by factors such as degree of supersaturation, the temperature of the solution, mixing, pH, flow velocity, intensity and the presence of impurities (or inhibitors). It is related to the kinetics of nucleation

2.4.1.4 Crystal growth

The stable nuclei, which are particles larger than the critical size, begin to grow into crystals of visible size as soon as they have been formed in a supersaturation system. This process is explained by several theories: surface energy theory, adsorption layer theory, kinematic theory, and diffusion-reaction theory. These theories have been covered extensively in the literature (Nielsen, 1970, Amjad and Demandis, 2015). Crystals grow by the continued addition of one layer of molecular units on another._ The units arrive at the crystal surface by diffusion, sometimes aided by convection, and are fitted to the crystal lattice. The details of adsorption of the units, and of their finding the right place and orientation, are not accurately known.

2.4.1.5 Aging

The contribution of the interfacial tension to the Gibbs free energy is proportional to the interfacial area. Therefore, the system cannot be deemed stable until the interfacial area is as small as possible. The

decrease of the interfacial area of a precipitate is called aging. In this stage, the scale texture changes to a more compact structure. The condition for permanent scale to develop is that there is a favourable combination of surface material, roughness, and hydrodynamics near the surface ensuring the crystals formed on a surface to remain attached to it, even when they are growing to a large size. Poor adhesion allows large crystals to be washed from the surface by the liquid stream and a coherent layer of scale covering the whole surface cannot develop.

The aging process takes place through (i) recrystallization of the primary particles, transforming e. g. needles, thin plates or dendrites into a more compact shape by surface wandering of adsorbed molecular units or by transport through the mother liquid, (ii) transformation of a crystal from a metastable modification into a stable modification by dissolution and reprecipitation, (iii) aggregation of primary particles followed by sintering (intergrowth) and (iv) Ostwald ripening, i. e., growth of the larger particles at the expense of the smaller ones (Nielsen, 1970).

For a simple system, with only the reactants present such as calcium and carbonate, precipitation and scale formation might proceed as illustrated in Figure 2-29 below (representation of the most important steps in the pathway from soluble ions to a macroscopic calcium carbonate scale deposit):

- Cationic and Anionic species such as Ca^{+2} and CO_3^{-2} collide to form ion pairs in the solution which subsequently form micro-aggregates (Supersaturation)
- Induction Time
- Micro-aggregates go on to become nucleation centres for crystallisation (Nucleation)
- Microcrystals are formed in the solution which agglomerate and adsorb to the surfaces to grow into larger microcrystals which ultimately deposit on the surface (Crystal growth and deposition)

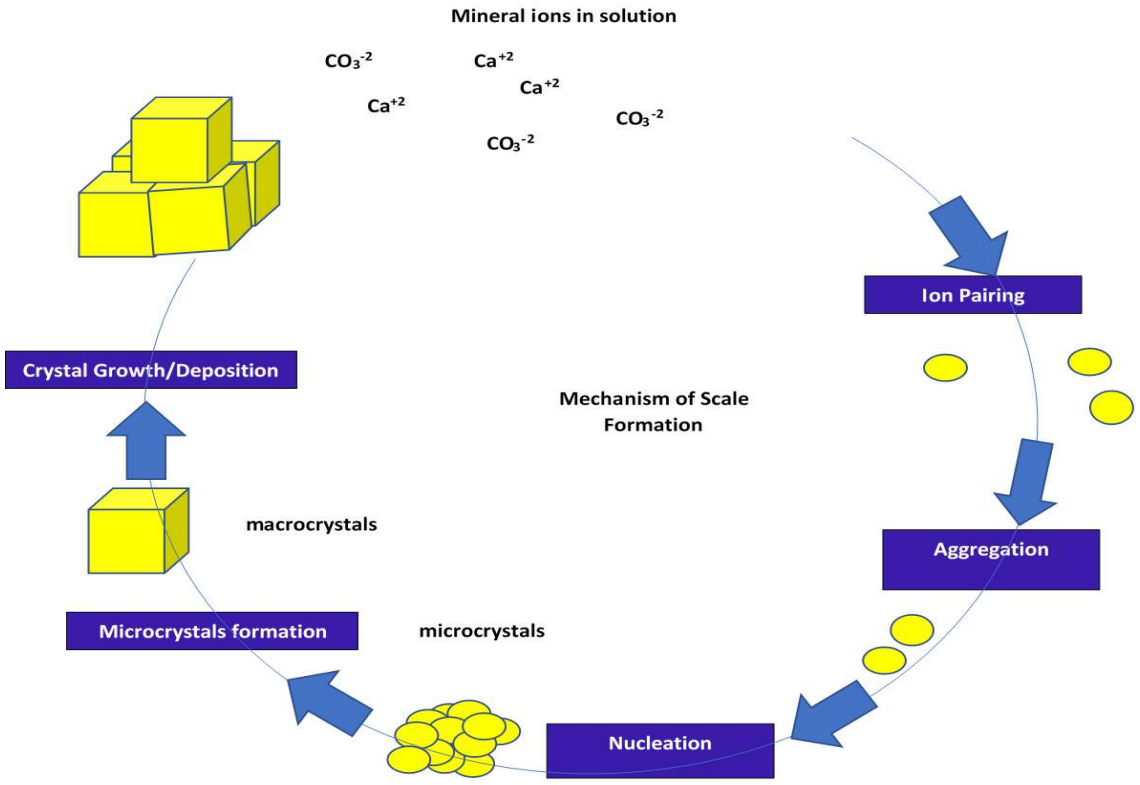

Figure 2-29: Schematic representation of the most important steps in the overall process of precipitation and deposition (adapted from Amjad and Demandis, 2015)

2.4.2 Common Minerals in Water Treatment Systems.

Table 2-5 on page 73 shows a summary of common components that precipitate from the water system

The most common components that precipitate from the water system and subsequently causing scaling or fouling are the carbonates and sulphates of calcium and magnesium. Other components include barium salts, strontium salts, silicates, and phosphates. Commonly observed water-formed deposits include calcium carbonate, calcium and barium sulphates, silica scales, iron-based scales, magnesium and calcium phosphates. Desalination is one area where these minerals cause issues during membrane desalination (e.g. Reverse Osmosis, Electro Dialysis, Forward osmosis, Nanofiltration) and thermal desalination (e.g. evaporative processes). Scale or fouling in these systems often result in poor water quality, increased operational pressures, increased energy costs, frequent downtime to clean the units, frequent membrane replacement, reduced plant availability, amongst others.

The following minerals are commonly formed under conditions experienced in water treatment processes, such as flocculation, clarification, settling, recarbonation, evaporation, ion exchange and membrane processes.

Table 2-5: Common Minerals in Water Treatment System

Mineral Deposit	Chemical Formula	PPT at amb T and P	Comments on formation	Factors and Conditions Affecting the Formation of Calcium carbonate
Calcium Carbonate (Calcite and Aragonite)	$CaCO_3$	Yes	calcium carbonate can precipitate from a supersaturated solution in a number of different polymorphs and these include calcite with a rhombohedral crystal structure, aragonite with an orthorhombic crystal structure and vaterite, which has hexagonal crystal structure. Each of the polymorphs has a different thermodynamic stability and reactivity and polymorphs may transform or dissolve, or both as the solution composition approaches equilibrium with thermodynamically stable phase. The reported stability products for calcite, aragonite and vaterite are 3.3×10^{-9}, 4.57×10^{-9} and 1.23×10^{-8}, respectively. Calcite is the most thermodynamically stable phase and vaterite the least stable phase at room temperature and under normal atmospheric pressure.	Formation is governed by factors such as temperature and pH. pH however plays a major role when compared to temperature. A pH increase from 7 to 8 was found to have five times the effect on precipitation than temperature change of 70 ^{o}C. Temperature influences the type of polymorphs phase development. Below 30^{o}C calcite is the only polymorph present. Vaterite is the most soluble and calcite the least soluble over a temperature range from 0 to 90 ^{o}C.
Calcium Sulphates (Anhydrite, Hemihydrite and Gypsum)	$CaSO_4$, $CaSO4.0.5H_2O$ and $CaSO_4.2H_2O$	Yes	Calcium Sulphate is one of the most prevalent scale in processes such as desalination (membrane and thermal). Calcium Sulphate exist as anhydrite, hemihydrite and gypsum. All these forms are more soluble than calcium carbonate and magnesium hydroxide. The most common is gypsum.	Formation of gypsum is governed by factors such as temperature, pressure, dissolved electrolytes and organics, and the presence of other minerals. Gypsum is the most formed deposit in membrane desalination and cooling systems where moderate temperatures (up to 50 ^{o}C) are employed, while calcium sulphate hemihydrite and anhydrite are the most common in high temperature applications such as thermal desalination. Calcium Sulphate precipitation is pH independent.
Barium Sulphate	$BaSO_4$	Yes	Not as common as the gypsum. Its precipitation is pH independent. It forms a very hard mineral called barite. Can be found in cooling systems and membrane desalination technologies. It is a problematic mineral to remove if it forms on the membrane surface.	
Magnesium based scales	$Mg(OH)_2$, $MgCO_3$ and $Mg_5(CO_3)_4(OH)_2.4H_20$)	yes	Magnesium scales such as magnesium hydroxide (brucite) ($Mg(OH)_2$, magnesium carbonate (magnesite) ($MgCO_3$), and hydroxymagnesite ($Mg_5(CO_3)_4(OH)_2.4H_2O$) are more common where water is used, especially where seawater is used. The most common magnesium scale is brucite which is also referred to as alkaline scale (like calcite). Other magnesium containing scale is magnesium silicate ($MgSiO_3$) and its hydrated form known as talc.	Formation of magnesium scales is influenced by temperature, pH, concentration of bicarbonate ions, magnesium concentration and total dissolved solids. Supersaturation of brucite depends on pH and occurs at pH above 10. Effect of temperature is significant for magnesium carbonate trihydrate as it mainly occurs at temperatures below 40 ^{o}C. Hydroxymagnesite forms at temperatures between 60 and 90 ^{o}C. Magnesium hydroxide is an inverse solubility salts formed above temperatures 95-100 ^{o}C, mainly due to the increase in hydroxyl ion formation at high temperature.
Silica Scales (Amorphous)	SiO_2	yes	Solubility of amorphous silica ranges from 120 to 150 mg/L, at 25 ^{o}C and pH <8-8.5. it is normaly classified as dissolved (reactive), colloidal (non-reactive), and particulate (suspended) silica. Amorphous silica can deposit on boilers, membranes, and colling towers	Formation of silica scale depend on silica concetration and pH. Solubility of amorphous silica is governed by temperature, pH, and the presence of other ions (aluminium) and organic compounds. The presence of magnesium in the water will lead to the formation of magnesium hydroxide whih subsequently react with silica (dissolved and colloidal) to form magnesium silicate which is hard to remove. Unlike other scales (calcite, gypsum), silica solubility increases with temperature and as a result, silica scale will form in the colder parts of the system. However, magnesium silicate decreases in solubility with increasing temperature, forming a dense scale on surfaces which is very difficult to remove. For membrane systems (brackish water application), aluminium silicates deposit such as clay ($Al_2O_3.SiO_2.xH_2O$, mulite
Iron Scales (magnetite, hematite, friic and ferrous hydroxide, geothite, akaganeite, lepidpcrocite and siderite)	Fe_3O_4; Fe_2O_3; $Fe(OH)_2$; $Fe(OH)_3$; $Fe_2O_3.H2O$; β-FeOOH; γ-FeOOH; $FeCO_3$	yes	Geothite forms under oxidising conditions from ferric salts and its formation is very slow. If a pH of a solution containing a signficant amount of ferric ion is raised, amorphous ($Fe(OH)_3$ (s)) will form initially. This can then overtime transform into less soluble geothite. Lepidocrocite formation is less likely than geothite formation.	Formation is governed by pH and Temperature. Iron based scales can be found in drinking water distribution lines, boiler feedwater heaters, steam generators, heat exchangers, cooling systems, membrane systems

CHAPTER 3 : ANALYSIS OF THE SELECTED CONCENTRATED BRINE STREAMS CHEMISTRY (DESKTOP STUDY USING OLI STREAM ANALYZER SOFTWARE)

OLI Stream Analyzer software was acquired, and its application on high ionic strength inorganic solutions were evaluated. OLI Stream Analyzer was used to gain a quantitative understanding of the various chemical principles and systems to be used in the investigation.

3.1 Introduction and Background

In this chapter, the OLI Stream Analyzer software was used to understand the speciation of the selected brine streams and draw solution as well as to calculate the thermo-physicochemical properties such as bulk osmotic pressure of the solutions. This information was useful when designing the FO experiment in terms of choosing appropriate operating conditions, i.e. temperature and providing an indication of possible mineral phases that could form. The following streams were identified for investigation during the experimental phase of the project: **leachate from ash dams**, **tubular reverse osmosis/spiral wound reverse osmosis brines**, **ion exchange high rinse portion**, **mother liquor (evaporative crystallizer brines)** and **combined regeneration effluent**. OLI Stream Analyzer software was used to determine the osmotic pressure of these streams and to predict the sequential precipitation of various minerals under different operating conditions.

Furthermore, the bulk osmotic pressure, as well as precipitation envelopes of the solutions, gives an indication on the fluxes as well as water recoveries that could be achieved for each stream and subsequently assist in choosing the appropriate streams for further evaluation during the experimental phase.

Chapter outline

Section 3.2 & 3.3 gives a brief description of the chemistry of the draw solution and the streams identified for FO technology evaluation. **Section 3.4** then provides the methodology used for thermodynamic modelling of identified streams using OLI Stream Analyzer. The results from the chemical speciation modelling are discussed in **Section 3.5** based on the following parameters: osmotic pressure differential, potential theoretical recoveries that could be achieved as well as speciation chemistry. **Section 3.6** highlights the conclusions and recommendations on which streams should be considered for the experimental studies are made based on the above-mentioned parameters.

3.2. Draw Solution Chemistry

Ammonium bicarbonate (NH_4HCO_3) was used as a draw solution in FO experiments as NH_4HCO_3 is highly soluble in water and can therefore generate a high driving force, which was key for both high water flux and recovery. Furthermore, NH_4HCO_3 decomposes quickly upon heating to produce fresh water. Ammonium bicarbonate also satisfies the characteristics for the best draw solution for the FO technology, namely (Ge et al., 2013):

- Highly soluble,
- Has low molecular weight (High Osmotic Pressure),
- High recoverability,
- Components of the draw solution does not have an adverse health effect which might render the product water not fit for use,
- No reaction with membranes and,
- Low energy requirements for separation and recycling.

The OLI Stream Analyzer was used to determine the solubility of NH_4HCO_3 in the temperature range of 0 to 100°C. The primary objective for doing this was to determine the maximum concentration of NH_4HCO_3 that could be achieved to saturate the solution as a function of temperature. A pressure of 1 atm and a temperature of 30°C were used to conduct a survey by composition calculation in order to determine the maximum concentration of NH_4HCO_3 required to saturate the solution. According to Lange's Handbook of Chemistry (Speight, 2005), the solubility of NH_4HCO_3 per 100 g of water is 36.6 and 59.2 g at 40 and 60°C, respectively. However, in Dean's Handbook of Organic Chemistry (Gokel, 2004), it is stated that NH_4HCO_3 starts to decompose into ammonia, carbon dioxide and water at 35°C, while complete decomposition is achieved beyond 60ºC. In the study conducted by Wanling et al. (2009), it was found that when 36.6 g of NH_4HCO_3 was dissolved in 100 g of water (equivalent to a molar concentration of 4.064M) at a temperature of 50 °C, the solution appeared slightly turbid, which suggested the presence of suspended solids of NH_4HCO_3. Also, gas bubbles were observed to be released from the solution, which suggested the decomposition of NH_4HCO_3 at this temperature. Decomposition of NH_4HCO_3 was not observed when the solution was kept at 30°C. The loss of ammonia is governed by the ammonia-ammonium equilibrium. Ammonium solution can be considered as a weak acid which dissociates into NH_3 and H^+ as indicated in the equation below:

$$\boldsymbol{NH_4^+ = NH_3 + H^+} \qquad \textbf{Equation 3-1}$$

(pKa at 25°C is 9.25)

The pKa value indicates the pH at which half of the ammoniacal N is NH_4^+ and half is NH_3. Together with pH, the pKa can be used to estimate the proportion of ammoniacal N as NH_3 using the equation (3-2):

$$\boldsymbol{pH = pKa - logNH_3/NH_4^+} \qquad \textbf{Equation 3-2}$$

The value of the pKa at 25°C is 9.25; however, this dissociation is temperature-sensitive. Equation 3-3 shows a temperature dependency of the pKa value for ammonia (Emerson *et al*., 1975)

$$\boldsymbol{pKa = 0.09018 + 2727.92/T} \qquad \textbf{Equation 3-3}$$

where T is the temperature in Kelvin.

The effect of temperature on the proportion of NH_3 in the mixture is substantial. For example, at a pH of 8, the proportion of ammoniacal N as NH_3 is about 2% at 10°C, and 13% at 40°C (Kissel and Cabrera, 2005). Another physical constant that affects the behaviour of ammoniacal N is the Henry's constant that describes the equilibrium of partitioning of NH_3 between a solution and the gaseous phase in contact with the solution. This constant is affected by temperature, with an approximately threefold increase in the proportion of NH_3 that partitions into the air when the temperature is raised from 10 to 40°C (Kissel and Cabrera, 2005). The discussion above shows that higher temperatures enhance ammonia loss from ammoniacal N due to its effect on both of these physical constants (i.e. pKa value and Henry's constant). It was for these reasons and the study conducted by Wanlin et al. discussed earlier that a temperature of 30°C was selected for this study to minimize the potential loss of ammonia from the draw solution.

The maximum concentration of NH_4HCO_3 was then used to conduct a temperature survey calculation to determine the distribution of NH_4HCO_3 species at various temperatures and the results are discussed later in this chapter.

3.3 Overview of Concentrated Streams Identified for Application

The following streams were identified in the introduction section for the study (Chapter 1): leachate from ash dams, tubular reverse osmosis/spiral wound reverse osmosis brines, ion exchange effluents and mother liquor. A brief description of the origin of these streams is given in this section.

3.3.1 Stream Analysis

The analysis of the stream is always necessary to both the thermodynamic and kinetic aspects of any chemical reaction. Standard water analysis techniques were used to characterise the various streams. Table 3-1 summarises methods used to characterise the streams identified for the study.

Table 3-1: Methods used to characterize streams identified for the study

Parameters	Units	Methods
Cations	mg/L	Inductive Coupled Plasma-Optical Emission Spectrometry/Mass Spectrometry (ICP-OES/MS) (3125 A/B)*
Anions	mg/L	Ion Selective Electrode and Flow Injection Chemistry (4500C)*
pH		Electrochemistry (4500A)*
Total Dissolved Solids (TDS)	mg/L	Gravimetric (2540C)*
Conductivity	µS/cm	Potentiometry (2510B)*
Ammonia/Ammonium	mg/L	Discrete Photometry ™ (visible) (Aquakem or Flow Injection Chemistry with Photometry (visible) (4500H)*
M & P Alkalinity	mg/L as $CaCO_3$	Electrometric Titration (2320B)*
Chemical Oxygen Demand	mg/L	Acid dichromate digestion and photometric test kit (5220D)*
Total Organic Carbon	mg/L	UV persulphate oxidation-NPOC-TOC (NPCO is Non-Purgeable Organic Carbon) (5310C)*

These methods are however based on the Standard Methods for the Examination of Water and Wastewater (Standard methods for the examination of water and wastewater, 2012)

* represent method number.

3.3.1.1. Mother Liquor

The mother liquor stream is the concentrate stream which results from the concentration of various streams, namely, leachate from ash dams and RO brines using Salty Water Evaporators. This stream is currently being disposed of to the evaporation dams. The typical flowrate for this stream is between 20-40 m^3/hr.

The components of concern in this stream were mainly calcium, fluoride, alkalinity, magnesium, sulphates and high TOC (refer to Figure 1a & b 1 & Table 1 in Appendix 1 for Kernel distribution, box plots and distributional percentiles for mother liquor stream). These contaminants have high potential to form sparingly soluble minerals which could foul the FO membrane. Barium, aluminium, silica and strontium were not analysed (These components were not routinely analysed, and the data used for the study was from the routine analysis).

3.3.1.2 Tubular Reverse Osmosis/Spiral Wound Reverse Osmosis Brine

This brine stream results from the treatment of leachate from ash dams using Tubular Reverse Osmosis (TRO)/Spiral Wound Reverse Osmosis (SRO) membrane process. This brine is currently being discharged to the ash handling facilities for disposal and reuse. The typical flowrate for this stream could range from 900 m^3/hr-1100 m^3/hr depending on the water recovery. Calcium and sulphates were the major ions of concern in this stream. The stream is also characterised by high TOC (refer to Figure 2a & b 1 & Table 2 in Appendix 1 for Kernel distribution, box plots and distributional percentiles for TRO/SROs brine stream).

3.3.1.3 Combined Regeneration Effluent

The ion exchange (IEX) Regeneration Effluents originates from the IEX units used for the preparation of boiler feed water for steam generation. The cationic resins use sulphuric acid to replace the metal ions with H+ ions. The anionic resins use sodium hydroxide to replace anions (such as SO_4^{-2}-, Cl^- and NO_3^-) with OH^- ions. After the regeneration chemical has been passed through the resin bed, the excess chemical must be rinsed out with high-quality water until the rinse water is sufficiently clean for further rinsing to have a low enough conductivity for the water to be acceptable as a product. The sodium softeners use a sodium chloride solution as a regeneration chemical to replace the Ca, Mg and various heavy metals with Na. The wastewater generated during the IEX resins regeneration process is called IEX Regeneration Effluents. The typical flowrate for this stream ranges from 150 m^3/hr-200 m^3/hr. Calcium and sulphates were the primary ions of concern in this stream (refer to Table 3 in Appendix 1 for distributional percentiles for combined regeneration effluent stream).

3.3.1.4 Ion Exchange Mixed Bed Regeneration Effluent

High Conductivity Portion (HRP) effluent (the regeneration effluent with a conductivity reading higher than 16 000 µS/cm) contains > 90% of the salts generated during the IEX regeneration process.

It is characterised by low pH, high concentrations of hardness, sulphates and silica with ca 2 – 3% NaCl content. The high concentration of sodium and chlorides is due to the hydrochloric acid and sodium hydroxide chemicals which are used for IEX resins regeneration. The stream has a typical flowrate ranging between 15 m^3/hr and 20 m^3/hr.

Although the flowrate is low, the salinity in this stream is very high. It is the main contributor to the final effluent total dissolved solids (TDS) content (refer to Table 4 in Appendix 1 for distributional percentiles for ion exchange mixed bed regeneration effluent).

3.4. Methodology for Thermodynamic Modelling

This section describes the protocol followed when doing thermodynamic modelling using OLI Stream Analyzer.

3.4.1 Statistical Analyses of the Data (streams)

Statistical analyses were conducted on the data from various streams except for combined regeneration effluent and ion exchange mixed bed regeneration streams as there was no sufficient data for these two streams. The distribution of each variable is visually presented using **standard box plots** as well as the **Kernel distribution estimates**. The Kernel distribution function estimate at a point is defined as shown in Equation 3-4.

Equation 3-4

$$f_h^n(x) = \frac{1}{n}\sum_{i=1}^{n} k(x - X_i)$$

For a sample, Xi,....., Xn, the bandwidth h controls the amount of the smoothing, and the kernel function K (.) controls the influence of the data points in the vicinity of x. In the current application, the standard normal distribution function as Kernel and data-driven bandwidth proposed by Polansky and Baker [Polansky, 2000] were used. The reader is referred to the work done by Simonoff [Simonoff, 1996] for detail discussion regarding Kernel distribution estimate. Some distributional percentiles have been calculated, specifically the 5^{th}, 10^{th}, 25th, 50^{th}, 75^{th}, 90^{th} and 95^{th}. The median (i.e., the 50^{th} % tile) of appropriate variables were used as input to the OLI Stream Analyzer program to generate various thermodynamic properties/ parameters for these streams. The results from the statistical analyses are shown in Appendix 1.

3.4.2 OLI Thermodynamic Modelling

Figure 3-1 shows the main components of OLI Stream Analyzer Simulator

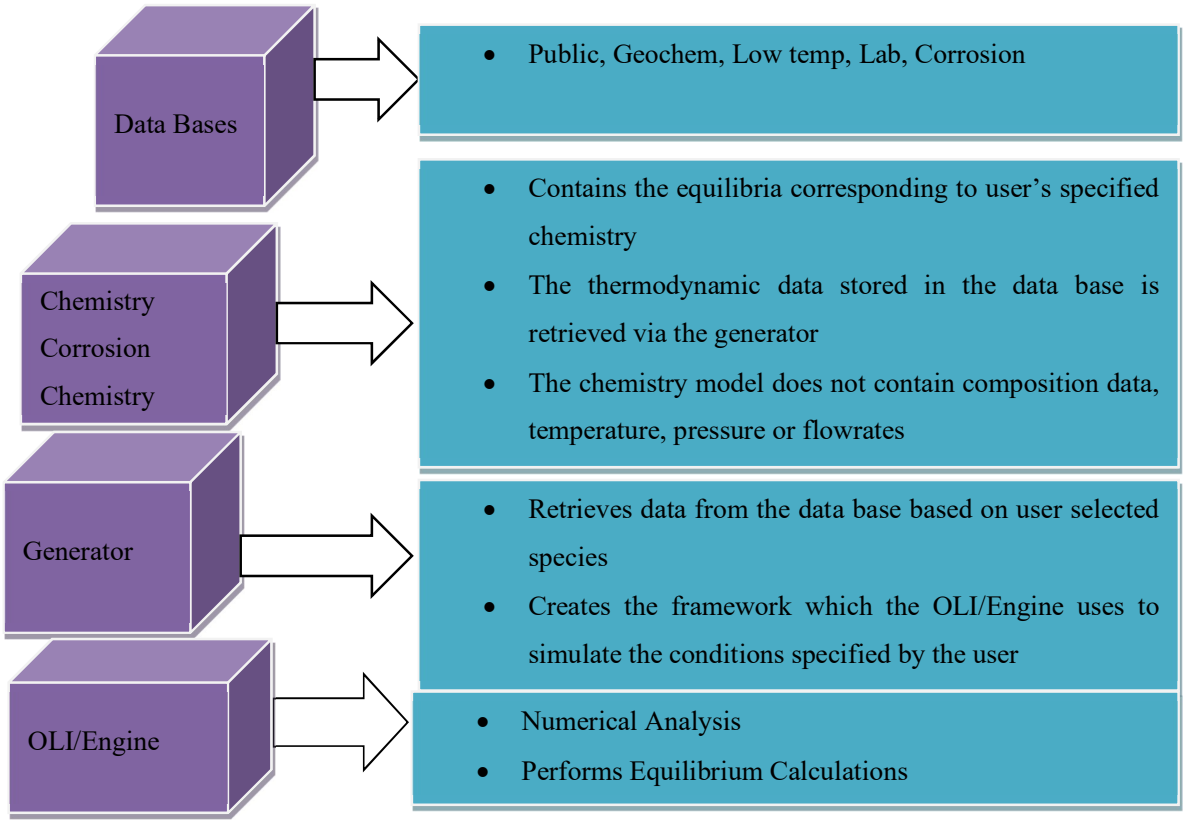

Figure 3-1: Components of the OLI Stream Analyzer software

Figure 3-2 shows a summary of the generic thermodynamic modelling procedure using the OLI Stream Analyzer (OLI Systems, Inc., 2014). The shaded blocks are the particular names of the steps used by OLI during the modelling process. The Water Analyzer block performs a reconciliation calculation for pH and Ion Charge balance (electroneutrality). OLI Water Analyzer adds or subtracts mass to balance electroneutrality and adds acid or base to adjust pH. The reconciled water analysis was then used to model the aqueous chemistry in the Stream block. The Mixed Solvent Electrolyte (MSE) thermodynamic framework model was used due to its ability to predict electrolyte behaviour for a wide concentration range; from infinite dilution to molten salts. The solid phase was included in the calculations, and the electrolyte engine generates a model that predicts all possible, solid species.

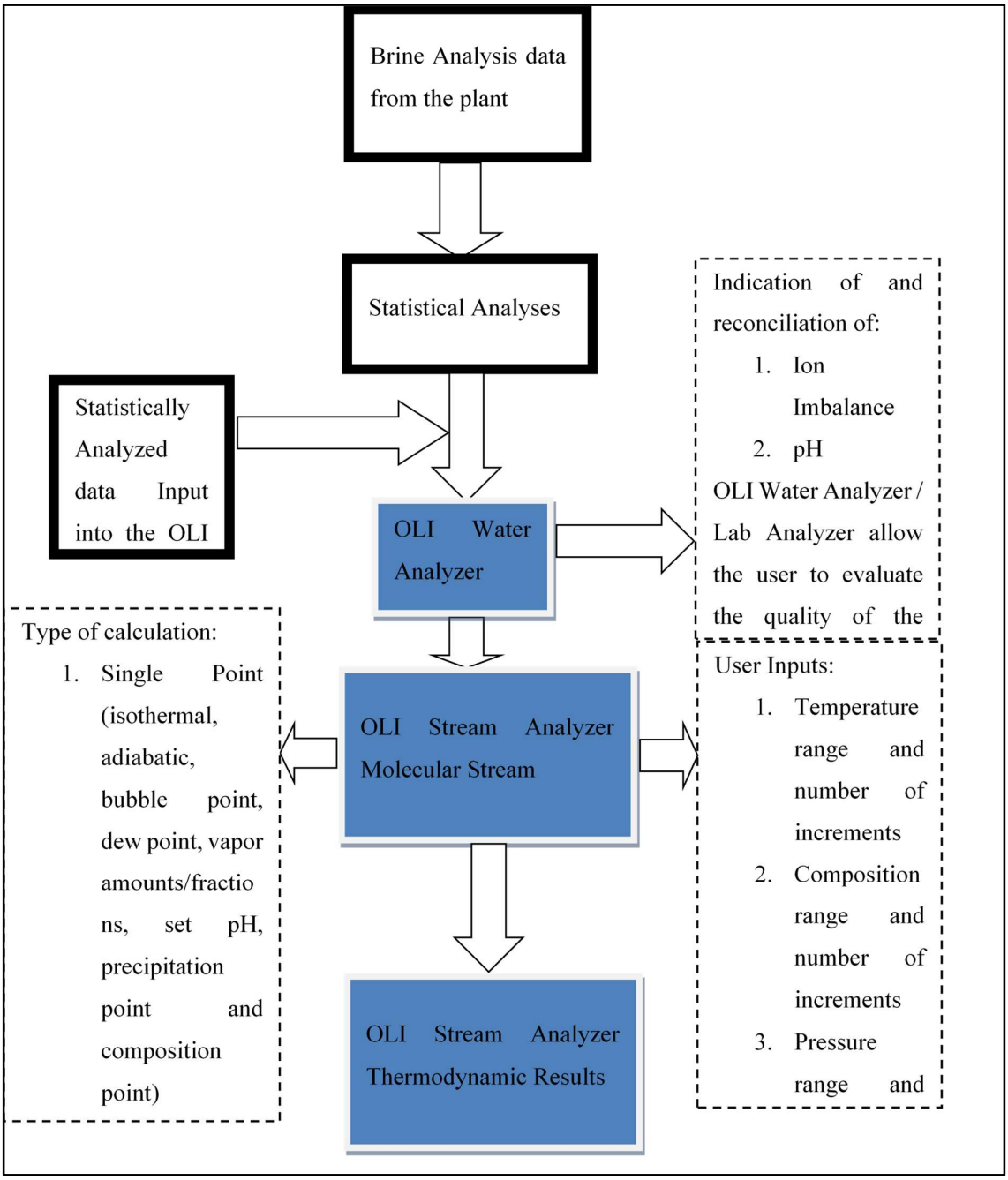

Figure 3-2: Generic thermodynamic modelling procedure using OLI Stream Analyzer

The OLI Stream Analyzer program is thermodynamic speciation software with certain limitations:

- Kinetics of precipitation of inorganic mineral phases is not considered.
- The effect of circulating scale inhibitors within the system cannot be modelled.
- The effect of organic compounds in the streams cannot be modelled.

OLI Stream Analyzer only computes an equilibrium result (i.e. what mineral is likely to form and how much of it will form at equilibrium).
The OLI does not predict kinetics, i.e. a mineral may show to be oversaturated from a thermodynamic theoretical perspective, but maybe kinetically inhibited for the given period (i.e. due to residence time, presence of antiscalant, organics or additives).

3.5. Results and Discussion

3.5.1 Evaluation of the Chemistry of Various Streams Using OLI Stream Analyzer

The following parameters were used as criteria to evaluate the suitability of the identified streams to be used as inputs to the FO process:

- Osmotic Pressure Differential (Draw Solution Osmotic Pressure-Feed Osmotic Pressure) - This is the driving force which gives an indication of the theoretical flux and maximum recovery that could be achieved.
- Speciation Chemistry - This is with respect to sequential precipitation of various minerals and gives an indication of maximum recovery that could be achieved.

3.5.1.1 Evaluation of the Solubility of Ammonium Bicarbonate and its Species as a Function of Temperature.

Ammonium bicarbonate was used as a draw solution in FO experiments as ammonium bicarbonate has a high solubility in water and can generate a high driving force, which was vital for good water flux and recovery.

Figure 3-3 below depicts the predicted maximum osmotic pressure and a corresponding concentration of a saturated solution of ammonium bicarbonate using OLI Stream Analyzer that could be achieved when ammonium bicarbonate was dissolved in water at 30°C.

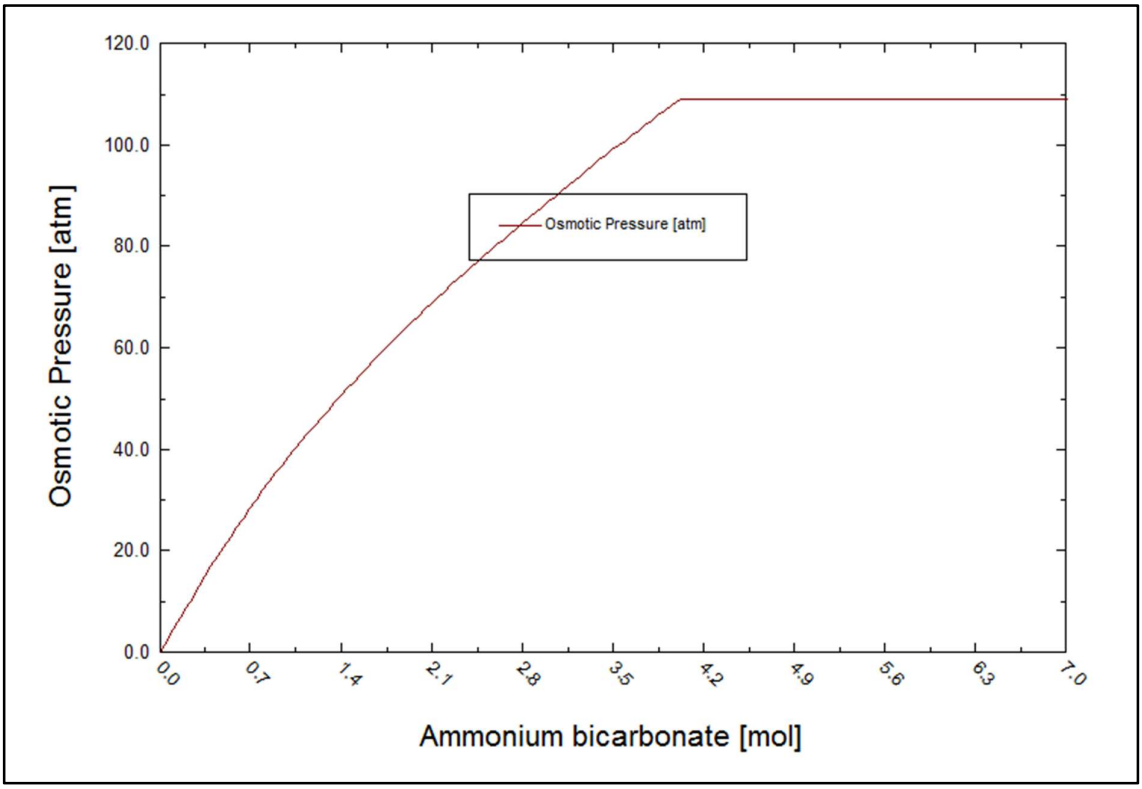

Figure 3-3: OLI Stream Analyzer predicted maximum osmotic pressure and corresponding concentration obtained when ammonium bicarbonate was dissolved in water at 30°C

The results from the simulation show that at 30°C the maximum osmotic pressure achievable was about 109 atm at an ammonium bicarbonate concentration of about 4M. Furthermore, the figure shows that increasing the ammonium bicarbonate beyond 4M does not increase osmotic pressure as the solution was saturated at these conditions.

Figure 3-4 depicts the speciation results obtained from an OLI Stream Analyzer's temperature survey calculation which was done to determine the distribution of ammonium bicarbonate species at various temperatures and fixed ammonium bicarbonate concentration (4M) and simulated as a closed system at atmospheric pressure (1 atm or 1 bar).

(a) (b)

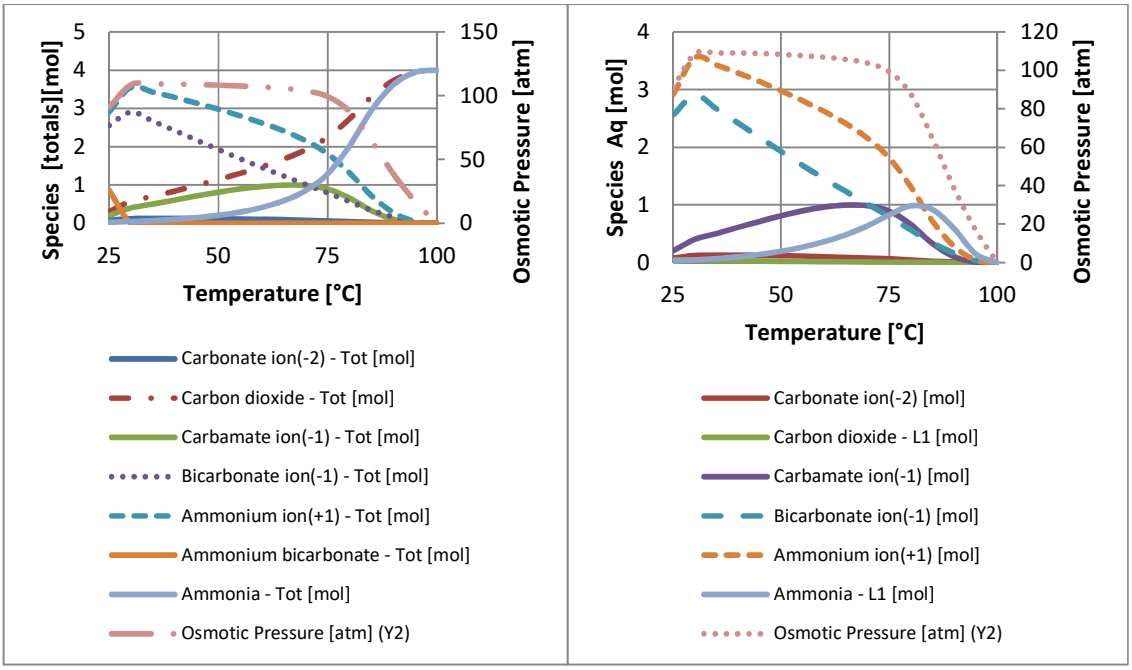

(c)

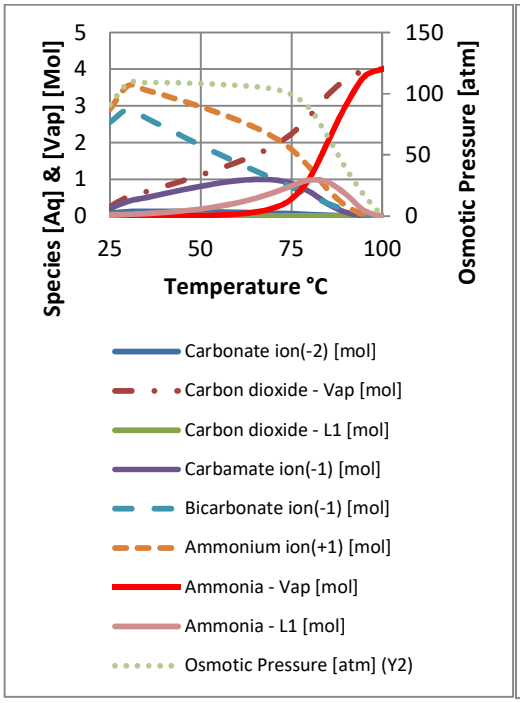

(d)

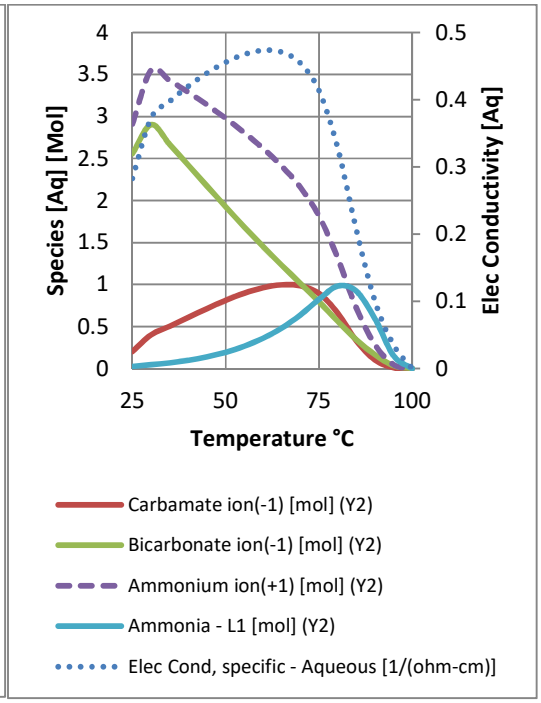

(e)

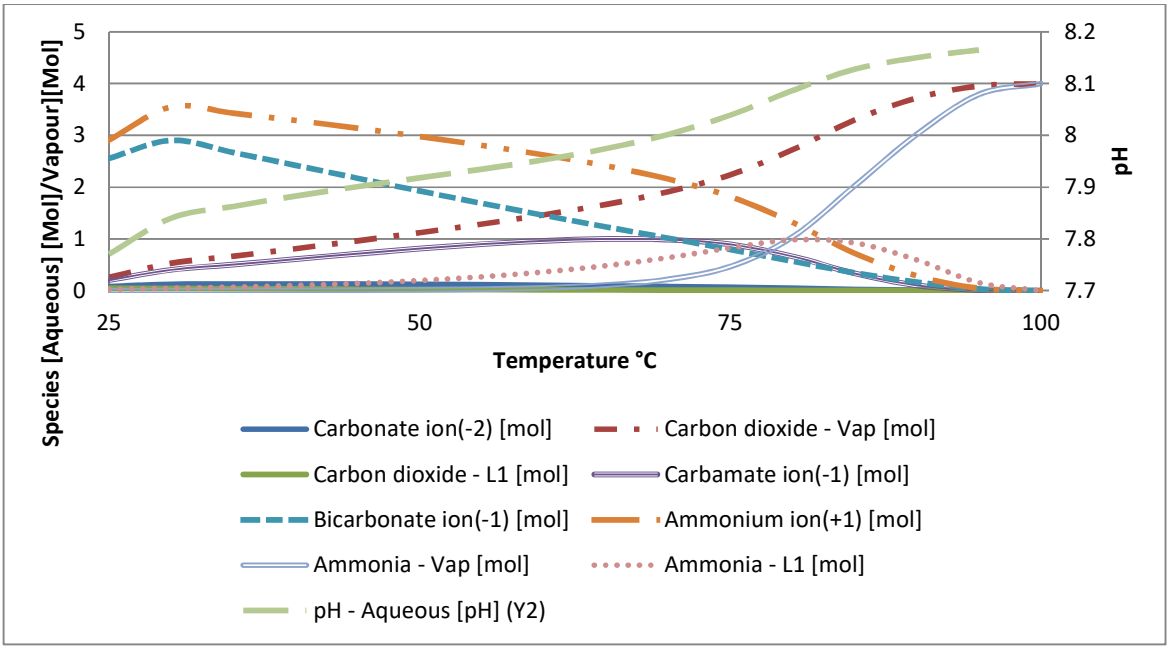

Figure 3-4: Distribution of ammonium bicarbonate species (4 M) at various temperatures

(a) Distribution of various ammonium bicarbonate species (totals), solution osmotic pressure as a function of temperature (species totals on the primary Y-axis and osmotic Pressure on the secondary Y-axis)

(b) Distribution of various ammonium bicarbonate species (aqueous), solution osmotic pressure as a function of temperature
(c) Distribution of various ammonium bicarbonate species (aqueous & vapour), solution osmotic pressure as a function of temperature (species aqueous & vapour on the primary Y-axis and osmotic pressure on the secondary Y-axis)
(d) Distribution various ammonium bicarbonate species (aqueous) and solution electrical conductivity as a function of temperature (species aqueous on the primary Y-axis and electrical conductivity on the secondary Y-axis)
(e) Distribution of various ammonium bicarbonate species (aqueous & vapour), solution pH as a function of temperature (species aqueous & vapour on the primary Y-axis and pH on the secondary Y-axis)

Figure 3-4 a, b & c shows that the dominant species at low temperatures were ammonium (+1) and bicarbonate (-1) ions. As the temperature increased, the concentrations of these two species start to decrease due to the formation of carbon dioxide (vapour), carbamate ion (-1) (aqueous), ammonia (aqueous). It was also evident from the graphs that the decomposition of ammonium bicarbonate into carbon dioxide and ammonia starts at a temperature above 30°C (in line with literature as discussed in section 3.2). The decline in the osmotic pressure was not immediate potentially due to the formation of carbamate and ammonia aqueous species which contributes to the osmotic pressure of the solution (also supported by electrical conductivity trend in Figure 3-4 (d)).

At temperatures above 70°C, a gradual decomposition of all the NH_4HCO_3 aqueous species (i.e. carbamate ion (-1), ammonium ion (+1), bicarbonate ion (-1) and ammonia) into ammonia (vapour) and carbon dioxide (vapour) was observed and this was also supported by the decrease in osmotic pressure of this solution. The equilibrium in the system between ionic and gaseous species shifts greatly towards the gaseous species at temperatures more than 70°C (Refer to vapour-liquid equilibrium equations below & Figure 3-4):

The loss of ammonia and carbon dioxide from the draw solution is acknowledged, this can however be engineered out when designing the draw solution regeneration system. Furthermore, draw solution recovery and regeneration was beyond the scope of the study.

$$NH_3(aq) + H_2O \rightleftharpoons NH_4 + + OH^- \quad \textbf{Equation 3-5}$$

$$NH_3(g) \rightleftharpoons NH_3(aq) \quad \textbf{Equation 3-6}$$

$$CO_2(aq) + H_2O \rightleftharpoons H^+ + HCO3^- \quad \textbf{Equation 3-7}$$

$$HCO3^- \rightleftharpoons H^+ + CO_3^{2-} \quad \textbf{Equation 3-8}$$

$$CO_2(g) \rightleftharpoons CO_2(aq) \quad \textbf{Equation 3-9}$$

$$H_2O \rightleftharpoons H^+ + OH^- \quad \textbf{Equation 3-10}$$

$$NH_3(aq) + HCO3^- \rightleftharpoons NH_2COO^- + H_2O \quad \textbf{Equation 3-11}$$

It is evident in Figure 3-4 (e) that the pH of the solution increased as the temperature was increased, which indicate that temperature and pH do play a role in driving the decomposition of the ammonium bicarbonate solution towards carbon dioxide and ammonia. The pH of the solution increased from ca. 7.8 to 8.2. The increase in pH is driven by the amount of ammonia in the aqueous phase (equation 3-5) which showed an increase as the temperature was increased.

3.5.1.2 Mother Liquor

Figure 3-5 shows the change in concentration of major ions and osmotic pressure in the bulk solution as water was removed from the mother liquor at 30°C and 1 atm, simulating the FO process.

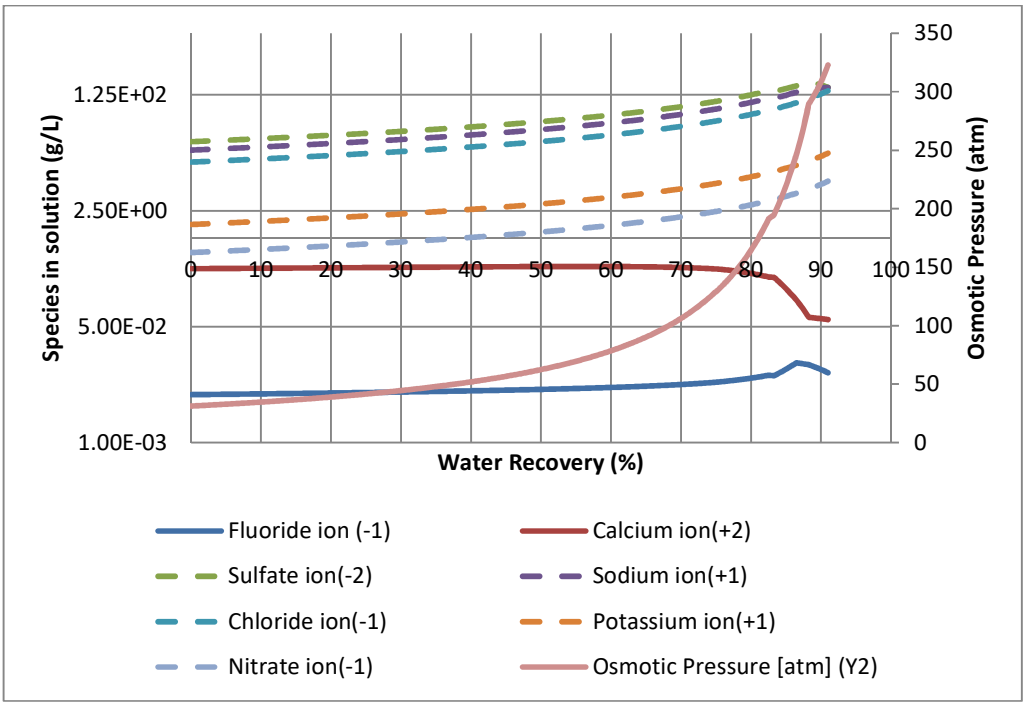

Figure 3-5: Change in concentration of major ions and osmotic pressure in the bulk solution as water was removed from the mother liquor at 30°C and 1 atm, simulating desalination using FO process.

It is apparent from Figure 3-5 that the bulk osmotic pressure of the feed increases as the water recovery was increased [Refer to equation 3-4 for water recovery definition]. This was because as the water was removed from the solution, the concentration of various species in the feed increased.

The dominant aqueous species which were contributing to osmotic pressure were sodium, chloride and sulphate. The removal of water concentrates the species in the solution, causing the saturation states of many minerals to increase (refer to Figure 3-6 below). The slight decline in sodium, sulphate and calcium ion concentration in the solution at about 82% water recovery was due to the formation of glauberite ($Na_2Ca(SO_4)_2$) mineral. The slight decline in sodium and sulphate ion concentration at about 88% water recovery was primarily due to the formation of sodium sulphate mineral. Fluoride ion concentration declined at about 86% water recovery was due to the precipitation of magnesium fluoride mineral.

The theoretical flux for the FO process is a function of membrane permeability (A), draw solution osmotic pressure (π_{draw}) and feed osmotic pressure (π_{feed}) as shown in equation 3-12 below [McGinnis, 2007].

Equation 3-12

$$\boldsymbol{J_{theo} = A(\pi_d - \pi_f)}$$

J_{theo} = Theoretical Flux, A = Membrane Permeability, π_{draw} = osmotic pressure of the concentrated draw solution, π_{feed} = osmotic pressure of the feed stream.

OLI Stream Analyzer software calculates osmotic pressure using Equation 3-13 below:

Equation 3-13

$$\boldsymbol{\pi = -RTLna_{H20}V_{H20}}$$

Where

$\boldsymbol{\pi}$ represents the osmotic pressure of the solution
R represents the gas constant
T represents the temperature of the solution
$\mathbf{a_{H20}}$ represents the activity of the water at temperature T
$\mathbf{V_{H2O}}$ represents the partial molal volume of water at temperature T

Theoretically, as the water is removed from the solution, the solution becomes concentrated, which increases its osmotic pressure. Consequently, at constant draw solution's osmotic pressure (i.e. 109 atm), the osmotic pressure differential, and thus the driving force and water flux (refer to equation 3-12) decrease.
Based on bulk osmotic pressure differential at 30°C, the maximum theoretical water recovery for this stream using a draw solution composed of a saturated solution of ammonium bicarbonate at a temperature of 30°C and 1 atm could be between 60 and 70% (refer to Figure 3-5 above).

Equation 3-14

$$\boldsymbol{Water\ Recovery} = \frac{\left(\boldsymbol{Starting\ mass\ of\ water\ (1\ kg) - remaining\ mass\ of\ water\ \ (kg)}\right)}{\boldsymbol{Starting\ mass\ of\ water\ (1\ kg)}} \boldsymbol{X100}$$

Equation 3-15 shows how theoretical osmotic pressure differential was calculated.

Equation 3-15

$$\Delta\boldsymbol{\pi} = \boldsymbol{\pi_d} - \boldsymbol{\pi_f}$$

$\boldsymbol{\Delta\pi}$ = Bulk or theoretical osmotic pressure difference between the draw solution and feed stream

$\boldsymbol{\pi_d}$ = osmotic pressure of the concentrated draw solution

$\boldsymbol{\pi_f}$= osmotic pressure of the feed stream

Figure 3-6 depicts sequential precipitation of various minerals and mass of the minerals formed during a simulation of the desalination of mother liquor stream as an equilibrium system at 30°C. Also included in the figure is the species in solution as water was removed from the solution.

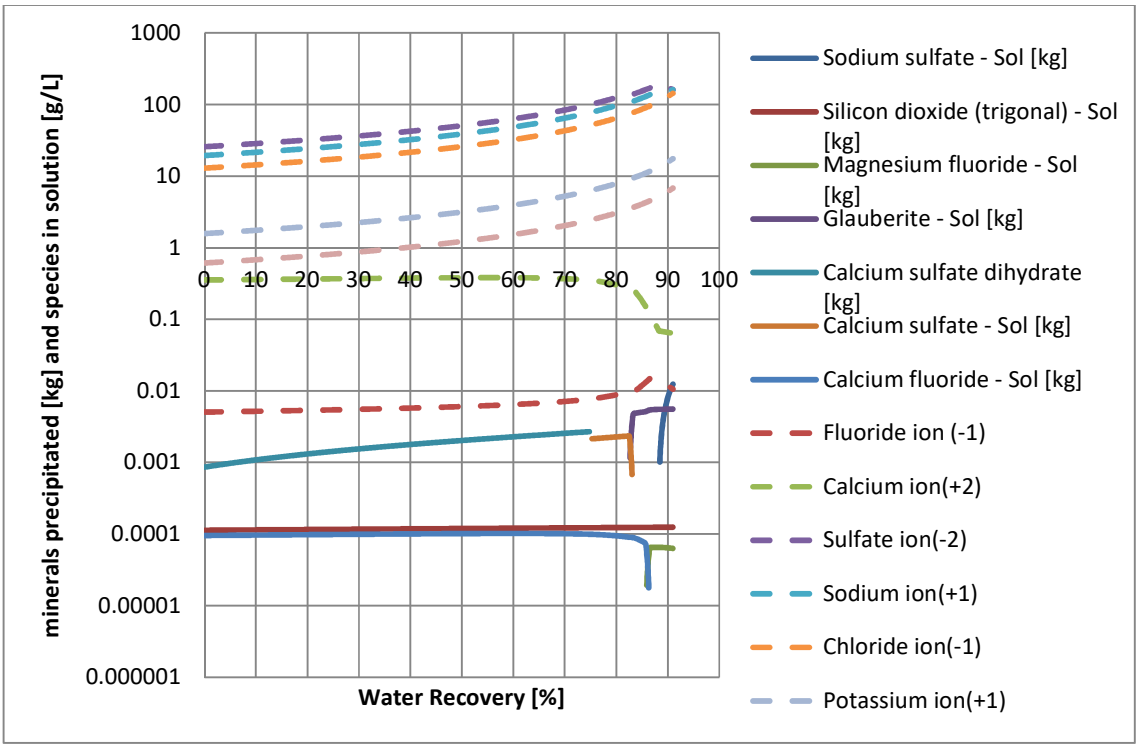

Figure 3-6: Sequential precipitation of various minerals and mass of the minerals precipitated during a reaction simulating the desalination of mother liquor stream as an equilibrium system at 30°C.

Figure 3-6 shows that initially calcium sulphate dihydrate, calcium fluoride and silicon dioxide precipitate with the mass of calcium sulphate dihydrate increasing as water recovery was increased. The other two minerals were, however showing marginal changes in mass precipitated.

At about 75% water recovery, the decreasing water activity as water was removed from the solution causes calcium sulphate dihydrate to dehydrate forming anhydrite which precipitates up to about 80% water recovery. At about 82% water recovery glauberite mineral starts to form. Glauberite occurs at higher concentrations of sodium sulphate in the presence of saturated calcium sulphate. With a high amount of calcium in this stream, the chances of forming glauberite were high. At about 85% water recovery, the mass of calcium fluoride precipitating decreases (due to decreasing calcium and fluoride ion concentration, refer to Figure 3-6) and magnesium fluoride starts to precipitate. Sodium Sulphate starts to form at about 88% water recovery as more water was removed from the solution. It is apparent from Figure 3-6 that calcium sulphate dihydrate forms in this stream in far greater mass than any other mineral.

Several studies have shown that strategies such as osmotic backwash, rinsing with pure water without using chemical cleaning reagents and increasing the cross-flow velocity during operation could be employed with success to manage FO fouling. This is because no hydraulic pressure is applied during the FO operation, and therefore the fouling layer is not as compacted as that observed during RO operation. Alternatively, in order to reduce the scaling potential of these minerals, pre-treatment of this stream in the form of antiscalant addition or softening (e.g. Conventional (Lime/Soda) or Ion Exchange) could be employed. For this stream, it appears as if the limiting parameter to water recovery in addition to potential precipitation of sparingly soluble salts (e.g. calcium sulphate dihydrate, silicon dioxide, calcium fluoride, magnesium fluoride) will be osmotic pressure of the draw solution (ammonium bicarbonate) as about 109 atm maximum osmotic pressure could be achieved due to the limitation associated with the solubility of ammonium bicarbonate at specified temperature.

3.5.1.3 Tubular Reverse Osmosis/Spiral Wound Reverse Osmosis Brine

This brine stream result from the treatment of leachate from ash dams using Tubular Reverse Osmosis (TRO)/Spiral Wound Reverse Osmosis (SRO) membrane process. This stream is currently being discharged to the ash handling facilities for disposal and reuse. Calcium and sulphates were the major contaminants of concern in this stream. Other contaminants of concern, which were not analysed, include barium, aluminium, silica and strontium.

Figure 3-7 shows the change in concentration of major ions and osmotic pressure in the bulk solution as water was removed from the TRO/SRO Brine stream at 30°C, simulating desalination using the FO process.

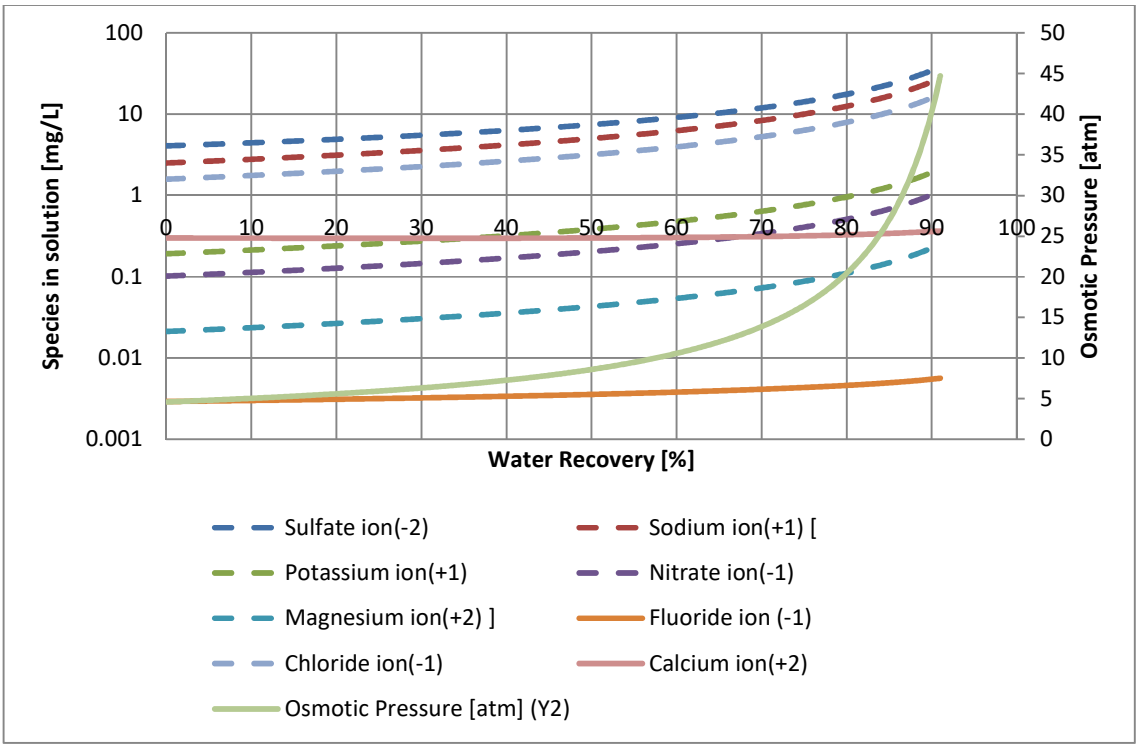

Figure 3-7: Change in concentration of major ions and osmotic pressure in the bulk solution as water was removed from the TRO/SRO Brine stream at 30°C and 1 atm, simulating desalinating using FO process.

Based on bulk osmotic pressure differential generated at 30°C, the theoretical water recovery for this stream using a draw solution composed of a saturated solution of ammonium bicarbonate at a temperature of 30°C could be at least 90% (Figure 3-7) implying that theoretically there will always be enough driving force (i.e. no osmotic pressure differential limitations) available to achieve higher water recoveries and higher fluxes. The major dominant ions contributing to the osmotic pressure were sodium, chloride and sulphate.

Figure 3-8 below depicts sequential precipitation of various minerals and mass of the minerals formed during a simulation of the desalination of TRO/SRO Brine stream as an equilibrium system at 30°C and 1 atm.

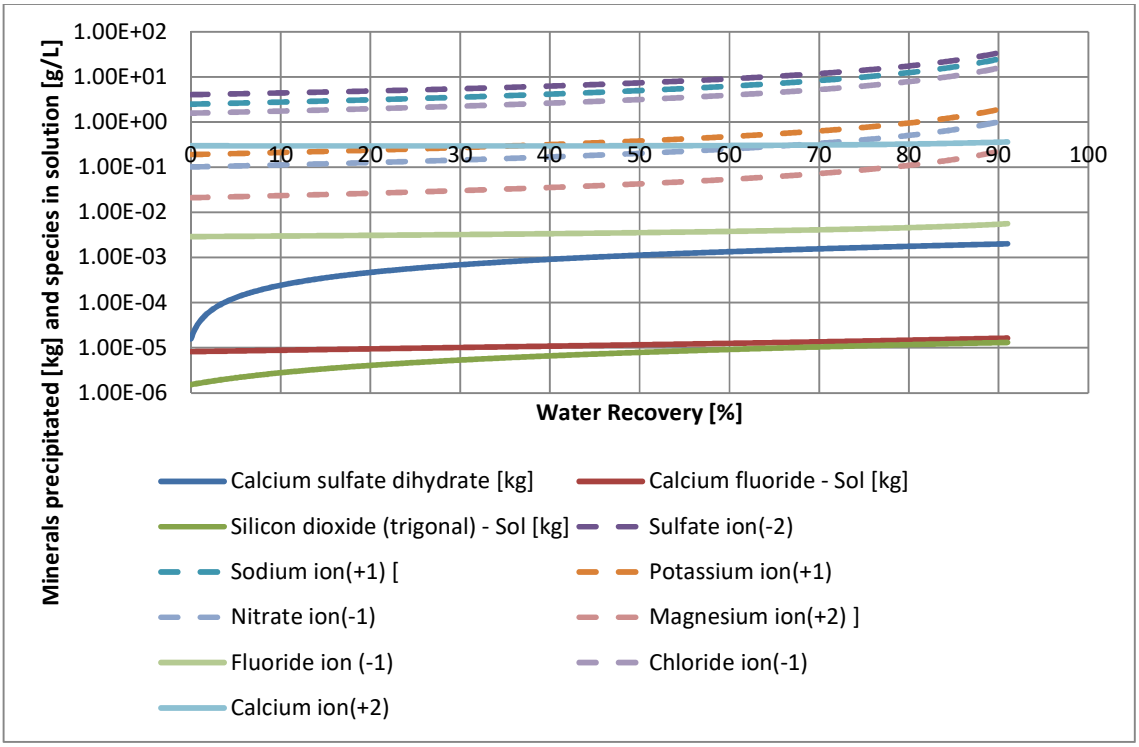

Figure 3-8: Sequential precipitation of various minerals, mass of the minerals precipitated, equilibrium solution osmotic pressure during a reaction simulating the desalination of TRO/SRO Brine stream as an equilibrium system at 30°C.

It is evident from Figure 3-8 that this stream is already saturated with calcium sulphate dihydrate, calcium fluoride and silicon dioxide. The mass of minerals precipitating increased as the water was removed from the solution. It is also apparent from Figure 3-8 that calcium sulphate dihydrate forms in this stream in far greater mass than any other mineral reflected. Studies conducted by Mi et al. (2008) showed that calcium sulphate scaling of the FO membrane is characterised by crystallisation in the bulk solution and deposition of particles which lead to the fouling layer formed being less compact due to the absence of hydraulic pressure in the FO process. This study also showed that calcium sulphate dihydrate fouling in the FO process was reversible, with greater than 90% recovery of FO membrane permeability following a water rinse without adding any chemicals and this strategy could be applied to manage other minerals which were precipitating. In other words, FO may offer an extraordinary advantage of significantly reducing or even removing the use of chemical cleaning. Conventional softening and ion exchange softening and antiscalants could be utilised as pre-treatment steps in order to minimise the potential formation of these minerals.

3.5.1.4 Combined Regeneration Effluent

There was only one set of analyses available on this stream, and as a result, statistical analyses could not be done. The one set of data available was used as feed to OLI Stream Analyzer program to get an indication on the chemistry of this stream.

Figure 3-9 shows the change in concentration of major ions and osmotic pressure in the bulk solution as water was removed from the Combined Regeneration Effluent stream at 30°C, simulating desalination using the FO process.

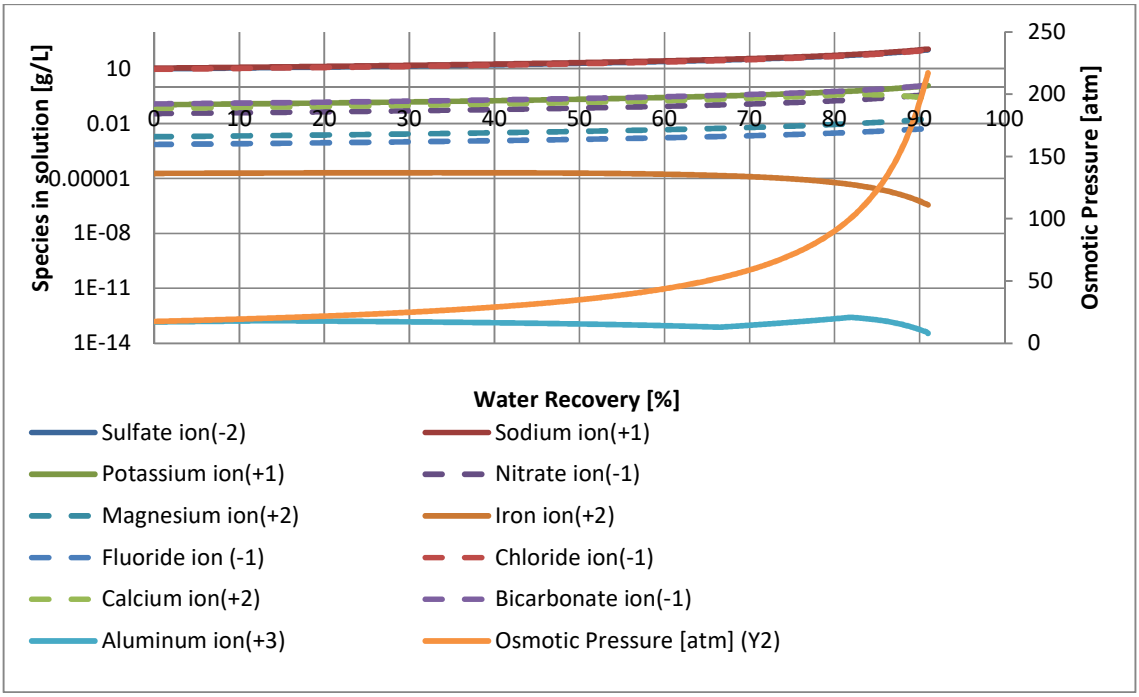

Figure 3-9: Change in concentration of major ions and osmotic pressure in the bulk solution as water was removed from the Combined Regeneration Effluent stream at 30°C and 1 atm, simulating desalination using FO process.

The Combined Regeneration Effluent stream has an osmotic pressure of about 18 atm, and as the water was removed from the solution, the stream osmotic pressure also increases due to an increase in the concentration of various components in this stream. The major ions contributing to the osmotic pressure were sodium, sulphate and chloride as depicted in Figure 3-9.

From Figure 3-9 above, the maximum theoretical water recovery for this stream using a draw solution composed of a saturated solution of ammonium bicarbonate at a temperature of 30°C could be about 80% before the osmotic pressure differential becomes limiting.

Figure 3-10 below depicts sequential precipitation of various minerals and mass of the minerals formed during a simulation of the desalination of combined regeneration effluent as an equilibrium system at 30°C.

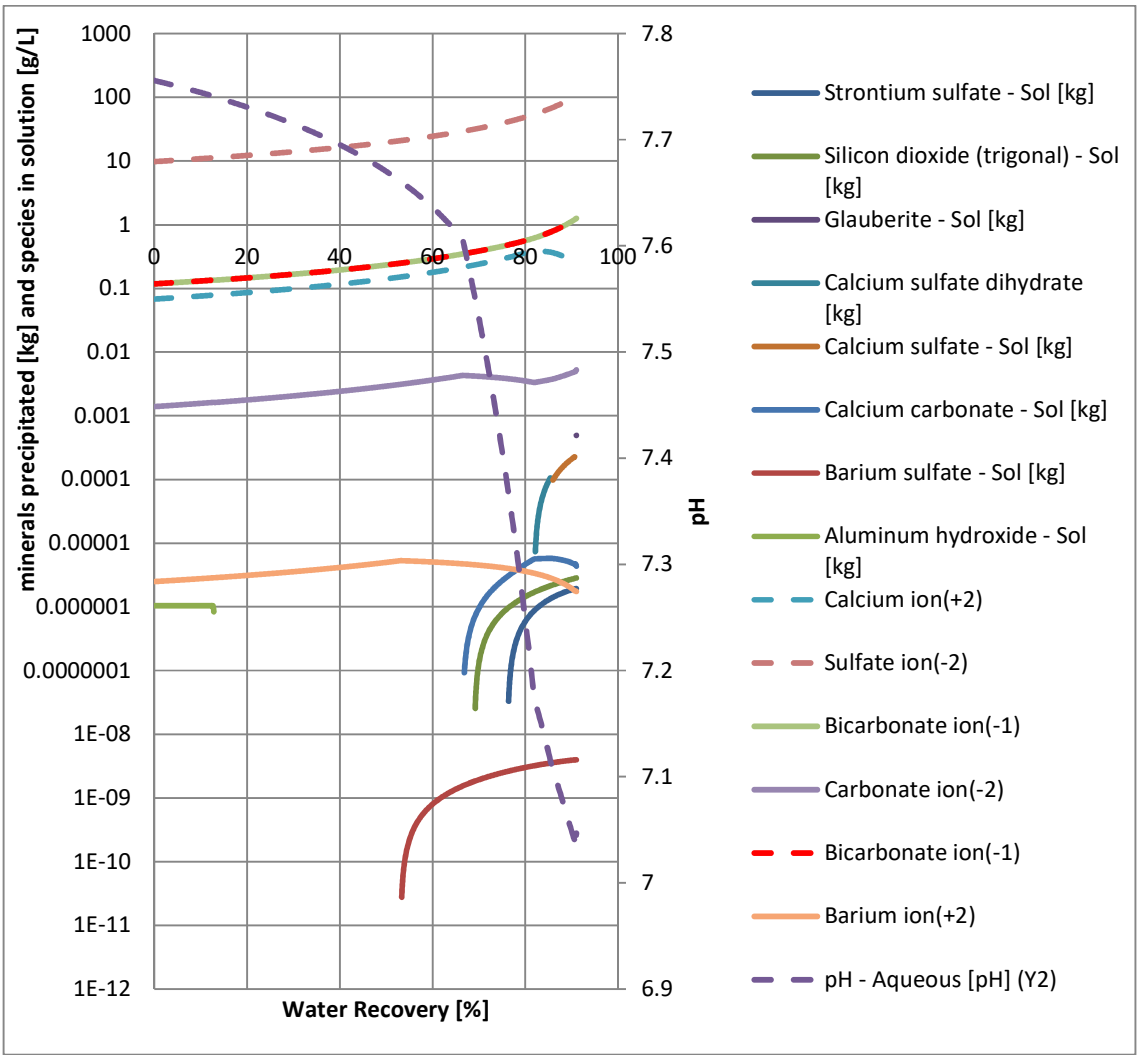

Figure 3-10: Sequential precipitation of various minerals and mass of the solids formed during a simulation of the desalination of combined regeneration effluent as an equilibrium system at 30°C.

Figure 3-10 indicates that this stream is already saturated with aluminium hydroxide from the beginning. At about 50-55% water recovery, barium sulphate starts to precipitate primarily due to the increase in barium and sulphate concentration as water was removed from the solution.

Calcium carbonate, silicon dioxide and strontium sulphate start to precipitate at 67%, 70% and 77% water recovery, respectively due to an increase in the concentration of calcium, carbonate, strontium, sulphate and silica concentration as water was removed from the solution (presence of supersaturated conditions).

The solution is supersaturated with respect to calcium carbonate, for example, if the ion activity product (IAP) for Ca^{+2} and CO_3^{-2} exceeds the calcite solubility product. In the case of calcite, pH also plays a role because generally at the pH of the solution, bicarbonate ions were converted to carbonates increasing the potential to form calcite.

Furthermore, at the temperature of simulation (30°C), calcite was the only polymorph present. At about 80% water recovery, calcium sulphate dihydrate starts to precipitate. The decreasing water activity causes gypsum to dehydrate to form calcium sulphate, as indicated in Figure 3-10. At about 90% water recovery, glauberite starts to precipitate. It is evident from the simulation results that, although high recoveries could be achieved on this stream, some pre-treatment to enable this will be required to remove sparingly soluble compounds precursors such as calcium, strontium, barium, aluminium and silica. This could be achieved through softening of the stream.

3.5.1.5 Ion Exchange Mixed Bed Regeneration Effluent (High Rinse Portion)

Figure 3-11 shows the change in concentration of major ions and osmotic pressure in the bulk solution as water was removed from the Ion Exchange Mixed Bed Regeneration stream at 30°C and 1 atm, simulating desalination using the FO process.

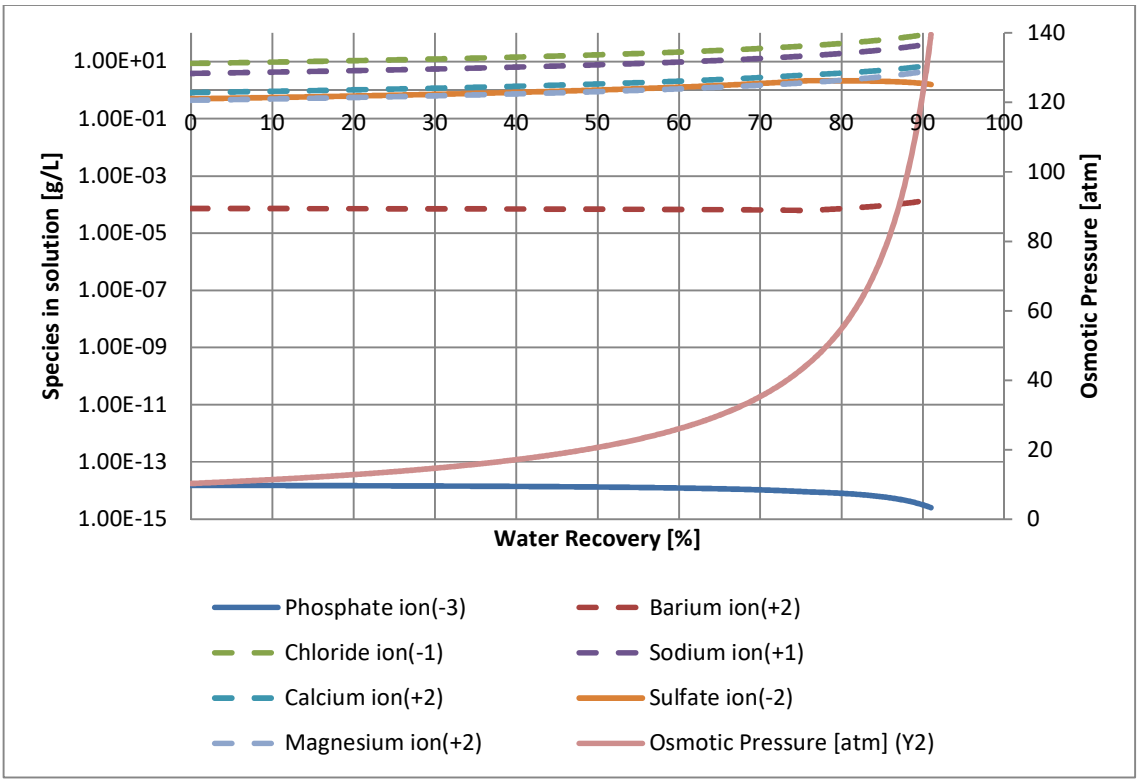

Figure 3-11: OLI simulation effects of desalination at 30°C on the chemistry of Ion Exchange Mixed Bed Regeneration stream with respect to variation in the stream's chemistry bulk composition and osmotic pressure.

Figure 3-11 shows that as the water was removed from the system, the stream osmotic pressure also increases due to an increase in the concentration of various components in this stream. The concentration of the components sodium and chloride increased since they were not part of solids formed during precipitation. The major components contributing to osmotic pressure were sodium and chloride. The ion exchange mixed bed regeneration stream has an osmotic pressure of about 10 atm, which was much less than that of seawater. Based on bulk osmotic pressure differential that could be generated at 30°C, the maximum theoretical water recovery for this stream using a draw solution composed of a saturated solution of ammonium bicarbonate at a temperature of 30°C and 1 atm could be about 90% if this stream is desalinated using FO process. The implication of this is that theoretically, there will always be enough driving force available to achieve higher recoveries and fluxes.

Figure 3-12 below depicts sequential precipitation of various minerals and mass of the solids formed during a reaction simulating the desalination of ion exchange mixed bed regeneration effluent as an equilibrium system at 30°C.

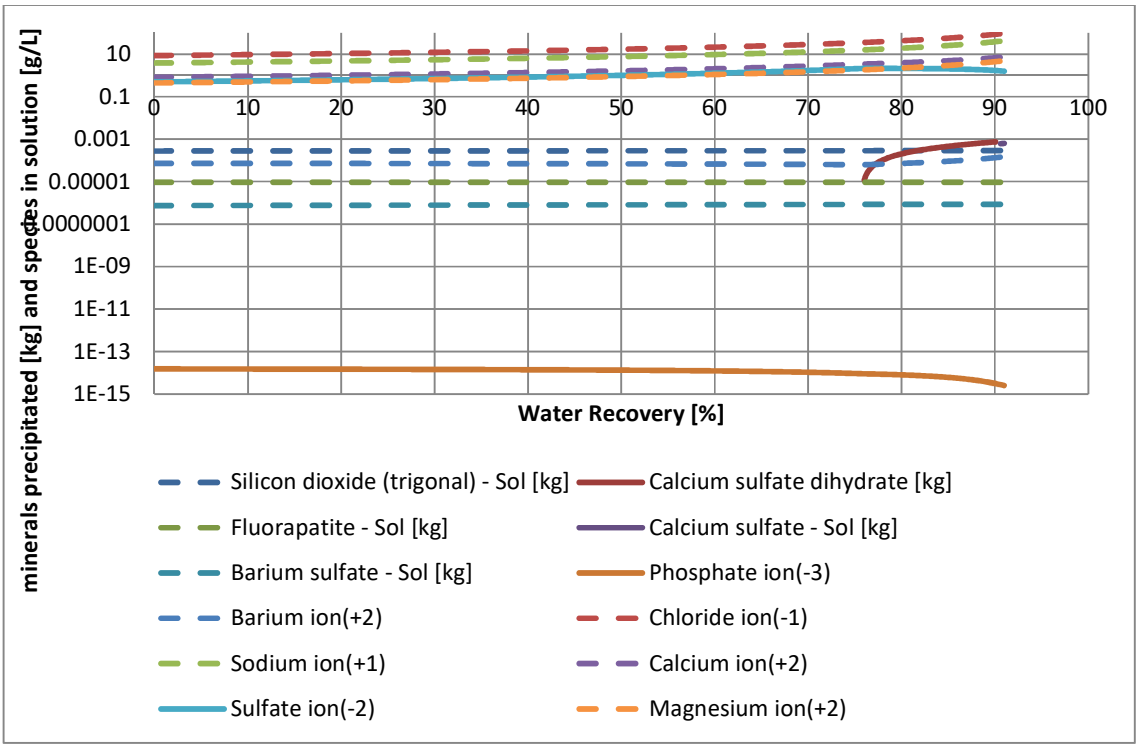

Figure 3-12: Sequential precipitation of various minerals and mass of the solids formed during a reaction simulating the desalination of ion exchange mixed bed regeneration effluent as an equilibrium system at 30°C.

Figure 3-12 shows that the ion exchange mixed bed regeneration stream is saturated with silicon dioxide, fluorapatite and barium sulphate. An almost similar amount (as mass) of silicon dioxide, fluorapatite, barium sulphate was precipitating as the solution becomes concentrated (the solution becomes supersaturated due to increasing individual ions concentration (e.g., calcium, sulphate, silica, barium). With further removal of the water, calcium sulphate dihydrate starts to precipitate at about 75% water recovery, and it forms in far greater mass than any other mineral in this system. At about 90% water recovery, the decreasing water activity of the solution causes the gypsum to dehydrate to calcium sulphate anhydrite. For this stream, pre-treatment in the form of softening to remove hardness and silica (responsible for barium sulphate, calcium sulphate (gypsum and anhydrite) and silica precipitation) will enable high water recovery of this stream.

3.6. Concluding Remarks

In this study, the OLI Stream Analyzer software was used to understand the speciation of the brine streams as well as to calculate the thermo-physicochemical properties such as osmotic pressure of the solution. This information was useful when designing the FO experiment with respect to choosing appropriate operating conditions, i.e. temperature and providing an indication of possible mineral phases that could form. The limitations associated with thermodynamic modelling should also be taken into consideration when interpreting the results discussed in this chapter. Furthermore, there were some components which were not available for some streams, and these components might add to the numbers of minerals precipitating in these streams. It must, however, be stated that the major components which were responsible for mineral formation were analysed for.

- Evaluation of the solubility of Ammonium Bicarbonate (NH_4HCO_3) and its species as a function of temperature.
    - The results generated by OLI Stream Analyzer 3.2 software indicate that in general, the solubility and osmotic pressure of a saturated solution of an NH_4HCO_3 draw solution increase as the solution temperature increases. Furthermore, the maximum concentration of ammonium bicarbonate that could be achieved to saturate the solution as a function of temperature was obtained to be 4 M.
    - The bulk osmotic pressure of a saturated solution at 30°C and 1 atm (temperature and pressure at which the experiments will be conducted) was about 109 atm. The high solubility and hence high bulk osmotic pressure at higher temperature was mainly due to ammonium carbamate species which was the most soluble species formed when ammonium bicarbonate was dissolved in water.
    - The bulk osmotic pressure of a saturated ammonium bicarbonate solution (109 atm) was much higher than the osmotic pressure of seawater undergoing 50% recovery (RO desalination), and this presents an opportunity for achieving higher water recovery and fluxes if FO process is used.
    - Temperature survey simulation using OLI Stream Analyzer program to determine the distribution of species at various temperatures and fixed ammonium carbonate concentration (4M) shows that that the dominant species at low temperatures were ammonium (+1) and bicarbonate (-1) ions. As the temperature increases, the concentrations of these two species start to decrease due to the formation of carbon dioxide (vapour), carbamate ion (-1) (aqueous), ammonia (aqueous). At temperatures above 70°C, a gradual decomposition of all the NH_4HCO_3 aqueous species (i.e. carbamate ion (-1), ammonium ion (+1), bicarbonate ion (-1) and ammonia) into ammonia (vapour) and carbon dioxide (vapour) was observed and this was also supported by the decrease in osmotic pressure of this solution.

- Evaluation of the chemistry of various streams using OLI Stream Analyzer 3.2 software
    - Mother Liquor
        - The initial bulk osmotic pressure of this stream was 30 atm, which could be classified as slightly higher than that of seawater.
        - Based on the bulk osmotic pressure of the saturated draw solution (NH_4HCO_3) and that of the feed as water was removed from the system, indications were that the maximum theoretical water recovery for this stream using a draw solution composed of a saturated solution of ammonium bicarbonate at a temperature of 30°C and 1 atm could be about 65%.
        - This stream is already saturated with the following minerals, namely, calcium sulphate dihydrate, calcium fluoride and silicon dioxide. As water was removed from the system, the mass of these species precipitating increases. As more water was removed from the system, species such as calcium sulphate and magnesium fluoride also precipitate. Calcium sulphate dihydrate and calcium sulphate, however, forms in much higher quantity than any other minerals in this stream.
    - Tubular Reverse Osmosis/Spiral Wound Reverse Osmosis Brine
        - The initial bulk osmotic pressure of this stream was about 5 atm which was much lower than that of seawater.
        - Indications based on the bulk osmotic pressure of the draw solution (NH_4HCO_3) and that of the feed stream as water was removed from the system (osmotic pressure differential generated at 30°C and 1 atm), were that the maximum theoretical water recovery for this stream using a draw solution composed of a saturated solution of ammonium bicarbonate at a temperature of 30°C could be as high as 90%.
        - As with the mother liquor stream, this stream is also already saturated with calcium sulphate dihydrate, calcium fluoride and silicon dioxide. The mass precipitating out of the solution increased as the water was removed from the system. Calcium sulphate dihydrate form in this stream in far greater mass than any other minerals.

    - Combined Regeneration Effluents
        - The initial bulk osmotic pressure of this stream was about 18 atm which was lower than that of seawater.

        - Indications based on the bulk osmotic pressure differential generated at 30°C shows that the maximum theoretical water recovery for this stream using a draw solution composed of a saturated solution of ammonium bicarbonate at a temperature of 30°C and 1 atm could be about 80%.
        - Minerals that were precipitating are barium sulphate, silicon dioxide, calcium carbonate; strontium sulphate and calcium sulphate dihydrate. As with the other streams, calcium sulphate dihydrate forms in much higher mass than any of these minerals.
    - Ion Exchange Mixed Bed Regeneration Effluent (High Rinse Portion)
        - The bulk osmotic pressure of this stream at 0% water recovery was about 10 atm which is lower than that of seawater.
        - Indication based on bulk osmotic pressure differential generated at 30°C is that the maximum theoretical water recovery for this stream using a draw solution composed of a saturated solution of ammonium bicarbonate at a temperature of 30°C could be about 90%.
        - Minerals that were precipitating are silicon dioxide, calcium sulphate dihydrate, fluorapatite, barium sulphate and aluminium hydroxide. Calcium sulphate dihydrate and silicon dioxide were the two minerals forming in much higher mass than the rest of the minerals with calcium sulphate being dominant, albeit forming at above 70%.
- Although all the streams earmarked for FO experimental evaluation were saturated with various minerals, several studies have shown that strategies such: osmotic backwash, rinsing with pure water without using chemical cleaning reagents and increasing the cross-flow velocity during operation could be employed with success to manage FO fouling. This is because no hydraulic pressure is applied during the FO operation, and therefore the fouling layer is not as compacted as that observed during RO operation. Alternatively, in order to reduce the scaling potential of these minerals, pre-treatment of these streams in the form of antiscalants addition or softening (e.g. Conventional or Ion Exchange) could be employed.
- Based on the results presented in this chapter, all the streams discussed in this chapter were recommended to be carried forward for FO process experimental studies.

The study provided vital information on how thermodynamic modelling can be used to identify critical parameters required for the designing of the FO experiments. This information included the use of speciation as a tool to identify concentration of the draw solution achievable, temperature for the experiments, water recovery achievable when concentrating identified brine streams and possible minerals that could precipitate during the concentration of the identified brine streams using FO process.

CHAPTER 4 : DEVELOPMENT AND VALIDATION OF EXPERIMENTAL EQUIPMENT AND PROCEDURES USING SODIUM CHLORIDE

In this chapter, some of the experiments cited in the literature were repeated to test and calibrate the equipment and the methods to be used. A supervisory control and data acquisition (SCADA) system were incorporated into the experimental equipment to keep experimental conditions constant and to acquire experimental data.

4.1 Objectives and Scope of the Study

This phase of the study was used to establish appropriate operating conditions with respect to membrane type, membrane orientation, draw solution concentration, feed solution concentration, temperature and cross-flow velocity to be used in the main experiments described in Chapter 5. In order to achieve these objectives, experiments were undertaken to evaluate the effects of various factors that impact the performance of the FO process and to determine their sole or combined effects on FO performance parameters (i.e. water flux and reverse salt flux) using sodium chloride as a feed solution. Sodium chloride was selected due to its stability and the fact that numerous studies have been conducted using sodium chloride which enable comparison of the results from this study. These operating conditions have been cited in the literature as playing a crucial role in the performance of the FO process (Wangling, 2009; Chen, 2011).

4.2 Material and Methods

4.2.1 Experimental Set up Description

A bench-scale test FO system was designed and built for this study. Figure 4-1 & 4-2 shows a PFD and a photograph of the FO bench-scale experimental set up utilised in this study.

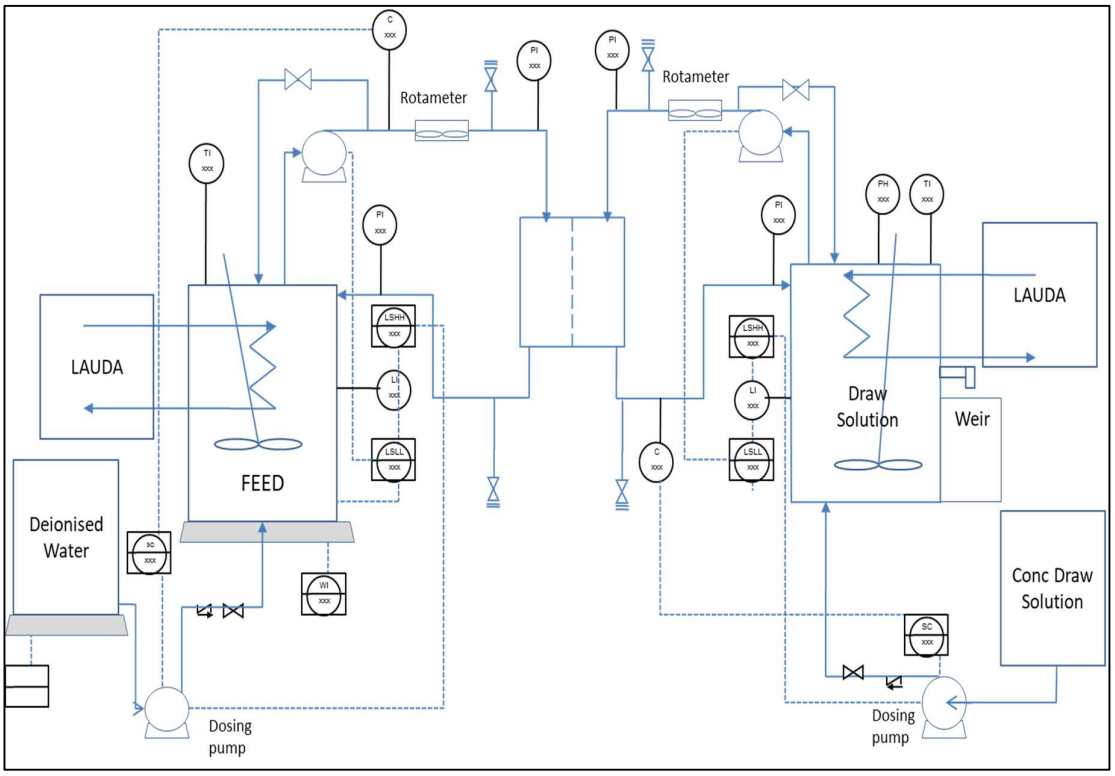

Figure 4-1: PFD of the FO bench scale experimental set up to be used for this study

A piping and instrumentation diagram (P&ID) of the experimental set up is attached in the Appendix 2.

Figure 4-2: Photograph of a Forward Osmosis Experimental Set up

The FO membrane cell (Sterlitech Corporation, Kent, USA) was constructed to have symmetric flow channels or chambers on both sides of the membrane which enables both the feed solution and draw solution (DS) to flow tangentially across the installed membrane. The active membrane surface area was 140 cm^2. Spacers (0.7874 mm) placed in the feed and the DS channels were used to support the membrane and enhanced mixing of the DS and feed solution.

Figure 4-3 shows the components of the FO membrane cell used for the experiments.

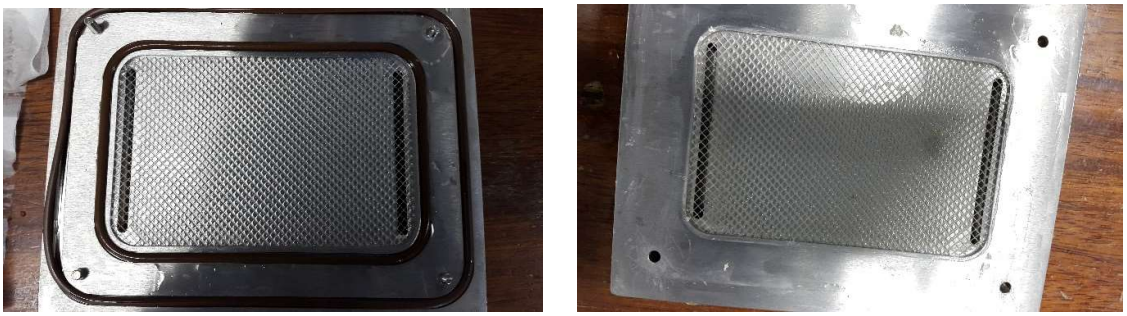

Figure 4-3: Components of the FO membrane cell used for the experiments

Two 15 L Perspex plastic tanks were constructed, and these were used to hold the feed (operating volume was 8 L) and the draw solution. A Hydra-Cell positive displacement pump (Warner Engineering) fitted with a variable speed drive motor was used to continuously circulate the feed solution between the feed tank and FO membrane cell. Similarly, a Hydra-Cell positive displacement pump (Warner Engineering) fitted with a variable speed drive was used to circulate the draw solution between the draw solution tank and FO membrane cell. The feed and draw solution flow rates were measured using a flow meter installed on the suction side of the feed and draw solution pumps, respectively. Coiled stainless steel tube heat exchangers were installed in both the feed and draw solution tanks, and the temperature in these tanks was controlled to a selected temperature using Lauda baths (Eco Silver-ECO 415). Feed and draw solution conductivities were measured using a K=1 cm^{-1} and K=10 cm^{-1} cell constant probes (Knick), respectively. Level switches installed in the feed tank and draw solution tank were used to control the levels in these tanks. Peristaltic pumps mounted on the feed and draw solution side of the membrane cell were used to manage the concentration of the feed and draw solution by dosing deionised (DI) water and concentrated draw solution, respectively. 15 L Perspex plastic tanks were used to hold DI water and concentrated draw solution. The DI water tank was placed on the analytical balance (Sartorius SIWRDCP-1-15-L from Taratec) that was connected to the DELTA V system to monitor the water flux through the membrane. This analytical balance was used when constant feed and constant draw solution philosophy was simulated (discussed in detail below). In this study, this balance was not used as the volume of water lost to the draw solution tank was very low when compared to the starting volume and also the change in feed water conductivity was very low to alter the osmotic pressure differential. An analytical balance (Sartorius SIWRDCP-1-15-L from Taratec) was provided (refer to P&ID in Appendix 2), and this was used to monitor the weight of water permeating through the membrane from the feed tank to the draw solution tank from which water flux was calculated, and the balance was also connected to the DELTA V system. Two 5 L containers on the feed side as well as on the draw solution side were used to hold pH correction chemicals and the dosing of these chemicals was controlled by the DELTA V system (There was no pH correction done during this study). The DELTA V system was developed and was utilised to manage and maintain experimental conditions. Also, the DELTA V system was used to acquire and record signals from conductivity probes, pH probes, temperature probes, pressure sensors, pumps speed, as well as readings from analytical balances. ASPEN Process Explorers 2006.5-Aspen One software was used to record the DELTA V data. Stirrers were used to keep the feed and draw solutions homogeneous.

Potential vapour losses when using ammonium bicarbonate as a draw solution was managed by conducting the experiments at a maximum temperature of 30ºC as well as covering the tanks.

Figure 4-3 below shows a screenshot of a DELTA V system being used to control the FO experiments:

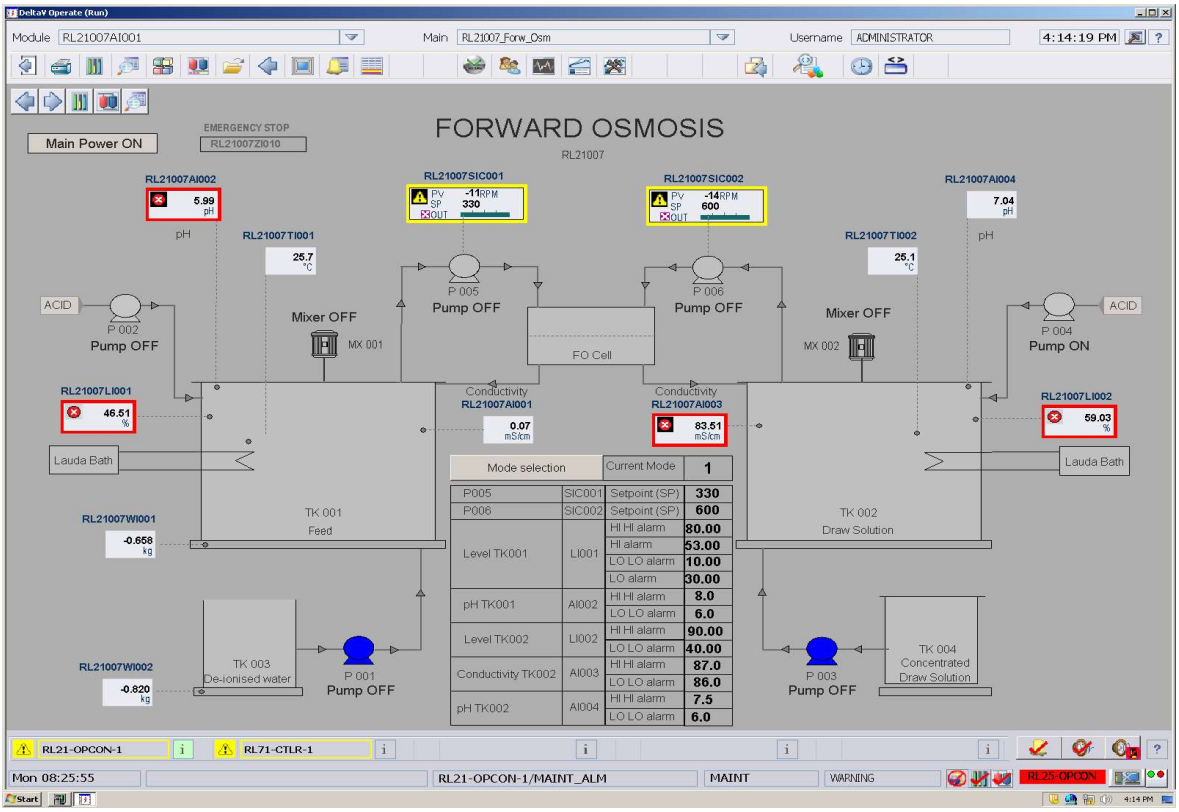

Figure 4-4: Screenshot for a DELTA V system during a typical experiment

4.2.2 Control Philosophy

The FO membrane cell system was designed to simulate the following scenario:

- Influence of constant feed and constant draw solution concentrations on forward osmosis process performance
- Influence of variable feed and constant draw solution concentrations on FO process performance
- Impact of variable feed and variable draw solution concentrations on FO process performance

Mode 1 was used during this phase of the study (description of the mode below must be read in together with the P&ID in Appendix 2).

Mode 1: Constant Feed Volume and Constant Draw Solution Conductivity

The tanks were filled with the relevant fluids before operation of the equipment.

The mass of the fluid in TK 001 and TK 003 were indicated by the electronic scales WI 001 and WI 002, respectively.

The temperature of the feed water in TK 001 was indicated by TI 001. The feed water was conveyed to the FO Cell ME 001 through a diaphragm pump P005. The speed of the diaphragm pump P005 was controlled by variable speed drive (VSD) SIC 001.
The contents of the tank were maintained homogenous by MX 001 which was operated at a constant speed.

The pH of the contents in TK 001 was indicated by pH meter AI 002, which has a low pH alarm AALL002 and a high pH alarm AAHH 002. When the pH of the contents in TK 001 exceeds the maximum setpoint, the alarm AAHH 002 was activated and triggers interlock I-06 to start the acid dosing pump P 002. When the pH of the contents in TK 001 reaches the minimum set point, the alarm AALL002 was activated and triggers the interlock I-05 to stop the acid dosing pump P002.
The conductivity of the contents in TK 001 was indicated by AI 001.

The level in TK 001 was indicated by LI 001 which had the following level alarms: level alarm high LAH 001, level alarm high high LAHH 001, level alarm low LAL 001 and level alarm low low LALL 001. The level in the tank TK 001 was maintained by dosing deionised water using P 001(there was no volume correction during these experiments as earlier). The deionised water dosing pump P 001 was started by I -12 which was activated by LAL 001 when the level in TK 001 drops below the low set point. When the level in TK 001 was above the high set point, LAH 001 was activated, which triggered I-13 to stop the pump P001. However, when the level in the tank exceeded its high high set point interlock I-01 was triggered to stop the feed pump P005 and the draw solution feed pump P006. If the level in TK001 dropped below the low low set point, the low-level alarm LALL 001 was activated and trigger interlock I- 02 to stop the feed pump P005 and the draw solution feed pump P006.

The draw solution in tank TK 002 was circulated through the FO cell ME 001 by diaphragm pump P006. The speed of pump P006 was controlled by the VSD SIC 002. The contents of the tank were maintained homogenous by MX 002 which was operated at a constant rate. The temperature of the feed water in TK 002 was indicated by TI 002.

The pH of the contents in TK 002 was indicated by pH meter AI 003, which had a low pH alarm AALL004 and a high pH alarm AAHH 004. When the pH of the contents in TK 002 exceeded the maximum setpoint, the alarm AAHH 004 was activated and triggered interlock I-08 to start the acid dosing pump P 004. When the pH of the contents in TK 002 reached the minimum set point, the alarm AALL004 was activated and triggers the interlock I-07 to stop the acid dosing pump P004.
The conductivity of the contents in TK 002 was controlled by AI 003. When the conductivity was below the minimum set point, the low conductivity alarm AALL 003 was activated, which triggered interlock

I-10 to start the concentrated draw solution pump P003. When the conductivity in TK 002 was above the maximum set point, high conductivity alarm AAHH 003 was activated, which triggered interlock I-09 to stop the concentrated draw solution pump P003.

The level in TK 002 was indicated by LI 002, which had a high high-level alarm LAHH 002 and a low low-level alarm LALL 002. When the level in the tank exceeded its maximum setpoint, interlock I-03 was triggered to stop P003 from dosing concentrated draw solution as well as the feed pump P005 and draw solution feed pump P 006. If the level in TK002 dropped below the minimum set point, the low, low-level alarm LALL 002 was activated and this triggered interlock I-04 to stop the draw solution feed pump P006 and feed pump P005.

4.2.3 Feed and Draw Solutions

Feed solutions used during this study ranged from deionised water to various concentrations of analytical grade sodium chloride depending on the parameter that was being evaluated. Analytical grade sodium chloride was also used as a draw solution for this study because it is simple, stable and easy to handle. Furthermore, this compound has been tested extensively in the literature, and as a result, there is a lot of data on its performance as a draw solution for FO process. Experiments using analytical grade ammonium bicarbonate as a draw solution were also conducted. The experimental results (for both sodium chloride and ammonium bicarbonate draw solutions) were only used for comparison purpose, and further separation of the draw solution was not considered as this was outside the overall scope of this project.

4.2.4 Membranes Tested

Two flat sheet FO membranes were tested during this study (i,e cellulose acetate and thin-film composite membranes). The first cellulose acetate (CA) membranes were prepared by Loeb and Sourirajan in the 1960s. These membranes (asymmetric CA membranes) have been used comprehensively in various applications such as RO. Hydration Technology Innovations (Beaudry, Thiel and York, 1999) developed and commercialised asymmetric cellulose-based membranes for FO applications for years. A commercially Cellulose Triacetate (CTA) specifically designed for osmotically driven processes was used for most of the experiments for the validation experiments. The CTAs membrane contains an inserted support screen and has a thick rejection layer (10-20 μm) which is thicker than commercially available composite membranes. However, this membrane has outperformed other commercially available membranes in osmotically driven membrane processes. The hydrophilic nature of the membrane ensured proper wetting and reduced ICP and increases water flux in osmotically driven membrane processes. It is for this reason that the HTI-CTA membrane has been comprehensively used in the research of osmotically driven membrane processes.

The HTI CTA membrane is not appropriate in many applications due to limited pH tolerance (pH 3-8) (Alsvik and Hagg, 2013).

The second membrane used in this study was a commercially available thin-film composite (TFC) membrane also manufactured by HTI (Smoke, 2012; Alsvik and Hagg, 2013). Membranes were wetted before used as indicated in the data sheets (refer to Appendix 2). Table 4-1 below summarises the HTI membranes physical and chemical properties (Coday et al., 2013).

Table 4-1: HTI Membrane Physical and Chemical Properties (adapted from Coday et al., 2013)

Membrane Parameter	unit	CTA	TFC
Pure water permeability coefficient (*A*)	L. $m^{-2}.h^{-1}bar^{-1}$	0.55	1.63
Salt Permeability coefficient (*B*)	m/s	$4.8x10^{-8}$	$8.3x10^{-8}$
Structural Parameter (*S*)	µm	463	690
Zeta Potential, Rejecting/Active layer	mV	-34.9	-38.6
Zeta Potential, Support layer	mV	-39.5	-9.5
Contact Angle		63.7	27.7

- *For a membrane to achieve high water flux in FO, a membrane should have a high water permeability coefficient (A)*
- *The salt permeability coefficient (B) need to be as low as possible to manage the diffusion of draw solution salts to the feed solution.*
- *Structural Parameter (S) also need to be as low as possible to manage ICP.*

4.2.5. Experimental Conditions

All experiments were conducted for a period of 2 hrs and single run was performed for each experiment combination. The cross-flow rates for the feed and draw solutions ranged from 1.5 L/min (33.3 $cm.s^{-1}$) to 2.7 L/min (60 $cm.s^{-1}$), maintained the same for both the feed and draw sides during each experiment. Co-current cross-flow was applied to both the feed and draw sides to find the effects on the FO performance. All the experiments were conducted under a co-current cross-flow mode.

The experimental temperature ranged from room 25ºC to 35ºC, being maintained the same for both the feed and draw solutions during the experiments. Only in experiments designed to investigate the effect of temperature on the FO performance, different temperatures were applied to feed and draw solutions.

Membranes were tested with either the active layer facing the feed solution (deionised water or sodium chloride) (FO) and the support layer in contact with the draw solution or active layer facing the draw solution (sodium chloride or ammonium bicarbonate) (PRO mode) and support layer facing the feed solution. This was done to quantify the impact of membrane orientation on FO performance. Tables 1, 2, 3, 4, 5, 6 and 7 in Appendix 2 shows the details of experimental conditions matrix used to evaluate the impact of various factors on FO performance. Descriptive statistics summaries for each run combination investigated are also appended (Appendix 2).

4.2.6 Calculation of Mass Transport

4.2.6.1 Determination of Water Flux

Water flux was calculated by monitoring the change in mass of the feed solution in TK 001 (deionised water or sodium chloride) on the analytical balance (WI 001, Sartorius SIWRDCP-1-15-L from Taratec). The gradient of mass versus time is the mass transfer rate through the membrane for a particular experiment.

Water flux (Jw) (L. $m^{-2}.h^{-1}$) was calculated by dividing the mass transfer rate by the water density and membrane surface area using the equation below (Tang, 2009; Cath et al., 2013; Hancock and Cath, 2009):

Equation 4-1

$$J_w = \frac{\Delta V_{feed}}{A_m X \Delta t} = \frac{\frac{\Delta m_{feed}}{\rho_{feed}}}{A_m X \Delta t}$$

Where ΔV_{feed} and Δm_{feed} is the change in volume and change in weight of the feed solution, respectively. ρ_{feed} represents the density of the feed solution and Δt represents the change in time (from the beginning to the end of the experiment).

4.2.6.2 Determination of Salt/Solute Flux

Salt Flux of the system was determined by quantifying the change in the conductivity of the feed solution after steady-state was reached, and over a selected time interval. A conductivity probe with K=1 cm^{-1} cell constant was specifically calibrated for diluted sodium chloride solutions.

There was a linear increase in the conductivity of the feed solution as a function of time as a result of the salts from the draw solution diffusing into the feed solution.

Salt flux (Js) was determined by first converting the feed solution conductivity to concentration using conversion factor derived from the linear relationship between the conductivity and the concentration (refer to the calibration curve of conductivity versus salt concentration for NaCl in Appendix 2). Salt flux was then calculated using the equation below (Xie et al., 2012):

Equation 4-2

$$J_s = \frac{V_t C_t - V_0 C_0}{A_m X \Delta t}$$

Where V_0 and V_t is the initial and final volume of the feed solutions respectively; C_0 and C_t represents the initial and final salt concentration in the feed solution respectively.

4.3 Results and Discussion

A series of experiments were undertaken to obtain a fundamental understanding of the FO process, using the laboratory-scale FO system operating under a variety of conditions, as described in section 4.2. Water flux and reverse salt flux were measured to examine the effects of various experimental conditions such as membrane orientation, temperature, flow rates, draw solute concentration, feed water concentration and membrane type (Experimental conditions are summarised in Tables 1, 2 and 3 in Appendix 2). This study was conducted primarily to evaluate and understand the fundamental characteristics of the FO process.

Analysis of the data collected during the experiment showed that water fluxes stabilise after about 30 minutes and it was for this reason that the data used to measure the parameters of interest were the data collected after 30 minutes had elapsed. Statistical analyses were conducted on the data.

The distribution of each variable is visually presented using standard box and whisker plots (maximum and minimum values, 25 percentile (bottom of the box), median (middle line in the box), average (black dotted line in the box) and 75 percentile (top of the box)).

Summary of the descriptive statistic for each experimental condition is presented in Appendix 2 (Table 9, 10 and 11)

4.3.1 Impact of FO Membrane Configuration on Water Flux and Reverse Salt Flux.

Figure 4-5 & 4-6 shows the water fluxes and salt fluxes, respectively, when the FO-CTA membrane was tested with the active layer facing the deionised water (AS-DI) and active layer facing the draw solution (AS DS) when using a 1 M NaCl as a draw solution

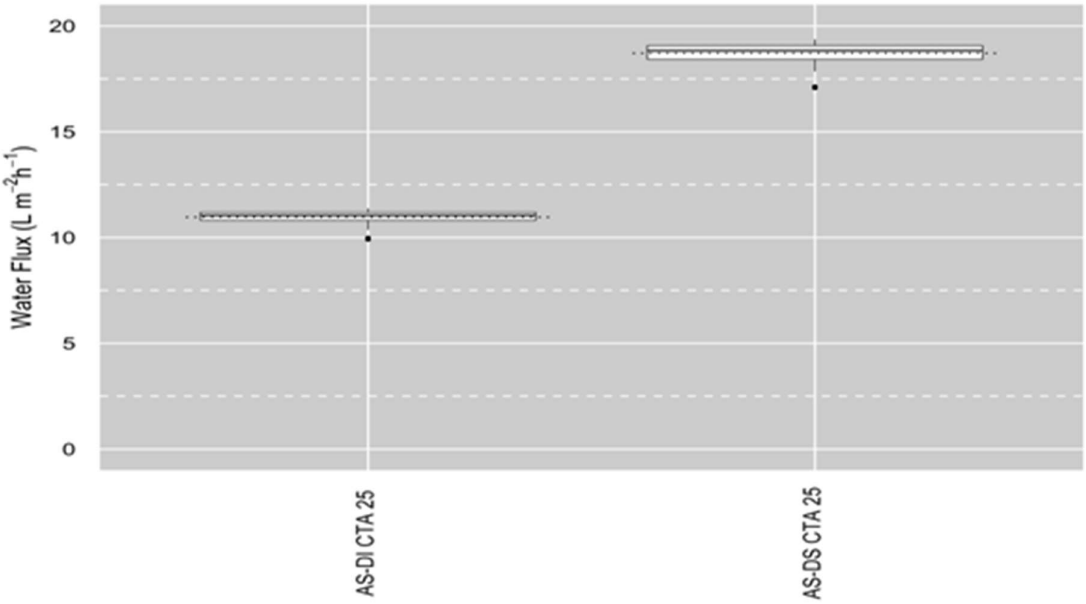

Figure 4-5: Impact of membrane configuration on the water flux (Feed solution: DI; Draw solution: 1 M NaCl; Co-current cross flow rate: 1.5 L/min; Temperature (DI and DS): 25ºC)

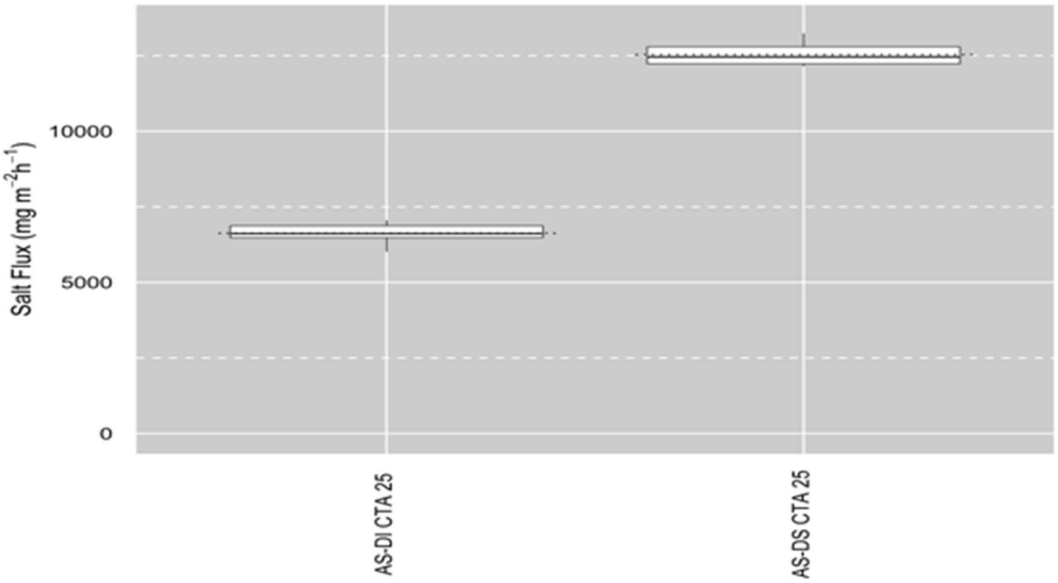

Figure 4-6: Impact of membrane configuration on the salt flux (Feed solution: DI; Draw solution: 1 M NaCl; Co-current cross flow rate: 1.5 L/min; Temperature (DI and DS): 25ºC)

By comparing the water fluxes and salt fluxes obtained under different membrane orientation, it was clear that the average water and salt fluxes obtained by the FO-CTA membrane under the AS-DS orientation (mean =18.71, SD = 0.5 $L.m^{-2}.h^{-1}$ and mean = 12540, SD = 356 $mg.m^{-2}.h^{-1}$, respectively) were consistently higher than those obtained under AS-DI orientation (mean = 10.96, SD = 0.3 $L.m^{-2}.h^{-1}$ and mean =6626, SD = 318 $mg.m^{-2}.h^{-1}$, respectively) under similar conditions. This is because the impact of the ICP experienced under AS-DS orientation is smaller when compared to that of AS-DI orientation (Cath et al., 2006; Chen, 2011/12). This indicates that dilutive ICP (experienced in AS-DI orientation) was more severe than the concentrative ICP (experienced in AS-DS orientation). Under the AS-DI orientation, the water dilutes the concentration of the draw solution within the porous membrane structure, resulting in a reduced effective osmotic pressure gradient, subsequently leading to lower water flux and salt flux.

It is also essential to note that due to the fact that the ratio between solute reverse flux and water flux should stay fairly constant (function of the membrane), higher water flux in the AS-DS mode may contribute to higher salt flux. The impact of ICP on FO water flux was discussed in detail in Chapter 2.

4.3.2 Impact of Feed and Draw Solution Temperature on Water Flux and Reverse Salt Flux.

Figures 4-7 & 4-8 shows the impact of temperature on water and salt fluxes when the FO-CTA membrane was operated with the dense layer or active layer facing the deionised water (AS-DI) and a dense layer or active layer facing the draw solution (AS-DS) using 1 M NaCl as a draw solution.

The temperature of the solution has a notable impact on FO process water and salt flux. The permeability of the water and salt through the FO membrane increases as the temperature increases (Baker, 2004; Mulder, 1996; McCutcheon et al., 2006; Garcia-Castello et al., 2009). The viscosity of water decreases at higher temperatures, which in turn increases the rate of water and salt diffusion through the membrane. Increasing the temperature leads to higher solute diffusion due to the increased solute diffusivity. Moreover, increasing the temperature leads to faster dissolution of the solutes into the membrane such that even hydrophobic neutral solutes absorb into the membrane at an order of magnitude higher rate at elevated temperatures. Fluxes (water and salt) are therefore inversely proportional to water viscosity, so the higher the temperature, the lower the water viscosity and the higher the flux. The temperature of the solution also influences osmotic pressure. As the temperature of the solution increases, the osmotic pressure of the solution also increases (Kim and Park, 2010).

It was clear from Figures 4-7 and 4-8 that increasing the temperature does have a positive impact on the FO water flux and salt flux. The water and salt fluxes for the AS-DI orientation showed an increase when the temperature was varied from 25ºC to 35ºC (mean = 10.96, SD = 0.3 $L.m^{-2}.h^{-1}$ and mean = 6626, SD = 318 $mg.m^{-2}.h^{-1}$, respectively to mean = 13.96, SD = 0.3 $L.m^{-2}.h^{-1}$ and mean = 8506, SD = 335 $mg.m^{-2}.h^{-1}$, respectively). These graphs represent the water flux and salt flux in the presence of dilutive ICP (for AS-DI) because DI water was in contact with the dense layer while the NaCl draw solution was in contact with the porous support layer. Under this orientation (AS-DI), ICP occurs within the porous support layer (Elimelech and McCutcheon, 2006).

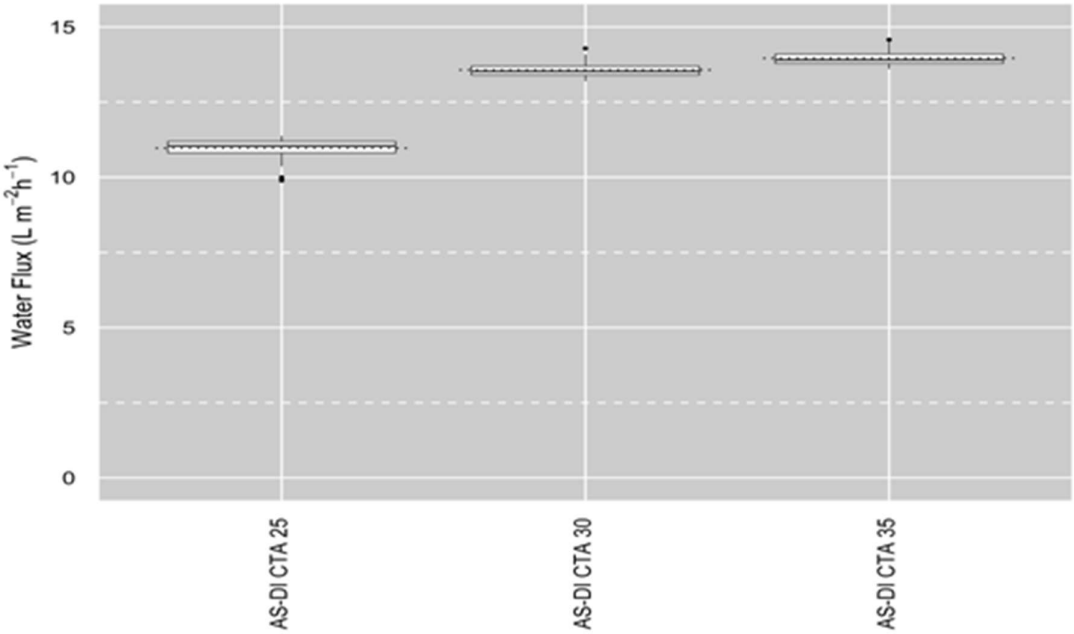

Figure 4-7: Impact of feed and draw solution temperature on the water flux (Membrane Orientation: AS-DI; Feed solution: DI; Draw solution: 1 M NaCl; Co-current cross flow rate: 1.5 L/min; Temperature (DI and DS): 25, 30, 35ºC)

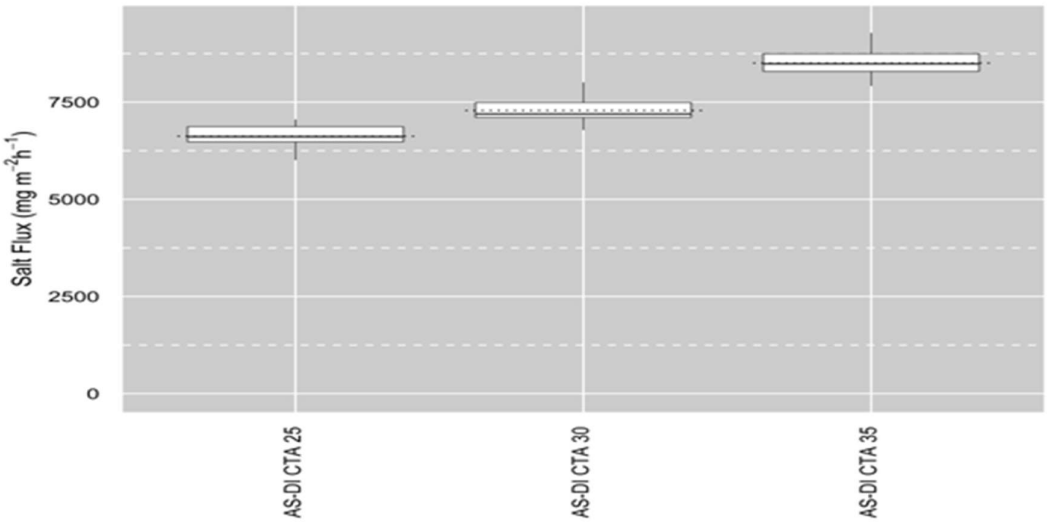

Figure 4-8: Effects of temperature on the salt flux (Membrane Orientation: AS-DI; Feed solution: DI; Draw solution: 1 M NaCl; Co-current cross flow rate: 1.5 L/min; Temperature (DI and DS): 25, 30, 35ºC)

Similarly, it was clear from Figures 4-9 and 4-10 that increasing the temperature does have a positive impact on the FO water flux and salt flux.

The average water and salt fluxes for the AS-DS orientation increased (from mean = 18.71, SD = 0.5 $L.m^{-2}.h^{-1}$ and mean = 12540, SD = 356 $mg.m^{-2}.h^{-1}$, respectively to mean = 22.64, SD = 0.2 $L.m^{-2}.h^{-1}$ and mean = 15260, SD = 453 $mg.m^{-2}.h^{-1}$) when the temperature was varied from 25ºC to 35ºC. These graphs represent the water flux and salt flux in the presence of concentrative ICP (for AS-DS) because DI water was in contact with the support layer while the NaCl draw solution was in contact with the dense layer.

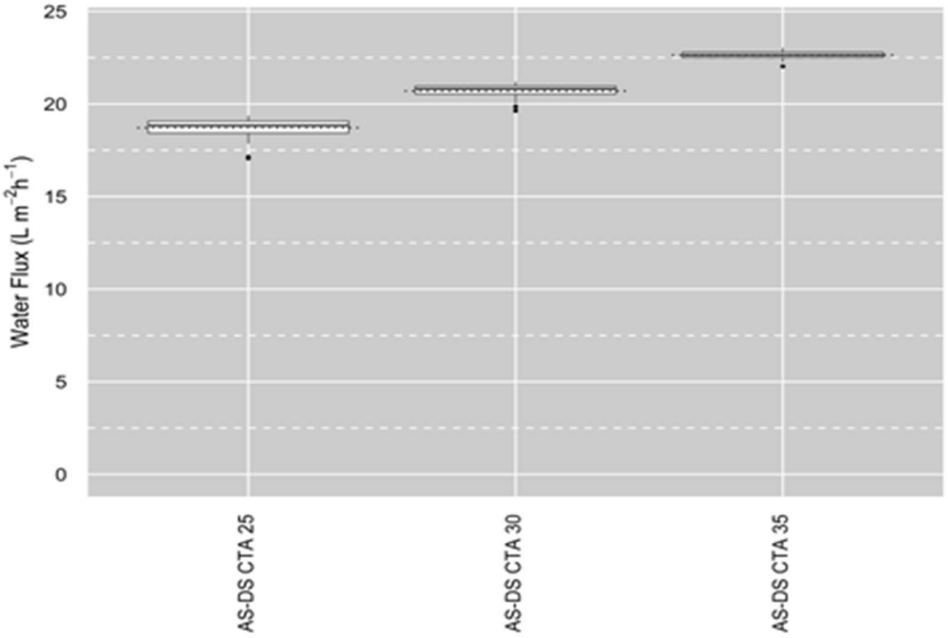

Figure 4-9: Impact of feed and draw solution temperature on the water flux (Membrane Orientation: AS-DS; Feed solution: DI; Draw solution: 1 M NaCl; Co-current cross flow rate: 1.5 L/min; Temperature (DI and DS): 25, 30, 35ºC)

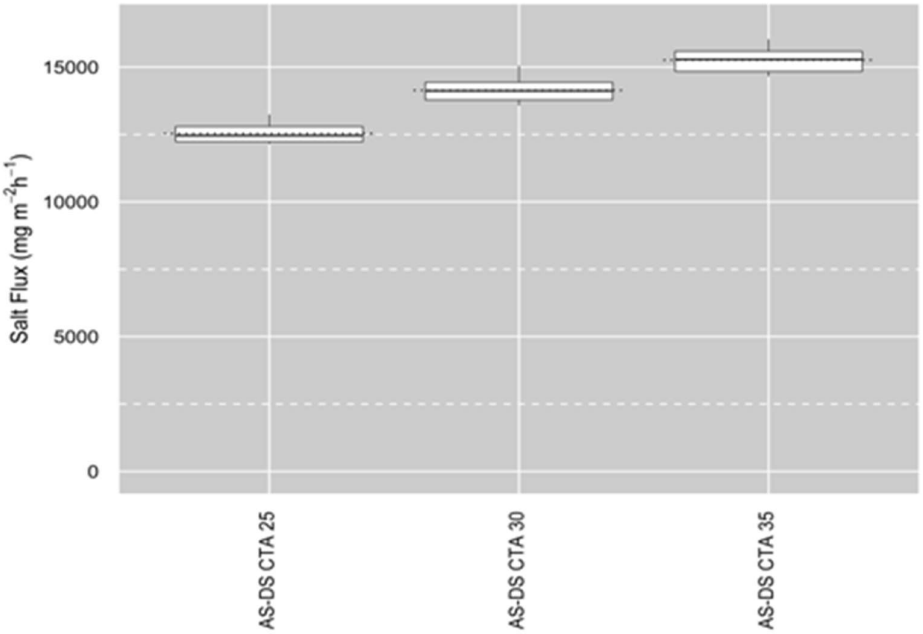

Figure 4-10: Effects of temperature on the salt flux (Membrane Orientation: AS-DS; Feed solution: DI; Draw solution: 1 M NaCl; Co-current cross flow rate: 1.5 L/min; Temperature (DI and DS): 25, 30, 35ºC)

It is worth noting that the improvements in fluxes due to increased temperature were marginal and this could be attributed to the ICP and ECP phenomenon which might still be playing a significant role at these temperatures (Liu, 2009).

4.3.3 Effects of Cross-flow Rate on Water Flux and Reverse Salt Flux.

Figure 4-11 shows the impact of cross-flow rate on water fluxes when the FO-CTA membrane was operated with the dense layer or active layer facing the deionised water (AS-DI).

It is theorised that the cross-flow rates of the FO experiments can affect the water flux. It was apparent in Figure 4-11 that as the cross-flow rate was increased from 1.5 to 2.7 L/min, the water flux also increased (average water flux increased from mean = 10.96 $L.m^{-2}.h^{-1}$ SD = 0.3 to mean = 13.18 SD = 0.4 $L.m^{-2}.h^{-1}$). The average salt flux increased from mean 6626 (SD = 318) to mean 6963 (SD = 245) $mg.m^{-2}.h^{-1}$, respectively, when the flow rate was increased from 1.5 to 2.7 L/min (refer to statistical description section in Appendix 2). Draw solution and Feed solution cross-flow rate affect ECP and draw solution cross-flow rate may indirectly affect ICP; and consequently, impact the water flux. This is because when the cross-flow rate is increased, higher turbulence in the flow channel decreases the impact of both ECP and ICP on the membrane performance.

In this study, ECP was minimised because deionised water was used as feed solution, and this implies that the increase in water flux observed was due to the impact of increased flow rate on ICP. Studies conducted by Hancock et al. showed that increasing the cross-flow rate on the feed solution side and draw solution side does have an impact on either the water flux or salt flux (Hancock and Cath, 2009; AL-Hemiri et al., 2009).

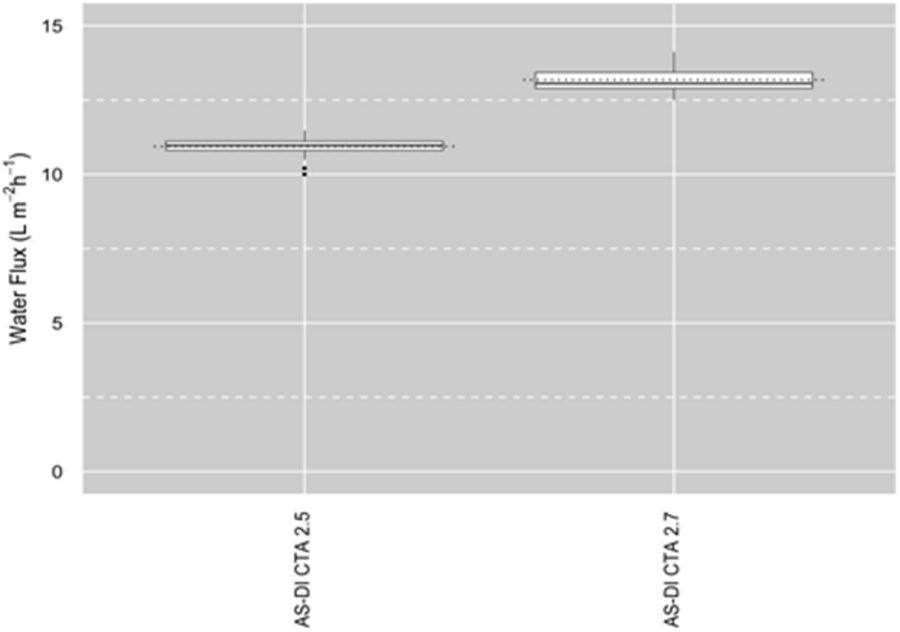

Figure 4-11: Effects of flow rate on the water flux (Membrane Orientation: AS-DI; Feed solution: DI; Draw solution: 1 M NaCl; Co-current cross flow rate: 2.5 & 2.7 L/min; Temperature (DI and DS): 25ºC).

4.3.4. Evaluation of the impact of using TFC membrane on Water Flux and Salt Flux.

Figure 4-12 and 4-13 shows the results obtained when evaluating the impact of using TFC membrane (under different membrane orientation) on Water Flux and Salt Flux.

By comparing the water fluxes and salt fluxes obtained under different membrane orientation, it is clear that average water and salt fluxes obtained using the FO-TFC membrane under the AS-DI orientation (mean = 14.8, SD = 0.3 L. $m^{-2}.h^{-1}$ and mean = 7812, SD = 118 $mg.m^{-2}.h^{-1}$, respectively) were consistently lower than those obtained under AS-DS orientation (mean = 30.69, SD = 0.2 $L.m^{-2}.h^{-1}$ and mean = 17920, SD = 661 $mg.m^{-2}.h^{-1}$, respectively) under similar conditions. This was because the impact of the ICP experienced under AS-DS orientation was smaller when compared to that of AS-DI configuration. This implies that dilutive ICP (experienced in AS-DI orientation) was more dominant than the concentrative ICP (experienced in AS-DS orientation).

Under the AS-DI configuration, the water permeating from the feed solution dilutes the concentration of the draw solution within the porous membrane structure, thereby causing a reduction in effective osmotic pressure differential, leading to lower water flux and salt flux.
It is also worth noting that the reverse salt flux was higher during the AS-DS orientation when compared to AS-DI orientation, mainly due to the ICP effects. Because the ratio between reverse solute flux and water flux is constant, higher water flux in the AS-DS configuration could contribute to higher salt flux.

When compared to the water fluxes obtained using the FO CTA membrane (evaluated in section 4.3.1-4.3-3), the FO TFC membrane produced higher fluxes, albeit not as high as those claimed by the membrane supplier. The higher water fluxes were supported by the high-water permeability for the TCF membrane when compared to the CTA membrane (refer to Table 4-1). Furthermore, the reverse salt flux observed on the FO TFC membrane was higher than those claimed by the membrane suppliers. Even though the performance observed using the FO TFC membrane did not match those claimed by the supplier, the water fluxes obtained shows that this membrane could be a viable alternative to the FO CTA membrane. Also, the high pH range (2-11) open the opportunity of applying the FO process to other applications. Water flux data on the FO TFC membrane reported elsewhere was also lower than that claimed by HTI (Kim and Park, 2011).

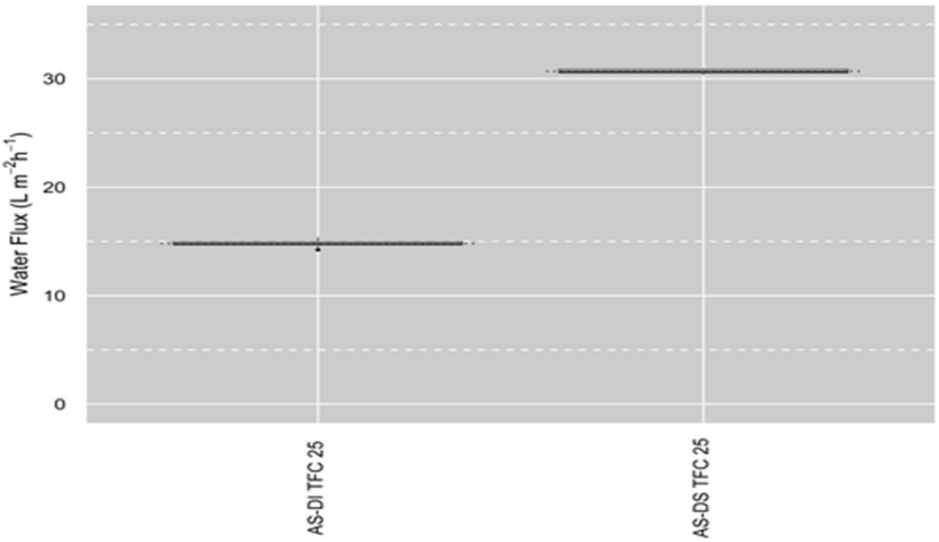

Figure 4-12: Impact of using TFC membrane under different configuration on the water flux (Membrane Orientation: AS-DI & AS-DS; Feed solution: DI; Draw solution: 1 M NaCl; Co-current cross flow rate: 1.5 L/min; Temperature (DI and DS): 25ºC).

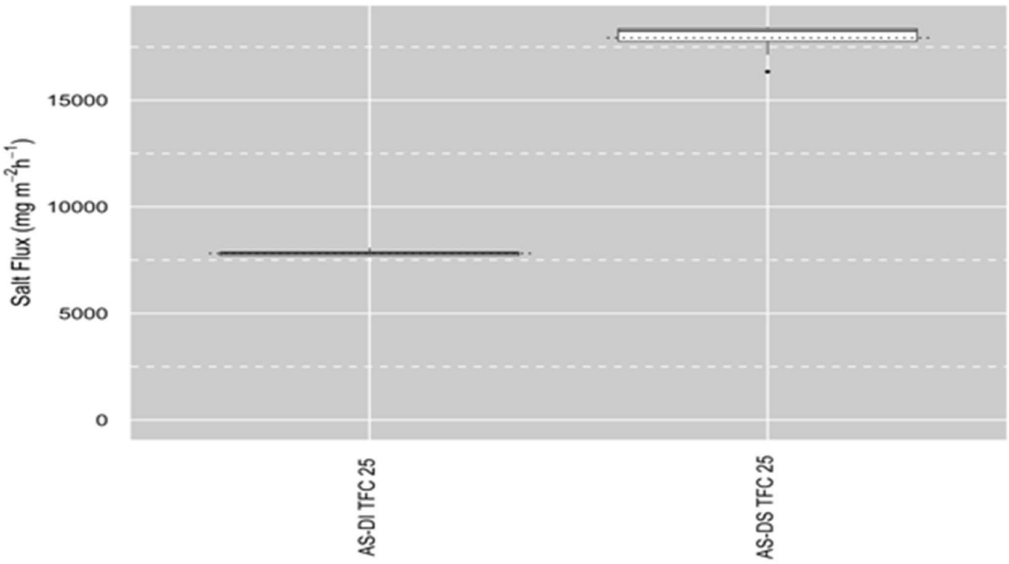

Figure 4-13: Impact of using TFC membrane under different configuration on the salt flux (Membrane Orientation: AS-DI & AS-DS; Feed solution: DI; Draw solution: 1 M NaCl; Co-current cross flow rate: 1.5 L/min; Temperature (DI and DS): 25ºC).

4.3.5 Impact of Draw Solution Concentration on FO Water Flux and Salt Flux

Figure 4-14 & 4-15 shows the impact of draw solution concentration on water and salt fluxes when the FO-CTA membrane was operated with the dense layer or active layer facing the deionised water (AS-DI).

The experiments were conducted using draw solutions with concentration ranging from 2 g/L to 70 g/L to examine the reliance of water flux and salt flux on NaCl concentration. The results of these experiments plotted in Figure 4-14 and 4-15 show that, as expected, water flux and salt flux increased with increasing draw solution concentration (AL-Hemiri et al., 2009; McCutcheon and Elimelech, 2007; McCutcheon et al., 2006; Achilli et al., 2010). In FO process, the rate of water permeation through the FO membrane is directly proportional to the osmotic pressure differential, which is influenced by the concentration of the draw solution. Increasing the concentration of draw solution enhances permeate flux due to increased driving force. However, increase in reverse solute flux is also expected to compensate the high-water flux observed in order to maintain the specific reverse solute flux (equation 5-1, discussed in detail in Chapter 5, section 5.9) of the membrane, as this parameter an intrinsic parameter of the membrane (Phillip, Yong and Elimelech, 2010; Hancock and Cath, 2009; She, 2016).

According to water flux equation 2-1 (Chapter 2), the increase in water flux should be linear with osmotic pressure difference and be a function of solute concentrations on both sides of the FO membrane. The relationship between water flux and osmotic pressure difference was, however, nonlinear in this experiment (Figure 4-14 (a and b)). In FO, the greater the differences in osmotic pressure as a driving force, the faster water moves through the membrane. Figure 4-14 shows greater permeate flow rate with a more concentrated draw solution. High osmotic pressure differential (i.e. high driving force) result in high water fluxes which generally cause more pronounced concentration polarisation effects (Chen, 2011/12; McCutcheon and Elimelech, 2007; McCutcheon et al., 2006), and a decrease in draw concentration facing porous support layer cause the ICP effects to be more severe. Salt flux (Figure 4-15) was expected to be linear according to equation 2-4. The concentration polarisation was responsible for nonlinear relationship observed for both the water flux and salt flux trend. The salt flux appears to decrease at very high DS concentrations. This was possibly an artefact, and it was also showing on the last point of the trend/graph. A comment was going to be made if more points were showing a decreasing trend.

(a)

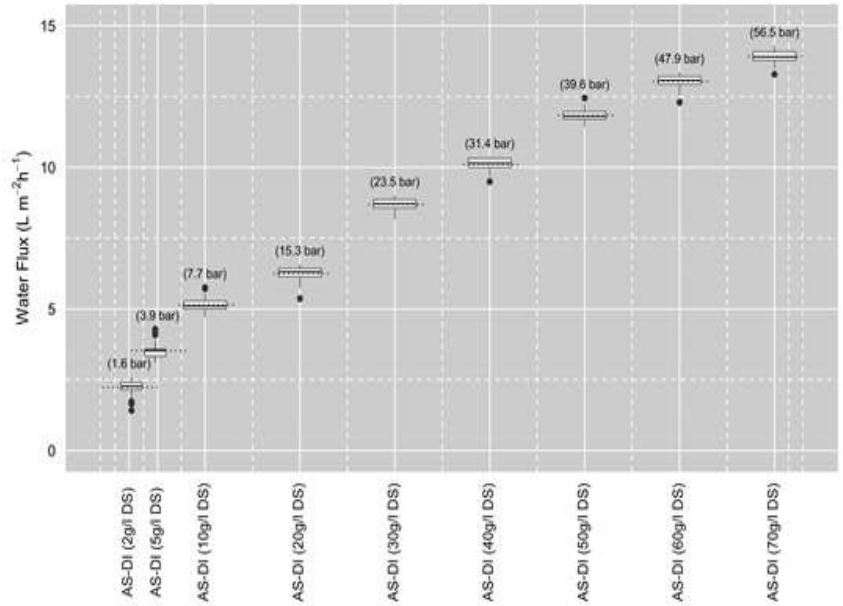

(b)

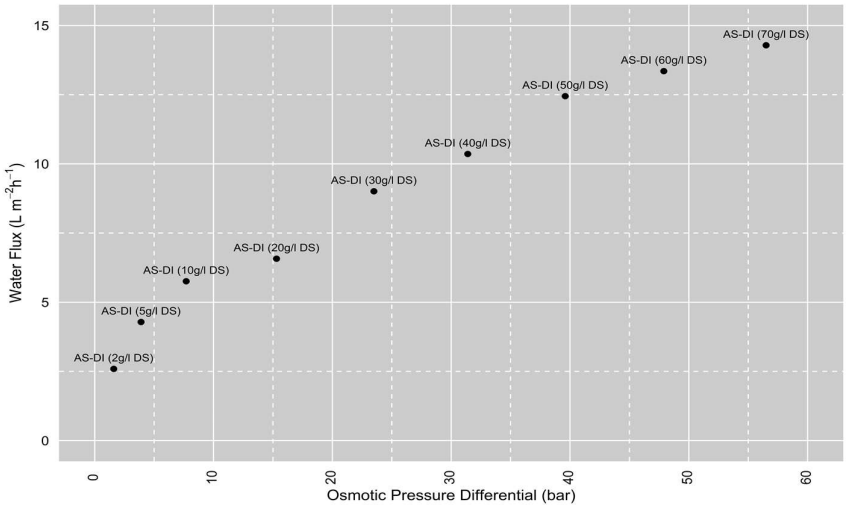

Figure 4-14: The impact of draw solution concentration on water flux (Membrane Orientation: AS-DI; Feed solution: DI; Draw solution: 2 g/L to 70 g/L NaCl; Co-current cross flow rate: 1.5 L/min; Temperature (DI and DS): 25ºC).

The values in brackets represent the osmotic pressure differential calculated using bulk osmotic pressures of the draw solution and deionised water (the osmotic pressure of DI was assumed to be 0). The bulk osmotic pressure differences of the draw solution and DI were calculated using a commercial software from OLI Systems Inc. (Olisystems.com, 2011).

(a)

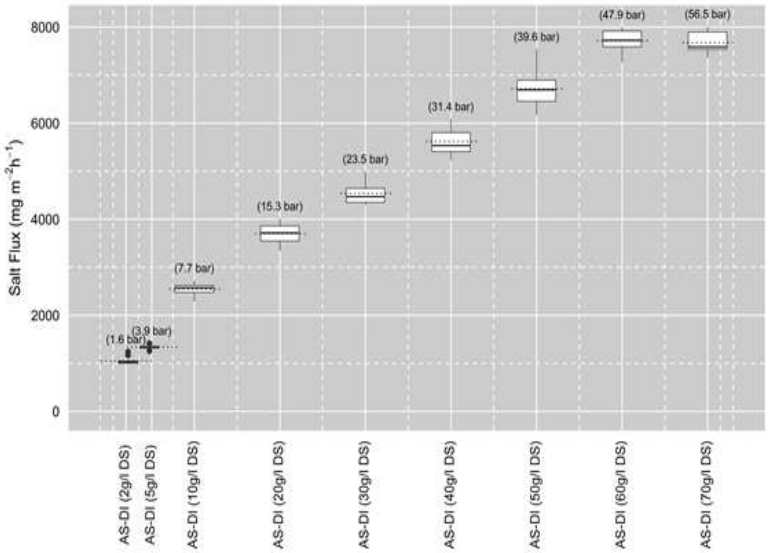

(b)

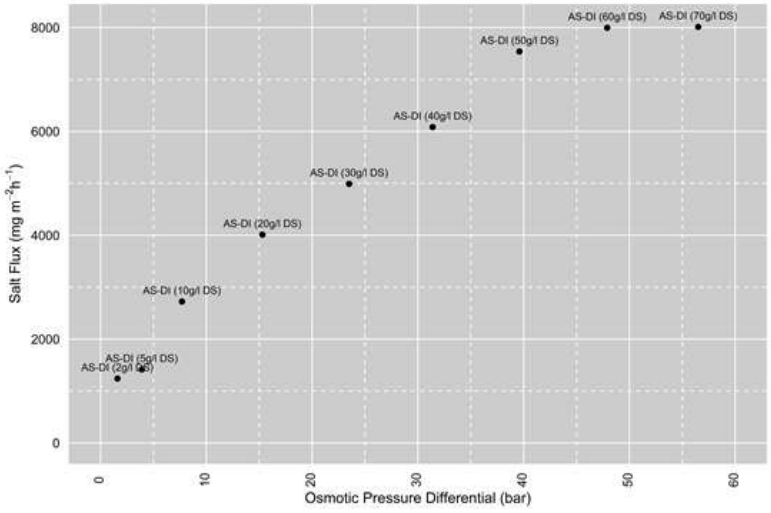

Figure 4-15: The impact of draw solution concentration on salt flux (Membrane Orientation: AS-DI; Feed solution: DI; Draw solution: 2 g/L to 70 g/L NaCl; Co-current cross flow rate: 1.5 L/min; Temperature (DI and DS): 25ºC).

The values in brackets represent the osmotic pressure differential calculated using bulk osmotic pressures of the draw solution and deionised water (the osmotic pressure of DI was assumed to be 0). The bulk osmotic pressure differences of the draw solution and DI were calculated using commercial software from OLI Systems Inc. (Olisystems.com, 2011).

The specific reverse solute flux (SRSF), a ratio of reverse solute flux (J_s) to forward water flux (J_w), a measure of membrane selectivity was calculated for the data presented in Figure 4-14 and 4-15. The graph showing the specific reverse solute flux trend for the data presented is shown in Appendix 2. The calculated ratio ranged between 400 and 590 mg/L. The calculated ratio was within the range of 400-600 mg/L reported by HTI for the CTA membrane (Coday, 2013 & HTI data sheet appended). The specific reverse solute flux is in general a constant value for a given membrane and is only dependent on the membrane intrinsic separation properties and working temperature. Theoretically, specific reverse solute flux is independent of the operating conditions, such as DS and FS concentration, membrane orientation and hydrodynamic conditions. In reality, the experimentally measured specific reverse solute flux may show some changes because the membrane separation properties may change with operating conditions and solution chemistry.

4.3.6 Impact of Feed Solution Concentration on FO Water Flux

Figure 4-16 shows the impact of feed solution concentration on water flux when the FO-CTA membrane was operated with the dense layer or active layer facing the deionised water (AS-DI).

Figure 4-16 shows that at constant draw solution concentration, as the concentration of the feed solution was increased, the measured water flux decreases. The experiments were conducted using feed solutions with concentration ranging from 10 g/L to 105 g/L to examine the dependency of water flux on feed concentration. As it was the case with the results discussed in section 4.3.5, the relationship between water flux and osmotic pressure differential was nonlinear, potentially due to both the concentrative ECP and dilutive ICP. Upon addition of different concentrations of NaCl on the feed side, flux decreases potentially due to the combined effect of reduced osmotic pressure driving force and concentration polarisation (ECP and ICP) (McCutcheon and Elimelech, 2007; McCutcheon et al., 2006; AL-Hemiri et al., 2009).

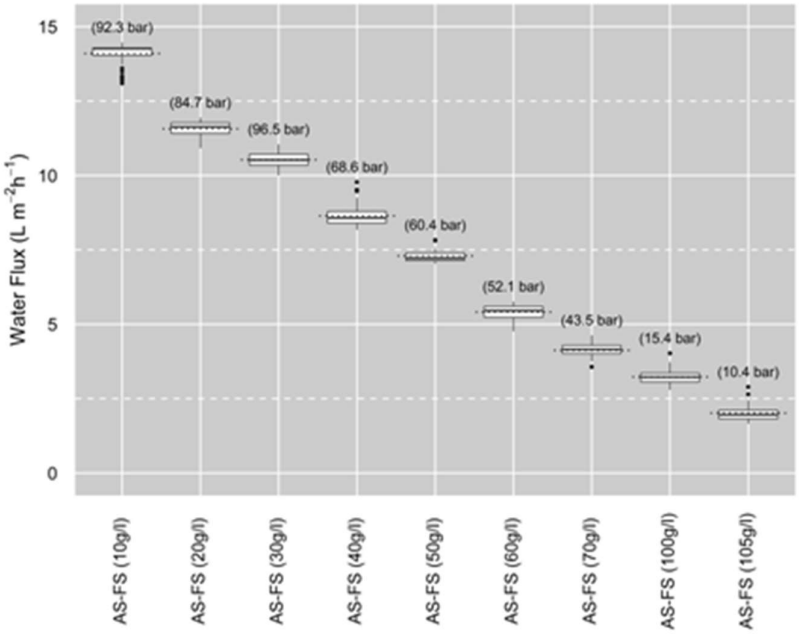

Figure 4-16: The impact of feed solution concentration on water flux (Membrane Orientation: AS-DI; Feed solution: 10 g/L to 105 g/L NaCl; Draw solution: 116 g/L NaCl; Co-current cross flow rate: 1.5 L/min; Temperature (Feed Solution and DS): 25ºC).

The values in brackets represent the osmotic pressure differential calculated using bulk osmotic pressures of the draw solution and deionised water (the osmotic pressure of DI was assumed to be 0). The bulk osmotic pressure differences of the draw solution and DI were calculated using commercial software from OLI Systems Inc. (Olisystems.com, 2011).

4.3.7 Effect of temperature, feed and draw solution concentration, membrane configuration and cross flow velocity on Forward Osmosis using Ammonium Bicarbonate as a draw solution.

Several experiments were also carried out to obtain a fundamental understanding of the FO process using ammonium bicarbonate as a draw solution instead of sodium chloride. Impact of FO membrane configuration, feed and draw solution temperature, draw solution concentration and feed solution concentration were evaluated (Experimental conditions are summarised in Tables 4, 5, 6 and 7 in Appendix 2). Summary of the descriptive statistic for each experimental condition is presented in Appendix 2 (Table 12, 13 and 14). Figure 4-17 below shows a graphical overview of the results obtained from the experiments. The graphs below show that membrane orientation, temperature, draw solution concentration and feed water concentration plays a role in the forward osmosis process.

The results obtained show the same trend with what was observed when sodium chloride was used as a draw solution (section 4.3.1-4.3.6).

Ammonium Bicarbonate draw solution has been extensively investigated by Elimelech and co-workers for FO application (Cath et al., 2006; McCutcheon et al., 2005, McCutcheon et al., 2006; Phillip et al., 2010). What was also notable from the results obtained when using ammonium bicarbonate as the draw solution was the high reverse flux when compared to sodium chloride. The main advantage of ammonium bicarbonate as a draw solution is that the draw solution can be recovered thermally. When heated to around 60ºC, NH_4HCO_3 solution decomposes to form ammonia and carbon dioxide gases, which could then be separated from the treated water. The NH_4HCO_3 draw solution could be regenerated by dissolving the ammonia and carbon dioxide gases back into the water. Given the fact that NH_4HCO_3 decomposes at low temperature the energy required in its recovery could be obtained from low-grade waste heat in the industries (e.g. Power Generation, Petrochemical, Pulp and Paper) (Jang, 2010). Subsequently, ammonium bicarbonate is being used on full scale as a draw solution in FO based membrane concentration of various wastewater streams because high water flux, water recovery could be achieved because of high osmotic pressure generated by NH_4HCO_3 (Pendergast et al., 2016; Pendergast et al., 2015)

(a)

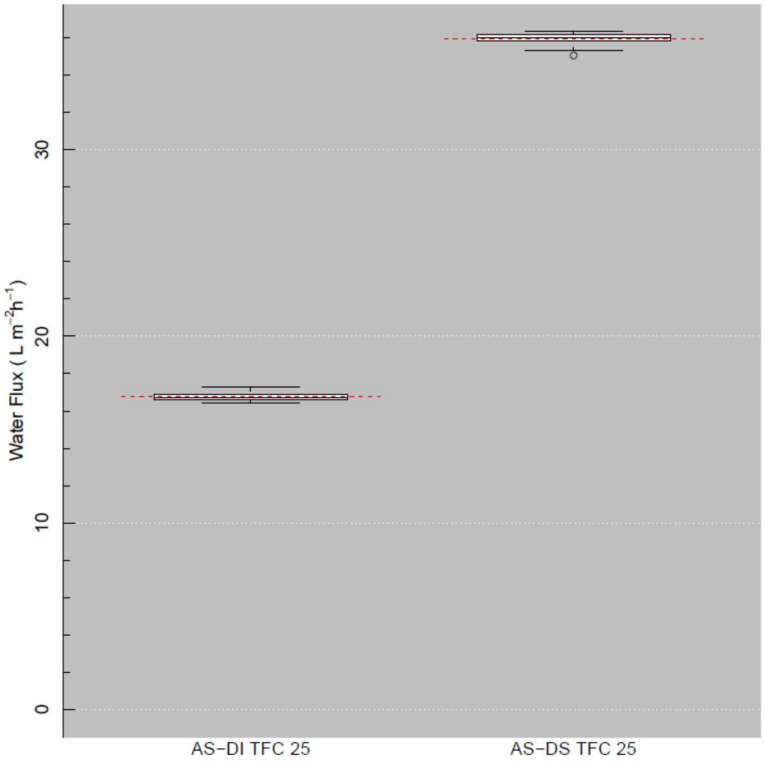
Water Flux (L m^{-2}h^{-1})
0
10
20
30
AS-DI TFC 25
AS-DS TFC 25

(b)

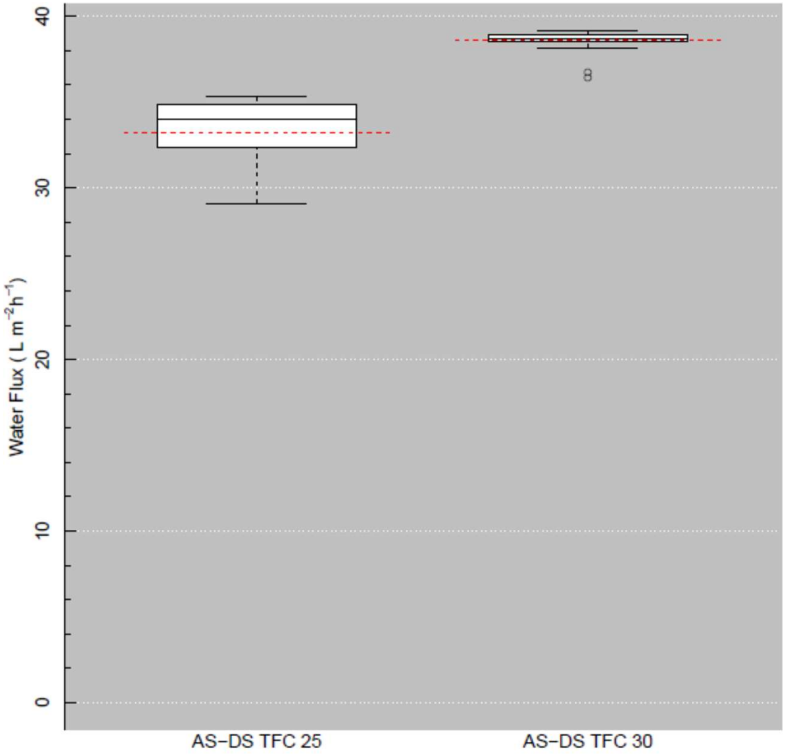
Water Flux (L m^{-2}h^{-1})
0
10
20
30
40
AS-DS TFC 25
AS-DS TFC 30

(c)

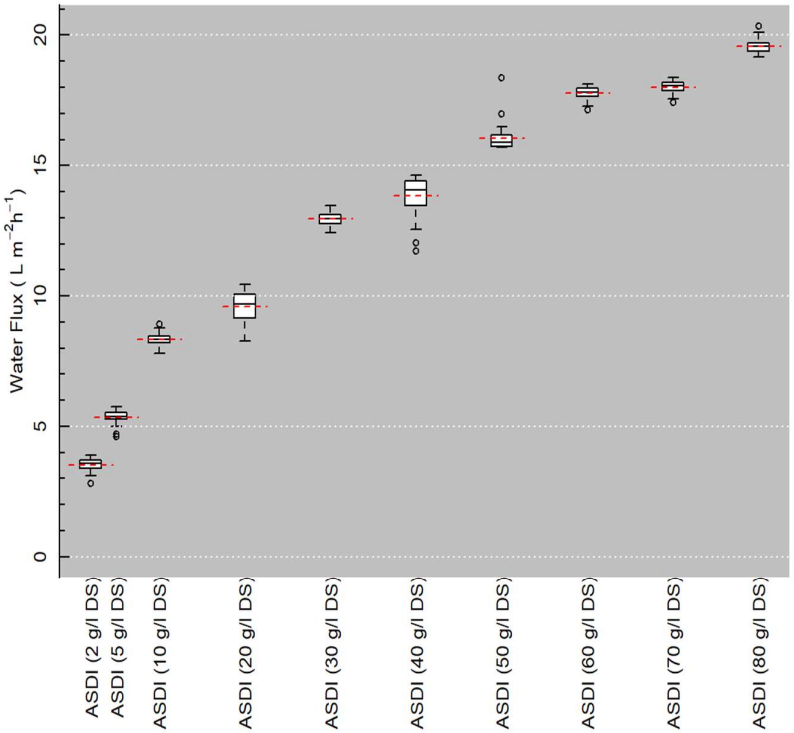
Water Flux (L m^{-2}h^{-1})
0
5
10
15
20
ASDI (2 g/l DS)
ASDI (5 g/l DS)
ASDI (10 g/l DS)
ASDI (20 g/l DS)
ASDI (30 g/l DS)
ASDI (40 g/l DS)
ASDI (50 g/l DS)
ASDI (60 g/l DS)
ASDI (70 g/l DS)
ASDI (80 g/l DS)

(d)

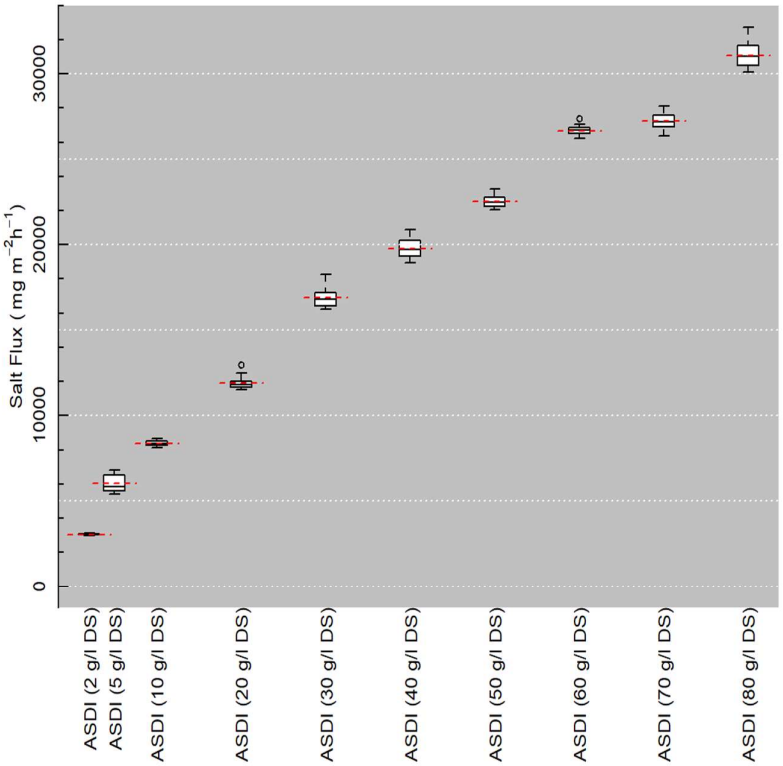
Salt Flux (mg m^{-2}h^{-1})
0
10000
20000
30000
ASDI (2 g/l DS)
ASDI (5 g/l DS)
ASDI (10 g/l DS)
ASDI (20 g/l DS)
ASDI (30 g/l DS)
ASDI (40 g/l DS)
ASDI (50 g/l DS)
ASDI (60 g/l DS)
ASDI (70 g/l DS)
ASDI (80 g/l DS)

(e)

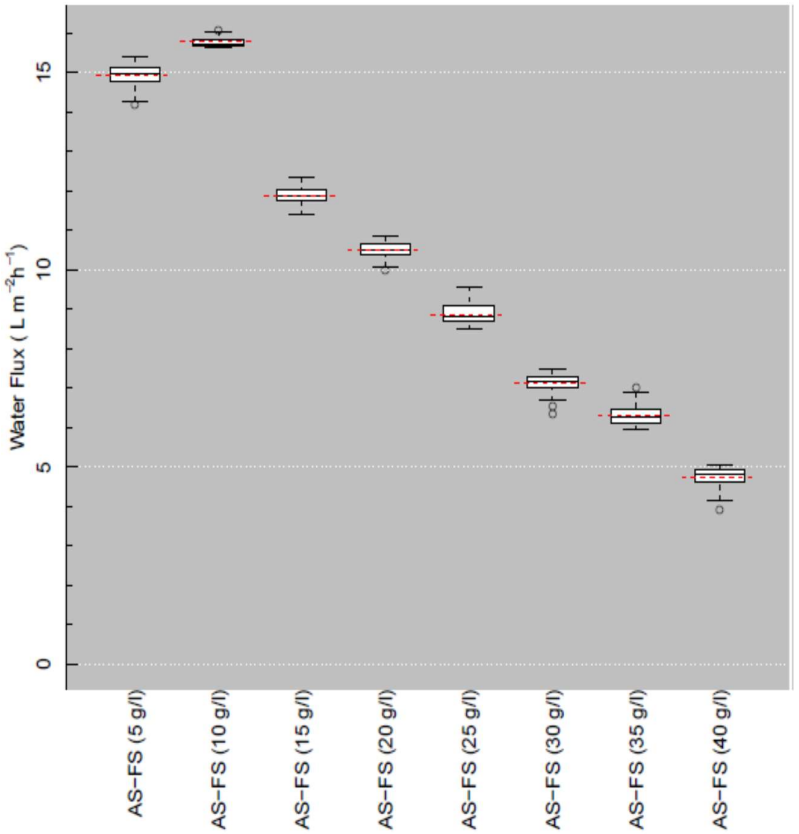
Water Flux (L m^{-2}h^{-1})
0
5
10
15
AS-FS (5 g/l)
AS-FS (10 g/l)
AS-FS (15 g/l)
AS-FS (20 g/l)
AS-FS (25 g/l)
AS-FS (30 g/l)
AS-FS (35 g/l)
AS-FS (40 g/l)

(f)

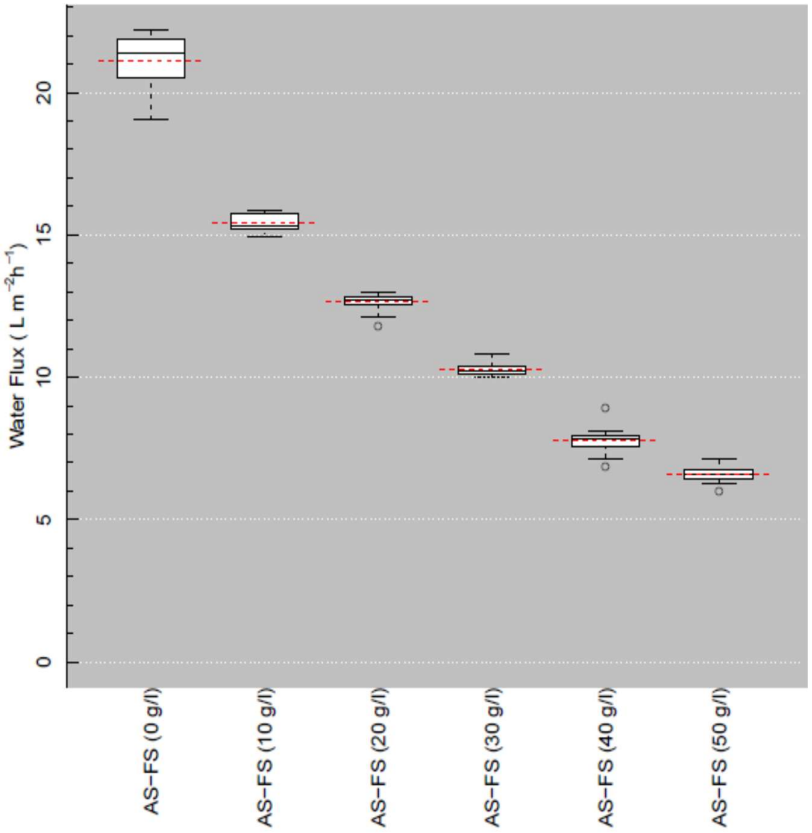
Water Flux (L m^{-2}h^{-1})
0
5
10
15
20
AS-FS (0 g/l)
AS-FS (10 g/l)
AS-FS (20 g/l)
AS-FS (30 g/l)
AS-FS (40 g/l)
AS-FS (50 g/l)

(g)

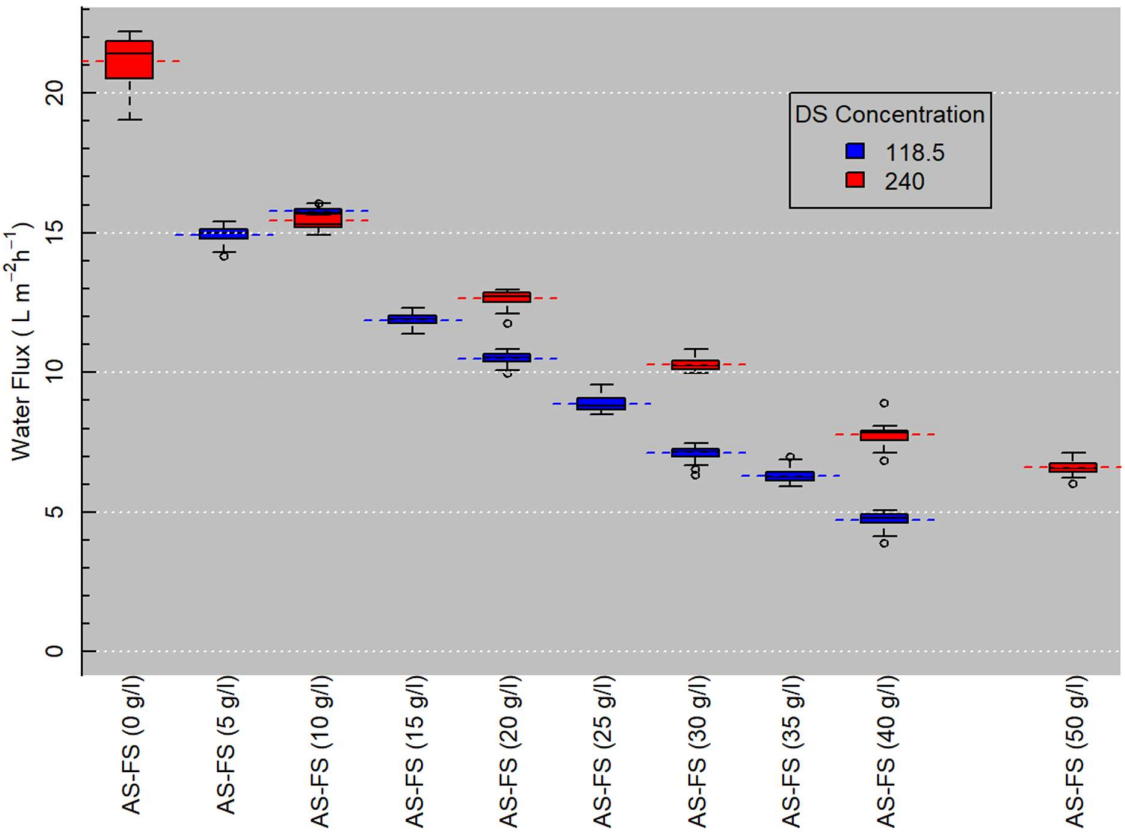

Figure 4-17: Summary of the results obtained from ammonium bicarbonate draw solution.

(a): Impact of membrane configuration on water flux (feed solution: DI; Draw solution: 1 M NH_4HCO_3; co-current cross flow rate: 1.5 L/min; Temperature (DI and DS): 25ºC

(b): Impact of temperature on water flux (feed solution: DI; Draw solution: 1 M NH_4HCO_3; co-current cross flow rate: 2.5 L/min; Temperature (DI and DS): 25 and 30 ºC

(c): Impact of draw solution concentration on water flux (membrane orientation: AS-DI; Feed solution: DI; Draw solution: 2-80 g/L NH_4HCO_3; co-current cross flowrate: 1.5 L/min; Temperature (DI and DS): 30 ºC

(d): Impact of draw solution concentration on salt flux (membrane orientation: AS-DI; Feed solution: DI; Draw solution: 2-80 g/L NH_4HCO_3; co-current cross flowrate: 1.5 L/min; Temperature (DI and DS): 30 ºC

(e): Impact of feed solution concentration on water flux (membrane orientation: AS-DI; Feed solution: 5-40 g/L NaCl; Draw solution: 1.5 M NH_4HCO_3; co-current cross flowrate: 1.5 L/min; Temperature (DI and DS): 30 ºC

(f): Impact of feed solution concentration on water flux (membrane orientation: AS-DI; Feed solution: 0-50 g/L NaCl; Draw solution: 3 M NH_4HCO_3; co-current cross flowrate: 1.5 L/min; Temperature (DI and DS): 30 ºC

(g): Impact of feed solution concentration on water flux (membrane orientation: AS-DI; Feed solution: 0-50 g/L NaCl; Draw solution: 1.5 & 3 M NH_4HCO_3; co-current cross flowrate: 1.5 L/min; Temperature (DI and DS): 30 ºC

4.4 Concluding Remarks

The results of this study provided an understanding into the forward osmosis process. As a result, this study facilitated a better understanding of the factors that drives FO process performance. This section summarises the findings from this study.

- Experimental results showed that the FO process could achieve a better performance when the membrane orientation was AS-DS (i.e. draw solution facing the active side of the membrane). This phenomenon was observed for both the CTA and TFC membrane.
- The critical phenomena affected by the various experimental factors and therefore greatly influenced the FO performance were found to be Internal concentration polarisation (ICP) as reported extensively in the literature.
    - When the FO process was tested with the feed solution facing the active side of the membrane (AS-DI), more severe internal ICP (dilutive ICP) occurs within the loose support layer of the FO membrane on the draw side, which resulted in a much lower water flux when compared to when the FO process was tested using AS-DS configuration.
    - When the FO configuration was AS-DS (i.e. active side facing the draw solution), internal ICP occurs (concentrative ICP) within the loose support layer of the FO membrane on the feed side, which would lower the effective driving force and cause the water flux to be lower than theoretically expected.
- This study also showed that apart from membrane orientation the FO process was also influenced by other factors such as temperature, cross-flow velocity, membrane type, draw solution type, draw solute concentration as well as feed solute concentration.
    - Increasing the temperature on both sides of the FO membrane cell resulted in increased water flux and salt flux. This phenomenon was observed for both orientation (i.e. AS-DI and AS-DS). The improvement in water flux as the temperature was increased was due to the decrease in water viscosity at higher temperatures.
    - Increasing the cross-flow velocity on both sides of the FO membrane channel resulted in an increased water flux. The increase in cross-flow velocity reduces the impact of concentration polarization on both side which increases the effective driving force and subsequently increase the water flux.
    - Increasing the draw solute concentration resulted in an increase in water flux and salt flux due to an increase in driving force. Increasing the concentration of draw solution enhances permeate flux due to increased driving force. However, increase in reverse solute flux was also expected in order to compensate for the high-water flux.

- Increasing the feed solute concentration (at constant draw solute concentration) resulted in a decrease in water flux. The osmotic driving force was expected to decrease as feed water concentration was increased. This was also supported by equation 2-1 in the Chapter 2.
- Water fluxes for FO-TFC membrane in both membrane orientations were consistently greater than those for the FO-CTA membrane. This observation was to be expected because the TFC membrane pure water permeability is greater than that of the CTA membrane (Table 4-1).
- Salt Fluxes for the FO-TFC membrane in both membrane orientations were consistently higher than those for the FO-CTA membrane due to its high salt permeability coefficient (Table 4-1). High salt fluxes negatively impact the FO process performance as it could lead to the fouling of the FO membrane due to enhanced inorganic scaling as a result of diffusion of scaling precursors ions in the draw solution as discussed in Chapter 2 (section 2.1.1.3).

- Based on the results derived from this study, the TFC membrane was recommended to be used for the FO experimental batch studies using selected synthetic concentrated brine streams evaluated in Chapter 3.
  - The FO-TFC membrane has a high pH tolerance in a 2-11 range, and as observed in this study, the water fluxes were higher than those obtained using FO-CTA membrane. The FO-CTA membrane is not appropriate for alkaline pH applications due to its limited pH tolerance (3-8). Ammonium bicarbonate draw solution (alkaline pH) will be used in this project as discussed in Chapter 3 under draw solution chemistry, and the FO-TFC membrane could offer a viable alternative as there will not be any pH correction required.
    - Studies discussed in the literature section of the dissertation showed that the use of ammonium bicarbonate draw solution gives high osmotic pressure differential which could result in higher water fluxes and recoveries. The higher water fluxes and recoveries could potentially reduce the CAPEX for the FO plant as well as the size of the brine handling system such as evaporative crystalliser.
  - Ammonium bicarbonate was also successfully used to evaluate various parameters that impact the performance of Forward Osmosis technology. Water fluxes obtained when the FO process was operated with ammonium bicarbonate draw solution (1 M) were generally higher than those obtained for sodium chloride (1 M) in both membrane orientations.

- Although the AS-DS configuration showed higher water fluxes than AS-DI, the AS-DS configuration is susceptible to severe fouling due to the potential precipitation of minerals into the support layer (discussed in Chapter 2 and demonstrated in Figure 2-8). In order to minimize the membrane-fouling effects the feed water faces the active layer in the typical membrane desalination configuration. This configuration will therefore be used for the bench-scale experiments.

This study provided an understanding of the various factors that drives FO process performance when using FO-TFC membrane and NH_4HCO_3 as a draw solution. This is adding to the new knowledge as most of the studies cited in the literature involving the use of NH_4HCO_3 as a draw solution have been conducted using FO-CTA membrane. The water flux and salt flux results obtained from this study provided vital information that can be used to improve the properties of the FO-TFC and FO membranes in general as membrane development is one of the major challenges hampering the fast commercialisation of the technology. The results from the study enabled the establishment of appropriate operating conditions for the main experiments conducted in Chapter 5. Through this study, TFC-FO membrane, ammonium bicarbonate draw solution concentration (3 M), feed and draw solution temperature of 30 ºC, feed and draw solution flow rates of 1.5 L/min (cross-flow velocity) and AS-DI membrane orientation were selected as suitable operating conditions for the main experiments in Chapter 5.

CHAPTER 5 : EVALUATION OF THE FO TECHNOLOGY AND ITS LIMITATIONS USING SYNTHETIC STREAMS WITH AMMONIUM BICARBONATE AS A DRAW SOLUTION

This phase of the study involved detailed bench-scale experiments using bench-scale FO unit described in Chapter 4 to evaluate the advantages and limitations of utilising forward osmosis technology to concentrate various high ionic strength streams selected based on results obtained from Chapter 3. Critical performance parameters such as water flux, solute back diffusion salt rejection and recoveries were monitored. For the bench-scale test in this phase of the study, the experimental set up was configured to simulate the influence of variable feed water concentrations and constant draw solution concentrations on FO process performance (simulating the impact of water recovery on flux and membrane fouling)

5.1. Objectives of this Phase of the Study

Although FO technology has shown much potential in various academic and full-scale applications, the technology still faces some critical challenges as extensively discussed in Chapter 1. These challenges primarily relate to the following aspects: internal and external concentration polarisation, membrane fouling, reverse solute diffusion, membrane development and the design of a fit for purpose draw solute. The details around these challenges have been covered extensively elsewhere (Alsvik and Hagg, 2013; Klaysom et al., 2013; Zhao et al., 2012). Fundamental understanding on the fouling tendencies of the FO process treating high salinity streams when employing specific set of operational parameters was therefore required for further advancement of this technology. For this phase of the study, the role of reverse solute diffusion phenomena on FO fouling when treating concentrated brine streams was evaluated.

The primary objective of this phase of the study was to evaluate the technical feasibility of treating selected synthetic concentrated brine streams using forward osmosis technology using HTI FO-TFC membrane and ammonium bicarbonate as a draw solution. Synthetic pure-component analogues of the selected industrial concentrated brine streams were used as feed solution. The following protocol was developed to achieve the primary objectives of this phase of the study:

- Short term batch experiments were undertaken using synthetic pure-analogues of the selected high salinity brine stream. Ammonium bicarbonate was used as a draw solution in all the experiments conducted. The selection of this draw solution was based on the literature review and results discussed in Chapter 4. Recovery of the draw solution was outside the scope of this study as it was concluded based on the

literature review that its recovery is well documented. A commercially available TFC-FO membrane coupons were used for the experiments.

- The TFC-FO membrane was chosen based on the results from Chapter 4 as well as its advantages discussed in the literature section of this dissertation. The advantages include wider pH range, higher flux and better rejection when compared to the CTA membrane.
- In order to simulate the impact of water recovery on water flux and membrane fouling, variable feed and constant draw solution concentration testing mode was followed. Although the AS-DS configuration showed higher water fluxes than AS-DI configuration as observed in Chapter 4 and cited in various literature, the AS-DS configuration is susceptible to severe fouling due to the potential precipitation of minerals into the support layer. In order to minimize the membrane-fouling effects the feed is made facing the active layer in the typical membrane desalination configuration. It was for these reasons that all the experiments in this phase of the study were completed using AS-DI configuration.
- Parameters such as temperature and feed and draw solution flowrate were crucial in the performance of the FO process as discussed in Chapter 4. These parameters were fixed for the all the experiments conducted in this phase.
- Critical performance parameters such as water flux, reverse solute diffusion, salt rejection, water recovery and membrane fouling were monitored and evaluated for all the experiments conducted.

5.2 Material and Methods

5.2.1 Experimental Set-up description

The description of the experimental setup used for this phase of the study was similar to that detailed in Chapter 4. The significant difference was in the control philosophy, which is described below. For the bench-scale test in this phase of the study, the experimental set up was configured to simulate the influence of variable feed water concentration and constant draw solution concentration on FO process performance.

5.2.1.1 Control Philosophy

The FO membrane cell system was designed to simulate the concentration of various brine streams at constant draw solution concentration. Figure 5-1 shows a simplified schematic diagram of the bench scale experimental set up used for this phase of the study. The tanks (feed, draw solution and concentrated draw solution tanks) were filled with relevant fluids before the operation of the equipment.

The level in the feed water tank can decrease by removing water through the process of forward osmosis (water flows from the feed side to the draw solution tank).

The amount of water removed from the feed tank to the draw solution tank was monitored by the change in the mass of the solution using the electronic scale. In order to keep the concentration of the draw solution constant, concentrated ammonium bicarbonate (4M) was dosed from the concentrated draw solution tank into the draw solution tank until setpoint conductivity in the draw solution tank was achieved. Potential vapour losses when using ammonium bicarbonate as a draw solution was managed by conducting the experiments at a maximum temperature of 30ºC as well as covering the tanks.

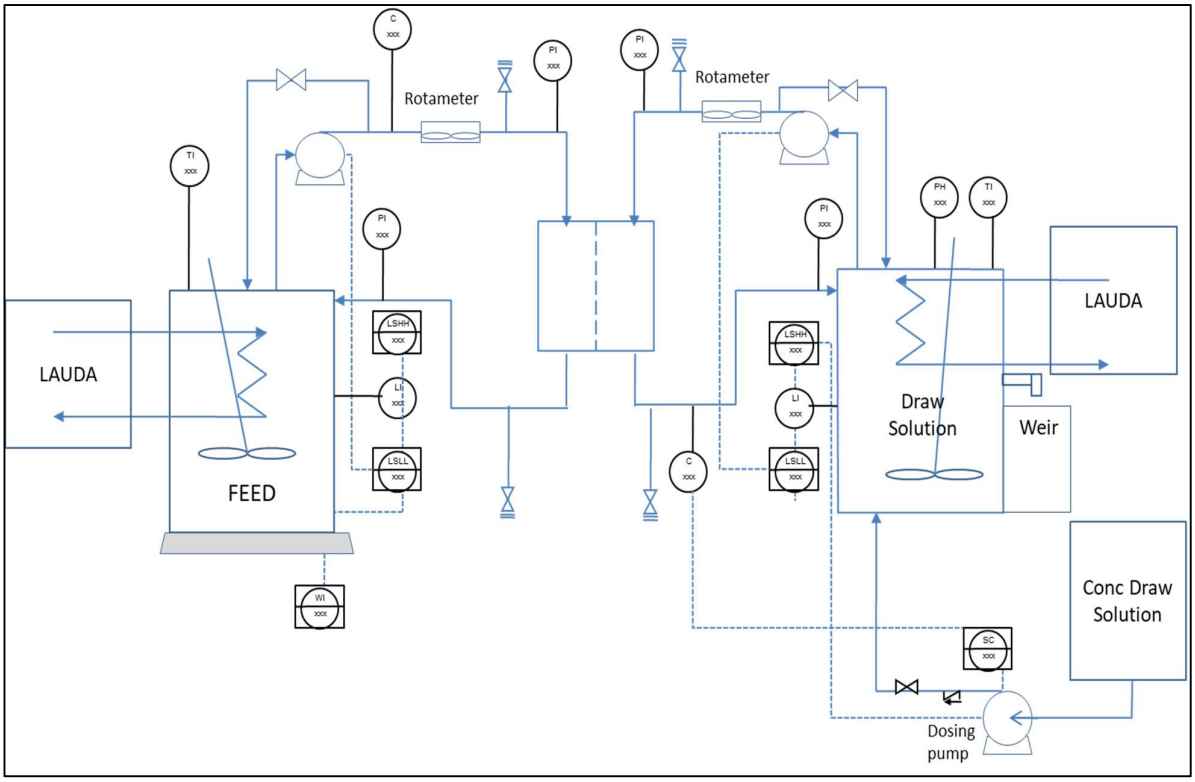

Figure 5-1: Simplified diagram of the experimental set up for bench scale evaluation of Forward Osmosis process to concentrate Synthetic pure-component analogues of the selected industrial concentrated brine streams.

5.3 Feed and Draw Solutions

5.3.1 Feed Solutions

Various types of feed solutions (FS) were used to evaluate forward osmosis process. The chemical composition of various FS used in the studies is shown in Table 5-1. These were the feed solutions selected based on survey studies conducted on numerous high ionic strength streams (Desktop study using OLI Stream Analyzer Software, covered in Chapter 3).

Model synthetic solutions (compounds simulated using OLI software and molecular output (apparent species)) were used to simulate (prepare) the actual streams.

Deionised water was used as the FS for membrane characterisation with respect to pure water flux and reverse salt flux before the baseline, and synthetic runs were undertaken.

Sodium Chloride was used as FS to simulate water fluxes and recoveries behaviours in the absence of membrane scaling or fouling (baseline run) for the streams of interest, namely, **High Rinse Portion**, **TRO/SRO Brine**, **Combined Regeneration Effluent** and **Mother Liquor**. The NaCl solutions were prepared in such a way that they have the same osmotic pressure as the synthetic solutions (Table 5-2).

Table 5-1: Composition of typical FS considered for all FO studies.

Parameter	High Rinse Portion (HRP)	TRO/SRO Brine	Combined Regeneration Effluent	Mother liquor
	mg/L	mg/L	mg/L	mg/L
NH_4^+	1.70	9.59	3.60	25.0
K^+	327.0	197.0	106.0	1574
Na^+	3840	2686	10580	19380
Ca^{+2}	865.9	508.0	105.0	809.7
Mg^{+2}	456.0	20.0	2.00	122.0
Sr^{+2}	6.80	N/A	1.07	N/A
Al^{+3}	0.80	N/A	0.36	N/A
Ba^{+2}	0.51	N/A	0	N/A
Fe^{+2}	0.24	0.15	0.04	N/A
Mn^{+2}	0.01	N/A	N/A	N/A
F^-	12.0	13.0	0.80	68.0
Cl^{-1}	8584	1618	9221	12840
NO_3^{-1}	63.0	108.0	35.0	610.7
SO_4^{-2}	601.9	4832	9881	26690
PO_4^{-3}	5.30	N/A	N/A	N/A
HCO_3^{-1}		45.0	122.0	225.0
pH	5.11	5.96	7.80	5.82
Osmotic Pressure (atm)	10.3	4.85	17.8	32.0

Feed solution Osmotic pressures were determined using OLI Stream Analyser 3.2. Median values were used for simulation.

Table 5-2 below shows the concentration of the NaCl used for baseline runs.

Table 5-2: Concentration of NaCl used for baseline runs

Parameter	High Rinse Portion (Baseline simulating non scaling)	TRO/SRO Brine (Baseline simulating non scaling)	Combined Regeneration Effluent (Baseline simulating non scaling)	Mother liquor (Baseline simulating non scaling)
	g/L	g/L	g/L	g/L
NaCl	13	6.5	23	40
Osmotic Pressure (atm)	10.3	4.85	17.8	32.0

Table 5-3 below shows a detailed composition of OLI model synthetic solutions (compounds simulated using OLI software and molecular output (apparent species)) used to simulate the actual streams in Table 5-1. Only the major compounds were used. Aqueous phase concentrations were used to make up the synthetic solutions

Table 5-3: Detailed composition of synthetic solutions simulating actual streams (the synthetic composition and concentration were generated using OLI Stream Analyzer 3.2 (OLI Systems Inc., Morris Plains, NJ, US)

Parameter	High Rinse Portion	TRO/SRO Brine	Combined Regeneration Effluent	Mother Liquor
	mg/L	mg/L	mg/L	mg/L
CaO ($Ca(OH)_2$)	372.2	701.8	146.9	763.9
FeO_2 ($FeCl_2$)	0.31			
$CaCl_2$ ($CaCl_2.2H_2O$)	1651			
NaCl	9727			
$MgCl_2$ ($MgCl_2.6H_2O$)	1786			
$AlCl_3$ ($AlCl_3.6H_2O$)	3.46			
KCl (KC l.$6H_2O$)	623.5			
K_2O (KCl.$6H_2O$)		220.1	125.7	1844
KF (KCl.$6H_2O$)		21.2	2.45	65.4
Sulphur Trioxide (H_2SO_4)	501.5	4027	8235	21820
HCl		1680	9483	13290
NaOH		4673	18400	33720
MgO		33.2	3.32	202.3
SiO_2(Fumed Si)			4.3	12.9
pH*	5.98	6.15	5.86	6.01
Osmotic Pressure (atm)	10.3	4.85	17.83	32.0

*pH of the resultants solutions was corrected to between pH 5-6 using either HCl or NaOH.

Compounds in brackets represent the actual compounds used. Some compounds (e.g. Dinitrogen Pentoxide, Sodium Fluoride and Potassium Fluoride) could not be sourced; their contribution to osmotic pressure was however minimal.

The FS were prepared by dissolving the salts of interest in DI water with the aid of a magnetic stirrer to ensure that all salts were fully dissolved and homogeneously mixed before the start of the experiments.

5.3.2 Draw Solution

All experiments were conducted using 3 M (ca. 90 atm Osmotic Pressure) ammonium bicarbonate as the draw solution. The 3 M ammonium bicarbonate solution was chosen as a draw solution to enable the use of 4 M solution to maintain constant concentration (3 M) in the draw solution tank. Furthermore, 3M draw solution was also evaluated in Chapter 4 (section 4.3.7) and the results showed higher water fluxes. The draw solution was prepared by dissolving ammonium bicarbonate salt in DI water to achieve a concentration of 3 M. Due to its lack of solubility at ambient temperature, gentle heat needed to be applied in order to afford complete dissolution of the salt. The heating temperature did not exceed 30ºC as above this temperature ammonium bicarbonate starts to decompose (covered in Chapter 3). As the mode of operation for these experiments was based on a constant draw solution concentration, a concentrated ammonium bicarbonate solution (4 M) was used to correct the conductivity of the draw solution to a set value in order to maintain a constant draw solution concentration. This was important to ensure that the change in water flux was not influenced by osmotic dilution. The successful preparation of 4 M ammonium bicarbonate was in line with the OLI results covered in Chapter 3.

5.4 Membranes Tested

An FO-TFC membrane was used for all the experiments. This was a commercially available FO membrane manufactured by Hydration Technology Innovations (HTI). This membrane was previously compared with the FO-CTA membrane, and the results showed that an FO-TFC membrane water flux in both membrane orientations was consistently higher than those for the FO-CTA membrane (discussed in detail in Chapter 4). Furthermore, the FO-TFC membrane has a high pH tolerance in a 2-11 pH range. The FO-CTA membrane was not appropriate for alkaline pH applications due to its limited pH tolerance (3-8). As stated in Section 5.3.2, an ammonium bicarbonate draw solution (alkaline pH) was used in this study and the FO-TFC membrane was preferred as there will not be any pH correction required. Virgin membrane coupons were cut to FO cell size and stored in distilled water overnight before use in each experiment (i.e. each experiment comprised of: pure water flux, non-scaling NaCl run simulating a particular stream osmotic pressure and scaling run using a synthetic analogue of a particular stream).

5.5. Experimental Conditions

All pure water flux experiments (experiments for characterising the membrane with respect to water flux and reverse salt flux using DI as feed water) were conducted for a 2-hr period (established in Chapter 4). The runs for the actual experiments using NaCl or Synthetic streams were conducted until 70% (equipment limitation) of water was recovered or until significant fouling was experienced, which result in an insignificant change in water flux. A run was completed for each experiment combination.

The cross-flow rates for the feed and draw solutions was 1.5 L/min (equivalent to 33.3 $cm.s^{-1}$ cross-flow velocity). All the experiments were conducted under a co-current flow.

The experimental temperature was 30ºC and was maintained for both the feed and draw solutions during the experiments. This temperature was selected based on the properties of ammonium bicarbonate discussed in the previous studies (Chapter 3 and 4). The solubility of ammonium bicarbonate is influenced by temperature; however, the literature review showed that above 30ºC, ammonium bicarbonate starts to decompose forming ammonia and carbon dioxide (Gokel, 2004 and Wanling et al.., 2009). The experimental pressure for all the experiments was 1 atm.

Membranes were tested with the active (rejecting) layer facing the feed solution (FO) and the support layer in contact with the draw solution. Tables 1, 2 and 3 in Appendix 3 shows the details of the experimental conditions matrix used for this study.

5.6 Calculation of FO Membrane Mass Transport

5.6.1 Determination of FO Membrane Water Flux

The rate of water permeation through the FO membrane was determined by calculating the change in mass of the feed solution on the analytical balance (WI 001, Sartorius SIWRDCP-1-15-L from Taratec). The gradient of the mass versus time graph gives the mass transfer rate through the FO membrane for an experiment. Water flux (J_w) (L. $m^{-2}.h^{-1}$) was calculated by dividing the mass transfer rate by the density of the water and membrane surface area using the equation 4-1 (Tang, 2009; Cath et al., 2013; Hancock and Cath, 2009):

5.6.2 Determination of Reverse Salt/Solute Flux (RSF) and Specific RSF (SRSF)

Solute transfer in a polymeric FO membrane occurs on both sides of the membrane as the membrane cannot completely reject solutes. In this study, the performance of the FO process was also measured in terms of reverse solute flux. Reverse Salt Flux values were calculated by measuring the steady-state increase of feed solution (Deionised Water) conductivity over a selected period. A conductivity probe (K=1 cm^{-1} cell constant) was specifically calibrated for dilute ammonium bicarbonate solutions at 30ºC. There was a liner increase in feed solution conductivity as a function of time due to the diffusion of draw solution solutes into the feed solution. Salt flux (Js, $mg.m^{-2}.h^{-1}$) was determined by first converting the feed solution conductivity to concentration using a conversion factor derived from the linear relationship between the conductivity and the concentration (refer to the calibration curve of conductivity versus salt concentration for ammonium bicarbonate in Appendix 3 (Figure 1)). Salt flux was then calculated using the equation 4-2 [Xie and Elimelech, 2012].

A term SRSF (g/L), a ratio of RSF to water flux, indicate the amount of draw solute lost by reverse diffusion per unit volume of water extracted from the FS as follows:

Equation 5-1

$$\boldsymbol{SRSF} = \frac{\boldsymbol{J_s}}{\boldsymbol{J_w}}$$

5.6.3. Water Recovery

At the end of the FO experiment (NaCl feed run and Synthetic feed run), water recovery for a particular experiment was determined by dividing the total volume of the permeate (calculated from the total weight decrease of the feed solution) by the initial volume of feed solution as indicated in equation 5-2 below.

Equation 5-2

$$\boldsymbol{Recovery}\ (\%) = \frac{\boldsymbol{V_{permeate}}}{\boldsymbol{V_{initial\ feed}}}\boldsymbol{X100}$$

5.7. Sample Analysis and Measurements

Samples of the feed and draw solution were collected at the beginning and the end of each experiment (Run). The collected samples were analysed for cations and anions using Inductively Coupled Plasma (ICP) and Ion Chromatography (IC), respectively. Alkalinity was analysed using standard titration methods. Buchi distillation method and the Spectroquant method were used to analyse for ammonium in the feed and draw solution. As experienced in other studies, analysing the samples was a challenge, especially the feed solutions ions (e.g. calcium, magnesium, potassium, chlorides, sulphates) in highly concentrated ammonium bicarbonate draw solution. Samples had to be analysed using several dilution factors because the concentration of the components from the feed solution was significantly lower relative to that of the DS.

5.8. FO Membrane Morphology

In order to characterise the membrane coupons before (virgin) and after the experiment (used), the following techniques were used: SEM, EDX(S), Raman Spectroscopy and XRD (for highly fouled coupons).

The following should be noted for the EDS characterisation of the samples: When the electron from the electron beam interacts with the samples, it resulted in the generation of two types of X-rays for Ca – one was the K alpha (between 3 – 4 keV), and the other was the L alpha (between 0 – 1 keV). This was due to the electrons from different energy levels within the Ca atom filling the vacancy created in the various atomic orbitals of the Ca. The K alpha was used for examining Ca since there was a severe overlap between C and Ca L alpha. Therefore, for the samples analysed, the K alpha of Ca was used for determining the Ca presence in the various samples. EDS spectra were obtained from an area of the sample that was several mm^2. The electron beam was rastered over this area and the sum of the spectra used to qualitatively determine which elements were present in each sample. Knowledge of which elements were present was used to assist with interpretation of the Raman spectra & XRD. The EDS results were not used quantitatively, so there was no reason to get lots of replicates.

5.9 Results and Discussion

A series of experiments were carried out to obtain the fundamental understanding of the FO process, using the laboratory-scale FO system operating under a variety of conditions. Water flux and reverse salt flux were calculated to characterise each membrane coupon before feed concentration experiments (simulating recovery) were undertaken using NaCl (simulating non-scaling conditions/impact of feed osmotic pressure) and Synthetic feed (simulating impact of synthetic feed). Experimental conditions are summarised in Table 1, 2, 3, 4, 5, 6, 7 and 8 (Appendix 3).

Analysis of the data collected during the experiment showed that water flux stabilised after about 30 min (established in Chapter 4); hence the data used to measure the parameters of interest was the data collected after 30 min had elapsed. Statistical analyses were conducted on the data (water flux and salt flux).

The distribution of each variable is visually presented using standard box and whisker plots (maximum and minimum values, 25 percentile (bottom of the box), median (middle line in the box), average (red dotted line in the box) and 75 percentile (top of the box)).
Summary of the descriptive statistic for each experimental condition is presented in Appendix 3 (Table 9, 10, 11 and 12)

5.9.1 High Rinse Portion Bench Scale Tests.

The results from bench-scale testing of the feasibility of using forward osmosis technology to treat High Rinse Portion stream are presented and discussed in this section.

5.9.1.1 Water Flux and Salt Flux (Pure Water as Feed)

Figures 5-2 & 5-3 show the water fluxes and salt fluxes, respectively, when the FO-TFC membrane was tested with the dense layer or active layer facing the deionised water (AS-DI) using 3 M ammonium bicarbonate as a draw solution.

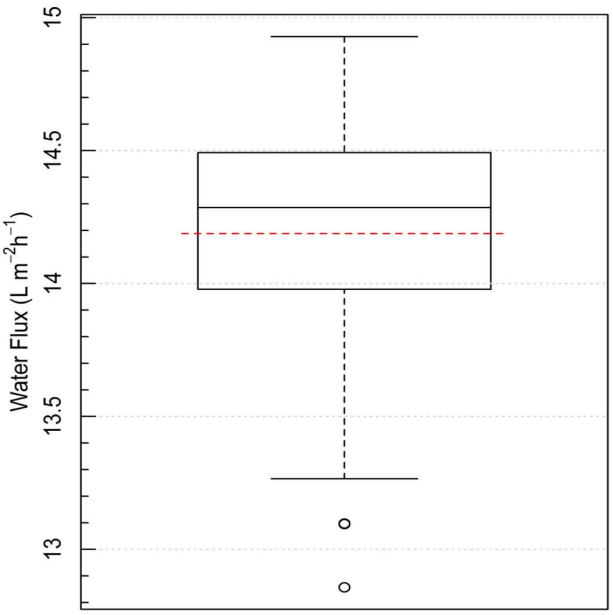

Figure 5-2: Water flux for High Rinse Portion run (Feed solution: DI; Draw solution: 3 M NH_4HCO_3; Co-current cross flow rate: 1.5 L/min; Temperature (DI and DS): 30ºC); Pressure: 1 atm.

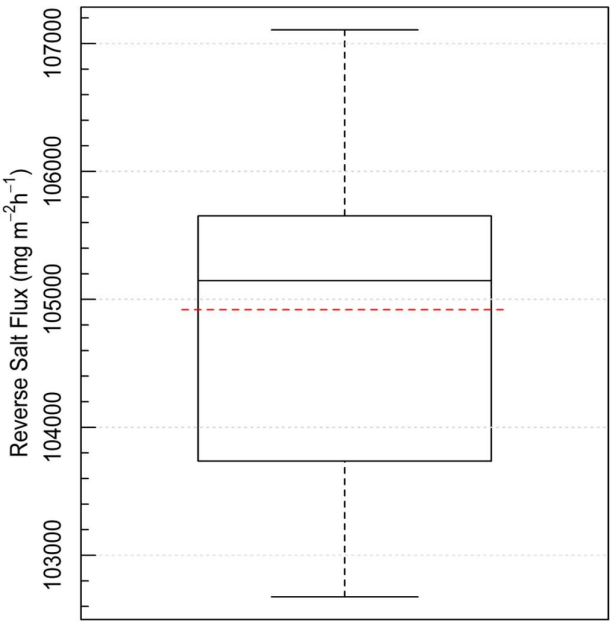

Figure 5-3: Reverse Salt Flux for High Rinse Portion run (Feed solution: DI; Draw solution: 3 M NH_4HCO_3; Co-current cross flow rate: 1.5 L/min; Temperature (DI and DS): 30ºC); Pressure: 1 atm

The average water and salt fluxes obtained for the membrane characterization run was 14.18 (SD = 0.5) $L.m^{-2}.h^{-1}$ and 104920 (SD = 1464) mg. $m^{-2}.h^{-1}$, respectively. The standard deviation shows that there was minimal variation in the water flux throughout the experiment and this was to be expected as the experiment was conducted at a constant draw solution concentration (i.e. constant osmotic pressure). The osmotic pressure exerted by the feed water was negligible to alter the osmotic driving force significantly. On average, the conductivity in the feed tank was 0.44 mS/cm, peaking at 0.67 mS/cm. These conductivities were very low when compared to that observed for the draw solution (mean = 141.3, SD = 0.87 mS/cm). It was evident from the reverse salt flux that there was a significant amount of draw solution that diffused back to the feed water tank (DI). This was also confirmed by the continuous increase in feed water conductivity as the run progressed. The Specific Reverse Salt Flux (SRSF) for this membrane using the average water flux and reverse salt flux according to Equation 5-3 was 7.4 g of ammonium bicarbonate per litre of product water. Previous studies conducted by other researchers, albeit using FO-CTA membrane have shown that loss of ammonium bicarbonate draw solution in the FO process could range between 2 and 3 g/L (Achill et al., 2010; Hancock and Cath, 2009). Furthermore, although the TFC membrane exhibited high water flux when compared to the CTA in other studies, the reverse salt flux of the TFC membranes was higher (Coday et al., 2013). The impact of this high SRSF will be discussed in detail later in this chapter.

5.9.1.2 Baseline and Synthetic Runs

In order to investigate the impact of decreasing osmotic driving force on the water recovery and flux, a non-scaling solution containing NaCl only was used as a baseline. After this, simulated synthetic High Rinse Portion solution was tested to evaluate the feasibility of using FO technology to treat this stream by monitoring impact on scaling, water flux and water recovery. Figure 5-4 shows the water flux as a function of water recovery during the baseline and synthetic run of HRP.

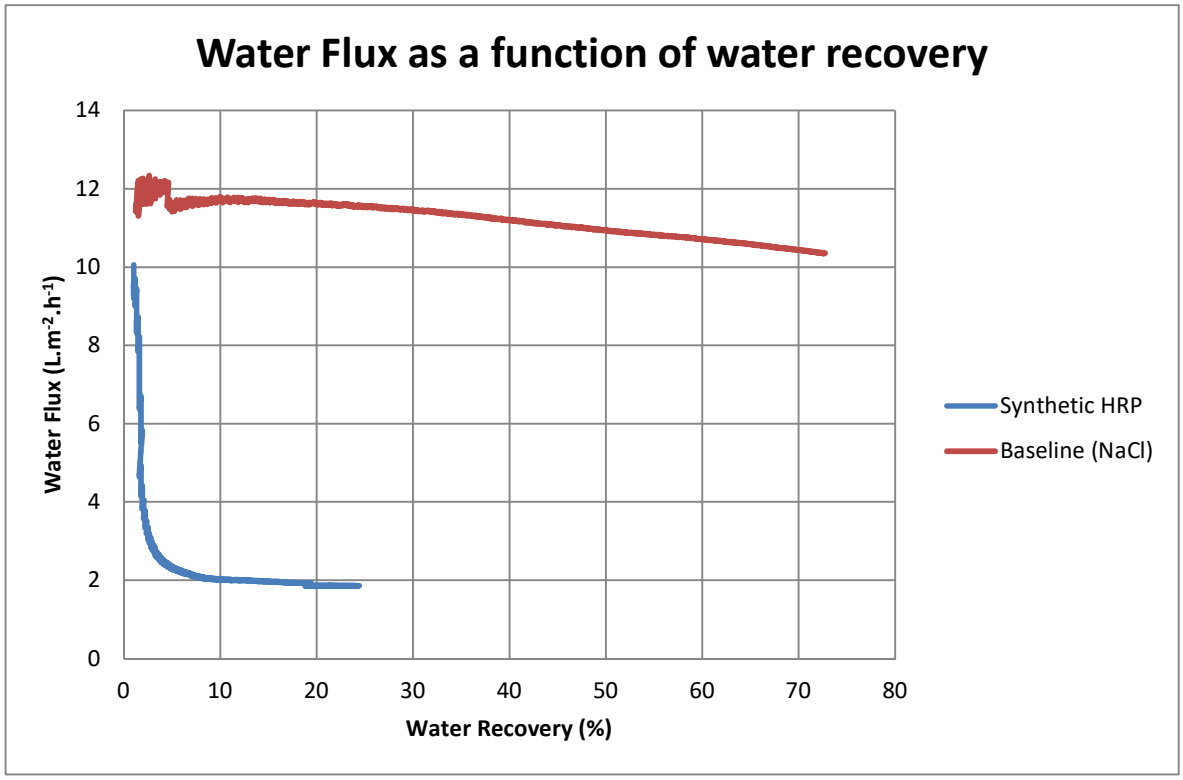

Figure 5-4: Water Flux as a function of water recovery for experiment conducted using NaCl and Synthetic HRP as feed solution

The initial flux during the baseline experiment with NaCl as a feed (bench-scale unit was operated until approximately 70% of the starting feed volume was recovered) was around 12 $L.m^{-2}.h^{-1}$ and decreased to a final water flux of approximately 10 $L.m^{-2}.h^{-1}$ as the feed solution concentration increased. The conductivity of the feed water increased from 20 mS/cm to 60 mS/cm due to the concentration of the feed solution as water was removed and reverse diffusion of salts from the draw solution into the feed solution. The increase in feed solution concentration resulted in a decrease in osmotic driving force even though the DS concentration was kept constant. For the synthetic solution, the initial flux was around 10 $L.m^{-2}.h^{-1}$, and the flux decreased to a final water flux of ca. 2 $L.m^{-2}.h^{-1}$ (experiment was conducted until approximately 24% of the original feed volume was recovered).

As indicated in Figure 5-4, the water flux trend was very different from that of the baseline run, and this was a clear indication of premature membrane fouling. As highlighted before, the synthetic feed solutions were corrected to a pH of between 5.5 and 6 (to manage scale associated with pH) before the experiment was started. The pH of the feed solution quickly became alkaline as soon as the experiment was started indicating potential diffusion of ammonium bicarbonate back to the feed solution. Table 14 in Appendix 3 shows a summary of results before and after the experiment for the synthetic run, and it was evident that there was a reverse diffusion of ammonium bicarbonate to the feed solution and this resulted in the increase in pH from between 5.5 and 6 to about 8 on average. The hypothesis around reverse salt diffusion was also supported by the SRSF (7.4 g/L) discussed in Section 5.9.1.1. For the same solute, the SRSF was found to be the same for any osmotic pressure differential, indicating that this ratio is a function of membrane's selectivity of the active layer and does not dependent on the DS concentration and membrane support structure. The inspection of the membrane coupon after the experiment showed that the membrane was severely fouled with white precipitate (Figure 5-5) and it was, therefore, essential to characterise the surface of the used membrane to determine the nature of the foulants.

Figure 5-5: Picture of the used membrane (Synthetic HRP feed solution)

5.9.1.3 FO Membrane Morphology

Morphology of new (unused) and used FO membranes was studied to show the effect of the HRP synthetic solution on the membrane performance.

It has been extensively reported in the literature that in the case of feed and draw solutions containing scale forming ions (e.g. Sr^{+2}, Ba^{+2}, Ca^{+2}, Mg^{+2}, SO_4^{-2}, F^{-1} and CO_3^{-2}), scaling due to minerals generally occurs on the membrane surface (active layer side of the membrane) when the feed solution components were concentrated above the solubility limits of various water-soluble minerals such as $CaCO_3$, $SrSO_4$, CaF, $BaSO_4$, $CaSO_4$ (Achilli et al., 2010). The feed and draw solution for this experiment contained scale precursors such as Ca^{+2}, Mg^{+2}, SO_4^{-2}, and CO_3^{-2}. Figure 5-6 and 5-8 show the SEM Morphology and EDS spectrum for the virgin and used membrane. The EDS spectrum shows that the virgin membrane contains C, O and S as the major elements. This was expected since the membrane was a TFC which is comprised of polyamide on polysulfone with an embedded polyester screen (Figure 5-7). The N from the polyamide polymer was not detected. Aluminium was found as a minor element in both membrane tests and may be due to the Al stub used for mounting the samples.

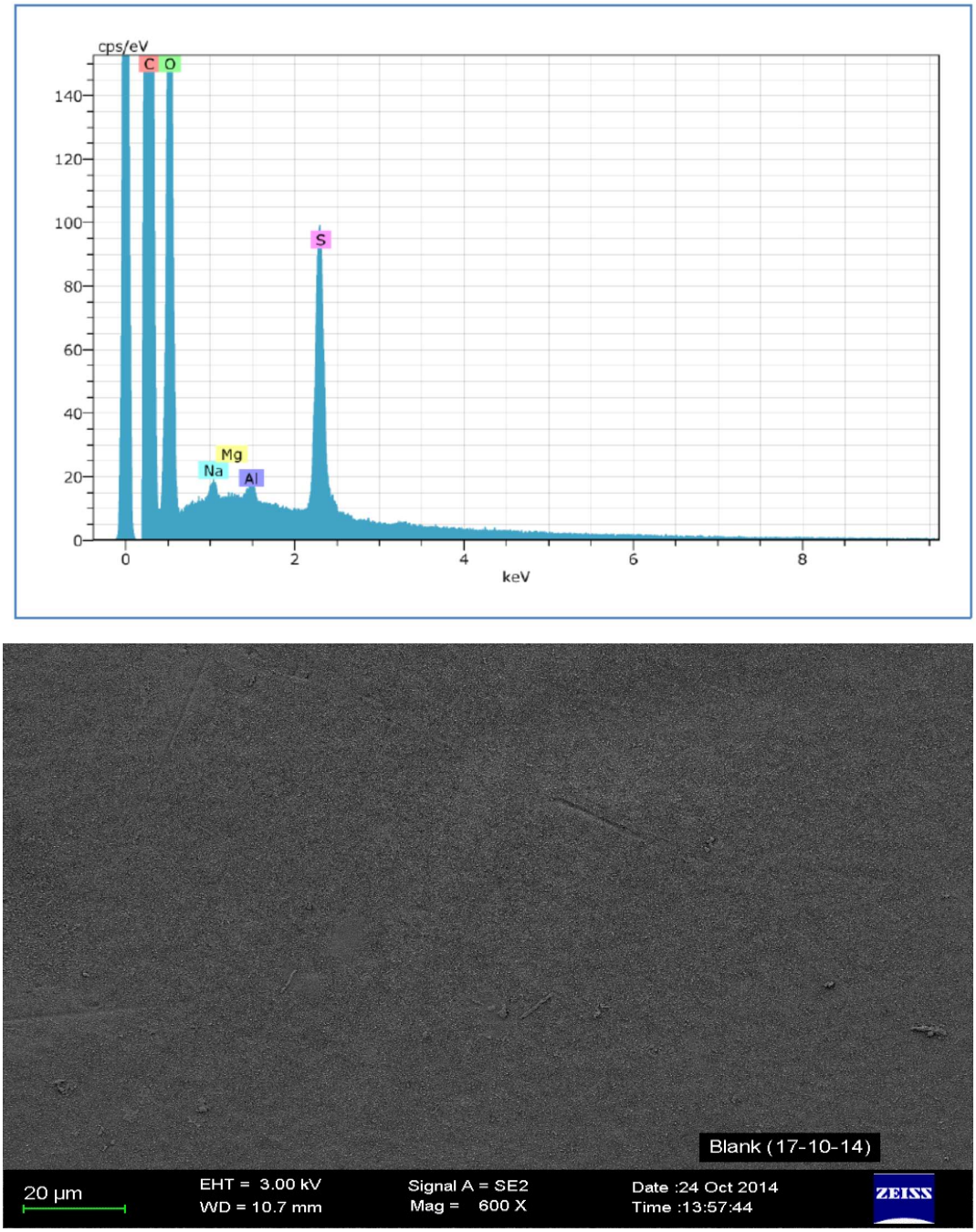

Figure 5-6: EDS Spectrum and SEM Morphology for the virgin membrane (Synthetic HRP as feed)

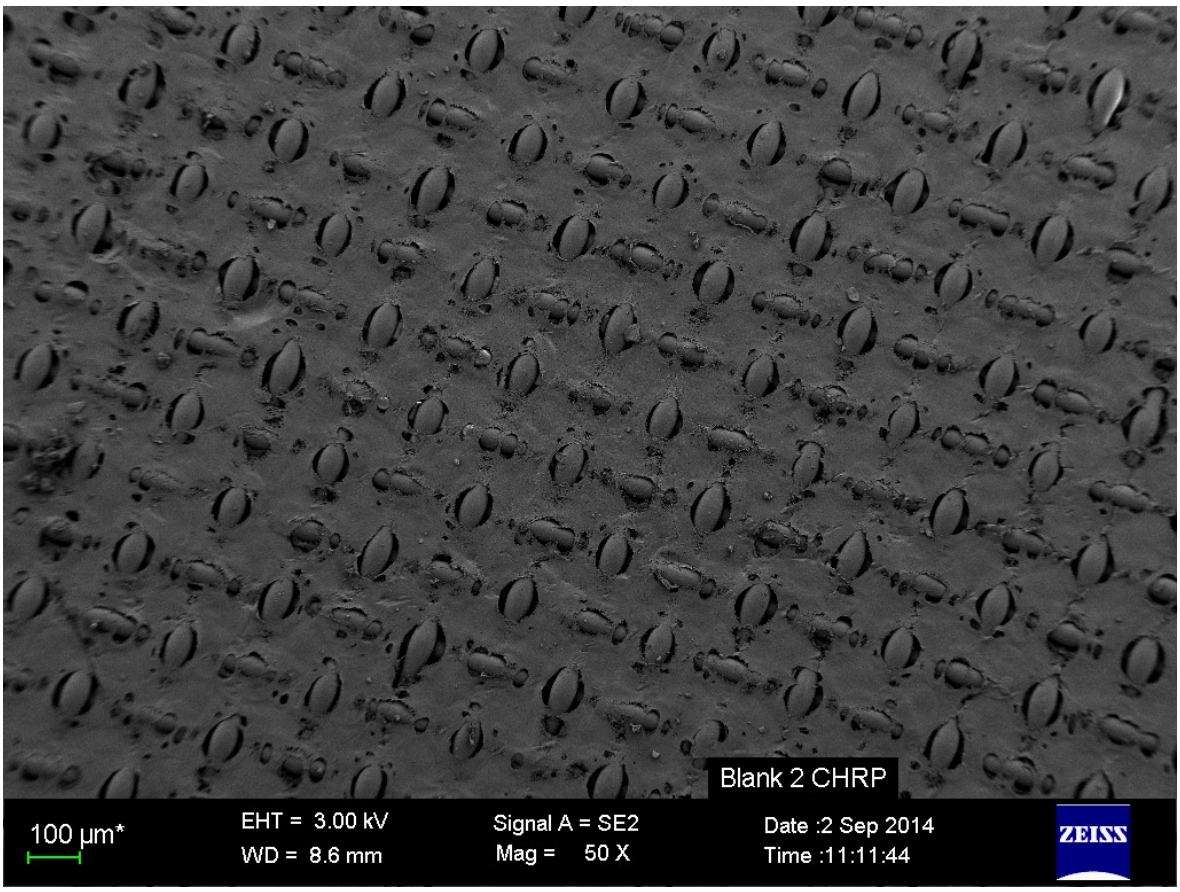

Figure 5-7: SEM Morphology showing a support layer of the virgin membrane (Synthetic HRP as feed)

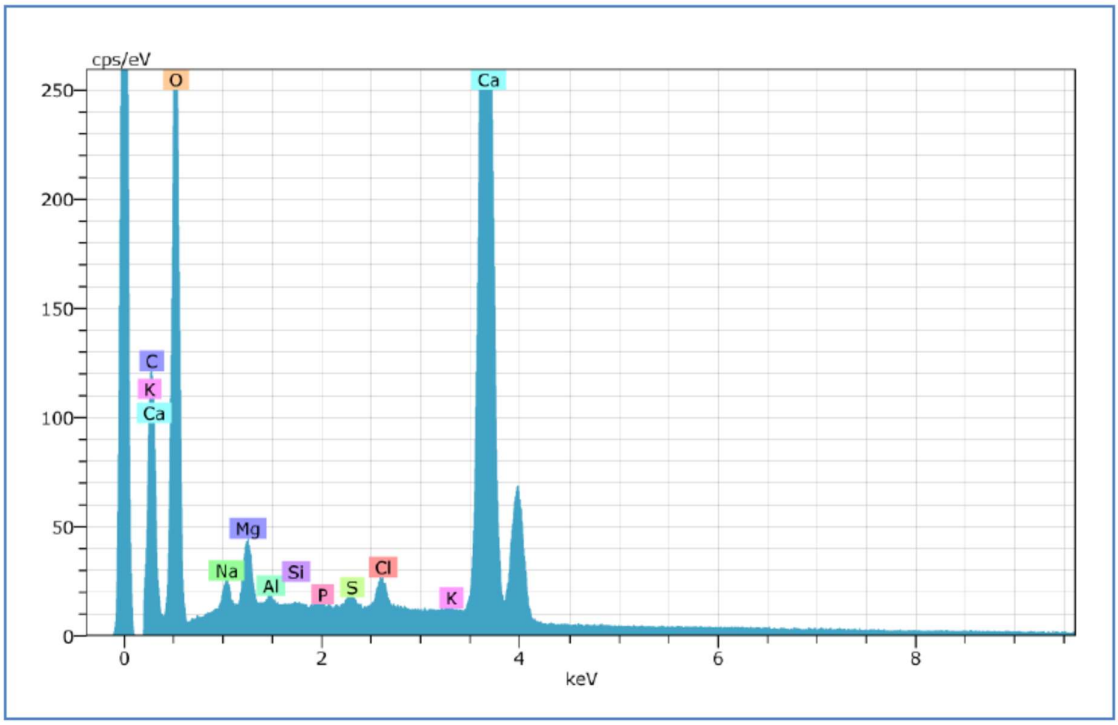

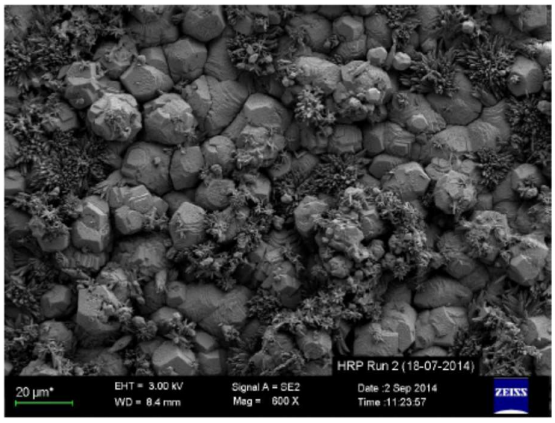

(d)

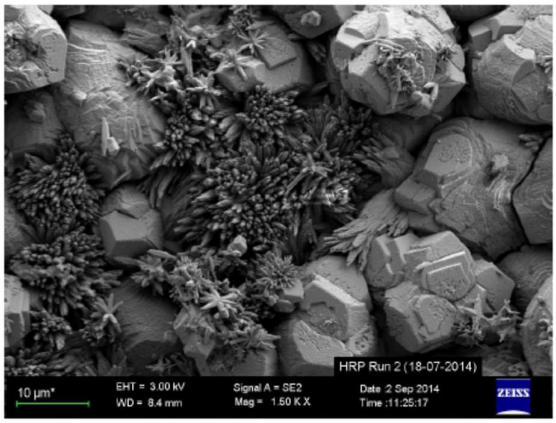

Figure 5-8: EDS Spectrum and SEM Morphology for the used membrane (Synthetic HRP as feed)

The EDS spectrum of the HRP Run is shown in Figure 5-8 and reveals that the membrane sample contained C, O and Ca as major elements. It is also evident from the SEM morphology that the membrane was severely fouled. Raman spectra obtained on the white particulates of the fouled membrane identified $CaCO_3$ to be present on the fouled membrane sample, but in different polymorphic forms. Both polymorphs have bands at 154 and 1085 cm^{-1} with the latter being the $\nu_s(CO_3^{2-})$ band. Aragonite has unique bands at ~205 and 704 cm^{-1} and calcite at ~279 and 709 cm^{-1} (refer to Appendix 3 for spectra).

The fouled membrane sample was further characterised using XRD, and the results showed the presence of aragonite and magnesium calcite ($Ca_{0.936}Mg_{0.064}$ (CO_3)) (Refer to Appendix 3 for X-ray diffractogram). From the FO membrane morphology results, it can be deduced that the steep flux decline observed in Figure 5-4 was associated with precipitation of calcium and magnesium-based compounds ($CaCO_3$ and $Ca_{0.936}Mg_{0.064}$ (CO_3)) onto the membrane surface. The EDS spectrum, SEM Morphology, Raman Spectroscopy and XRD of the same run conducted using a new membrane coupon showed similar results (results not shown). In that particular run, however, two additional bands were identified with Raman Spectroscopy which was associated with magnetite and ferrihydrite. The mineral precipitating based on OLI Stream Analyser simulation as discussed in Chapter 3 for this stream were silica, calcium sulphate dihydrate, fluorapatite, barium sulphate and aluminium hydroxide.

5.9.2 TRO/SRO Brine Bench Scale Tests.

The results from bench-scale testing of the feasibility of using forward osmosis technology to treat TRO/SRO brine stream are presented and discussed in this section.

5.9.2.1 Water Flux and Salt Flux (Pure Water as Feed)

Figures 5-9 & 5-10 show the water fluxes and salt fluxes, respectively, when the FO-TFC membrane was tested with the active layer facing the deionised water (AS-DI) using 3 M ammonium bicarbonate as a draw solution.

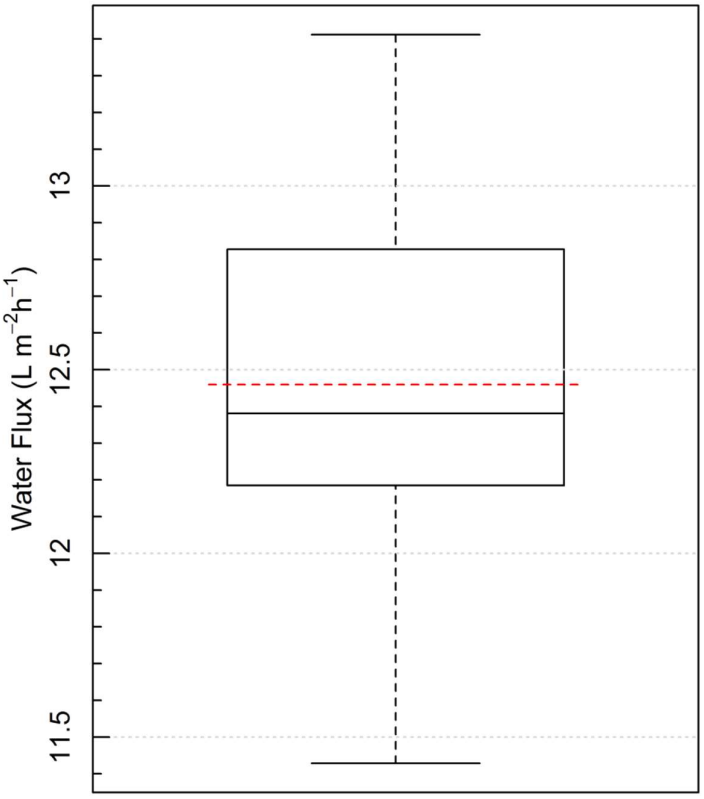

Figure 5-9: Water flux for TRO/SRO Brine run (Feed solution: DI; Draw solution: 3 M NH_4HCO_3; Co-current cross flow rate: 1.5 L/min; Temperature (DI and DS): 30°C); Pressure: 1 atm

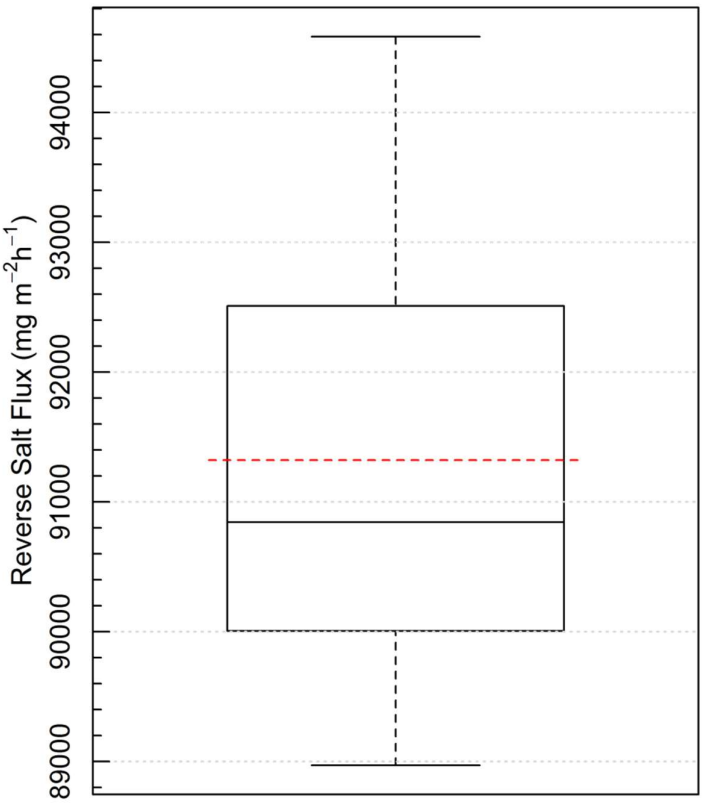

Figure 5-10: Reverse Salt Flux for TRO/SRO brine run (Feed solution: DI; Draw solution: 3 M NH_4HCO_3; Co-current cross flow rate: 1.5 L/min; Temperature (DI and DS): 30ºC); Pressure: 1 atm

The average water and salt fluxes obtained for the membrane characterization run was 12.5 (SD = 0.4) $L.m^{-2}.h^{-1}$ and 91322 (SD = 1778) mg. $m^{-2}.h^{-1}$, respectively. The standard deviation shows that there was minimal variation in the water flux throughout the experiment, and this was to be expected as the run was conducted at constant draw solution concentration (constant osmotic pressure). The osmotic pressure exerted by the feed water was negligible and thus was not expected to alter the osmotic driving force significantly. On average, the conductivity in the feed tank was 0.38 mS/cm with a maximum of at 0.57 mS/cm. These conductivities were very low when compared to that observed for the draw solution (mean = 143.3, SD = 0.81 mS/cm). It is evident from the reverse salt flux plot that there was a significant amount of draw solution that diffused back to the feed water tank (DI). This was also confirmed by the continuous increase in feed water conductivity as the run progressed. The Specific Reverse Salt Flux (SRSF) for this membrane using the average water flux and reverse salt flux according to Equation 5-3 was 7.3 g of ammonium bicarbonate per litre of product water, and this was similar to that of the TFC-FO membrane used for the HRP runs.

The SRSF is a function of draw solution and membrane intrinsic separation properties, and therefore it was expected that the SRSF will be comparable. Theoretically, the SRSF is independent of the operating conditions, such as DS and FS concentration, membrane orientation and hydrodynamic conditions (She et al., 2016)

5.9.2.2 Baseline and Synthetic Runs

In order to investigate the impact of decreasing osmotic driving force on the water recovery and flux, a non-scaling solution containing NaCl only was used as a baseline (refer to Table 5-2). After this, simulated synthetic TRO/SRO brine solution water (refer to Table 5-1 & 5-3) was tested to evaluate the feasibility of treating the TRO/SRO brine stream using FO technology. Figure 5-11 below shows the water flux as a function of water recovery during the baseline and synthetic run.

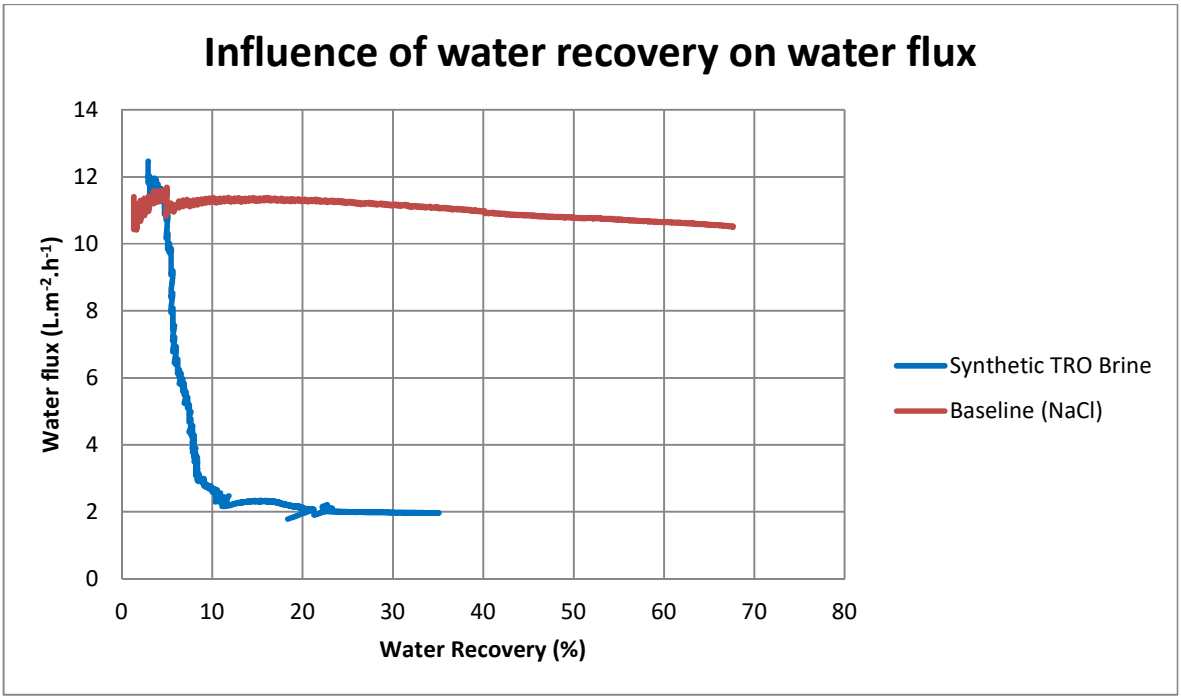

Figure 5-11: Influence of water recovery on water flux for the experiment conducted using NaCl or Synthetic TRO/SRO Brine as feed solution.

The initial flux during the baseline experiment with NaCl as a feed (bench-scale unit was operated until about 70% of the starting feed volume was recovered) was around 11 $L.m^{-2}.h^{-1}$ and decreased to a final water flux of about 10 $L.m^{-2}.h^{-1}$ as the feed solution concentration increased.

The conductivity of the feed water increased from 10 mS/cm to about 30 mS/cm indicating concentration of the feed solution as water was removed and diffusion of salts from the draw solution into the feed (a phenomenon known as reverse salt diffusion).

The increase in feed solution concentration resulted in a decrease in osmotic driving force even though the DS concentration was kept constant, and this resulted in the decline in water flux as discussed above. For the Synthetic solution, the initial water flux was around 12.5 $L.m^{-2}.h^{-1}$, and the water flux decreased to ca. 2 $L.m^{-2}.h^{-1}$ (the experiment was conducted until about 34% of the original feed water volume was recovered). The water flux of the synthetic solution started off slightly higher than that of the baseline solution, although they should have had the same starting osmotic pressure. The "phenomenon" was not investigated further during the study as the differences were not deemed as significant during the execution of the experiments.

As indicated in Figure 5-11, the water flux trend was very different from that of the baseline run, and this was a clear indication of premature membrane fouling. The pH of the feed solution quickly became alkaline as soon as the run was started indicating diffusion of ammonium bicarbonate back to the Synthetic TRO/SRO brine feed solution. Table 15 in Appendix 3 shows a summary of results before and after the experiment for the synthetic run, and it was evident that there was a reverse diffusion of ammonium bicarbonate solute to the feed solution and this resulted in the increase in pH from between 5.5 and 6 to about 8 on average. The inspection of the membrane coupon after the experiment showed that the membrane was also severely fouled with white precipitate (Figure 5-12) (similar to that observed for the Synthetic HRP feed solution).

Figure 5-12: Picture for the used membrane (Synthetic TRO/SRO Brine feed solution)

5.9.2.3 FO Membrane Morphology

Morphology of new (unused) and used FO membranes was studied to show the effect of synthetic TRO/SRO brine solution on the membrane performance.

The feed and draw solution for this run contained scale precursors such as Ca^{+2}, Mg^{+2}, SO_4^{-2}, and CO_3^{-2}. Figure 5-13 shows the EDS spectrum and SEM Morphology for the used membrane.

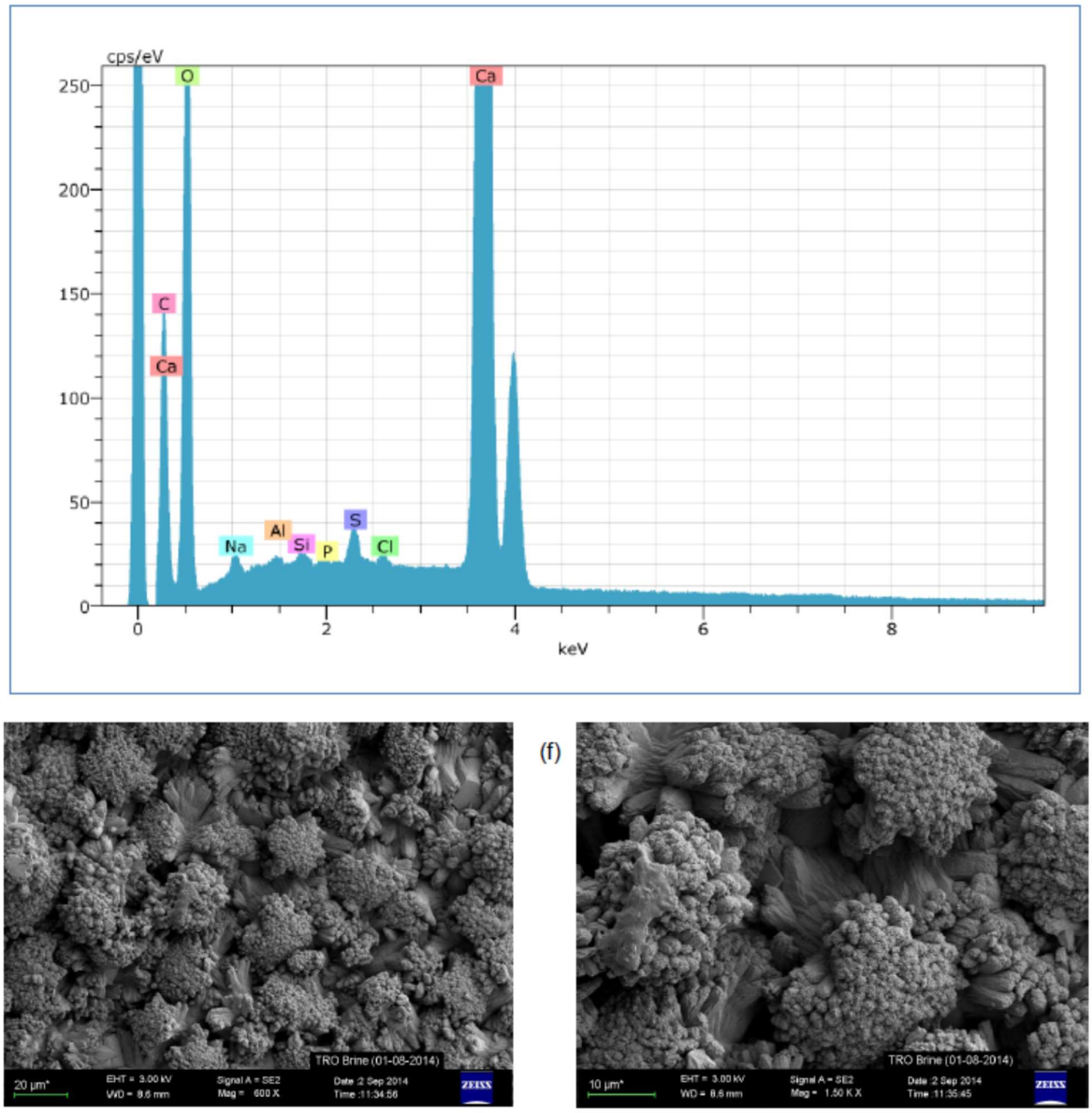

Figure 5-13: EDS Spectrum and SEM Morphology for the used membrane (Synthetic TRO/SRO Brine feed solution)

The EDS spectrum of Synthetic TRO/SRO Brine feed solution is shown in Figure 5-13. The EDS spectrum shows that C, O and Ca were major elements in this membrane sample with the minor elements being Na, Si, P, and Cl. It was also evident from the SEM morphology that the membrane was severely fouled.

Raman spectra obtained on the white particulates of the fouled membrane identified $CaCO_3$ (Aragonite and Calcite) to be present on the membrane sample, but in different polymorphic forms. Both polymorphs have bands at 154 and 1085 cm^{-1} with the latter being the $\nu_s(CO_3^{-2})$ band. Aragonite has unique bands at ~205 and 704 cm^{-1} and calcite at ~279 and 709 cm^{-1}.

The fouled membrane sample was further characterised using XRD, and the results showed the presence of aragonite and magnesium calcite ($Ca_{0.936}Mg_{0.064}$ (CO_3)) (Refer to Appendix 3 for X-ray Diffractogram). From the FO membrane morphology results, it can be deduced that the steep flux decline observed in Figure 5-13 is associated with the precipitation of calcium and magnesium-based compounds ($CaCO_3$ and $Ca_{0.936}Mg_{0.064}$ (CO_3)) on to the membrane surface due to the interaction of scaling precursors in the feed solution (Ca^{2+} and Mg^{2+}) and draw solution (CO_3^{2-}). The mineral precipitating from this stream as water recovery was increased based on OLI Stream Analyser simulation discussed in Chapter 3 were silica, calcium sulphate dihydrate and fluorapatite. This contrast shows that different fouling mechanism was at play.

5.9.3 Combined Regeneration Effluent Bench Scale Tests.

The results from bench-scale testing of the feasibility of using forward osmosis technology to treat Combined Regeneration Effluent stream are presented and discussed in this section.

5.9.3.1 Water Flux and Salt Flux (Pure Water as Feed)

Figures 5-14 & 5-15 show the water fluxes and salt fluxes, respectively, when the FO-TFC membrane was tested with the active layer facing the deionised water (AS-DI) using 3 M ammonium bicarbonate as a draw solution.

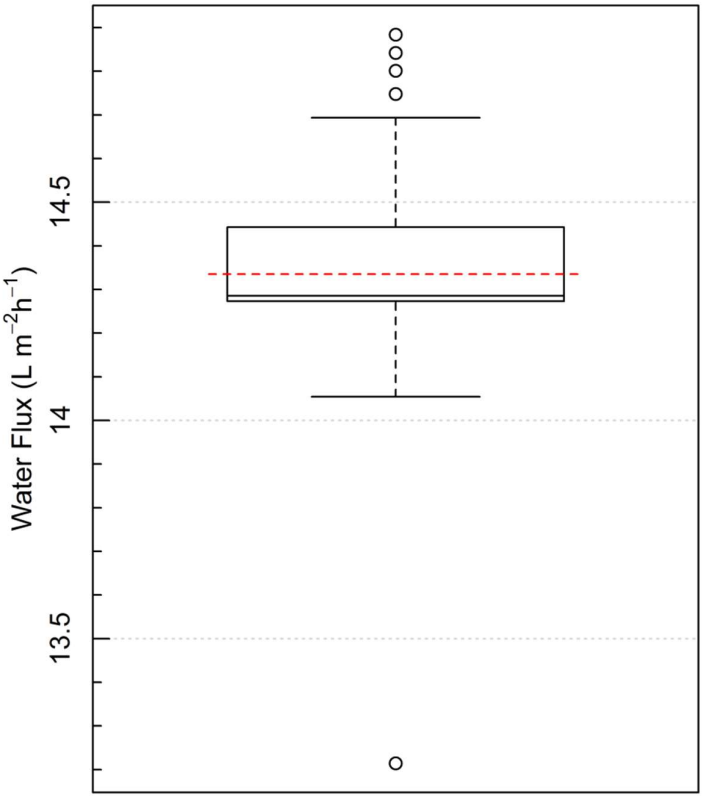

Figure 5-14: Water flux for Combined Regeneration Effluent run (Feed solution: DI; Draw solution: 3 M NH_4HCO_3; Co-current cross flow rate: 1.5 L/min; Temperature (DI and DS): 30ºC); Pressure: 1 atm.

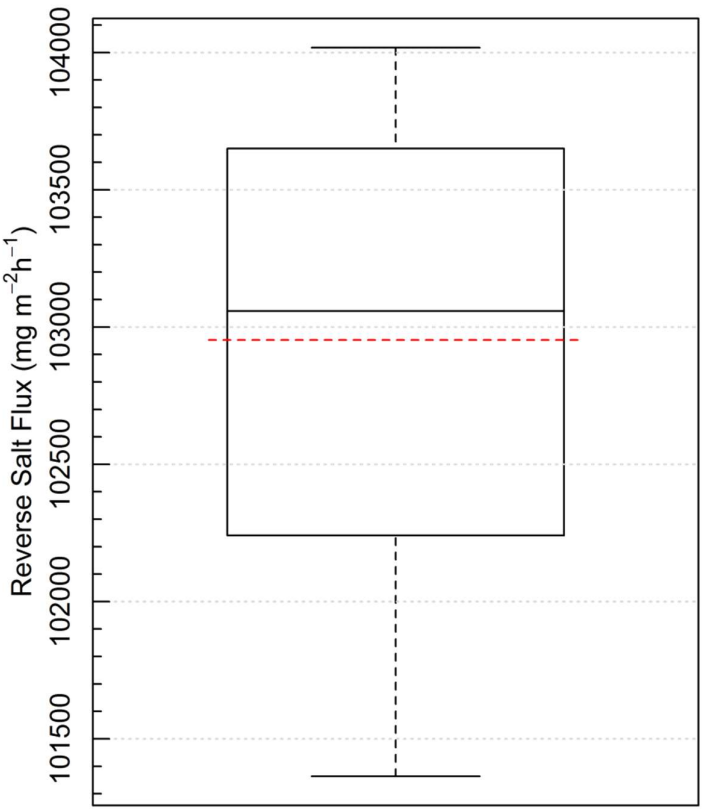

Figure 5-15: Reverse Salt Flux for Combined Regeneration Effluent run (Feed solution: DI; Draw solution: 3 M NH_4HCO_3; Co-current cross flow rate: 1.5 L/min; Temperature (DI and DS): 30ºC); Pressure: 1 atm.

The average water and salt fluxes obtained for the membrane characterization run was 14.3 (SD = 0.3) L.m^{-2}.h^{-1} and 102950 (SD = 821.0) mg m^{-2}.h^{-1}, respectively. The standard deviation shows that there was minimal variation in the water flux throughout the experiment, and this was to be expected as the run was conducted with constant draw solution osmotic pressure. The osmotic pressure exerted by the feed water was negligible to alter the osmotic driving force significantly. On average, the conductivity in the feed tank was 0.45 mS/cm with a maximum of 0.66 mS/cm. These conductivities were very low when compared to that observed for the draw solution (mean = 142.4, SD = 0.96 mS/cm). It is evident from the reverse salt flux plot that there was a significant amount of draw solution that diffused back to the feed water tank (DI). This was also confirmed by the continuous increase in feed water conductivity as the run progressed. The Specific Reverse Salt Flux (SRSF) for this membrane using the average water flux and reverse salt flux according to Equation 5-3 was 7.4 g of ammonium bicarbonate per litre of product water and this was comparable to that of the TFC-FO membrane used for the HRP and TRO/SRO Brines runs.

5.9.3.2 Baseline and Synthetic Runs

Sodium chloride solution was used as a baseline to investigate the impact of decreasing osmotic driving force on the water recovery and flux (refer to Table 5-2). After this, simulated synthetic Combined Regeneration Effluent solution (refer to Table 5-1 & 5-3) was tested to evaluate the feasibility of treating this stream using FO technology. Figure 5-16 below shows the influence of water recovery on water flux as observed during the baseline and synthetic run.

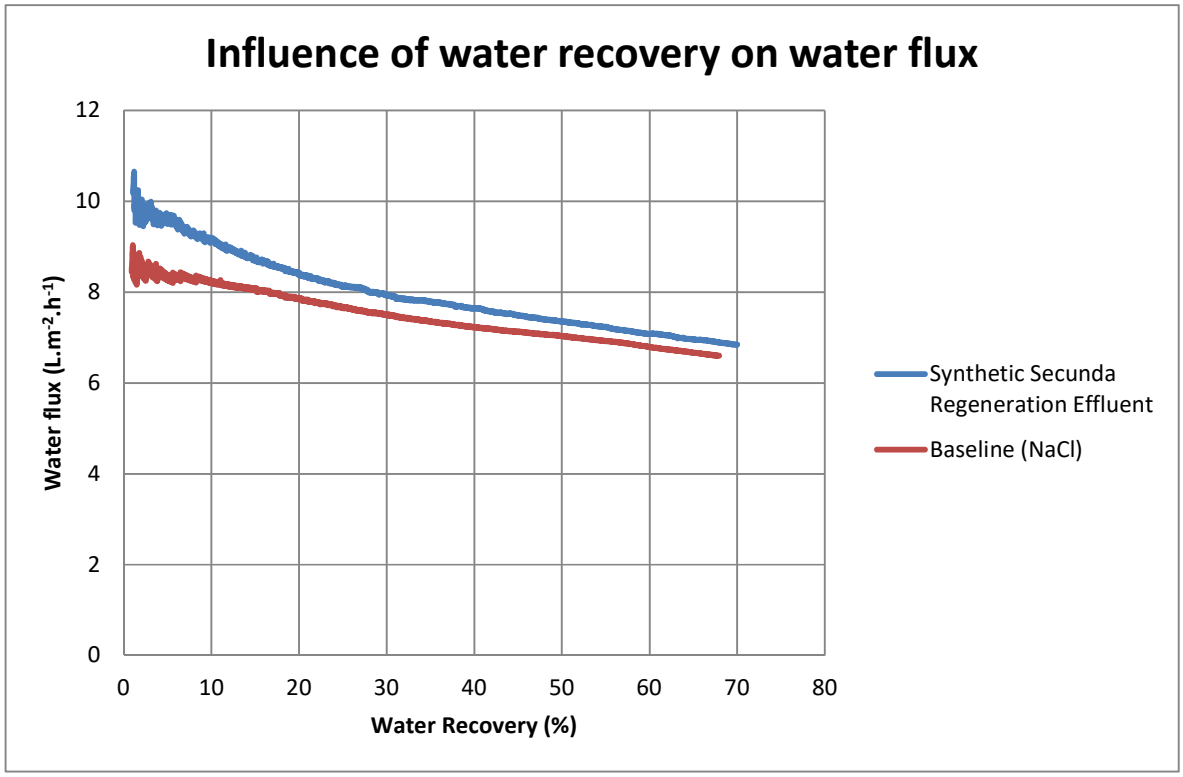

Figure 5-16: Influence of water recovery on water flux for experiment conducted with NaCl or Synthetic Combined Regeneration Effluent as feed solution.

The initial flux during the baseline experiment with NaCl as a feed (bench-scale unit was operated until about 70% of the starting feed volume was recovered) was around 9 $L.m^{-2}.h^{-1}$, and it decreased to a final water flux of roughly 6.6 $L.m^{-2}.h^{-1}$ as the feed solution concentration increases. The conductivity of the feed water increased from 36 mS/cm to about 90 mS/cm, indicating that the feed was concentrated. The increase in feed solution concentration resulted in a decrease in osmotic driving force even though the DS concentration was kept constant, which resulted in the decline in flux. For the Synthetic solution, the initial flux was around 10.6 $L.m^{-2}.h^{-1}$, and the flux decreased to a final water flux of ca. 6.9 $L.m^{-2}.h^{-1}$ (experiment was conducted until about 70% of the original feed volume was recovered). The water flux of the synthetic solution started off higher than that of the base solution, although they should have had the same starting osmotic pressure.

This "phenomenon" was not investigated further during the study as the differences were not deemed as significant during the execution of the experiments. The conductivity of the synthetic Combined Regeneration Effluent feed solution increased from 36 mS/cm to about 90 mS/cm, which was very similar to that observed for the non-scaling baseline feed solution. As indicated in Figure 5-16 above, the water flux trend was very similar to that of the baseline run, and this was a clear indication that there was no significant change in membrane performance or no significant membrane fouling induced by Combined Regeneration Effluent. Although there was reverse salt diffusion, indications were that the concentration of the scaling precursors in the feed, specifically Ca^{+2}, played a major role when it comes to membrane fouling. The Combined Regeneration Effluent solution has the lowest Ca^{+2} concentration (approximately 100 mg/L) when compared to that of the other three solutions (High Rinse Portion (~860 mg/L), TRO/SRO Brine (500 mg/L) and Mother Liquor (545 mg/L)). The inspection of the membrane coupon after the experiment showed that the membrane was also clean (Figure 5-17) with no noticeable membrane fouling which contrasted with the HRP and TRO/SRO Brine synthetic solutions' used membranes.

Figure: 5-17: Picture for the used membrane (Synthetic Combined Regeneration Effluent feed solution)

5.9.3.3 FO Membrane Morphology

Morphology of the used membrane was studied to evaluate the effect of synthetic Combined Regeneration Effluent solution on the membrane performance.

The feed and draw solution for this experiment also contained scale precursors such as Ca^{+2}, Mg^{+2} (low concentration when compared to other streams), SO_4^{-2}, SiO_2 and CO_3^{-2}. Figure 5-18 shows the EDS spectrum and SEM Morphology for the used membrane.

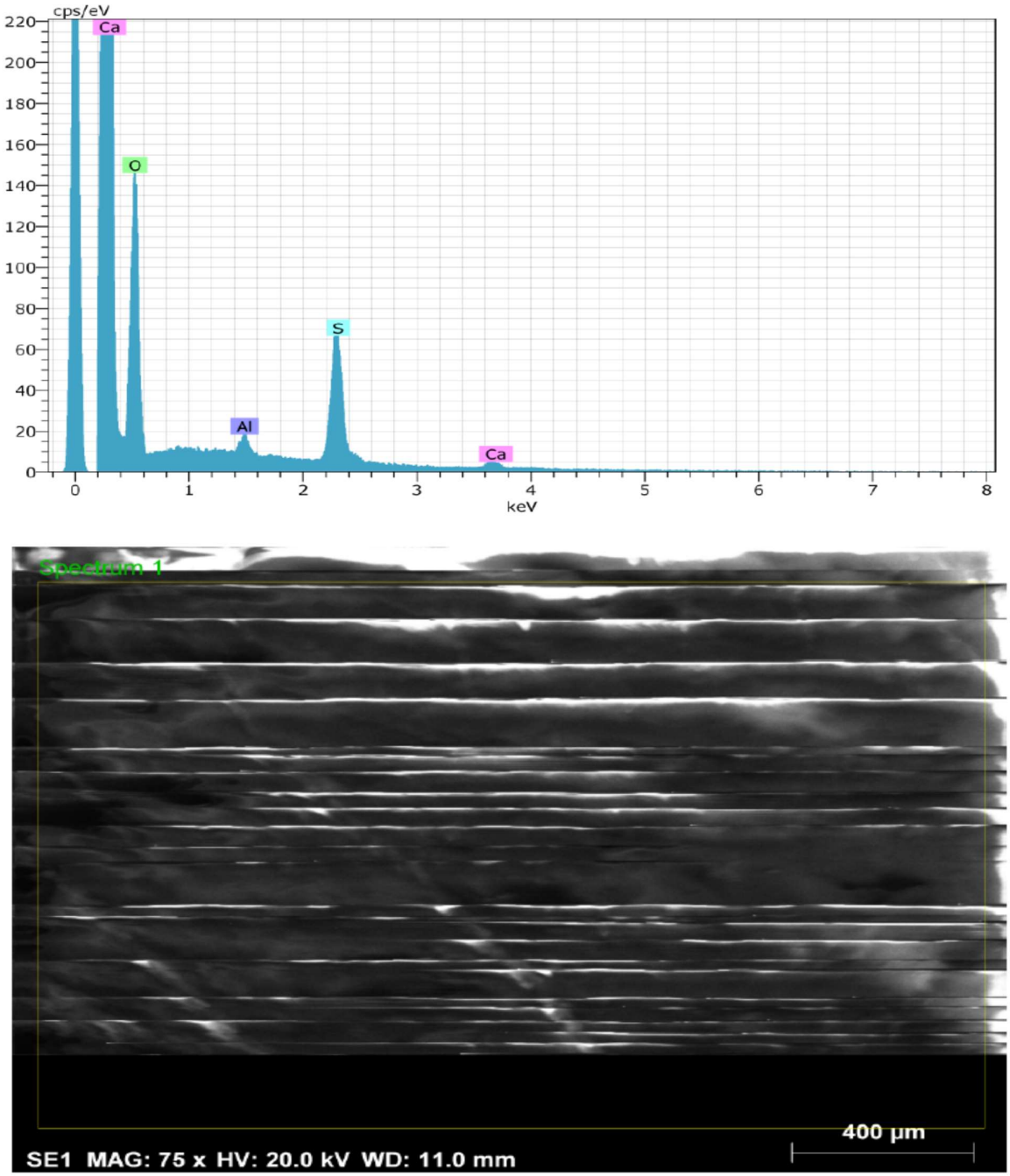

Figure 5-18: EDS Spectrum and SEM Morphology for the used membrane (Synthetic Combined Regeneration Effluent feed solution)

The EDS spectrum of Synthetic Combined Regeneration Effluent feed solution is shown in Figure 5-18. The EDS spectrum shows that C (overlap with Ca peak L alpha), O and S (building blocks for the virgin membrane, refer to Figure 5-6) were major elements in this membrane sample. It was evident from the EDS spectrum that intensity of the distinct Ca peak (between 3 and 4 KeV) that was observed for the HRP and TRO/SRO Brine synthetic solution has decreased significantly, and Ca peak was considered minor.

It was also evident from the SEM morphology that the noticeable fouling that was observed for the HRP and TRO/SRO Brine solution runs was absent, and the used membrane appeared clean. Raman spectra obtained for this membrane showed the presence of both Aragonite and Calcite indicating that although the membrane fouling was not severe based on the hydraulic performance (Figure 5-16) and visual observation (Figure 5-17), some fouling did occur on the membrane surface, but this did not contribute significantly to the decline in water flux as the water recovery was increased. Furthermore, this could also suggest that the minerals that precipitated could be managed hydraulically through cross-flow rate. OLI Stream Analyzer simulation for this stream, discussed in Chapter 3 predicted the formation of aluminium hydroxide, calcium sulphate dihydrate and silica as water recovery was increased. The formation of these minerals was not observed even at 70% water recovery. The dominating factor which contributed to the decline in water flux as the water recovery was increased could be attributed mainly to the decrease in osmotic driving force rather than fouling. The results from this run highlight a critical point about the impact of the concentration of scale precursors in the feed solution on FO membrane fouling. The implication of this is that for high hardness brine streams a hardness removal step (complete or partial hardness removal), in particular, calcium hardness may be required to make the FO process viable. Oasys Water, Inc., a company which was in the forefront of commercialising the FO process using patented TFC-FO membrane and NH_3/CO_2 draw solution, included a softening step in its pilot-scale demonstration & commercial plants treating high salinity brines (McGinnis et al., 2013) and (Pendergast et al., 2016).

5.9.4 Mother Liquor Bench Scale Tests.

The results from bench-scale testing of the feasibility of using forward osmosis technology to treat Mother Liquor stream are presented and discussed in this section.

5.9.4.1 Water Flux and Salt Flux (Pure Water as Feed)

Figures 5-19 & 5-20 show the water fluxes and salt fluxes, respectively, when the FO-TFC membrane was tested with the active layer facing the deionised water (AS-DI) using 3 M ammonium bicarbonate as a draw solution.

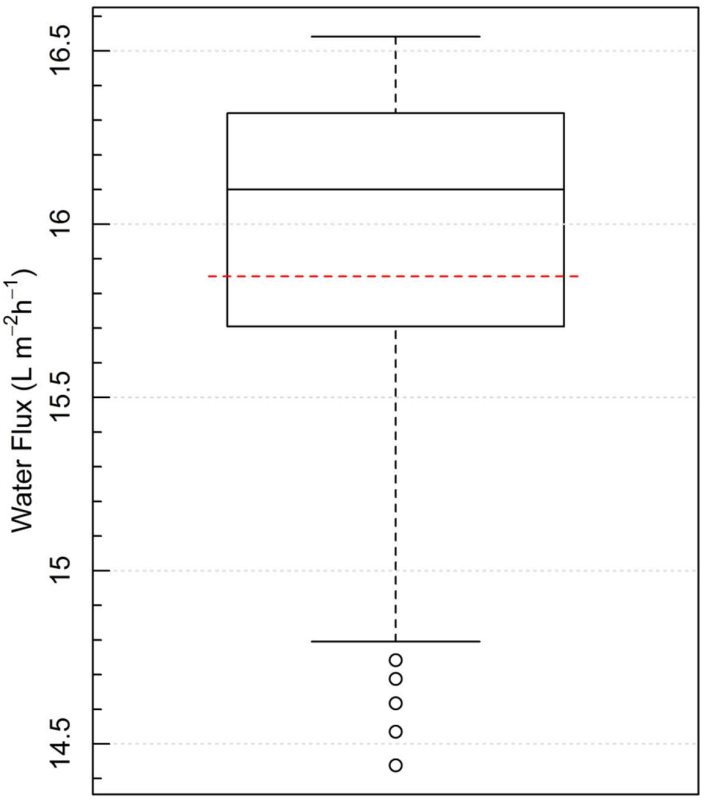

Figure 5-19: Water flux for Mother Liquor run (Feed solution: DI; Draw solution: 3 M NH_4HCO_3; Co-current cross flow rate: 1.5 L/min; Temperature (DI and DS): 30ºC); Pressure: 1 atm.

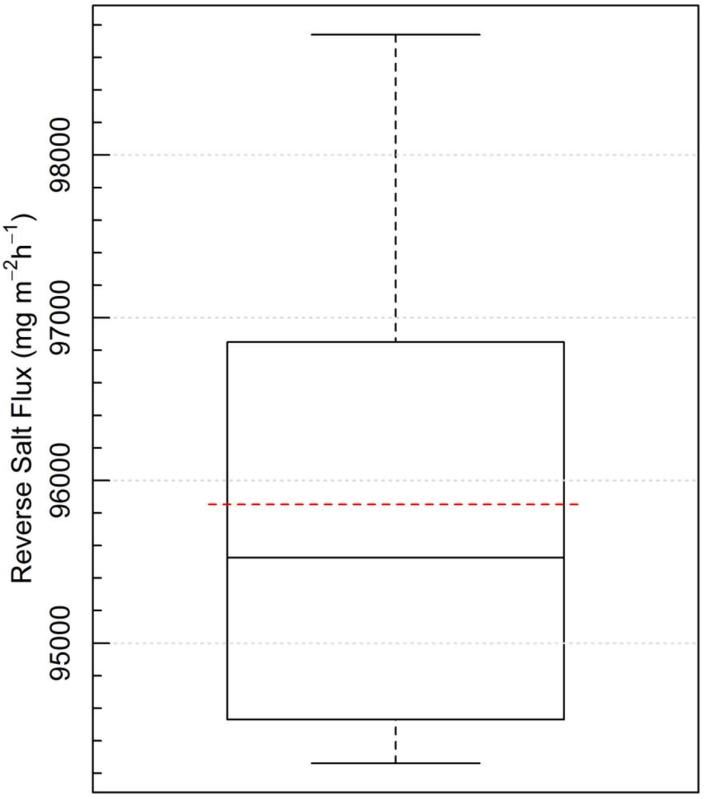

Figure 5-20: Salt Flux for Mother Liquor run (Feed solution: DI; Draw solution: 3 M NH_4HCO_3; Co-current cross flow rate: 1.5 L/min; Temperature (DI and DS): 30ºC); Pressure: 1 atm.

The average water and salt fluxes obtained for the membrane characterisation run was 15.8 (SD = 0.6) $L.m^{-2}.h^{-1}$ and 95852 (SD = 1494) $mg.m^{-2}.h^{-1}$, respectively. The standard deviation shows that there was minimal variation in the water flux throughout the experiment, and this was to be expected as the run was conducted at constant draw solution concentration. The osmotic pressure exerted by the feed water was negligible to alter the osmotic driving force significantly. On average, the conductivity in the feed tank was 0.42 mS/cm with a maximum of at 0.63 mS/cm. These conductivities were very low when compared to that observed for the draw solution (mean = 141.8, SD = 0.5 mS/cm). It was evident from the reverse salt flux plot that there was a significant amount of draw solution that diffused back to the feed water tank (DI). This was also confirmed by the continuous increase in feed water conductivity as the run progressed. The Specific Reverse Salt Flux (SRSF) for this membrane using the average water flux and reverse salt flux was 6.1 g of ammonium bicarbonate per litre of product water, and this was marginally lower to that of the TFC-FO membrane used for the HRP, TRO/SRO Brine and Combined Regeneration Effluent runs.

The marginal difference could potentially be attributed to the difference in selectivity of the membrane coupons used for this study. The SRSF was, however, still very high and its impact when interacting with the synthetic Mother Liquor feed solution could still be very significant.

5.9.4.2 Baseline and Synthetic Runs

To investigate the impact of decreasing osmotic driving force on the water recovery and flux, sodium chloride solution (osmotic pressure same as that of the synthetic Mother Liquor solution to be used) was used as a baseline. After this, the simulated synthetic Mother Liquor solution was tested to evaluate the feasibility of using FO technology to treat this stream. Figure 5-21 below shows influence of water recovery on water flux during the baseline and synthetic run.

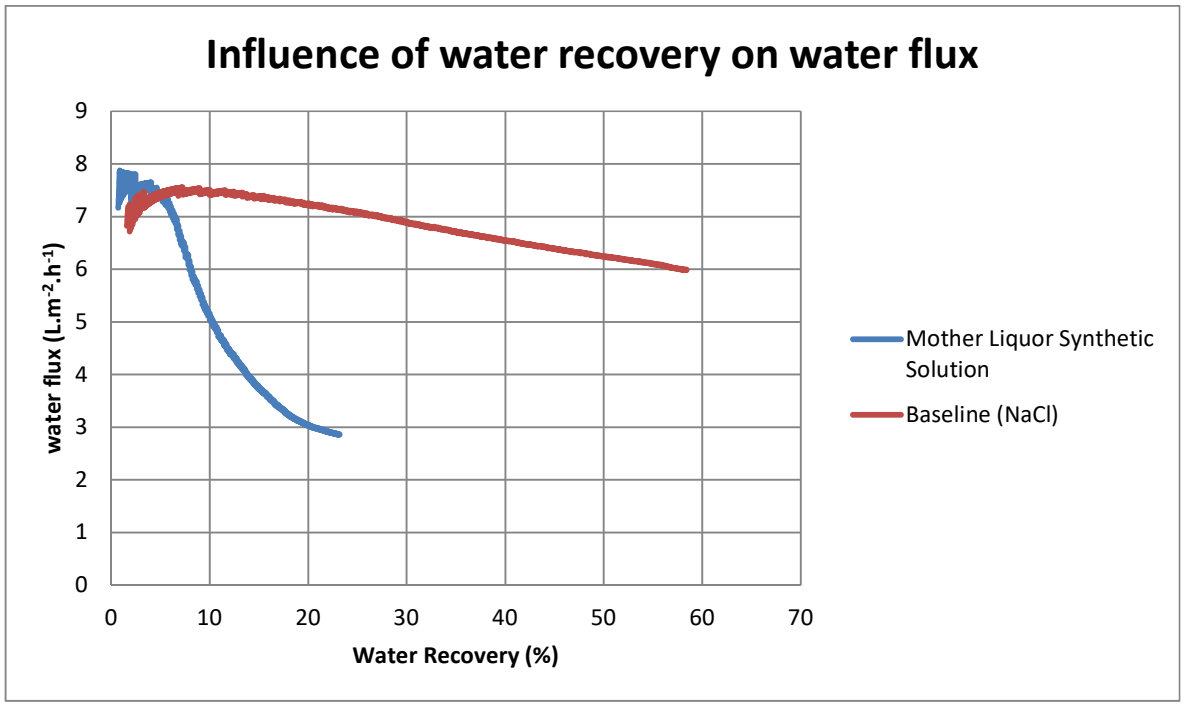

Figure 5-21: Influence of water recovery on water flux for experiment conducted with NaCl or Synthetic Mother Liquor as feed solution.

Figure 5-21 above shows that for the mother liquor runs, the experiment took slightly longer to reach a steady-state in terms of water flux.

The initial flux during the baseline experiment (after the steady-state was established) with NaCl as a feed (bench-scale unit was operated until about 58% of the starting feed volume was recovered) was around 7.5 $L.m^{-2}.h^{-1}$, and it decreased to a final water flux of roughly 6 $L.m^{-2}.h^{-1}$ as the feed solution concentration or osmotic pressure increases. It is worth noting that the starting water flux for the mother liquor was low when compared to that of other streams, this was however expected because this stream is highly saline (blowdown from the evaporator).

The conductivity of the feed water increased from 56 mS/cm to about 110 mS/cm, indicating that the feed solution was concentrated. The increase in feed solution concentration resulted in a decrease in osmotic driving force even though the DS concentration was kept constant, which resulted in the decline in flux as discussed in the above paragraph. The run was stopped at 58% feed volume recovery as the permeation rate had become very low due to the decreasing osmotic driving force. For the Synthetic solution, the initial flux (after steady state was established) was around 7.8 $L.m^{-2}.h^{-1}$, and the flux decreased to a final water flux of ca. 2.9 $L.m^{-2}.h^{-1}$ (operated until approximately 22% feed volume recovery). The water flux of the synthetic solution started off higher than that of the base solution, although they should have had the same starting osmotic pressure. This "phenomenon" was not investigated further during the study as the differences were not deemed as significant during the execution of the experiments. As indicated in Figure 5-21 above, the water flux trend was very different from that of the baseline run, and this was a clear indication of potential premature membrane fouling. Table 17 in Appendix 3 shows a summary of results before and after the experiment for the synthetic run, and it was evident that there was a reverse diffusion of ammonium bicarbonate solute to the feed solution and this resulted in the increase in pH from between 5.5 and 6 to about 8.6 on average. The inspection of the membrane coupon after the experiment showed that the membrane was also severely fouled with white precipitate (Figure 5-22) (similar to that observed for the Synthetic HRP and TRO/SRO Brine feed solutions).

Figure 5-22: Picture for the used membrane (Synthetic Mother Liquor feed solution)

5.9.4.3 FO Membrane Morphology

Morphology of virgin and used membranes was studied to evaluate the effect of synthetic Mother Liquor solution on the membrane performance.

The feed and draw solution for this experiment contained scale precursors such as Ca^{+2}, Mg^{+2}, SO_4^{-2}, SiO_2 and CO_3^{-2}. Figure 4-23 shows the EDS spectrum and SEM Morphology for the used membrane.

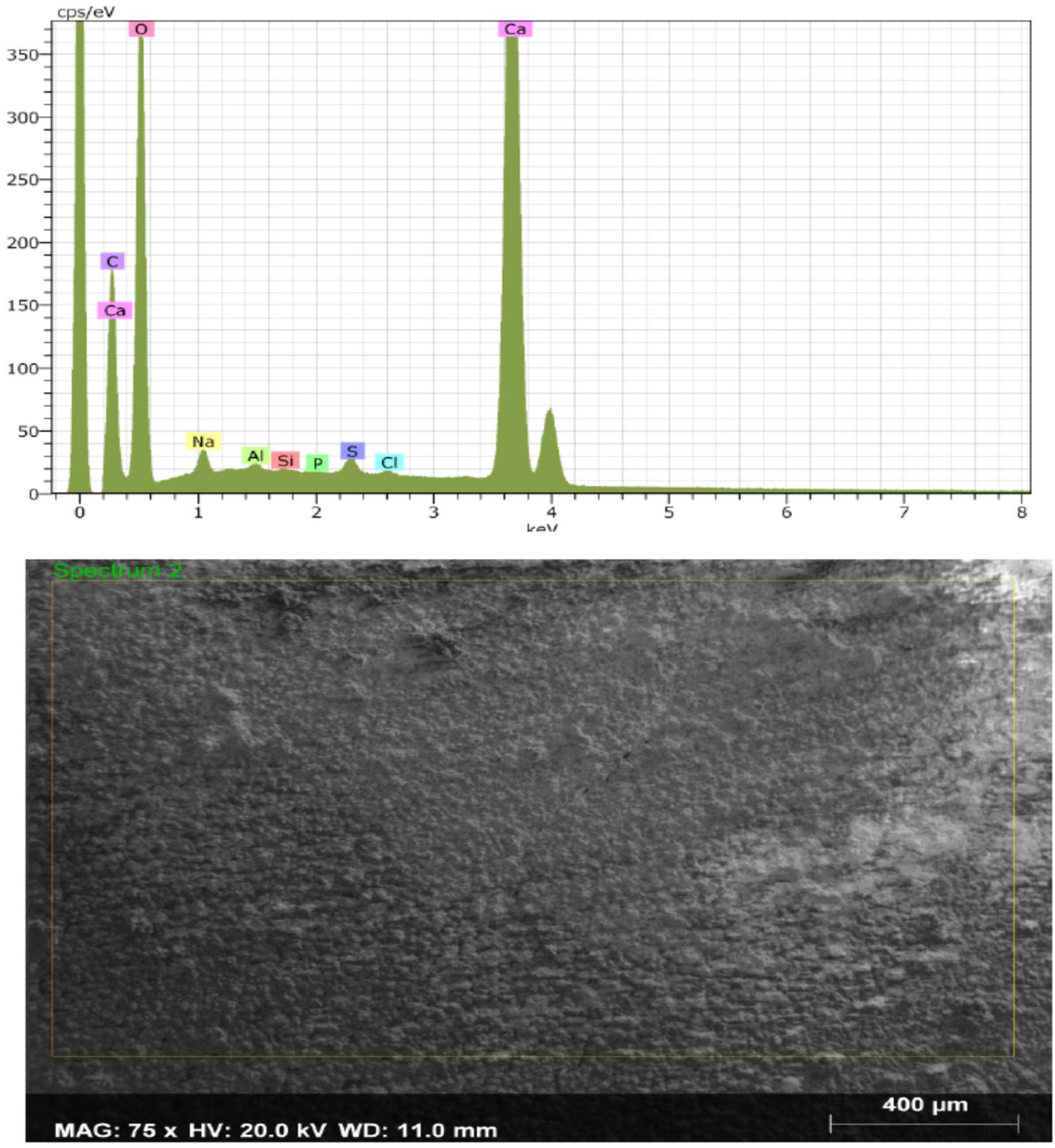

Figure 5-23: EDS Spectrum and SEM Morphology for the used membrane (Synthetic Mother Liquor feed solution)

The EDS spectrum of Synthetic Mother Liquor feed solution is shown in Figure 5-23. The EDS spectrum shows that C, O and Ca were major elements in this membrane sample with the minor elements being Na, Si, P, Al, and Cl. It was also evident from the SEM morphology that the membrane was severely fouled. Raman spectra obtained on the white particulates of the fouled membrane identified $CaCO_3$ to be present on the membrane sample, but in different polymorphic forms. Both polymorphs have bands at 154 and 1085 cm^{-1} with the latter being the ν_s (CO_3^{-2}) band. Aragonite has unique bands at ~205 and 704 cm^{-1} and calcite at ~279 and 709 cm^{-1} (refer to Appendix 2 for spectra). The EDS spectrum, SEM Morphology and Raman Spectroscopy of the same run conducted using a new membrane coupon showed similar results (results not shown). The mineral precipitating as water recovery was increased based on OLI Stream Analyser simulation were silica, calcium sulphate dihydrate and fluorapatite.

5.9.5. Evaluation of the impact of hardness removal on FO process using Mother Liquor as feed solution

A follow-up study was conducted using Mother Liquor as a feed solution in order to understand the impact of calcium concentration on FO membrane fouling. This study was important as it would give an indication of the amount of hardness (specifically calcium based) that could be tolerated when treating this stream.

Table 5-4 below summarises the feed composition of baseline and Mother Liquor solutions used for follow up experiments.

Table 5-4: Detailed composition of baseline and synthetic solutions (Mother Liquor at various calcium concentration) simulating actual streams (the synthetic composition and concentration were generated using OLI Stream Analyzer 3.2 (OLI Systems Inc., Morris Plains, NJ, US)

Parameter	Baseline Runs (NaCl)	Mother Liquor (~Near Zero Point)	Mother Liquor (~Mid-Point)	Mother Liquor (~High-Point)
	mg/L	mg/L	mg/L	mg/L
$Ca(OH)_2$	-	3.26	469.6	973.5
NaCl	46000			
$KCl.6H_2O$	-	7351.6	7349.7	7348.0
H_2SO_4	-	27269.2	27261.86	27203.06
HCl		11818	11815	11812
NaOH		36240.84	34846.67	34238.76
MgO		162.6	202.3	202.4
pH* (after pH adjustment)	-	6.49	5.02	5.82
Osmotic Pressure (atm)	37.5	37.7	37.5	37.3

Figure 5-24 below shows the influence of water recovery on water flux during the baseline, and synthetic Mother Liquor runs.

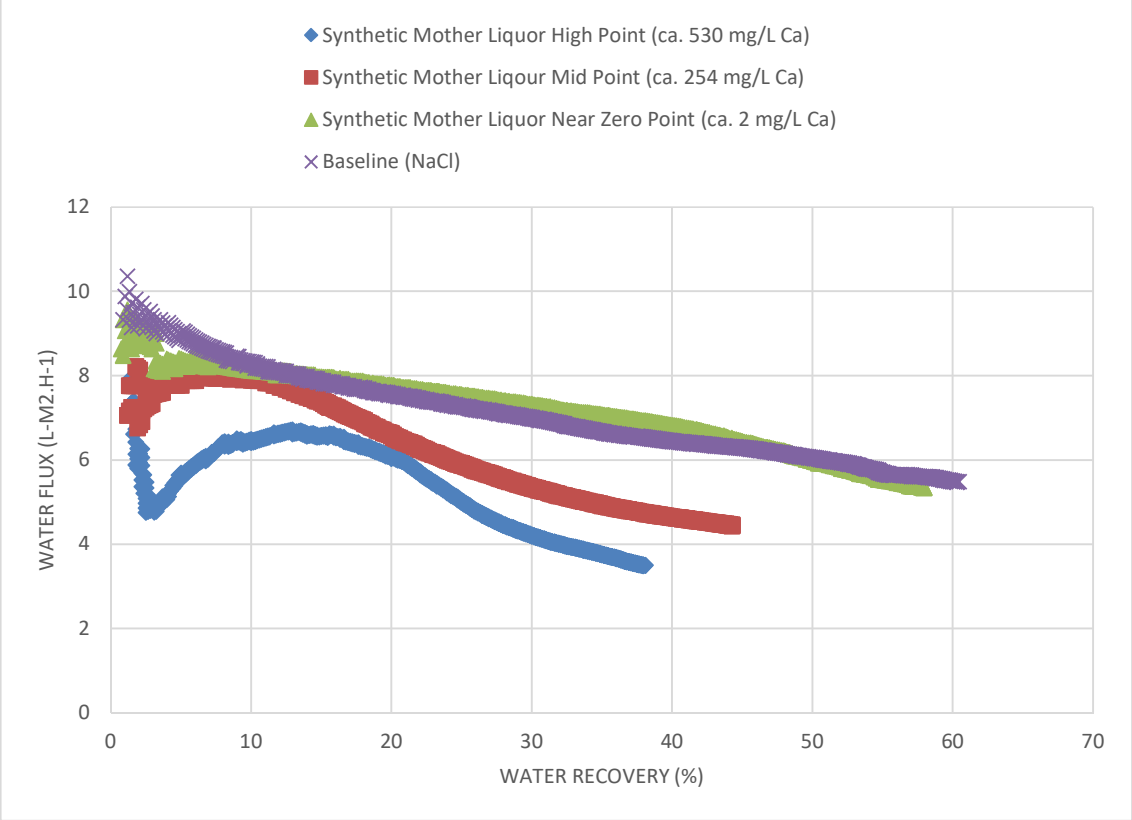

Figure 5-24: Influence of water recovery on water flux during the baseline and synthetic Mother Liquor run (Zero Calcium concentration point).

As indicated in Figure 5-24, the water flux trend for the synthetic Mother Liquor feed solution at almost zero calcium concentration (ca. 2 mg/L) was very similar to that of the baseline run (NaCl), and this was a clear indication that there was no change in FO membrane performance or FO membrane fouling induced by softened synthetic Evaporator Blowdown feed solution. The SEM-EDX spectra and visual inspection of the used membrane coupon showed that the membrane coupon had no noticeable fouling on the surface.

Figure 5-25 below shows SEM-EDX spectra confirming that there was no noticeable fouling on the membrane surface. Visual inspection of the membrane after the run also confirmed this.

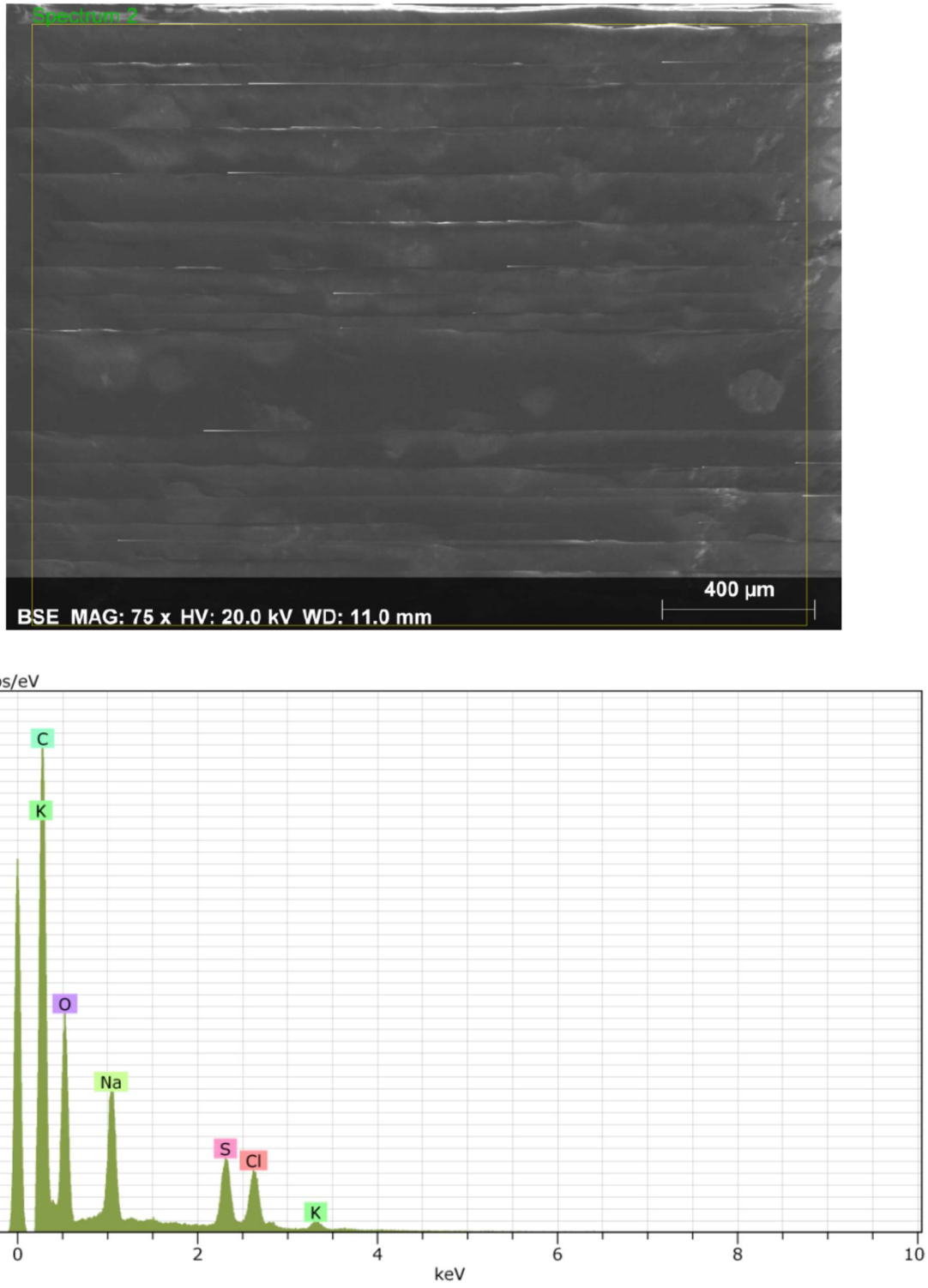

Figure 5-25: SEM and EDS spectra for Mother Liquor Zero Point Run

It was also evident from water flux vs water recovery trends in Figure 5-24 that, for feed solutions containing calcium concentration at ca. 250 mg/L and ca. 530 mg/L, fouling of the membrane was observed. The synthetic Mother Liquor feed solution containing ca. 250 mg/L calcium concentration, however, showed less fouling when compared to the feed solution containing ca. 530 mg/L (comparing water flux decline and water recovery achieved). The initial flux for the Mother Liquor experiment at mid-point calcium concentration was ca. 8 $L.m^{-2}.h^{-1}$, and it decreased to approximately 4.4 $L.m^{-2}.h^{-1}$ (45% water recovery). It was however clear from the Mother Liquor Mid-Point Calcium trend that there was a continuous decline in the flux when the water recovery was increased, and this was very much similar to the trends observed for the Mother Liquor experiment discussed in section 5.9.4.

The EDS spectrum of Synthetic Mother Liquor feed solution (Mid-Point Calcium concentration) is shown in Figure 5-26. The EDS spectrum shows that C, O and Ca were major elements in this membrane sample with the minor elements being Na, S, P, Al, and Cl. It was also evident from the SEM morphology that the membrane was fouled. The FTIR spectra of the Mother Liquor sample at Mid-Point Calcium concentration showed bands at 1443, 1082, 852, 712 and 699 cm^{-1} and these bands were assigned to $CaCO_3$. These results again confirm the impact of calcium concentration, as observed in section 5.9.4.

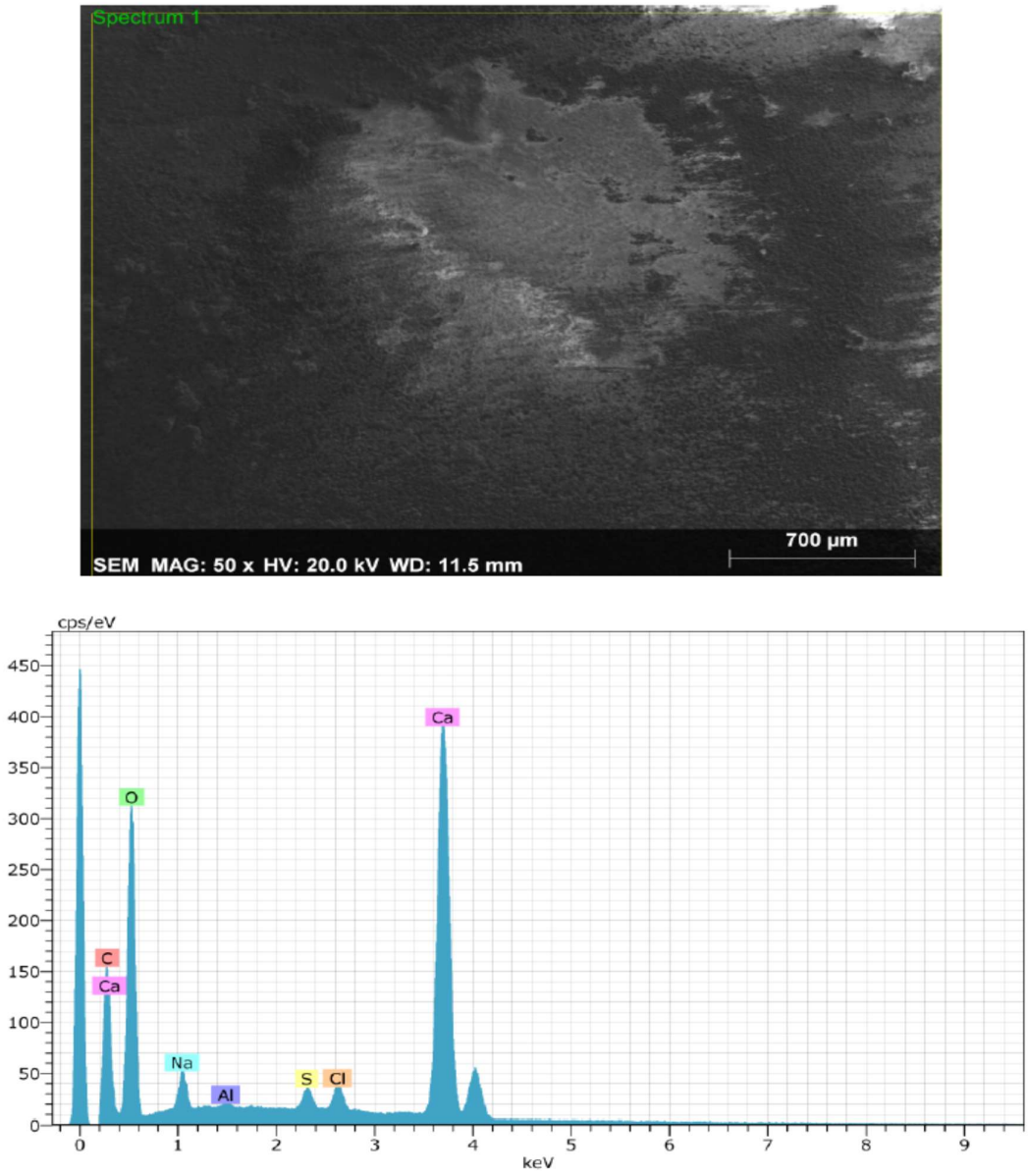

Figure 5-26: SEM and EDS Spectra for Mother Liquor Mid-Point Calcium concentration run

Figure 5-24 also shows that for the high point calcium scenario, the initial water flux was approximately 8 $L.m^{-2}.h^{-1}$ which decreased to approximately 3.5 $L.m^{-2}.h^{-1}$ when the experiment was stopped at 38% water recovery. It is also worth noting that there appears to be an initial sharp decline in water flux from 8 $L.m^{-2}.h^{-1}$ to approximately 5 $L.m^{-2}.h^{-1}$ and after that, the water flux starts to increase and stabilised at about 6.5 $L.m^{-2}.h^{-1}$. The water flux starts to decrease from 20% water recovery until the end of the experiment. It is hypothesised that the initial drop in water flux at the beginning of the experiment could be due to a sudden rush in draw solution solutes back to the feed solution as a result of high-water flux. It, however, appears as if this initial fouling was not permanent as indicated by the increase again in water flux.

The increase in water flux observed for scenarios in Figure 5-24 occurred after the initial decline. This decline was deemed "initial non-permanent fouling" removable hydraulically (cross-flow rate). Once this "non-permanent fouling" was removed, there was an increase in the water flux which was followed by decline as water recovery was increased. The decrease was due to scaling of the membrane as supported by the SEM/EDS spectra. This hypothesis was however not tested during the execution of the experiments. It is included in the recommendation section for future investigation.

Figure 5-27 below shows the SEM and EDS spectra for Mother Liquor High Point Calcium concentration run.

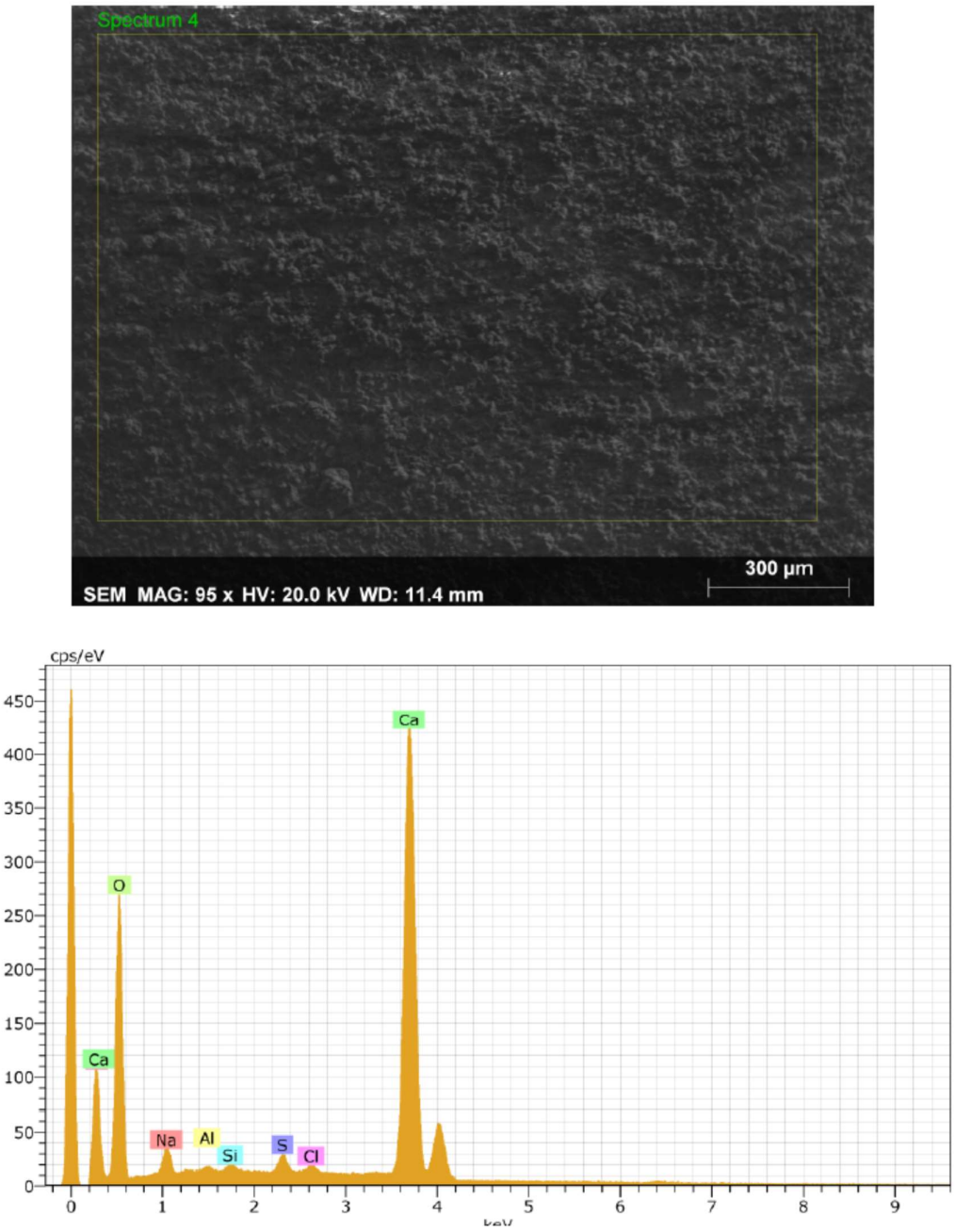

Figure 5-27: SEM and EDS Spectra for Mother Liquor High Point Calcium concentration run

The EDS spectrum shows that C, O and Ca were major elements in this membrane sample with the minor elements being Na, S, P, Al, and Cl. It was also evident from the SEM morphology that the membrane was heavily fouled.

The FTIR spectra of the Mother Liquor sample at High-Point Calcium concentration showed bands at 1443, 1082, 852, 712 and 699 cm^{-1} and these bands were assigned to $CaCO_3$.

The result from the evaluation of the impact of hardness concentration indicates that complete softening of the Mother Liquor feed solution might not be required as the performance of the FO process could potentially be sustained by just removing just enough calcium from the feed water. Although the EDS and Infrared spectra confirmed calcium carbonate precipitation for both cases (i.e. middle and high calcium concentration), SEM morphology and visual observation showed that the high calcium concentration membrane coupon was heavily fouled when compared to the middle calcium concentration membrane coupon.

The draw solution induced calcium carbonate scaling discussed in this dissertation was also observed by Li et al. (2015) when evaluating the feasibility of using the FO process to desalinate Sea Water using Ammonium Bicarbonate as a draw solution. The SRSF observed in Li et al. (2015) study was 12 g/L (even higher than what was observed during this study). It must, however, be stated that Li et al. (2015) used Cellulose Triacetate (CTA) membrane). Li et al. (2015) showed that the scaling occurs very early in the process, as observed during this study. The EDS spectrum of the membrane coupon from these authors study showed that the surface of the membrane coupon contained Ca as a major element (similar to what was observed with the High Rinse Portion, TRO/SRO Brine and Mother Liquor streams). Scaling observed in their study showed a typical aragonite cluster (similar to what was observed for brine streams evaluated in this study). The potential fouling mechanism observed in this study was similar to the mechanism 2 highlighted by She et al. (2016) in Figure 2-10. Fouling mechanism 2 involves the enhancement of inorganic fouling of the FO membrane due to the reverse salt diffusion of scaling precursors in the draw solution to the feed.

Li et al. (2015), however, indicated that the membrane permeability lost due to the experienced scaling could be recovered (albeit not 100%) using hydraulic cleaning (increased cross-flow velocity). The impact of increasing cross-flow velocity on water flux (albeit for non-scaling solutions) was also observed during this study (refer to chapter 4).

Al-Furaiji (2009) investigated the treatment of hyper-saline produced water using FO process. Severe scaling effects were observed when using NH_3-CO_2 draw solution, which resulted in a reduction in the forward osmosis water flux and recoveries. Calcium carbonate was also found to be the main component that caused the observed scaling. Formation of the calcium carbonate was found to be due to the interaction between the calcium ions that exist in the feed solution with carbonate ions from the draw solution. Furthermore, the transport of draw solution to the feed side of the membrane causes a pH increase at the feed side which subsequently promotes favourable conditions for calcium carbonate precipitation.

5.10 Contaminants Rejection

One of the most important criteria for an ideal FO membrane is its ability to achieve high contaminants rejection (organic, particulate and inorganic) to ensure that the desalinated water is suitable for re-use or discharge. In this study, feed water and draw solution were characterised in order to assess the selectivity of the TFC-FO membrane used. Analysing samples generated during the bench-scale FO experiments requires the quantification of the concentration of components (cations or anions or organic matter) at very low levels in the presence of an extremely higher concentration of ammonium bicarbonate in the draw solution. Because the membranes used in the FO process cannot reject all the components (as it is the case in RO membranes), the ions of interest in the draw solution samples were those that diffused through the FO membrane from the feed solution to the draw solution.

In order to analyse the cations, the FO draw solutions required a sample pre-treatment procedure to remove the ammonia in excess. The high ammonia content of draw solution destabilises the plasma conditions, affecting the accuracy of the ICP-OES analysis. A standard addition method was tested for the analysis of draw solution but proved to be unsuitable. A customised method was developed, which showed that the draw solution could be analysed using an ICP-OES method after the proper pretreatment to remove ammonia. It must, however, be stated that the procedure to pre-treat the sample was very long and despite the pre-treatment steps cations analysis remained the challenge. For anions, the ion chromatography (IC) was found to be reliable to quantify the anions in the feed and draw solution. Based on Table 18 & 19 (refer to Appendix 3), it was evident that in general the most predominant ions in the draw solution (Ca^{+2}, Na^{+}, Cl^{-} and SO_4^{-2}) did not contaminant the draw solution (there were however some exceptions which could be attributed to the difficulty experienced when analysing the cations) implying that the selectivity of the TFC-FO membrane used was good, and the distillate from the draw solution regeneration step will be of good quality.

5.11 Concluding Remarks

This study investigated the potential of forward osmosis technology to desalinate high salinity brines and its limitations using synthetic streams with ammonium bicarbonate as a draw solution. Synthetic pure-component analogues of the selected industrial concentrated brine streams, namely, High Rinse Portion (Ion Exchange Regeneration Effluent), Tubular Reverse Osmosis (TRO)/Spiral Wound Reverse Osmosis (SRO) Brine, Ion Exchange Regeneration Effluent and Mother Liquor were used as feed solution. Critical performance parameters such as water flux, reverse solute diffusion, salt rejection, water recovery and membrane fouling were monitored and evaluated.

The batch studies conducted using deionised water as feed (membrane characterisation in terms of flux and reverse salt flux) have shown that specific reverse salt flux for the membrane coupons used was on average ranging from 6 to 7.4 g of ammonium bicarbonate per litre of the product water for the different brine streams. This specific reverse salt flux was high and has the potential to impact the feed water chemistry and subsequently result in draw solution induced membrane fouling due to the interaction of scaling precursors in the feed (Ca^{+2}, Mg^{+2}, SO_4^{-2}) with the scale precursors (CO_3^{-2}) in the draw solution. The results from the batch studies conducted using synthetic High Rinse Portion, TRO/SRO Brine, Combined Regeneration Effluent and Mother Liquor solutions showed that the High Rinse Portion, TRO/SRO Brine and Mother Liquor streams have high fouling propensity when compared to the Combined Regeneration Effluent. This observation was based on both the hydraulic performance as well as membrane morphology studies conducted on the used membrane coupons. The Combined Regeneration Effluent solution happens to have the lowest Ca^{+2} (~100 mg/L) concentration when compared to that of the other three solutions [High Rinse Portion (~860 mg/L), TRO/SRO Brine (~500 mg/L) and Mother Liquor (~545 mg/L)].

Furthermore, the experiments conducted to evaluate the impact of calcium concentration in the feed stream (zero calcium concentration point, mid calcium concentration point and high calcium concentration point) using Mother Liquor as feed showed that the concentration of scaling precursors in the feed, specifically Ca^{+2} plays a major role when it comes to membrane fouling when using ammonium bicarbonate as the draw solution due to the formation of draw solution induced calcite scale. Furthermore, it was clear that calcium concentrations have a major influence on the amount of scale formed and therefore, the degree of hardness was the primary parameter governing the scaling power of the selected brine streams. The fouling mechanism observed during this study was different to that of RO process and other FO processes reported (using NaCl as a draw solution) in which scaling is due to the supersaturation of the salts in the feed solution rather than the interaction of the feed with diffused draw solution ions (Scale precursor ions).

It was also evident in the batch studies that the most predominant scale for the streams that showed fouling tendency was calcium carbonate and none of the streams showed any calcium sulphate-based precipitate even though thermodynamic simulation has predicted calcium sulphate dihydrate precipitation even at lower water recovery (e.g. TRO/SRO Brine and Mother Liquor Stream). The potential explanation for this is that it is only when all carbonates were removed or depleted in the solution that calcium sulphate will then start to precipitate. With a continuous supply of carbonates from draw solution, there will always be enough carbonates in the solution, which then favours the formation of calcium carbonate.

This study provided new information on the interaction of the components of the draw solution with the feed water when using FO-TFC membrane and NH_4HCO_3 as a draw solution. The study showed that complete hardness removal in the feed water is not required for the FO process as some hardness could be tolerated as shown by the study conducted to show the impact of calcium concentration on the performance of the FO process. These results could lead to further reduction in the capital cost for the technology as only partial softening of the feed water could be required. Furthermore, there could be reduction in operational cost associated with softening chemicals. The mechanism of fouling was also demonstrated in this study, which confirm that the high specific reverse salt flux was responsible for the scale formation which contributed to water flux decline observed. The high specific reverse salt flux observed reinforced the need for more research on draw solution and FO membrane.

CHAPTER 6 : CONCLUSIONS AND RECOMMENDATIONS

The results from this study provided an insight into the FO process as an alternative desalination technology for high salinity brine streams. As a result, this study facilitated a better understanding of the FO performance, and investigation into the feasibility of adopting the FO technology for desalination, brine treatment and other possible applications. This chapter summarises the findings and recommends possible future work that can extend this study.

6.1 Conclusions

6.1.1 Preliminary Studies

During the preliminary study (Section 4.3), performances in terms of water flux and reverse salt flux under various experimental conditions were monitored and compared for the FO process

- When the FO configuration was AS-DS (i.e. active side facing the draw solution), internal ICP occurs within the loose support layer of the FO membrane on the feed side, which would lower the effective osmotic driving force and cause the water flux to be lower.
- When the FO process was tested with the feed solution (deionised water) facing the active side of the membrane (AS-DI), more severe internal ICP (dilutive ICP) occurs within the loose support layer of the FO membrane on the draw side, which resulted in a much lower water flux when compared to when the FO process was tested using AS-DS configuration.
- Increasing the temperature of the solutions on both side of the membrane resulted in an increased water flux and salt flux. This phenomenon was observed for both membrane orientations (i.e. AS-DI and AS-DS)
- Increasing the cross-flow velocity on both side of the membrane channel resulted in an increased water flux
- Increasing the draw solute concentration resulted in an increase in water flux and salt flux due to an increase in osmotic driving force. The greater the difference in osmotic pressure, as a driving force, the greater the water flux.
- Increasing the feed solute concentration (at constant draw solute concentration) resulted in a decrease in water flux due to decrease in osmotic driving force.
- A FO-TFC membrane water flux in both membrane orientations was consistently higher than those for the FO-CTA membrane. The FO-TFC membrane is pH tolerant in a 2 to 11 range and as observed in this study the water fluxes were higher than those obtained using FO-CTA membrane.

- The FO-CTA membrane is not appropriate for alkaline pH applications (i.e. when ammonium bicarbonate is used as a draw solution) due to its limited pH tolerance (3-8).
- Water fluxes and Salt fluxes obtained when the FO process was operated with ammonium bicarbonate draw solution (1 M) were generally higher than those obtained for sodium chloride (1 M) in both membrane orientations.

Results from the preliminary study showed that the FO process can achieve a better performance when the membrane orientation was AS-DS (i.e. active side of the membrane facing draw solution) as opposed to AS-DI (i.e. active side of the membrane facing the deionised water). This phenomenon was observed for both the CTA and TFC membranes. It must be stated however that the FO process configuration for this study was AS-DI (i.e. active layer facing feed solution) (Section 4.3.1). The key phenomena affected by the various experimental factors and therefore greatly influenced the FO performance was found to be internal concentration polarization (ICP) as reported extensively in the literature (Section 2.1.1.1).

Although the AS-DS configuration showed higher water fluxes than AS-DI, the AS-DS configuration is susceptible to severe fouling due to the potential precipitation of minerals into the support layer. In order to minimize the membrane-fouling effects the feed is made facing the active layer in the typical membrane desalination configuration. The preliminary study also showed that apart from membrane orientation the FO process was also influenced by additional factors such as temperature, cross flow velocity, membrane type, draw solute concentration, feed solute concentration and draw solution type. (Section 4.3.1 to 4.3.7)

6.1.2 Batch Studies Using Various Synthetic Solutions

The batch study (Section 5.9.1 to 5.11) investigated the feasibility of using forward osmosis technology to desalinate selected high salinity brine streams and its limitations using synthetic or generic streams. The studies were conducted using FO-TFC membrane and ammonium bicarbonate as a draw solution. Synthetic pure-component analogues of the selected industrial concentrated brine streams were used as feed solutions. Critical performance parameters such as water flux, reverse solute flux, water recovery and membrane fouling were monitored and evaluated. This section summarizes the findings from this study.

Water Flux and Reverse Salt Flux Tests-Membrane Characterization

- Experimental results showed that for the FO-TFC membrane coupons used the averaged water fluxes ranged from 12 $L.m^{-2}.h^{-1}$ to 15.8 $L.m^{-2}.h^{-1}$ with the average reverse salt flux ranging from 91322 $mg.m^{-2}.h^{-1}$ to 10492 $mg.m^{-2}.h^{-1}$.

- The resultant specific reverse salt flux for the membrane coupons used on average ranged from 6.to 7.4 g of ammonium bicarbonate per litre of the product water.
- This specific reverse salt flux was high and has the potential to impact the feed water chemistry and subsequently result in draw solution induced membrane fouling.
- With an exception of one membrane coupon which had a specific reverse salt flux of 6.1 g/L, the other coupons had a similar specific reverse salt flux (ca. 7 g/L) supporting the fact that this ratio relates to the membrane's selectivity of active layer as well as the type of the draw solution used.

High Rinse Potion (HRP) Evaluation (Ion Exchange High Rinse Portion Regeneration Waste)

- For the Synthetic HRP solution, the initial flux was around 10 $L.m^{-2}.h^{-1}$ and the flux declined to a water flux of ca. 2 $L.m^{-2}.h^{-1}$ (at ca. 24% water recovery) indicating that the water flux decline was potentially due to draw solution induced membrane fouling.

Membrane surface characterization conducted on the used membrane (Section 5.9.1.3) showed that the membrane surface was fouled with aragonite and calcite. Because the starting synthetic HRP had no alkalinity, the membrane surface characterization studies together with feed water quality after the run confirmed the reverse diffusion of ammonium bicarbonate into the feed solution. Formation of the aragonite and calcium carbonate was found to be due to the interaction between the calcium ions that exists in the feed solution with carbonate ions from the draw solution. Furthermore, the transport of draw solution to the feed side of the membrane causes a pH increase at the feed side which subsequently promotes favourable conditions for calcium carbonate precipitation.

Tubular Reverse Osmosis (TRO)/Spiral Wound Reverse Osmosis (SRO) Brine Evaluation (Reverse Osmosis Brine)

- For the Synthetic TRO/SRO Brine solution, the initial water flux was around 12.5 $L.m^{-2}.h^{-1}$ and the flux declined to a water flux of ca. 2 $L.m^{-2}.h^{-1}$ (operated until ca. 34% feed volume recovery) indicating that the water flux decline was potentially due to draw solution induced membrane fouling. The pH of the feed solution became alkaline as soon as the run was started indicating the reverse diffusion of ammonium bicarbonate into the feed solution.
- Membrane surface characterization conducted (Section 5.9.2.3) showed that the membrane was fouled with aragonite and calcite.

Combined Regeneration Effluent Evaluation

- For the Synthetic Combined Regeneration Effluent solution, the initial water flux was around 10.6 $L.m^{-2}.h^{-1}$ and the water flux declined to ca. 6.9 $L.m^{-2}.h^{-1}$ (operated until ca. 70% feed volume recovery) indicating that the water flux decline was due to the decrease in osmotic pressure driving force (as observed with non-scaling solution) rather than membrane fouling.

Furthermore, the water flux trend observed was very similar to that of the non-scaling baseline feed solution (sodium chloride). This was an indication of insignificant membrane fouling. Although there was reverse salt diffusion of draw solution into the feed solution, indications were that the concentration of scaling precursors in the feed, especially Ca^{+2} could be playing a role when it comes to membrane fouling. The calcium concentration in this stream was low when compared to that of the other streams.

- Membrane surface characterization studies showed that the fouling observed for the other two streams discussed above was absent and the membrane at the end of the trial appeared clean (visual observation). Raman spectra obtained on some particles (although very sparse) found on the membrane showed the presence of both aragonite and calcite.

The results from this run (combined regeneration effluent) highlighted a very important point about the impact of concentration of scale precursors in the feed solution on FO membrane fouling. The potential implication for this result is that for high hardness brine streams, a hardness removal step (albeit not complete softening) could be required in order to make FO process viable.

Mother Liquor-Evaporator Blowdown (Brine from Thermal Evaporator)

- For the Synthetic Mother Liquor solution, the initial flux was around 7.8 $L.m^{-2}.h^{-1}$ and the flux declined to a water flux of ca. 2.9 $L.m^{-2}.h^{-1}$ (operated until ca. 22% feed volume recovery) indicating that the water flux decline was potentially due to draw solution induced membrane fouling.
- Membrane surface characterization studies also showed that the membrane was also fouled with aragonite and calcite.
- The experiments conducted to evaluate the impact of three calcium concentration in the feed stream (zero calcium concentration, mid calcium concentration and high calcium concentration) using Mother Liquor Evaporator Blowdown as feed showed that the concentration of scaling precursors in the feed, specifically Ca^{+2} plays a major role when it comes to membrane fouling when using ammonium bicarbonate as the draw solution due to the formation of draw solution induced calcite scale. This was as a result of high specific reverse salt diffusion which was observed during this study.

The implication of the results from this study is that for high hardness brine streams, a hardness removal step, calcium hardness could be required in order for FO process to be technically feasible when using ammonium bicarbonate as a draw solution. The softening of the stream to remove hardness where ammonium bicarbonate is used as draw solution is becoming prominent as discussed in the literature review (section 2.1.2) (OASYS Water case studies (demonstration MBC plants & full MBC scale plants)).

The findings from the batch study (Section 5.9.1 to 5.11) provide an important implication for the selection of draw solution and the development of improved FO membranes in the FO process.

6.1.3 Reflections on the treatment of selected concentrated brine streams using forward osmosis technology.

In this study, forward osmosis was evaluated in the treatment of selected concentrated brine streams. Calcium carbonate scaling (calcite or aragonite) formed due to the interaction between the calcium ions in the feed solution with carbonate ions from the draw solution reduces water flux and water recoveries achievable. Moreover, the feed solution pH increase observed in this study enhances scaling deposition as it significantly affects the solubility of calcium carbonate. It was also observed in this study that the concentration of the calcium ions in the feed does have an impact on the formation of calcium carbonate scale, implying that some hardness can be tolerated in the feed to the forward osmosis process. It can therefore be concluded that in the absence of some hardness removal, ammonium bicarbonate draw solution was not suitable for treating concentrated brine streams that contain a high concentration of calcium ions. It was also observed in this study that a better forward osmosis process performance with sustainable fluxes and no scaling was observed when hardness ions (calcium and magnesium) were removed from the feed solution (softening). This was also supported by forward osmosis performance observed when non scaling sodium chloride was used as feed solution for baseline experiments (osmotic pressure similar to synthetic brine solutions). Based on the results from this study, FO technology using ammonium bicarbonate as a draw solution can be considered as an alternative technology to treat concentrated brine streams from inland industries provided some pre-treatment to remove scaling precursors such as calcium is incorporated in the flow scheme.

6.1.4 Future Outlook

In this study, the feasibility of using the FO process as an alternative to conventional brine concentrators to concentrate high salinity brine streams was evaluated to enable brine volume reduction and water reuse. The concentrated brine stream produced could then be further processed to recover salt and achieve zero liquid discharge. The conventional brine concentrators currently employed in the petrochemical and power generating industry are the evaporation ponds, thermal evaporators and crystallizers. Although evaporation ponds are well-known options and offer simple alternative, land requirement and potential contamination of groundwater remains a challenge. Evaporation ponds are not appropriate for cases where water reuse is a priority. Thermal evaporators and crystallizers are also proven technologies; however, thermal evaporative processes tend to be energy-intensive. Expensive equipment may be required to minimize corrosion in cases where the high salinity water to be concentrated is corrosive. Despite their perceived robustness, the thermal evaporators and crystallizers still requires pre-treatment to remove scaling components such as barium, calcium, strontium, magnesium etc.

Scaling and fouling are common problems in these processes and may precipitate on the equipment surface (e.g. plugging heat exchanger tubes) and impede the desalination process by reducing the heat transfer rate.

The scaling of the equipment impacts plant availability due to frequent downtimes required for cleaning the equipment. This is a reality in the petrochemical and power generating industry due to the absence of pre-treatment steps to remove scaling components. The evaluation of the FO process conducted in this study showed that the process does have the potential to be used as an alternative brine concentrator despite the fouling experienced in streams with a high concentration of scaling components. The research also showed that a certain concentration of scaling components could be tolerated, which could further advantage this technology when it comes to capital cost compared to thermal evaporators/crystallisers. Since the driving force for the FO technology is osmotic pressure differential, exotic material, high-pressure pumps, pressure vessels are not a requirement. This offers FO technology a capital cost advantage compared to thermal evaporators/crystallizers. As discussed in the literature review section, the FO technology has full-scale plants installed over the years. Despite the advances that have been made in the advancement of FO technology, which led to the commercialization of the technology, there are still several key technical issues that need to be addressed. Some of these issues were once again proven during this study, namely the importance of an ideal membrane that limits ICP, offer high water fluxes, and provide low SRSF. Furthermore, it was also evident from this study that more studies on the types of the draw solution are still required as the draw solution impacts the performance of the FO technology with respect to water flux, salt flux and membrane fouling. Many in-depth experiments and research are still required, as highlighted in the recommendations (section 6.2) to address FO technology challenges relevant to the study completed.

6.2 Recommendations

The treatment of selected concentrated brine streams was investigated experimentally in this dissertation using forward osmosis process. Even though ammonium bicarbonate draw solution has the advantage of easy to recover, it was not efficient enough to treat all the brine streams selected for this study. Despite the fundamental understanding of FO technology achieved, this study had some limitations which require further evaluation.

- A laboratory-scale equipment was used for all the research work, as a result no pilot or full-scale extrapolation of the performance could be made. The experimental study was limited to batch tests, and long-term performance was not evaluated.
    - Evaluation of the technology on pilot scale for this application in order to achieve the following:
        - Acquire long term performance data
        - FO membrane cleaning protocols evaluation (i.e. osmotic backwash, chemical cleaning, increased cross-flow velocity etc.)
        - Recovery of draw solution and product water
        - Verification of pre-treatment (Chemical Softening, Multi-Media Filtration, Antiscalant dosing etc.)
        - Evaluation of the impact of organics in the feed water (synthetic pure inorganic solutions were used for the study)
        - Evaluation of the impact of Draw Solution concentration (driving force) on FO membrane fouling.
- The experimental study was limited to a HTI membrane (TFC-FO) and an ammonium bicarbonate draw solution.
    - The development of improved FO membranes remains a challenge to move FO technology from laboratory research to industrial applications even though there has been a positive development with respect to full-scale applications of FO technology in areas such as Sea Water Desalination and Oil and Gas Waste Stream (e.g. Produced Water, Fracking Water). In this study, a TFC-FO membrane from HTI was used to generate the results observed, and it is therefore recommended that in the future, TFC-FO membranes from other suppliers be evaluated. An ideal membrane should have the following characteristics to address issues such as low water fluxes and reverse solute diffusion observed during this study:
        - High water permeability and selectivity
        - Minimized Internal Concentration Polarization
        - High mechanical strength and stability

- Synthetic solutions were used as feed to the FO process.
    - Plant feed solutions need to be evaluated.
- Testing of other available draw solutions
    - It was evident during this experimental study that the draw solution played a major role in as far as low water fluxes, membrane fouling, and reverse solute diffusion is a concern. Therefore, it is recommended that other draw solutions be evaluated in the future to address challenges associated with ammonium bicarbonate draw solution. However, some steps can be studied to improve the FO process using ammonium bicarbonate draw solution (e.g. buffering the feed solution at low pH to increase the solubility of calcium carbonate and reduce its deposition on the FO membrane surface). Also, pre-treatment steps such as anti-scalant dosing and softening to manage scale formation require further evaluation if ammonium bicarbonate is to be used as a draw solution. A fit for purpose draw solution has the following characteristics:
        - Ability to generate high osmotic pressure
        - Can be recovered efficiently and reused in the process to reduce chemical and energy cost.
        - Reduce Internal Concentration Polarization, leading to high flux and lower CAPEX
        - Not toxic
        - It cannot compromise the integrity of the FO membrane.
        - Should not cause scaling or fouling on the FO membrane surface (both on the feed or draw solution side of the membrane)
        - The rate of its diffusion to the feed solution side should be minimal to reduce chemical cost.
- There were instances where the water flux showed initial decrease, which was followed by an increase, and it was hypothesised that this was due to the initial “non-permanent” fouling that occurs (removable by cross-flow). Once this fouling was removed, it was hypothesised that the water flux would increase and thereafter start to decrease as water recovery was increased. This hypothesis requires further investigation.

- Modelling of the onset of fouling
    - This aspect was beyond the scope of the current study.
        - The recommendation involves combining the speciation modelling, water flux, and salt flux to model when precipitation would occur, resulting in fouling of the membrane. This could then be compared to when fouling did actually occur experimentally. This would provide a very powerful tool to predict the maximum water recovery that could be achieved before catastrophic fouling.

REFERENCES

Achilli, A., Cath, T. and Childress, A., 2010. Selection of inorganic-based draw solutions for forward osmosis applications. *Journal of Membrane Science*, 364(1-2), pp.233-241.

Achilli, A., Cath, T., Marchand, E. and Childress, A., 2009. The forward osmosis membrane bioreactor: A low fouling alternative to MBR processes. *Desalination*, 239(1-3), pp.10-21.

Ahmed, M., Shayya, W., Hoey, D. and Al-Handaly, J., 2002. Brine Disposal from Inland Desalination Plants. *Water International*, 27(2), pp.194-201.

Al-Furaiji, M., 2016. *Hyper-Saline Produced Water Treatment for Beneficial Use*. PhD. University of Twente.

Al-Mayahi, A. and Sharif, A., 2004. *SOLVENT REMOVAL PROCESS*. 7,879,243.

Alsvik, I. and Hägg, M., 2013. Pressure Retarded Osmosis and Forward Osmosis Membranes: Materials and Methods. *Polymers*, 5(1), pp.303-327.

Amjad, Z. and Demadis, K., 2015. *Mineral Scales and Deposits*. Amsterdam: Elsevier.

Anderko, A., Wang, P. and Rafal, M., 2002. Electrolyte solutions: from thermodynamic and transport property models to the simulation of industrial processes. *Fluid Phase Equilibria*, 194-197, pp.123-142.

Baker, R., 2013. *Membrane Technology and Applications*. Hoboken, N.J.: Wiley.

Bamaga, O., Yokochi, A., Zabara, B. and Babaqi, A., 2011. Hybrid FO/RO desalination system: Preliminary assessment of osmotic energy recovery and designs of new FO membrane module configurations. *Desalination*, 268(1-3), pp.163-169.

Bartholomew, T., Mey, L., Arena, J., Siefert, N. and Mauter, M., 2017. Osmotically assisted reverse osmosis for high salinity brine treatment. *Desalination*, 421, pp.3-11.

Batchelder, G., 1965. *Process for The Demineralization of Water*. 3,171,799.

Beaudry, E., Thiel, R. and York, R., 1999. Full Scale Experience of Direct Osmosis Concentration Applied to Leachate Management. In: *Proceedings for Sardinia '99 Seventh International Landfill Symposium held in Oct. 1999.*

Bethke, C., 1996. *Geochemical Reaction Modeling*. New York: Oxford University Press.

Blandin, G., Ferrari, F., Lesage, G., Le-Clech, P., Héran, M. and Martinez-Lladó, X., 2020. Forward Osmosis as Concentration Process: Review of Opportunities and Challenges. Membranes, 10(10), p.284.

Boo, C., Lee, S., Elimelech, M., Meng, Z. and Hong, S., 2012. Colloidal fouling in forward osmosis: Role of reverse salt diffusion. *Journal of Membrane Science*, 390-391, pp.277-284.

Cath, T., Adams, D. and Childress, A., 2005. Membrane contactor processes for wastewater reclamation in space. *Journal of Membrane Science*, 257(1-2), pp.111-119.

CATH, T., CHILDRESS, A. and ELIMELECH, M., 2006. Forward osmosis: Principles, applications, and recent developments. *Journal of Membrane Science*, 281(1-2), pp.70-87.

Cath, T., Elimelech, M., McCutcheon, J., McGinnis, R., Achilli, A., Anastasio, D., Brady, A., Childress, A., Farr, I., Hancock, N., Lampi, J., Nghiem, L., Xie, M. and Yip, N., 2013. Standard Methodology for Evaluating Membrane Performance in Osmotically Driven Membrane Processes. *Desalination*, 312, pp.31-38.

Chekli, L., Phuntsho, S., Kim, J., Kim, J., Choi, J., Choi, J., Kim, S., Kim, J., Hong, S., Sohn, J. and Shon, H., 2016. A comprehensive review of hybrid forward osmosis systems: Performance, applications and future prospects. *Journal of Membrane Science*, 497, pp.430-449.

Chen, C., 2011. *EN-63AB Fabrication and Comparison Of RO-Like And NF-Like Forward Osmosis Membranes*. A Final Year Project presented to the Nanyang Technological University in partial fulfilment of the requirement for the Degree of Bachelor of Engineering. Singapore. Nanyang Technological University: Nanyang Technological University. Singapore.

Chen, X. and Yip, N., 2018. Unlocking High-Salinity Desalination with Cascading Osmotically Mediated Reverse Osmosis: Energy and Operating Pressure Analysis. *Environmental Science & Technology*, 52(4), pp.2242-2250.

Choice Reviews Online, 2012. Standard methods for the examination of water and wastewater. 49(12), pp.49-6910-49-6910.

Chun, Y., Mulcahy, D., Zou, L. and Kim, I., 2017. A Short Review of Membrane Fouling in Forward Osmosis Processes. *Membranes*, 7(2), p.30.

Chung, T., Zhang, S., Wang, K., Su, J. and Ling, M., 2012. Forward osmosis processes: Yesterday, today and tomorrow. *Desalination*, 287, pp.78-81.

Coday, B., Heil, D., Xu, P. and Cath, T., 2013. Effects of Transmembrane Hydraulic Pressure on Performance of Forward Osmosis Membranes. *Environmental Science & Technology*, 47(5), pp.2386-2393.

Coday, B., Xu, P., Beaudry, E., Herron, J., Lampi, K., Hancock, N. and Cath, T., 2014. The sweet spot of forward osmosis: Treatment of produced water, drilling wastewater, and other complex and difficult liquid streams. *Desalination*, 333(1), pp.23-35.

Conway, B., Bockrish, J. and Yeager, E., 1983. Comprehensive Treatise of Electrochemistry. *Plenum Press, New York*, p.P11.

Davenport, D., Deshmukh, A., Werber, J. and Elimelech, M., 2018. High-Pressure Reverse Osmosis for Energy-Efficient Hypersaline Brine Desalination: Current Status, Design Considerations, and Research Needs. *Environmental Science & Technology Letters*, 5(8), pp.467-475.

de Bod, S., 2012. *The South African Water Management Framework: Lethabo Power Station as A Case Study*. Master of Engineering. North-West University-South Africa.

Deng, B., 2013. Effects of Polysulfone (PSf) Support Layer on the Performance of Thin-Film Composite (TFC) Membranes. *Journal of Chemical and Process Engineering*.

Durham, B. and Mierzejewski, M., 2003. Water reuse and zero liquid discharge: a sustainable water resource solution. *Water Science and Technology: Water Supply*, 3(4), pp.97-103.

Elimelech, M., 2007. Yale constructs forward osmosis desalination pilot plant. *Membrane Technology*, 2007(1), pp.7-8.

Emerson, K.; Russo, R.C.; Lund, R.E. et al. (1975) Aqueous ammonia equilibrium calculations: Effect of pH and temperature. *Journal of Fisheries Research Board of Canada*, v.32, p.2379-2383.

Eskom.co.za. 2019. *Company Information Overview*. [online] Available at: <http://www.eskom.co.za/OurCompany/CompanyInformation/Pages/Company_Information.aspx> [Accessed 25 September 2019].

Ferguson, R., Ferguson, B. and Stancavage, R., 2011. Modeling Scale Formation and Optimizing Scale Inhibitor dosages in Membrane Systems. In: *AWWA Membrane Technology Conference*. Kimberton, PA 19442: French Creek Software, Inc., pp.1-19.

Forwardosmosistech.com. 2016. *Industrial FO-Based ZLD System | Forwardosmosistech*. [online] Available at: <https://www.forwardosmosistech.com/fo-systems-are-now-one-step-closer-to-mass-adoption/> [Accessed 6 June 2016].

Frank, B., 1972. *Desalination of Seawater*. US Patent 3,670,897.

Garcia-Castello, E., McCutcheon, J. and Elimelech, M., 2009. Performance evaluation of sucrose concentration using forward osmosis. *Journal of Membrane Science*, 338(1-2), pp.61-66.

Ge, Q., Ling, M. and Chung, T., 2013. Draw solutions for forward osmosis processes: Developments, challenges, and prospects for the future. *Journal of Membrane Science*, 442, pp.225-237.

gewater.com. 2008. *Brine Concentrators*. [online] Available at: <http://www.gewater.com/products/equipment/thermal.evaporative/brine_concentration> [Accessed 22 September 2019].

Gitari, M., Fatoba, O., Nyamihingura, A., Petrik, L., Vadapali, V., Nel, K., October, A., Dlamini, L., Gericke, G. and Mahlaba, J., 2009. Chemical Weathering in a Dry Ash Dump: An Insight from Physicochemical and Mineralogical Analysis of Drilled Cores. Lexington, KY, USA: 2009 World of Coal Ash (WOCA) conference. May 4-7.

Glater, J. and Coyen, Y., 2003. *Brine Disposal from Land-Based Membrane Desalination Plants: A Critical Assessment*. [online] Polyucla.edu.sep. Available at: <http://polysep.ucla.edu/Publications/Papers. PDF/Brine%20DISPOSAL.> [Accessed 22 September 2019].

Glew, D., 1965. *Process for Liquid Recovery and Solution Concentration*. US Patent 3,216,930.

Goh, P., Ismail, A., Ng, B. and Abdullah, M., 2019. Recent Progresses of Forward Osmosis Membranes Formulation and Design for Wastewater Treatment. *Water*, 11(10), p.2043.

Goh, P., Matsuura, T., Ismail, A. and Ng, B., 2017. The Water-Energy Nexus: Solutions towards Energy-Efficient Desalination. *Energy Technology*, 5(8), pp.1136-1155.

Gokel, G. and Dean, J., 2004. *Dean's Handbook of Organic Chemistry*. New York: McGraw-Hill.

Gray, G., McCutcheon, J. and Elimelech, M., 2006. Internal concentration polarization in forward osmosis: role of membrane orientation. *Desalination*, 197(1-3), pp.1-8.

Haghtalab, A., 1990. *Thermodynamics of Aqueous Electrolyte Solutions, PhD Thesis*. PhD. Department of Chemical Engineering, McGill University, Montreal, Quebec, Canada.

Hancock, N. and Cath, T., 2009. Solute Coupled Diffusion in Osmotically Driven Membrane Processes. *Environmental Science & Technology*, 43(17), pp.6769-6775.

Hancock, N., 2013. *Engineered Osmosis for Energy Efficient Separations: Optimizing Waste Heat Utilization FINAL SCIENTIFIC REPORT DOE F 241.3, Report, January 13, 2013*. [online] Available at: <. (https://digital.library.unt.edu/ark:/67531/metadc829878/m1/2/> [Accessed 23 September 2019].

Hancock, N., Xu, P., Roby, M., Gomez, J. and Cath, T., 2013. Towards direct potable reuse with forward osmosis: Technical assessment of long-term process performance at the pilot scale. *Journal of Membrane Science*, 445, pp.34-46.

Hanrahan, G., 2010. *Modelling of Pollutants in Complex Environmental Systems*.

Haupt, A. and Lerch, A., 2018. Forward Osmosis Application in Manufacturing Industries: A Short Review. *Membranes*, 8(3), p.47.

Helgeson, H. C. 1969. "Thermodynamics of Hydrothermal Systems at Elevated Temperatures and Pressures." Am. J. Sci. 267:729-804.

Helgeson, H. and Kirkham, D., 1974. Theoretical prediction of the thermodynamic behaviour of aqueous electrolytes at high pressures and temperatures; I, Summary of the thermodynamic/electrostatic properties of the solvent. *American Journal of Science*, 274(10), pp.1089-1198.

Helgeson, H. and Kirkham, D., 1974. Theoretical prediction of the thermodynamic behaviour of aqueous electrolytes at high pressures and temperatures; II, Debye-Huckel parameters for activity coefficients and relative partial molal properties. *American Journal of Science*, 274(10), pp.1199-1261.

Helgeson, H. and Kirkham, D., 1976. Theoretical prediction of the thermodynamic properties of aqueous electrolytes at high pressures and temperatures. III. Equation of state for aqueous species at infinite dilution. *American Journal of Science*, 276(2), pp.97-240.

Helgeson, H., Kirkham, D. and Flowers, G., 1981. Theoretical prediction of the thermodynamic behaviour of aqueous electrolytes by high pressures and temperatures; IV, Calculation of activity coefficients, osmotic coefficients, and apparent molal and standard and relative partial molal properties to 600 degrees C and 5kb. *American Journal of Science*, 281(10), pp.1249-1516.

Hickenbottom, K., Hancock, N., Hutchings, N., Appleton, E., Beaudry, E., Xu, P. and Cath, T., 2013. Forward osmosis treatment of drilling mud and fracturing wastewater from oil and gas operations. *Desalination*, 312, pp.60-66.

HOLLOWAY, R., CHILDRESS, A., DENNETT, K. and CATH, T., 2007. Forward osmosis for concentration of anaerobic digester centrate. *Water Research*, 41(17), pp.4005-4014.

Htiwater.com. 2010. *Forward Osmosis Technology | HTI Water*. [online] Available at: <http://www.htiwater.com/technology/forward_osmosis/index.html> [Accessed 13 May 2010].

Jang, H., 2010. *Design of Ammonia-Carbon Dioxide Forward Osmosis Desalination Process*. MSc Thesis. KAIST, South Korea

Juby, G., Zacheis, A., Shih, W. and Ravishanker, P., 2008. *Evaluation and Selection of Available Processes for A Zero-Liquid Discharge*. Desalination and Water Purification Research and Development. Available from the National Technical Information Service: U.S. Department of the Interior, PP 1-40.

Kaplan, R., Mamrosh, D., Salih, H. and Dastgheib, S., 2017. Assessment of desalination technologies for treatment of a highly saline brine from a potential CO2 storage site. Desalination, 404, pp.87-101.

Khan, J., Shon, H. and Nghiem, L., 2019. From the Laboratory to Full-Scale Applications of Forward Osmosis: Research Challenges and Opportunities. *Current Pollution Reports*, 5(4), pp.337-352.

Kim, H., Park, S., Choi, Y., Lee, S. and Choi, J., 2018. Fouling due to CaSO4 scale formation in forward osmosis (FO), reverse osmosis (RO), and pressure assisted forward osmosis. *DESALINATION AND WATER TREATMENT*, 104, pp.45-50.

Kim, Y. and Park, S., 2011. Experimental Study of a 4040 Spiral-Wound Forward-Osmosis Membrane Module. *Environmental Science & Technology*, 45(18), pp.7737-7745.

Kissel, D.E and Cabrera, M.L (2005). Chemical Reactions of Ammoniacal N. *Encyclopaedia of Soils in the Environment*

Klaysom, C., Cath, T., Depuydt, T. and Vankelecom, I., 2013. ChemInform Abstract: Forward and Pressure Retarded Osmosis: Potential Solutions for Global Challenges in Energy and Water Supply. *ChemInform*, 44(39), p.no-no.

Koppol, A., Bagajewicz, M., Dericks, B. and Savelski, M., 2004. On zero water discharge solutions in the process industry. *Advances in Environmental Research*, 8(2), pp.151-171.

Korak, K. and Arias, P., 2015. *Forward Osmosis Evaluation and Applications for Reclamation (Final Report 2015-01-7911)*. Research and Development Office Advanced Water Treatment. Research and Development Office U.S. Department of the Interior, Bureau of Reclamation, PO Box 25007, Denver CO 80225-0007: U.S. Department of the Interior, Bureau of Reclamation, pp 1- 49.

Kragl, U., 1997. Basic Principles of Membrane Technology. (2. Aufl.) VonM. Mulder. Kluwer Academic Publishers, Dordrecht, 1996. 564 S., geb. 174.00.ISBN 0–7923–4247-X. *Angewandte Chemie*, 109(12), pp.1420-1421.

Kravith, R. and Davis, J., 1975. Desalination of seawater by direct osmosis. *Desalination*, 16, pp.151-155.

Lay, W., Chong, T., Tang, C., Fane, A., Zhang, J. and Liu, Y., 2010. Fouling propensity of forward osmosis: investigation of the slower flux decline phenomenon. *Water Science and Technology*, 61(4), pp.927-936.

Lee, K., Baker, R. and Lonsdale, H., 1981. Membranes for power generation by pressure-retarded osmosis. *Journal of Membrane Science*, 8(2), pp.141-171.

Lee, S., Boo, C., Elimelech, M. and Hong, S., 2010. Comparison of fouling behaviour in forward osmosis (FO) and reverse osmosis (RO). *Journal of Membrane Science*, 365(1-2), pp.34-39.

Lee, S., Elimelech, M., Boo, C., Kim, C. and Hong, S., 2009. *Recent and Future Development in Forward Osmosis Technology*.

Li, L., Shi, W. and Yu, S., 2019. Research on Forward Osmosis Membrane Technology Still Needs Improvement in Water Recovery and Wastewater Treatment. Water, 12(1), p.107.

Li, Z., Valladares Linares, R., Bucs, S., Aubry, C., Ghaffour, N., Vrouwenvelder, J. and Amy, G., 2015. Calcium carbonate scaling in seawater desalination by ammonia–carbon dioxide forward osmosis: Mechanism and implications. *Journal of Membrane Science*, 481, pp.36-43.

Liberman, I., 2005. *RO Membrane Cleaning Method*. 7,658,852 B2.

Linares, R., Li, Z., Elimelech, M., Amy, G. and Vrouwenvelder, H., 2017. Recent Developments in Forward Osmosis Processes. *Water Intelligence Online*, 16, p.9781780408125.

Liu, L., Wang, M., Wang, D. and Gao, C., 2009. Current Patents of Forward Osmosis Membrane Process. *Recent Patents on Chemical Engineeringe*, 2(1), pp.76-82.

Loehe, J. and Donohue, M., 1997. Recent advances in modelling thermodynamic properties of aqueous strong electrolyte systems. *AIChE Journal*, 43(1), pp.180-195.

MacHarg, J. and Pique, G., 2002. How to Design and Operate SWRO Systems Build Around a New Pressure Exchanger Devic. In: *IDA World Congress on Desalination and Water Reuse*. Bahrain: IDA World Congress on Desalination and Water Reuse.

Mahlaba, J., Kearsley, E. and Kruger, R., 2012. Microstructural and Mineralogical Transformation of Hydraulically Disposed Fly Ash—Implications to the Environment. *Coal Combustion and Gasification Products*, 4(1), pp.21-27.

Mariah, L., 2006. *Membrane Distillation of Concentrated Brines*. PhD Dissertation. University of KwaZulu-Natal, South Africa.

Martinetti, C., Childress, A. and Cath, T., 2009. High recovery of concentrated RO brines using forward osmosis and membrane distillation. *Journal of Membrane Science*, 331(1-2), pp.31-39.

Martinetti, C., Childress, A. and Cath, T., 2009. High recovery of concentrated RO brines using forward osmosis and membrane distillation. *Journal of Membrane Science*, 331(1-2), pp.31-39.

McCutchen, J. and Elimelech, M., 2007. Modeling water flux in forward osmosis: Implications for improved membrane design. *AIChE Journal*, 53(7), pp.1736-1744.

McCutcheon, J. and Elimelech, M., 2006. Influence of concentrative and dilutive internal concentration polarization on flux behaviour in forward osmosis. *Journal of Membrane Science*, 284(1-2), pp.237-247.

McCutcheon, J., McGinnis, R. and Elimelech, M., 2005. A novel ammonia—carbon dioxide forward (direct) osmosis desalination process. *Desalination*, 174(1), pp.1-11.

McCutcheon, J., McGinnis, R. and Elimelech, M., 2006. Desalination by ammonia–carbon dioxide forward osmosis: Influence of draw and feed solution concentrations on process performance. *Journal of Membrane Science*, 278(1-2), pp.114-123.

McGinnis, R. and Elimelech, M., 2007. Energy requirements of ammonia–carbon dioxide forward osmosis desalination. *Desalination*, 207(1-3), pp.370-382.

McGinnis, R. and Elimelech, M., 2008. Global Challenges in Energy and Water Supply: The Promise of Engineered Osmosis. *Environmental Science & Technology*, 42(23), pp.8625-8629.

McGinnis, R. and McCutcheon, J., 2007. *Presentation-Forward Osmosis Energy Use, Comparison To RO, MSF, MED*.

McGinnis, R., 2002. *Osmotic Desalination Process*. 6,391,205.

McGinnis, R., Hancock, N., Nowosielski-Slepowron, M. and McGurgan, G., 2013. Pilot demonstration of the NH3/CO2 forward osmosis desalination process on high salinity brines. *Desalination*, 312, pp.67-74.

Mecha, C., 2017. Applications of Reverse and Forward Osmosis Processes in Wastewater Treatment: Evaluation of Membrane Fouling, Osmotically Driven Membrane Processes. In: H.

Du, A. Thompson and X. Wang, ed., *Osmotically Driven Membrane Processes - Approach, Development and Current Status*. [online] Available at: <https://www.intechopen.com/books/osmotically-driven-membrane-processes-approach-development-and-current-status/applications-of-reverse-and-forward-osmosis-processes-in-wastewater-treatment-evaluation-of-membrane> [Accessed 15 February 2020].

Mehta, G. and Loeb, S., 1978. Internal polarization in the porous substructure of a semipermeable membrane under pressure-retarded osmosis. *Journal of Membrane Science*, 4, pp.261-265.

Melia, T.P., 1965. Crystal nucleation from aqueous solution, J. Appl. Chem. 1, pp 5 345-357.

Menon, A., Haechler, I., Kaur, S., Lubner, S. and Prasher, R., 2020. Enhanced solar evaporation using a photo-thermal umbrella for wastewater management. *Nature Sustainability*, 3(2), pp.144-151.

Mi, B. and Elimelech, M., 2008. Chemical and physical aspects of organic fouling of forward osmosis membranes. *Journal of Membrane Science*, 320(1-2), pp.292-302.

Mi, B. and Elimelech, M., 2010. Gypsum Scaling and Cleaning in Forward Osmosis: Measurements and Mechanisms. *Environmental Science & Technology*, 44(6), pp.2022-2028.

Mi, B. and Elimelech, M., 2010. Organic fouling of forward osmosis membranes: Fouling reversibility and cleaning without chemical reagents. *Journal of Membrane Science*, 348(1-2), pp.337-345.

Moch, I. and Harris, C., 2002. What Seawater Energy Recovery System Should I Use? A Modern Comparative Study. Bahrain: IDA World Congress on Desalination and Water Reuse.

Modernwater.com. 2011. *Forward Osmosis Desalination - Modern Water*. [online] Available at: <https://www.modernwater.com/desalination-systems/forward-osmosis-desalination> [Accessed 24 June 2011].

Morillo, J., Usero, J., Rosado, D., El Bakouri, H., Riaza, A. and Bernaola, F., 2014. Comparative study of brine management technologies for desalination plants. *Desalination*, 336, pp.32-49.

Muftah, H., 2011. Reject Brine Management. *Desalination, Trends and Technologies*.

Muhammad, O., 2010. *Membrane Distillation of Concentrated Brines*. MSc. University of Pretoria, South Africa.

Murray, P., Cobban, B. and Faller, K., 1995. *Electrodialysis And Electrodialysis Reversal (M38)*. Denver: American Water Works Association.

Nathoo, J., Jivanji, R. and Lewis, A., 2009. Freezing your brines off: Eutectic Freeze Crystallization for Brine Treatment. In: *International Mine Water Conferences*. Cilla Taylor Conferences.

Nie1sen, A.E., 1970. Precipitation, *Crotica Chemica ACTA,* 42, pp. 319-333

Ng, H., Tang, W. and Wong, W., 2006. Performance of Forward (Direct) Osmosis Process: Membrane Structure and Transport Phenomenon. *Environmental Science & Technology*, 40 (7), pp.2408-2413.

Nyamhingura, A., 2009. *Characterization and Chemical Speciation Modelling Of Saline Effluents At Sasol Synthetic Fuel Complex-Secunda And Tutuka Power Station.* Master of Science. University of Western Cape.

Oasys. 2014. *Oasys Water - Case Studies*. [online] Available at: <http://oasyswater.com/solutions/case-studies-2/> [Accessed 26 June 2014].

Olisystems.com. 2011. [online] Available at: <https://www.olisystems.com/oli-studio-stream-analyzer> [Accessed 7 July 2011].

Pendergast, M., Nowosielski-Slepowron, M. and Tracy, J., 2016. Going big with forward osmosis. *Desalination and Water Treatment*, 57(55), pp.26529-26538.

Pendergast, M., Nowosielski-Slepowron, M. and Tracy, J., 2014. Forward Osmosis Based Membrane Concentration of Wastewater Streams in Coal-Fired Power Generation. Orlando, Florida: Proceedings of the 2015 International Water Conference.

Petrik, L., Gitari, W., Etchebers, O., Nel, J., Vadapalli, V., Fatoba, O., Nyamihingura, A., Akinyemi, S. and Antonie, M., 2007. *Towards the Development of Sustainable Salt Sinks: Fundamental Disposal of Brines Within Inland Ash Dams*. Environmental and Nano Sciences Group (ENS), Chemistry Department, University of the Western Cape.

Phillip, W., Yong, J. and Elimelech, M., 2010. Reverse Draw Solute Permeation in Forward Osmosis: Modelling and Experiments. *Environmental Science & Technology*, 44(13), pp.5170-5176.

Phuntsho, S., 2012. *A Novel Fertilizer Drawn Forward Osmosis Desalination for Fertigation*. PhD. School of civil and Environmental Engineering, Faculty of Engineering and Information Technology, University of Technology, Sydney (UTS).

Phuntshoa, S., Shona, HK., Hong,S, Leeb, S. and Vigneswarana, S., 2011. A novel low energy fertilizer driven forward osmosis desalination for direct fertigation: Evaluating the performance of fertilizer draw solutions. *Journal of Membrane Science*, 375, pp. 172-181Pitzer, K., 1975. Thermodynamics of electrolytes. V. effects of higher-order electrostatic terms. *Journal of Solution Chemistry*, 4(3), pp.249-265.

Pitzer, K., 1977. Electrolyte theory - improvements since Debye and Huckel. *Accounts of Chemical Research*, 10(10), pp.371-377.

Pitzer, K., 1979. *Theory: Ion Interaction Approach, Activity Coefficients in Electrolyte Solutions*. 3rd ed. Boca Raton: CRC Press, Boca Raton, pp. 157-208.

Pitzer, K., 1991. *Activity Coefficients in Electrolyte Solutions*. 2nd ed. Boca Raton, FL: CRC Press, Boca Raton, FL.

Polansky, A. and Baker, E., 2000. Multistage plug in bandwidth selection for kernel distribution function estimates. *Journal of Statistical Computation and Simulation*, 65(1-4), pp.63-80.

Qin, J., Liberman, B. and Kekre, K., 2009. Direct Osmosis for Reverse Osmosis Fouling Control: Principles, Applications and Recent Developments. *The Open Chemical Engineering Journal*, 3(1), pp.8-16.

Rafa, M., Berthold, J., Scrivner, N. and Grise, S., 1994. *Models for Electrolyte Solutions, Models for Thermodynamic and Phase Equilibria Calculations*. Sandler, SI (éd.), Marcel Dekker, Inc., NY, pp. 601-670.

Ras, C. and Van Blottsnitz, H., 2013. *An Assessment of The Key Factors That Influence the Environmental Sustainability of a Large Inland Industrial Complex*. Volume III: Development and assessment of technological interventions for cleaner production at the scale of the complex. [online] Water Research Commission, pp.5-71. Available at: www.wrc.org.za [Accessed 8 April 2020].

Reiss, R., 1981. *Nonparametric estimation of smooth distribution functions, Scandinavian Journal of Statistics*, 8(2), pp.116-119.

Ren, J. and McCutcheon, J., 2014. A new commercial thin film composite membrane for forward osmosis. *Desalination*, 343, pp.187-193.

Renon, H., 1986. Electrolyte Solutions. *Fluid Phase Equilibria*, 30, pp.181-195.

Rioyo, J., Aravinthan, V., Bundschuh, J. and Lynch, M., 2017. A review of strategies for RO brine minimization in inland desalination plants. *DESALINATION AND WATER TREATMENT*, 90, pp.110-123.

Rogers, D., Brouckaert, C. and Hobbs, P., 2013. *An Assessment of The Key Factors That Influence the Environmental Sustainability of A Large Inland Industrial Complex*. Volume II: Inventory of inland salt production and key issues for integrated cleaner production for waste salt management at the highveld mining and industrial complex. [online] Water Research Commission, pp.1-73. Available at: www.wrc.org.za [Accessed 8 April 2020]

Sahebi, S., Phuntsho, S., Eun Kim, J., Hong, S. and Kyong Shon, H., 2015. Pressure assisted fertiliser drawn osmosis process to enhance final dilution of the fertiliser draw solution beyond osmotic equilibrium. *Journal of Membrane Science*, 481, pp.63-72.

Sandler, S., 1994. *Models for Thermodynamic And Phase Equilibria Calculations*. New York: M. Dekker.

Sasol.com. 2019. *Company Overview | Sasol*. [online] Available at: <https://www.sasol.com/about-sasol/overview-0> [Accessed 25 September 2019].

Schantz, A., Xiong, B., Dees, E., Moore, D., Yang, X. and Kumar, M., 2018. Emerging investigators series: prospects and challenges for high-pressure reverse osmosis in minimizing concentrated waste streams. *Environmental Science: Water Research & Technology*, 4(7), pp.894-908.

Scribd. 2008. *Unisim Design OLI Interface Reference Guide | Solubility | Gibbs Free Energy*. [online] Available at: <https://www.scribd.com/document/6808398/UniSim-Design-OLI-Interface-Reference-Guide> [Accessed 23 November 2011].

Semiat, R., 2008. Energy Issues in Desalination Processes. *Environmental Science & Technology*, 42(22), pp.8193-8201.

Sethi, S., Walker, S. and Drewes, J., 2006. Existing and Emerging Concentrate Minimization and Disposal Practices for Membrane Systems. *Florida Water Resources Journal*, pp. 38-48.

She, Q., Jin, X., Li, Q. and Tang, C., 2012. Relating reverse and forward solute diffusion to membrane fouling in osmotically driven membrane processes. *Water Research*, 46(7), pp.2478-2486.

She, Q., Wang, R., Fane, A. and Tang, C., 2016. Membrane fouling in osmotically driven membrane processes: A review. *Journal of Membrane Science*, 499, pp.201-233.

Shon, H., Phuntsho, S., Zhang, T. and Surampalli, R., 2015. *Forward Osmosis: Fundamentals and Application*. Reston: American Society of Civil Engineers.

Smalley, R., 2005. Future Global Energy Prosperity: The Terawatt Challenge. *MRS Bulletin*, 30(6), pp.412-417.

Snyman, G., 2008. *Technical Input Performance Base Contract Desalination Secunda Rev 2 Internal Unpublished Report*. Secunda: Sasol.

Speight, J., Lange, N. and Dean, J., 2005. *Lange's Handbook of Chemistry (16Th Edition)*. New York, USA: McGraw-Hill Professional Publishing.

Support.olisystems.com. 2006. *Getting Started with Hysys™ OLI™*. [online] Available at: <http://support.olisystems.com/Documents/Manuals/Getting%20Started%20with%20Hysys%20OLI.pdf?cv=1> [Accessed 23 November 2011].

Tang, W. and Ng, H., 2008. Concentration of brine by forward osmosis: Performance and influence of membrane structure. *Desalination*, 224(1-3), pp.143-153.

Tanger, J., 1986. *Calculation of Standard Partial Molal Thermodynamic Properties Of Aqueous Ions And Electrolytes At High Pressures And Temperatures*. PhD. University of California, Berkeley.

Valladares Linares, R., Li, Z., Sarp, S., Bucs, S., Amy, G. and Vrouwenvelder, J., 2014. Forward osmosis niches in seawater desalination and wastewater reuse. *Water Research*, 66, pp.122-139.

Wanling, T., 2009. *Forward (Direct) Osmosis: A Prospective Membrane Process*. PhD. National University of Singapore.

Water Desalination Report, 2010. *FO Plant Completes 1-Year of Operation*. Volume 46, Issue 44.

Water Desalination Report, 2011. *FO Takes A Giant Step Forward*.

Water Desalination Report, 2014. *FO: RO'S New Best Friend*. Vol 50, issue 32.

Waterlines Report, 2008. *Emerging Trends in Desalination: A Review*. Series No 9. UNESCO, Canberra.

Wateronline.com. 2015. *Changxing Power Plant Debuts the World's First Forward Osmosis-Based Zero Liquid Discharge Application*. [online] Available at: <https://www.wateronline.com/doc/changxing-power-plant-debuts-the-world-s-first-forward-osmosis-based-zero-liquid-discharge-application-0001> [Accessed 20 August 2015].

Watson, I., Morin, O. and Henthorne, L., 2003. *Desalting Handbook for Planners*. 3rd ed. [Denver, Colo.]: Bureau of Reclamation, Denver Federal Center, pp.1-316.

Whitlock, D., Daigger, G. and McCoy, N., 2007. The Future of Sustainable Water Management: Using a Value Chain Analysis to achieve a Zero Waste Society. In: *WEFTEC. 07*.

Xie, M., Nghiem, L., Price, W. and Elimelech, M., 2012. Comparison of the removal of hydrophobic trace organic contaminants by forward osmosis and reverse osmosis. *Water Research*, 46(8), pp.2683-2692.

Yangali-Quintanilla, V., Li, Z., Valladares, R., Li, Q. and Amy, G., 2011. Indirect desalination of Red Sea water with forward osmosis and low-pressure reverse osmosis for water reuse. *Desalination*, 280(1-3), pp.160-166.

Yip, N., Tiraferri, A., Phillip, W., Schiffman, J. and Elimelech, M., 2010. High Performance Thin-Film Composite Forward Osmosis Membrane. *Environmental Science & Technology*, 44(10), pp.3812-3818.

Younos, T., 2009. Environmental Issues of Desalination. *Journal of Contemporary Water Research & Education*, 132(1), pp.11-18.

Zemaitis, J., 1986. *Handbook of Aqueous Electrolyte Thermodynamics*. New York: Design Institute for Physical Property Data.

Zhao, S., Zou, L., Tang, C. and Mulcahy, D., 2012. Recent developments in forward osmosis: Opportunities and challenges. *Journal of Membrane Science*, 396, pp.1-21.

APPENDIX 1: STATISTICAL ANALYSES OF FEED STREAMS

Figure 1a and 1b shows a Kernel distribution estimates and box plots for the Mother Liquor stream. A script was written by the statistician and this script was used to generate the kernel distribution estimates and box plots.

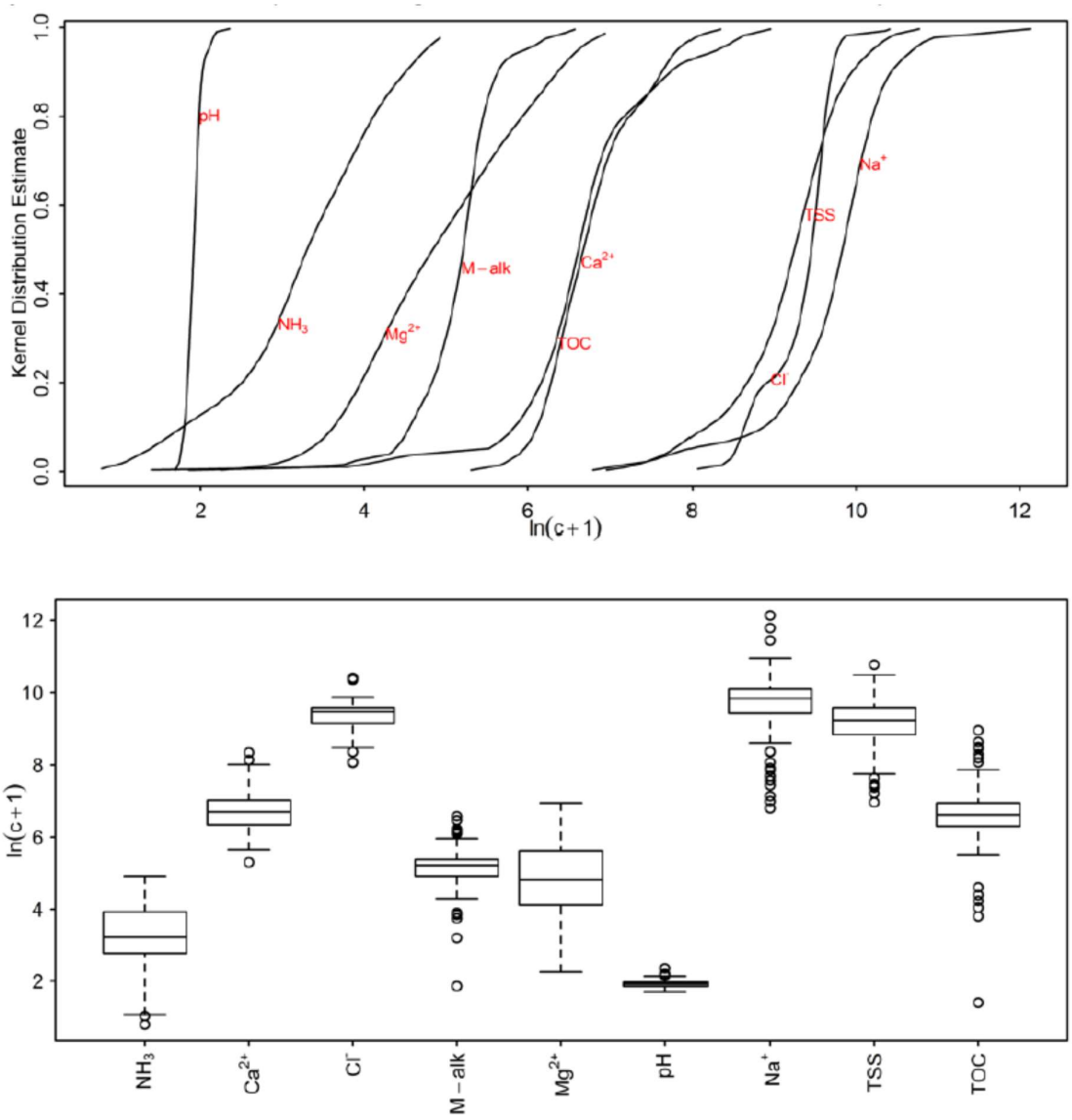

Figure 1: Kernel distribution estimates and box plots for mother liquor stream

Table 1 summarizes some distributional percentiles for the mother liquor stream and the 50th % tile (median) of the appropriate variable was used as input to OLI Stream Analyzer program. The following equations were used to obtain actual values for Kernel distribution estimate. For box plots the same equations are used but x is replaced with y

Equation 6-1

$$\ln(C+1) = \log_e(C+1)$$

Equation 6-2

$$x = \log_e(C+1)$$

$$e^x = C+1$$

$$C = e^x - 1$$

C is the concentration of the component of interest.

Table 1: Summary of distributional percentiles for the mother liquor stream

Component	units	Quantiles as %						
		5th	10th	25th	50th	75th	90th	95th
Ammonia	mg/L	3.0	5.2	15.0	24.0	49.5	88.1	111.0
Calcium	mg/L	403.8	469.7	566.2	810.1	1114.9	2029.5	2398.7
Chloride	mg/L	5151.9	5690.8	9351.7	12844.9	14549.9	16208.8	16972
M-Alkalinity	mg/L	79.8	94.4	136.7	184.9	216.8	271.2	371.7
Magnesium		30.9	41.4	60.0	122.1	276.1	557.8	680.4
pH	mg/L	4.8	5.1	5.4	5.8	6.2	6.4	7.0
Sodium	mg/L	2899.1	7330.3	12360.0	18574.0	24154.0	32871.0	44102.1
Suspended Solids	mg/L	2490.3	3549.0	6845.0	10256.0	14585.5	20065.0	26218.3
TOC	mg/L	275.3	369.9	549.0	748.6	1036.6	2278.2	3925.0

Number of analyses used for STATS=169

These data did not have silica, potassium, aluminium, barium, strontium, sulphates and nitrate

Median data for silica, potassium, nitrate and sulphates were adapted from the design document [Snyman, 2008]

According to OLI Stream Analyzer 3.2 software, the above water quality was imbalance in as far as the charge is concerned. The imbalance was on the anion and OLI dominant ion charge balance method was used to address the imbalance. OLI Stream Analyzer added 26688 mg/L of sulphates ion to address the charge imbalance.

Figure 2a and 2b shows a Kernel distribution estimates and box plots for Tubular Reverse Osmosis/Spiral Wound Reverse Osmosis Brine.

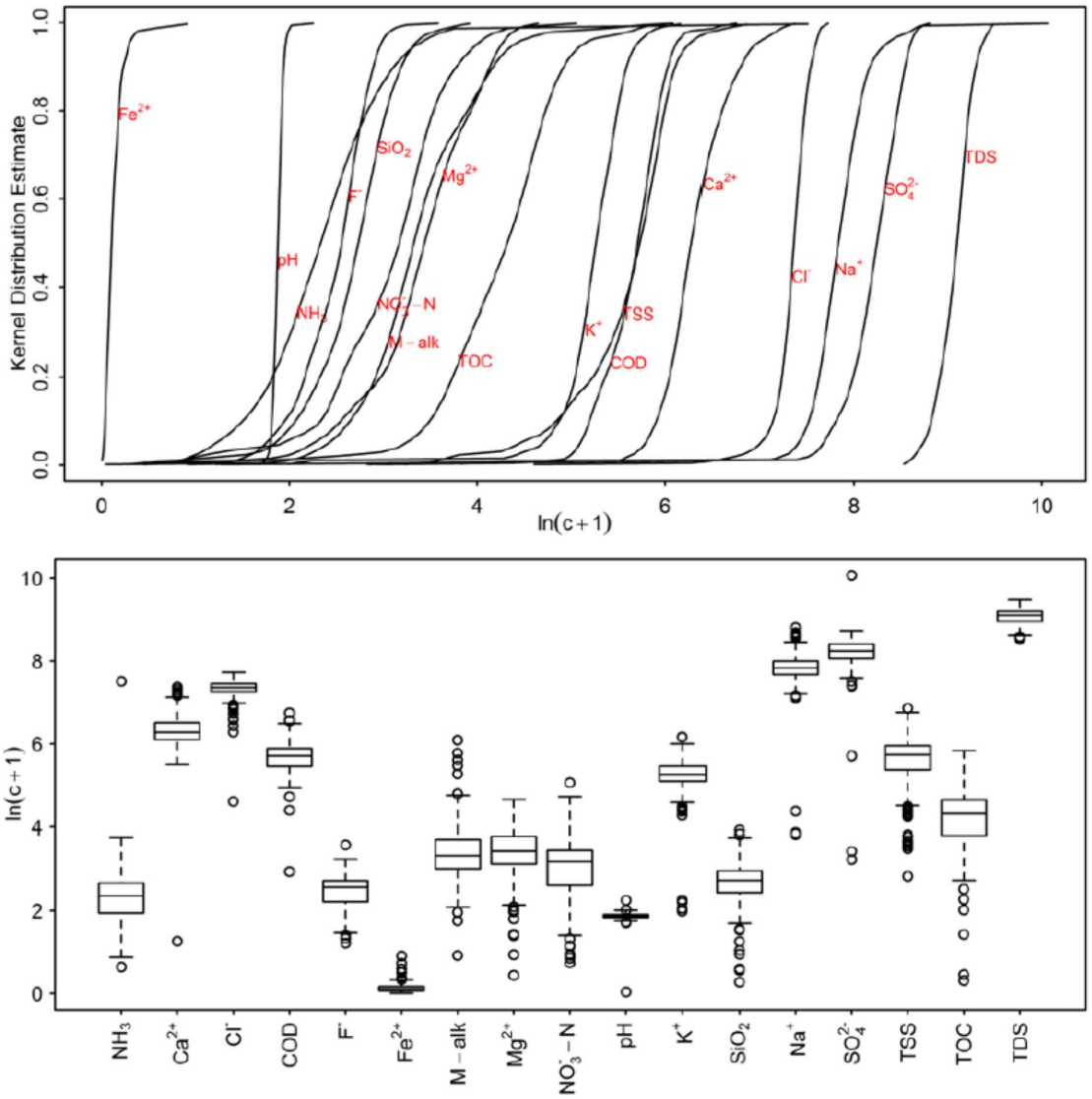

Figure 2: Kernel distribution estimates and box plots for Tubular Reverse Osmosis/Spiral Wound Reverse Brine.

Table 2 summarizes some distributional percentiles for the Tubular Reverse Osmosis (TRO/SRO) Brine stream and the 50th % tile (median) of the appropriate variable was used as input to OLI Stream Analyzer program.

Table 2: Distributional percentiles for the TRO/SRO Brine stream

Component	units	Quantiles as %						
		5th	10th	25th	50th	75th	90th	95th
Ammonia	mg/L	2.7	3.5	6.0	9.6	13.5	20.7	26.3
Calcium	mg/L	332.5	368.0	445.5	530.0	670.5	884.6	989.0
Chloride	mg/L	1095.6	1255.3	1423.6	1571.6	1719.5	1857.4	1978.1
COD	mg/L	164.1	181.2	232.0	300.0	359.5	411.4	440.0
Fluoride	mg/L	4.76	6.0	8.3	12.0	14.3	16.8	18.1
Iron	mg/L	0.03	0.04	0.06	0.12	0.19	0.25	0.33
M-Alkalinity	mg/L	11.0	13.3	19.4	27.0	40.0	61.9	77.7
Magnesium	mg/L	8.4	11.7	21.8	30.2	43.2	60.1	67.2
Nitrate-N	mg/L	6.00	9.95	12.68	23.15	30.73	41.84	50.67
pH		5.1	5.2	5.3	5.5	5.8	5.9	6.1
Potassium	mg/L	112.5	130.4	162.1	191.9	233.2	263.4	288.9
Silica	mg/L	5.3	7.0	10.5	14.4	18.4	23.0	26.0
Sodium	mg/L	1680.5	1847.9	2148.4	2509.8	2959.0	3443.4	4067.4
Sulphate	mg/L	2164.5	2453.0	3147.5	3800.0	4506.3	5075.7	5317.0
Suspended Solids	mg/L	87.2	125.4	214.0	308.0	384.0	435.6	513.4
TOC	mg/L	26.2	33.1	44.4	73.7	102.8	132.0	158.8
Total Dissolved Solids	mg/L	6368.7	6828.1	7755.3	9001.1	9830.8	10785.0	11555.9

Number of analysis used for STATS=301

According to OLI Stream Analyzer 3.2 software, the above water quality was imbalance in as far as the charge is concerned. The imbalance was on the anion and the software used dominant ion charge balance method to address the imbalance. OLI stream Analyzer added 817 mg/L of sulphate ion to balance the charge

Table 3 shows a summary of combined regeneration effluent used as input to OLI Stream Analyzer program

Table 3: Summary of Combined Regeneration Effluent Stream

Combined Regeneration Effluent Stream		
Parameters	Valid N	Value
TDS (mg/L)	1	30838.0
pH	1	7.8
Suspended Solids	1	2378.0
Conductivity (µS/cm)	1	30840.0
Total Organic Carbon (mg/L)	1	3.5
M-Alk (mg/L as $CaCO_3$)	1	100.0
Free and Saline Ammonia (NH_3-N) (mg/L)	1	2.8
Total Phosphate (PO_4-P) (mg/L)	1	0.4
Potassium (K) (mg/L)	1	106.0
Sodium (Na) (mg/L)	1	10520.0
Calcium (Ca) (mg/L)	1	105.0
Magnesium (Mg) (mg/L)	1	<2
Silica(SiO_2) (mg/L)	1	4.4
Strontium (Sr) (mg/L)	1	1.1
Aluminium (Al) (mg/L)	1	0.4
Barium (Ba) (mg/L)	1	<0.025
Iron (Fe) (mg/L)	1	0.04
Manganese (Mn) (mg/L)	1	<0.025
Fluoride (F) (mg/L)	1	0.8
Chloride (Cl) (mg/L)	1	9221.0
Nitrate (NO_3-N) (mg/L)	1	7.8
Sulphates (SO_4) (mg/L)	1	9881.0

Only one data point was used as this stream is not currently monitored and therefore special analysis (Water lab report number: 28685) was conducted in order to complete the modelling.

According to OLI Stream Analyzer 3.2 software, the above water quality was imbalance in as far as the charge is concerned. The imbalance was on the cation and the software used dominant ion charge balance method to address the imbalance. OLI Stream Analyzer added 56.16 mg/L of sodium ion to balance the charge.

Due to insufficient data a statistical analysis (Kernel Distribution Estimate and Box Plot) of the data could not be conducted and as a result a median was used to do the OLI Stream Analyzer simulation.

Table 4 shows a summary of mixed bed regeneration effluent (High Rinse Portion)

Table 4: Summary of Ion Exchange Mixed Bed Regeneration Effluent (high Rinse Portion)

Ion Exchange Mixed Bed Regeneration Effluent (High Rinse Portion)						
Parameters	Valid N	Mean	Median	Minimum	Maximum	Std.Dev.
TDS (mg/L)	6.0	28517.0	28050.0	15600.0	46000.0	10312.0
pH	6.0	1.3	1.3	1.0	1.5	0.2
COD (mg/L)	6.0	523.2	544.5	328.0	670.0	126.8
M-Alk (mg/L as $CaCO_3$)	6.0	<1.4	<1.4	<1.4	<1.4	0.0
P-Alkalinity	6.0	<0.8	<0.8	<0.8	<0.8	0.0
Ammonia (NH_3) (mg/L)	6.0	1.6	1.6	1.1	2.3	0.4
Phosphate (PO_4) (mg/L)	6.0	5.6	5.3	4.5	7.1	0.9
Potassium (K) (mg/L)	6.0	310.2	326.5	219.0	409.0	75.1
Sodium (Na) (mg/L)	6.0	2317.0	2388.0	1287.0	2997.0	559.5
Calcium (Ca) (mg/L)	6.0	913.7	865.5	623.0	1252.0	224.7
Magnesium (Mg) (mg/L)	6.0	485.5	456.0	344.0	627.0	101.7
Silica (SiO_2) (mg/L)	6.0	262.2	288.9	94.2	318.8	85.5
Strontium (Sr) (mg/L)	6.0	6.8	6.8	4.8	8.4	1.2
Aluminium (Al) (µg/L)	6.0	798.8	784.9	605.0	1098.0	165.9
Barium (Ba) (µg/L)	6.0	574.2	507.7	415.0	791.6	175.2
Iron (Fe) (µg/L)	6.0	260.7	240.0	159.0	442.0	99.3
Manganese (Mn) (µg/L)	6.0	12.2	11.5	8.0	18.0	4.1
Fluoride (F) (mg/L)	6.0	11.2	12.0	2.0	19.0	6.6
Chloride (Cl) (mg/L)	6.0	9925.0	8585.0	6295.0	19456.0	4778.0
Nitrate (NO_3) (mg/L)	6.0	75.2	62.5	43.0	125.0	30.3
Sulphates (SO_4) (mg/L)	6.0	610.7	602.5	276.0	895.0	220.9
Conductivity (µS/cm)	6.0	41155.0	40185.0	28120.0	61650.0	11715.0

Median values were used to conduct the simulation.

According to OLI Stream Analyzer 3.2 software, the above water quality was imbalance in as far as the charge is concerned. The imbalance was on the cation and the software used dominant ion charge balance method to address the imbalance. OLI Stream Analyzer added 1452 mg/L of sodium ion to balance the charge.

APPENDIX 2: EXPERIMENTAL CONDITIONS; STATISTICAL SUMMARY; FO MEMBRANE SPCIFICATION & P&ID FOR FO UNIT (PRELIMINARY STUDIES)

Table1: Impact of membrane orientation, temperature and flow rate on forward osmosis water and salt flux

Impact of membrane orientation, temperature and flow rates on FO water and salt flux			
Experimental Conditions	Value	Units	Notes
Testing modes: active layer facing deionised water (AS-DI) and active layer facing draw solution (AS-DS) PRO mode)			
Deionised and Draw solution temperatures	25	˚C	
	30	˚C	
	35	˚C	
Draw solution concentration	1	M NaCl	58.44 g/L NaCl
Deionised water concentration	0	Deionised water	
Deionised and Draw solution pH			Not adjusted. The pH was within the appropriate range for FO CTA and FO TFC membrane
Deionised and Draw solution flow rates	1.5	L/min	
	2.5	L/min	
	2.7	L/min	

Deionised and Draw solution flow direction	co-current		
Spacers	0.7874	mm	Spacers were installed in the deionised and draw solution flow channel to promote turbulence or mixing
Deionised and Draw solution pressures	~0	bar	there was no pressurization of the system (operating at atmospheric pressure)
Membrane Type	FO CTA		all the parameters were evaluated
	FO TFC		only membrane orientation was evaluated
Membrane Orientation	FO Mode		
	PRO Mode		

Table 2: Impact of draw solution concentration on Forward Osmosis water and salt flux

Impact of draw solution concentration on FO water and salt flux			
Experimental Conditions	Value	Units	Notes
Testing modes: active layer facing deionised water (AS-DI)			
Deionised and Draw solution temperatures	25	˚C	
Draw solution concentration	2	g/L NaCl	
	5	g/L NaCl	
	10	g/L NaCl	
	20	g/L NaCl	
	30	g/L naCl	
	40	g/L NaCl	
	50	g/L NaCl	
	60	g/L NaCl	
	70	g/L NaCl	
Deionised water concentration	0	Deionised water	
Deionised and Draw solution pH			Not adjusted. The pH was within the appropriate range for FO CTA and FO TFC membrane
Deionised and Draw solution flow rates	1.5	L/min	
Deionised and Draw solution flow direction	co-current		
Spacers	0.7874	mm	Spacers were installed in the deionised and draw solution flow channel to promote turbulence or mixing
Deionised and Draw solution pressures	~0	bar	there was no pressurization

			of the system (operating at atmospheric pressure)
Membrane Type	FO CTA		all the parameters were evaluated
	FO TFC		only membrane orientation was evaluated
Membrane Orientation	FO Mode		
	PRO Mode		

Table 3: Impact of feed solution concentration on Forward Osmosis water flux

Impact of feed solution concentration on FO water and salt flux			
Experimental Conditions	Value	Units	Notes
Testing modes: active layer facing deionised water (AS-DI)			
Feed and Draw solution temperatures	25	˚C	
Feed solution concentration	10	g/L NaCl	
	20	g/L NaCl	
	30	g/L NaCl	
	40	g/L NaCl	

	50	g/L NaCl	
	60	g/L NaCl	
	70	g/L NaCl	
	100	g/L NaCl	
	105	g/L NaCl	
Draw Solution	116	g/L NaCl	
Feed and Draw solution pH			Not adjusted. The pH was within the appropriate range for FO CTA and FO TFC membrane
Feed and Draw solution flow rates	1.5	L/min	
Feed and Draw solution flow direction	co-current		
Spacers	0.7874	mm	Spacers were installed in the deionised and draw solution flow channel to

			promote turbulence or mixing
Feed and Draw solution pressures	~0	bar	there was no pressurization of the system (operating at atmospheric pressure)
Membrane Type	FO CTA		all the parameters were evaluated
	FO TFC		only membrane orientation was evaluated
Membrane Orientation	FO Mode		
	PRO Mode		

Table 4: Impact of membrane orientation, temperature and flowrate on forward osmosis water and salt flux (NH_4HCO_3 draw solution)

Impact of membrane orientation, temperature and flow rate on forward osmosis water and salt flux			
Experimental Conditions	Value	Units	Notes
Testing modes: active layer facing deionised water (AS-DI) (FO mode) and active layer facing draw solution (AS-DS) (PRO)			
Deionised and Draw solution temperatures	25	˚C	
	30	˚C	
Draw solution concentration	1	M NH4HCO3	83.4 g/L
Concentrated Draw solution concentration	2	M NH4HCO3	167 g/L
Deionised water concentration	0	M NaCl	Deionised water
Deionised and Draw solution pH			Not adjusted. The pH where within the appropriate range for FO CTA and FO TFC membrane
Deionised and Draw solution flow rates	1.5	L/min	
	2.5	L/min	
Deionised and Draw solution flow direction	co-current		
Spacers	0.7874	mm	Spacers were installed in the deionised water and draw solution flow channel to promote turbulence or mixing
Deionised and draw solution pressures	~0	bar	there was no pressurization of the system
Membrane Type	FO TFC		
Membrane Orientation	FO mode		
	PRO mode		

Table 5: Impact of draw solution concentration on FO water flux

Impact of draw solution concentration on FO water flux			
Experimental Conditions	Value	Units	Notes
Testing modes: active layer facing deionised water (AS-DI) (FO mode)			
Deionised and Draw solution temperatures	30	˚C	
Feed concentration	2	g/L NH4HCO3	
	5	g/L NH4HCO3	
	10	g/L NH4HCO3	
	20	g/L NH4HCO3	
	30	g/L NH4HCO3	
	40	g/L NH4HCO3	
	50	g/L NH4HCO3	
	60	g/L NH4HCO3	
	70	g/L NH4HCO3	
	80	g/L NH4HCO3	
CDS concentration	167	g/L NH4HCO3	2 M
Deionised and Draw solution pH			Not adjusted. The pH where within the appropriate range for FO CTA and FO TFC membrane
Deionised and Draw solution flow rates	1.5	L/min	
Deionised and Draw solution flow direction	co-current		
Spacers	0.7874	mm	Spacers were installed in the deionised water and draw solution flow channel to promote turbulence or mixing
Deionised and draw solution pressures	~0	bar	there was no pressurization of the system
Membrane Type	FO CTA		
Membrane Orientation	FO mode		

Table 6: Impact of feed solution concentration on FO water flux (NH_4HCO_3 draw solution)

Impact of feed solution concentration on FO water flux			
Experimental Conditions	Value	Units	Notes
Testing modes: active layer facing deionised water (AS-DI) (FO mode)			
Deionised and Draw solution temperatures	30	˚C	
Feed concentration	5	g/L NaCl	
	10	g/L NaCl	
	15	g/L NaCl	
	20	g/L NaCl	
	25	g/L NaCl	
	30	g/L NaCl	
	35	g/L NaCl	
	40	g/L NaCl	
DS concentration	118	g/L NH4HCO3	1.5 M
CDS concentration	167	g/L NH4HCO3	2 M
Deionised and Draw solution pH			Not adjusted. The pH where within the appropriate range for FO CTA and FO TFC membrane
Deionised and Draw solution flow rates	1.5	L/min	
Deionised and Draw solution flow direction	co-current		
Spacers	0.7874	mm	Spacers were installed in the deionised water and draw solution flow channel to promote turbulence or mixing
Deionised and draw solution pressures	~0	bar	there was no pressurization of the system
Membrane Type	FO CTA		
Membrane Orientation	FO mode		

Table 7: Impact of feed solution concentration on FO water flux (NH_4HCO_3 draw solution)

Impact of feed solution concentration on FO water flux			
Experimental Conditions	Value	Units	Notes
Testing modes: active layer facing deionised water (AS-DI) (FO mode)			
Deionised and Draw solution temperatures	30	˚C	
Feed concentration	0	g/L NaCl	
	10	g/L NaCl	
	20	g/L NaCl	
	30	g/L NaCl	
	40	g/L NaCl	
	50	g/L NaCl	
DS concentration	240	g/L NH4HCO3	3 M
CDS concentration	316	g/L NH4HCO3	4 M
Deionised and Draw solution pH			Not adjusted. The pH where within the appropriate range for FO CTA and FO TFC membrane
Deionised and Draw solution flow rates	1.5	L/min	
Deionised and Draw solution flow direction	co-current		
Spacers	0.7874	mm	Spacers were installed in the deionised water and draw solution flow channel to promote turbulence or mixing
Deionised and draw solution pressures	~0	bar	there was no pressurization of the system
Membrane Type	FO CTA		
Membrane Orientation	FO mode		

Table 8: Standard relationship between measured conductivity and prepared sodium chloride salt concentration

Standard Relationship between conductivity and NaCl salt concentration		
NaCl Concentration (g/L)	Measured Conductivity (mS/cm)	Ratio (new)
0.010	0.022	0.45
0.020	0.044	0.45
0.030	0.064	0.47
0.040	0.090	0.44
0.050	0.110	0.45
0.060	0.127	0.47
0.070	0.151	0.46
0.080	0.169	0.47
0.090	0.187	0.48
0.100	0.212	0.47

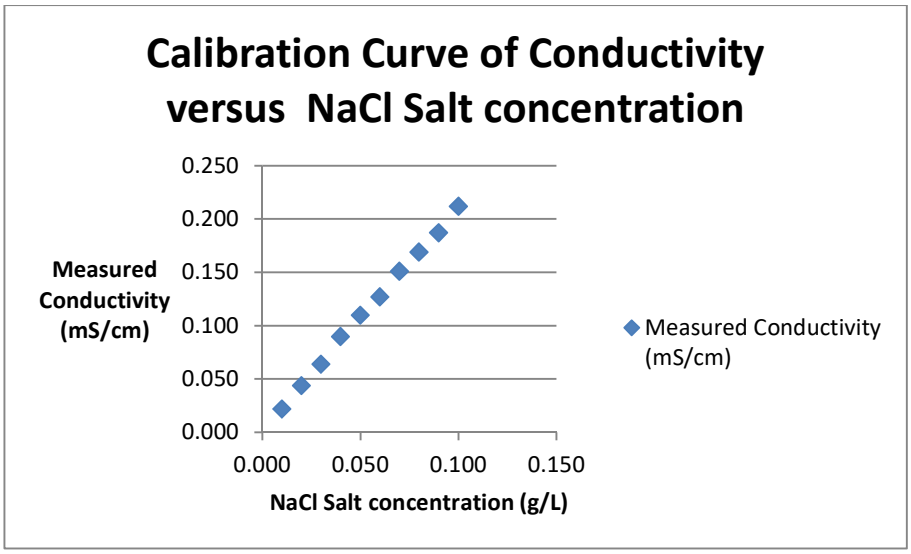

Figure1: Calibration curve of conductivity vs sodium chloride salt concentration

HTI OsMem™ CTA-ES Membrane

Features:

- The OsMem™ CTA-ES Membrane is HTI's fouling resistant and most chlorine resistant FO membrane with an embedded support.
- The OsMem™ CTA-ES Membrane is used in all spiral-wound FO elements that use CTA (Expedition, HydroWell, and 2521FO-CTA, 4040FO-CTA, and 8040FO-CTA).
- The OsMem™ CTA-ES Membrane is cast on 40" (1-m) wide rolls.
- The OsMem™ CTA-ES Membrane coupons are shipped "dry," where vegetable-based glycerin replaces the water.

Typical FO Performance (Rejection Layer Contacting Feed):

- Water Permeation: 5.3 GFD (gallons per square foot each day) (9.0 LMH – liters per square meter each hour)
- Salt Rejection: 99%

Test Conditions: **Feed**: 1 gpm (4 lpm) tap water feed at 77°F (25°C) fed at the bottom into a 4" (100 mm) by 0.2" (5 mm) open channel with an initial volume of 0.40 gal (1.5 L) and an exit pressure of 5 psi (35 kPa).
Draw: 7 gph (26 lph) 1 M NaCl (58.5 g/L) at the bottom at 2 psi (15 kPa) feed into a 4" (100 mm) by 0.055" (1.4 mm) channel of two 30-mil (0.76 mm) diamond-type polypropylene feed spacers (strands spaced at 11 strands per inch (25.4 mm)) with an initial volume of 0.13 gal (0.5 L).
Membrane Area: 0.22 ft² (0.020 m²)
Rejection: {1 – [(mol NaCl transferred to feed)/(L water removed)/(1 M)]}

Typical uPRO* Performance (Rejection Layer Contacting Draw Solution):

- Water Permeation: 7 GFD (gallons per square foot each day) (12 LMH – liters per square meter each hour)
- Salt Rejection: 99%

Test Conditions: **Feed**: 7 gph (26 lph) tap water at the bottom at 2 psi (15 kPa) feed into a 4" (100 mm) by 0.055" (1.4 mm) channel of two 30-mil (0.76 mm) diamond-type polypropylene feed spacers (strands spaced at 11 strands per inch (25.4 mm)) with an initial volume of 0.26 gal (1.0 L).
Draw: 1 gpm (4 lpm) 1 M NaCl (58.5 g/L) at 77°F (25°C) fed at the bottom into a 4" (100 mm) by 0.2" (5 mm) open channel with an initial volume of 0.2 gal (0.8 L) and an exit pressure of 5 psi (35 kPa).
Membrane Area: 0.22 ft² (0.020 m²)
Rejection: {1 – [(mol NaCl transferred to feed)/(L water removed)/(1 M)]}
***uPRO**: unpressurized Pressure Retarded Osmosis membrane orientation

Hydration Technology Innovations
2484 Ferry St. SW Albany, OR 97322 USA 541-917-3335 info@htiwater.com http://www.htiwater.com

HTI OsMem™ CTA-ES Membrane (page 2)

Operating Limits and Guidelines:

• Membrane Requirements	Membrane coupons are shipped in glycerin. Should be soaked in water for 30 minutes prior to use. After glycerin extraction, membrane must be kept moist at all times. Do not allow to freeze. Exercise care in handling.
• Membrane Type	Cellulose Triacetate (CTA) with embedded polyester screen support
• Maximum Operating Temperature	160°F (71°C)
• Maximum Transmembrane Pressure	10 psi (70 kPa), if supported
• pH Range	3 to 8
• Maximum Chlorine	2 ppm
• Cleaning Guidelines	Use only cleaning chemicals approved for CA/CTA RO membranes
• Storage Guidelines	Store out of direct sunlight with a couple mL of water

FO Membrane Notes:

The membrane is initially cast on rolls. On a roll, the rejection layer is to the inside of the roll and is the shiny side; on drying, the membrane will curl towards the rejection layer.

FO membranes behave similarly to RO membranes in that dissolved gases are not rejected well. Their ions are rejected, but the (often small) fraction that exists as a dissolved gas is not rejected. Small polar, water-soluble organics, such as urea, methanol, and ethanol, are also not rejected well.

Brief Startup Description:

If the process is being run with the draw solution contacting the rejection layer (uPRO), make sure that there is water in the cell on the supported side to draw from. Start the pump on the unsupported side. Adjust the flowrate with the inlet valve and the exit pressure to 5 psi (35 kPa) with the exit valve. Start the side with the membrane support and adjust to the desired inlet pressure of 2 psi (15 kPa). Monitor volume or weight changes, temperature, and concentrations with time.

Brief Shutdown Descriptions:

Turn off the pumps and drain the high osmotic pressure solution first. Then drain the low osmotic pressure solution. Rinsing is recommended. The membrane can be stored in the cell – preferably drained.

HTI OsMem™ TFC-ES Membrane

Features:

- The OsMem™ TFC-ES Membrane is HTI's fastest and highest rejecting FO membrane.
- The OsMem™ TFC-ES Membrane is used in all spiral-wound FO elements that use TFC.
- The OsMem™ TFC-ES Membrane is cast on 40" (1-m) wide rolls.
- The OsMem™ TFC-ES Membrane coupons are shipped "dry," where vegetable-based glycerin replaces the water.

Typical FO Performance (Rejection Layer Contacting Feed):

- Water Permeation: 12 GFD (gallons per square foot each day) (20 LMH – liters per square meter each hour)
- Salt Rejection: 99.6% as defined in Test Conditions

Test Conditions: **Feed**: 1 gpm (4 lpm) tap water feed at 77°F (25°C) fed at the bottom into a 4" (100 mm) by 0.2" (5 mm) open channel with an initial volume of 0.40 gal (1.5 L) and an exit pressure of 10 psi (40 kPa).
Draw: 20 gph (75 lph) 1 M NaCl (58.5 g/L) at the bottom at 6 psi (40 kPa) feed into a 4" (100 mm) by 0.06" (1.5 mm) channel of three 20-mil (0.51-mm) epoxy-coated permeate spacer with the bottom two oriented normal to flow and the membrane-contacting spacer parallel to the flow with an initial volume of 0.13 gal (0.5 L).
Membrane Area: 0.22 ft² (0.020 m²)
Rejection: {1 – [(mol NaCl transferred to feed)/(L water removed)/(1 M)]}

Typical uPRO* Performance (Rejection Layer Contacting Draw Solution):

- Water Permeation: 24 GFD (gallons per square foot each day) (40 LMH – liters per square meter each hour)
- Salt Rejection: 99.6% as defined in Test Conditions

Test Conditions: **Feed**: 20 gph (75 lph) tap water at the bottom at 6 psi (40 kPa) feed into a 4" (100 mm) by 0.06" (1.5 mm) channel of three 20-mil (0.51-mm) epoxy-coated permeate spacer with the bottom two oriented normal to flow and the membrane-contacting spacer mounted parallel to the flow with an initial volume of 0.26 gal (1.0 L).
Draw: 1 gpm (4 lpm) 1 M NaCl (58.5 g/L) at 77°F (25°C) fed at the bottom into a 4" (100 mm) by 0.2" (5 mm) open channel with an initial volume of 0.2 gal (0.8 L) and an exit pressure of 10 psi (70 kPa).
Membrane Area: 0.22 ft² (0.020 m²)
Rejection: {1 – [(mol NaCl transferred to feed)/(L water removed)/(1 M)]}
***uPRO**: unpressurized Pressure Retarded Osmosis membrane orientation

Hydration Technology Innovations
2484 Ferry St. SW Albany, OR 97322 USA 541-917-3335 info@htiwater.com http://www.htiwater.com

Table 9: Descriptive statistics results for the impact of membrane orientation, temperature and flow rate on water and salt flux experiments

Descriptive Statistics

Variable: Flux

	GroupDescrip	FluxDescrip	Mean	St. Deviation	Valid N	Median	25th Percentile	75th Percentile	Minimum	Maximum
1	AS-DI CTA 25	Salt (mg m^-2h^-1)	6625.59	318.458	10	6613.62	6480.04	6870.83	6010.34	7055.01
2	AS-DI CTA 30	Salt (mg m^-2h^-1)	7285.66	314.956	15	7196.45	7107.71	7491.87	6783.11	8010.12
3	AS-DI CTA 35	Salt (mg m^-2h^-1)	8506.31	335.492	27	8488.37	8292.05	8744	7915.62	9283.23
4	AS-DS CTA 25	Salt (mg m^-2h^-1)	12536.49	365.009	10	12459.62	12230.13	12792.45	12142.89	13238.87
5	AS-DS CTA 30	Salt (mg m^-2h^-1)	14137.9	441.368	15	14117.12	13782.05	14431.52	13571.75	15054.03
6	AS-DS CTA 35	Salt (mg m^-2h^-1)	15260.34	452.618	14	15282.66	14839.18	15584.12	14650.32	16033.47
7	AS-DI CTA 2.5	Salt (mg m^-2h^-1)	7295.95	417.065	10	7328.02	6941.78	7562.71	6723.32	8018.72
8	AS-DI CTA 2.7	Salt (mg m^-2h^-1)	6963.04	245.804	12	6936.48	6809.17	7024.62	6624.55	7574.84
9	AS-DS CTA 2.5	Salt (mg m^-2h^-1)	12563.31	703.146	13	12576.98	12291.67	13159.5	11183.52	13530.56
10	AS-DI TFC 25	Salt (mg m^-2h^-1)	7811.94	118.348	18	7814.26	7712.04	7877.03	7658.42	8071.25
11	AS-DS TFC 25	Salt (mg m^-2h^-1)	17924.14	661.068	11	18248.99	17759.35	18355.18	16335.74	18434.64
12	AS-DI CTA 25	Water (Lm^-2h^-1	10.96	0.332	45	11.04	10.81	11.19	9.89	11.37
13	AS-DI CTA 30	Water (Lm^-2h^-1)	13.57	0.246	48	13.52	13.4	13.69	13.2	14.29
14	AS-DI CTA 35	Water (Lm^-2h^-1)	13.96	0.258	31	13.91	13.79	14.1	13.6	14.57
15	AS-DS CTA 25	Water (Lm^-2h^-1)	18.71	0.518	49	18.83	18.42	19.07	17.06	19.36
16	AS-DS CTA 30	Water (Lm^-2h^-1)	20.69	0.354	49	20.8	20.54	20.95	19.63	21.2
17	AS-DS CTA 35	Water (Lm^-2h^-1)	22.64	0.216	34	22.64	22.5	22.79	22.03	23.02
18	AS-DI CTA 2.5	Water (Lm^-2h^-1	10.94	0.269	49	10.97	10.81	11.11	10	11.48
19	AS-DI CTA 2.7	Water (Lm^-2h^-1	13.18	0.413	33	13.06	12.9	13.43	12.5	14.12
20	AS-DS CTA 2.5	Water (Lm^-2h^-1	19.54	0.673	36	19.65	19.12	20.05	17.96	20.98
21	AS-DI TFC 25	Water (Lm^-2h^-1	14.8	0.263	49	14.78	14.68	14.97	14.22	15.4
22	AS-DS TFC 25	Water (Lm^-2h^-1)	30.69	0.192	36	30.67	30.54	30.87	30.33	30.95

Table 10: Descriptive statistics results for the impact of draw solution concentration on water and salt flux experiments

Descriptive Statistics

Variable: Flux

	GroupDescrip	FluxDescrip	Mean	St. Deviation	Valid N	Median	25th Percentile	75th Percentile	Minimum	Maximum
1	AS-DI (2g/l DS	Salt (mg^-2h^-1	1048.09	75.8	13	1025.82	1003.06	1048.38	984.53	1239.31
2	AS-DI (5g/l DS	Salt (mg^-2h^-1	1337.34	42.726	12	1326.61	1319.51	1357.32	1258.75	1414.49
3	AS-DI (10g/l DS	Salt (mg^-2h^-1	2543.96	126.077	11	2573.19	2477.92	2622.32	2286.79	2722.15
4	AS-DI (20g/l DS	Salt (mg^-2h^-1	3696.47	213.895	14	3714.42	3546.24	3861.18	3341.98	4010.35
5	AS-DI (30g/l DS	Salt (mg^-2h^-1	4541.29	237.607	12	4468.88	4349.81	4643.48	4294.42	4990.3
6	AS-DI (40g/l DS	Salt (mg^-2h^-1	5617.41	254.248	19	5533.49	5406.34	5803.39	5220.85	6083.51
7	AS-DI (50g/l DS	Salt (mg^-2h^-1	6716.54	342.515	23	6694.25	6455.02	6895.42	6167.47	7538.53
8	AS-DI (60g/l DS	Salt (mg^-2h^-1	7715.43	226.568	14	7723.93	7589.64	7915.55	7271.78	7995.65
9	AS-DI (70g/l DS	Salt (mg^-2h^-1	7675.18	235.201	10	7587.21	7536.64	7895.78	7361.11	8013.47
10	AS-DI (2g/l DS	Water (Lm^-2h^-1	2.23	0.253	43	2.27	2.14	2.41	1.41	2.59
11	AS-DI (5g/l DS	Water (Lm^-2h^-1	3.53	0.261	49	3.53	3.33	3.58	3.1	4.29
12	AS-DI (10g/l DS	Water (Lm^-2h^-1	5.15	0.227	49	5.1	5	5.28	4.71	5.76
13	AS-DI (20g/l DS	Water (Lm^-2h^-1	6.25	0.266	35	6.31	6.14	6.43	5.37	6.57
14	AS-DI (30g/l DS	Water (Lm^-2h^-1	8.69	0.217	49	8.71	8.57	8.86	8.16	9.01
15	AS-DI (40g/l DS	Water (Lm^-2h^-1	10.11	0.219	34	10.14	10	10.31	9.49	10.36
16	AS-DI (50g/l DS	Water (Lm^-2h^-1	11.84	0.215	49	11.81	11.71	11.96	11.43	12.45
17	AS-DI (60g/l DS	Water (Lm^-2h^-1	13.03	0.235	34	13.07	12.93	13.21	12.3	13.35
18	AS-DI (70g/l DS	Water (Lm^-2h^-1	13.91	0.234	48	13.9	13.77	14.08	13.28	14.29

Table 11: Descriptive statistics results for the impact of feed solution concentration on water flux experiments

Descriptive Statistics

Variable: Flux

	GroupDescrip	FluxDescrip	Mean	St. Deviation	Valid N	Median	25th Percentile	75th Percentile	Minimum	Maximum
1	AS-FS (10g/l)	Water (Lm^-2h^-1	14.1	0.341	47	14.26	14.03	14.29	13.1	14.47
2	AS-FS (20g/l)	Water (Lm^-2h^-1	11.57	0.264	34	11.64	11.42	11.77	10.92	11.94
3	AS-FS (30g/l)	Water (Lm^-2h^-1	10.53	0.211	48	10.52	10.35	10.71	10	11.05
4	AS-FS (40g/l)	Water (Lm^-2h^-1	8.64	0.35	49	8.57	8.4	8.79	8.17	9.78
5	AS-FS (50g/l)	Water (Lm^-2h^-1	7.3	0.209	49	7.22	7.14	7.4	7.03	7.83
6	AS-FS (60g/l)	Water (Lm^-2h^-1	5.41	0.242	46	5.46	5.24	5.6	4.76	5.76
7	AS-FS (70g/l)	Water (Lm^-2h^-1	4.13	0.228	49	4.15	4.02	4.29	3.57	4.63
8	AS-FS (100g/l)	Water (Lm^-2h^-1	3.23	0.24	47	3.23	3.07	3.36	2.8	4.03
9	AS-FS (105g/l)	Water (Lm^-2h^-1	2.01	0.271	34	1.96	1.82	2.11	1.66	2.89

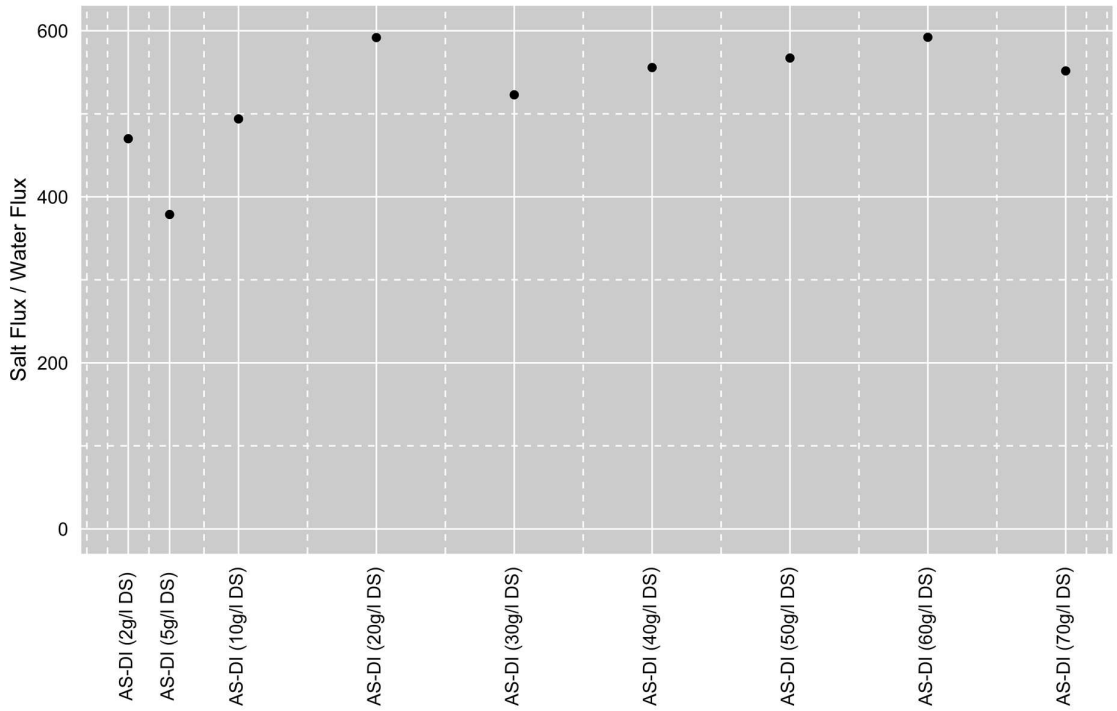

Figure 2: Specific Reverse Solute Flux for the CTA membrane

Table 12: Descriptive statistics results for the impact of membrane orientation, temperature and flow rate on water and salt flux experiments (NH_4HCO_3 draw solution)

item	group1	group2	n	mean	sd	median	min	max	Variable
1	AS-DI TFC 25	1.5	49	16.75	0.22	16.71	16.41	17.26	Water.Flux
2	AS-DS TFC 25	1.5	34	35.94	0.3	35.98	35.06	36.32	Water.Flux
1	AS-DI TFC 25	1.5	6	29940.2	1411.97	29306.69	29030.02	32704.43	Salt.Flux
2	AS-DS TFC 25	1.5	17	28545.12	787.39	28538.33	26270.13	29583.02	Salt.Flux
1	AS-DS TFC 25	2.5	34	33.25	1.98	34	29.07	35.31	Water.Flux
2	AS-DS TFC 30	2.5	35	38.6	0.56	38.71	36.43	39.17	Water.Flux
1	AS-DS TFC 25	2.5	25	31041.54	430.18	31010.83	29781.31	31754.76	Salt.Flux
2	AS-DS TFC 30	2.5	9	38190.09	1148.32	37946.83	36375.53	39995.67	Salt.Flux

Table 13: Descriptive statistics results for the impact of draw solution concentration on water and salt flux experiments

item	group1	n	mean	sd	median	min	max	Variable
1	ASDI (2 g/l DS)	36	3.53	0.23	3.57	2.84	3.9	Water.Flux
2	ASDI (5 g/l DS)	34	5.35	0.26	5.38	4.62	5.75	Water.Flux
3	ASDI (10 g/l DS)	34	8.34	0.22	8.32	7.81	8.92	Water.Flux
4	ASDI (20 g/l DS)	36	9.59	0.56	9.7	8.25	10.44	Water.Flux
5	ASDI (30 g/l DS)	35	12.95	0.24	12.95	12.43	13.47	Water.Flux
6	ASDI (40 g/l DS)	34	13.83	0.74	14.05	11.72	14.64	Water.Flux
7	ASDI (50 g/l DS)	36	16.06	0.5	15.88	15.69	18.36	Water.Flux

8	ASDI (60 g/l DS)	35	17.78	0.24	17.81	17.16	18.12	Water.Flux
9	ASDI (70 g/l DS)	35	18.01	0.23	18.05	17.42	18.38	Water.Flux
10	ASDI (80 g/l DS)	34	19.58	0.25	19.56	19.18	20.35	Water.Flux
1	ASDI (2 g/l DS)	14	3049.24	35.14	3046.21	3002.05	3114.9	Salt.Flux
2	ASDI (5 g/l DS)	12	6023.14	533.17	5854.3	5397.09	6800.73	Salt.Flux
3	ASDI (10 g/l DS)	28	8385.97	157.92	8385.73	8121.92	8677.72	Salt.Flux
4	ASDI (20 g/l DS)	26	11903.43	325.03	11833.82	11531.59	12961.16	Salt.Flux
5	ASDI (30 g/l DS)	35	16927.98	580.85	16813.23	16209.2	18242.24	Salt.Flux
6	ASDI (40 g/l DS)	34	19770.71	541.29	19718.63	18947.5	20871.61	Salt.Flux
7	ASDI (50 g/l DS)	35	22535.66	348.55	22494.7	22025.06	23265.36	Salt.Flux
8	ASDI (60 g/l DS)	34	26672.69	251.05	26691.57	26218.91	27374.71	Salt.Flux
9	ASDI (70 g/l DS)	34	27252.98	424.28	27183.29	26342.9	28105.47	Salt.Flux
10	ASDI (80 g/l DS)	34	31087.07	679.18	31002.75	30093.96	32697.16	Salt.Flux

Table 14: Descriptive statistics results for the impact of feed solution concentration on water flux experiments (NH_4HCO_3 draw solution)

item	group1	vars	n	mean	sd	median	min	max	Variable	Conc
1	AS-FS (5 g/l)	1	36	14.92	0.29	14.99	14.17	15.38	Water.Flux	118.5
2	AS-FS (10 g/l)	1	34	15.78	0.12	15.73	15.65	16.06	Water.Flux	118.5
3	AS-FS (15 g/l)	1	34	11.88	0.21	11.88	11.38	12.32	Water.Flux	118.5

4	AS-FS (20 g/l)	1	34	10.5	0.21	10.51	9.99	10.85	Water.Flux	118.5
5	AS-FS (25 g/l)	1	34	8.87	0.27	8.82	8.49	9.57	Water.Flux	118.5
6	AS-FS (30 g/l)	1	35	7.12	0.25	7.15	6.33	7.47	Water.Flux	118.5
7	AS-FS (35 g/l)	1	34	6.31	0.26	6.28	5.94	7	Water.Flux	118.5
8	AS-FS (40 g/l)	1	34	4.74	0.27	4.79	3.9	5.06	Water.Flux	118.5
1	AS-FS (0 g/l)	1	35	21.12	0.9	21.39	19.05	22.19	Water.Flux	240
2	AS-FS (10 g/l)	1	35	15.44	0.31	15.3	14.92	15.84	Water.Flux	240
3	AS-FS (20 g/l)	1	34	12.65	0.27	12.71	11.77	12.98	Water.Flux	240
4	AS-FS (30 g/l)	1	34	10.29	0.24	10.24	9.98	10.84	Water.Flux	240
5	AS-FS (40 g/l)	1	36	7.77	0.34	7.86	6.86	8.93	Water.Flux	240
6	AS-FS (50 g/l)	1	34	6.6	0.23	6.58	6.01	7.12	Water.Flux	240

P&ID Lab unit forward osmosis RL21

APPENDIX 3: EXPERIMENTAL CONDITIONS; STATISTICAL SUMMARY & ANALYTICAL RESULTS FROM BATCH EXPERIMENTS

Table 1: Experimental conditions for non-scaling Synthetic HRP solution (NaCl baseline run)

SELECT MODE 2 ON THE DELTA V			
Synthetic Solution for HRP Sasolburg			
Water Flux Behaviour in the absence of scaling			
Experimental Conditions	Value	Units	Notes
Testing modes: active layer facing Feed water (AS-DI) (FO mode).			**Constant Draw Solution and Variable Feed Solution Concentration (Feed Solution is allowed to concentrate)**
Feed and Draw solution temperatures	30	˚C	
Draw solution concentration	3	M NH4HCO3	240 g/L NH4HCO3
Concentrated Draw solution concentration	4	M NH4HCO3	316 g/L NH4HCO3
Feed concentration	0.22500	M NaCl	13 g/L NaCl (10 bar osmotic pressure)
Feed and Draw solution pH			Not adjusted.
Feed and Draw solution flow rates	1.5	L/min	
Feed Solution Starting Volume	8	L	
Feed and Draw solution flow direction	co-current		
Spacers	0.7874	mm	Spacers were installed in the deionised water and draw solution flow channel to promote turbulence or mixing
Feed and draw solution pressures	~0	bar	there was no pressurization of the system
Membrane Type	FO TFC		
Membrane Orientation	FO mode		

Analysis	
Feed Sample at the beginning	Draw Solution Samples at the beginning
Feed Sample at the end of the run	Draw Solution Sample at the end of the run
Full Analysis to qunatify both reverse and forward solute diffusion	
Monitor the feed solution starting volume and end volume	
Monitor the concentrated draw solution volume (beginning, during and end of the run)	

Table 2: Experimental conditions for scaling Synthetic HRP solution

SELECT MODE 2 ON THE DELTA V			
Synthetic Solution for HRP Sasolburg			
Water Flux Behaviour in the presence of scaling			
Experimental Conditions	Value	Units	Notes
Testing modes: active layer facing Feed water (AS-DI) (FO mode).			**Constant Draw Solution and Variable Feed Solution Concentration (Feed Solution is allowed to concentrate)**
Feed and Draw solution temperatures	30	˚C	
Draw solution concentration	3	M NH4HCO3	240 g/L NH4HCO3
Concentrated Draw solution concentration	4	M NH4HCO3	316 g/L NH4HCO3
Feed concentration			Synthetic HRP Sasolburg Solution (10 bar osmotic pressure)
Feed and Draw solution pH			Synthetic feed solution was corrected to pH between 5 and 6.5 before the experiment was conducted
Feed and Draw solution flow rates	1.5	L/min	
Feed Solution Starting Volume	6.8	L	
Feed and Draw solution flow direction	co-current		
Spacers	0.7874	mm	Spacers were installed in the deionised water and draw solution flow channel to promote turbulence or mixing
Feed and draw solution pressures	~0	bar	there was no pressurization of the system
Membrane Type	FO TFC		
Membrane Orientation	FO mode		

Analysis	
Feed Sample at the beginning	Draw Solution Samples at the beginning
Feed Sample at the end of the run	Draw Solution Sample at the end of the run
Full Analysis to qunatify both reverse and forward solute diffusion	
Monitor the feed solution starting volume and end volume	
Monitor the concentrated draw solution volume (beginning, during and end of the run)	

Table 3: Experimental conditions for non-scaling Synthetic TRO/SRO Brine solution (NaCl baseline run)

SELECT MODE 2 ON THE DELTA V			
Synthetic Solution for TRO Brine			
Water Flux Behaviour in the absence of scaling			
Experimental Conditions	Value	Units	Notes
Testing modes: active layer facing Feed water (AS-DI) (FO mode).			**Constant Draw Solution and Variable Feed Solution Concentration (Feed Solution is allowed to concentrate)**
Feed and Draw solution temperatures	30	˚C	
Draw solution concentration	3	M NH4HCO3	240 g/L NH4HCO3
Concentrated Draw solution concentration	4	M NH4HCO3	316 g/L NH4HCO3
Feed concentration	0.1125	M NaCl	6.5 g/L NaCl (5 bar osmotic pressure)
Feed and Draw solution pH			Not Adjusted
Feed and Draw solution flow rates	1.5	L/min	
Feed Solution Starting Volume	6.8	L	
Feed and Draw solution flow direction	co-current		
Spacers	0.7874	mm	Spacers were installed in the deionised water and draw solution flow channel to promote turbulence or mixing
Feed and draw solution pressures	~0	bar	there was no pressurization of the system
Membrane Type	FO TFC		
Membrane Orientation	FO mode		

Analysis	
Feed Sample at the beginning	Draw Solution Samples at the beginning
Feed Sample at the end of the run	Draw Solution Sample at the end of the run
Full Analysis to quantify both reverse and forward solute diffusion	
Monitor the feed solution starting volume and end volume	
Monitor the concentrated draw solution volume (beginning, during and end of the run)	

Table 4: Experimental conditions for scaling Synthetic TRO/SRO Brine solution

SELECT MODE 2 ON THE DELTA V			
Synthetic Solution for TRO Brine			
Water Flux Behaviour in the presence of scaling			
Experimental Conditions	Value	Units	Notes
Testing modes: active layer facing Feed water (AS-DI) (FO mode).			**Constant Draw Solution and Variable Feed Solution Concentration (Feed Solution is allowed to concentrate)**
Feed and Draw solution temperatures	30	˚C	
Draw solution concentration	3	M NH4HCO3	240 g/L NH4HCO3
Concentrated Draw solution concentration	4	M NH4HCO3	316 g/L NH4HCO3
Feed concentration			U69 Synthetic Brine Solution (5 bar osmotic pressure)
Feed and Draw solution pH			Synthetic feed solution was corrected to pH between 5 and 6.5 before the experiment was conducted
Feed and Draw solution flow rates	1.5	L/min	
Feed Solution Starting Volume	5.5	L	
Feed and Draw solution flow direction	co-current		
Spacers	0.7874	mm	Spacers were installed in the deionised water and draw solution flow channel to promote turbulence or mixing
Feed and draw solution pressures	~0	bar	there was no pressurization of the system
Membrane Type	FO TFC		
Membrane Orientation	FO mode		

Analysis	
Feed Sample at the beginning	Draw Solution Samples at the beginning
Feed Sample at the end of the run	Draw Solution Sample at the end of the run
Full Analysis to quantify both reverse and forward solute diffusion	
Monitor the feed solution starting volume and end volume	
Monitor the concentrated draw solution volume (beginning, during and end of the run)	

Table 5: Experimental conditions for non-scaling Synthetic Regen Effluent solution (NaCl baseline run)

SELECT MODE 2 ON THE DELTA V			
Synthetic Solution for Secunda Regen Effluent			
Water Flux Behaviour in the absence of scaling			
Experimental Conditions	Value	Units	Notes
Testing modes: active layer facing Feed water (AS-DI) (FO mode). **Constant Draw Solution and Variable Feed Solution Concentration (Feed Solution is allowed to concentrate**			
Feed and Draw solution temperatures	30	˚C	
Draw solution concentration	3	M NH4HCO3	240 g/L NH4HCO3
Concentrated Draw solution concentration	4	M NH4HCO3	316 g/L NH4HCO3
Feed concentration	0.4	M NaCl	23 g/L NaCl (18 bar osmotic pressure)
Feed and Draw solution pH			Not Adjusted
Feed and Draw solution flow rates	1.5	L/min	
Feed Solution Starting Volume	6.8	L	
Feed and Draw solution flow direction	co-current		
Spacers	0.7874	mm	Spacers were installed in the deionised water and draw solution flow channel to promote turbulence or mixing
Feed and draw solution pressures	~0	bar	there was no pressurization of the system
Membrane Type	FO TFC		
Membrane Orientation	FO mode		
Analysis			
Feed Sample at the beginning	Draw Solution Samples at the beginning		
Feed Sample at the end of the run	Draw Solution Sample at the end of the run		
Full Analysis to quantify both reverse and forward solute diffusion			
Monitor the feed solution starting volume and end volume			
Monitor the concentrated draw solution volume (beginning, during and end of the run)			

Table 6: Experimental conditions for scaling Synthetic Regen Effluent solution

SELECT MODE 2 ON THE DELTA V			
Synthetic Solution for Secunda Regen Effluent			
Water Flux Behaviour in the presence of scaling			
Experimental Conditions	Value	Units	Notes
Testing modes: active layer facing Feed water (AS-DI) (FO mode). **Constant Draw Solution and Variable Feed Solution Concentration (Feed Solution is allowed to concentrate**			
Feed and Draw solution temperatures	30	˚C	
Draw solution concentration	3	M NH4HCO3	240 g/L NH4HCO3
Concentrated Draw solution concentration	4	M NH4HCO3	316 g/L NH4HCO3
Feed concentration			Synthetic Secunda Regen Effluent Solution(18 bar osmotic pressure)
Feed and Draw solution pH			Synthetic feed solution was corrected to pH between 5 and 6.5 before the experiment was conducted
Feed and Draw solution flow rates	1.5	L/min	
Feed Solution Starting Volume	6.8	L	
Feed and Draw solution flow direction	co-current		
Spacers	0.7874	mm	Spacers were installed in the deionised water and draw solution flow channel to promote turbulence or mixing
Feed and draw solution pressures	~0	bar	there was no pressurization of the system
Membrane Type	FO TFC		
Membrane Orientation	FO mode		
Analysis			
Feed Sample at the beginning	Draw Solution Samples at the beginning		
Feed Sample at the end of the run	Draw Solution Sample at the end of the run		
Full Analysis to quantify both reverse and forward solute diffusion			
Monitor the feed solution starting volume and end volume			
Monitor the concentrated draw solution volume (beginning, during and end of the run)			

Table 7: Experimental conditions for non-scaling Synthetic Mother Liquor solution (NaCl baseline run)

SELECT MODE 2 ON THE DELTA V			
Synthetic Solution for Unit 66 Mother Liquor			
Water Flux Behaviour in the absence of scaling			
Experimental Conditions	Value	Units	Notes
Testing modes: active layer facing Feed water (AS-DI) (FO mode).			**Constant Draw Solution and Variable Feed Solution Concentration (Feed Solution is allowed to concentrate)**
Feed and Draw solution temperatures	30	˚C	
Draw solution concentration	3	M NH4HCO3	240 g/L NH4HCO3
Concentrated Draw solution concentration	4	M NH4HCO3	316 g/L NH4HCO3
Feed concentration	0.6875	M NaCl	40 g/L NaCl (32 bar osmotic pressure)
Feed and Draw solution pH			Not adjusted.
Feed and Draw solution flow rates	1.5	L/min	
Feed Solution Starting Volume	6.9	L	
Feed and Draw solution flow direction	co-current		
Spacers	0.7874	mm	Spacers were installed in the deionised water and draw solution flow channel to promote turbulence or mixing
Feed and draw solution pressures	~0	bar	there was no pressurization of the system
Membrane Type	FO TFC		
Membrane Orientation	FO mode		
Analysis			
Feed Sample at the beginning	Draw Solution Samples at the beginning		
Feed Sample at the end of the run	Draw Solution Sample at the end of the run		
Full Analysis to quantify both reverse and forward solute diffusion			
Monitor the feed solution starting volume and end volume			
Monitor the concentrated draw solution volume (beginning, during and end of the run)			

Table 8: Experimental conditions for scaling Synthetic Mother Liquor solution

Water Flux Behaviour in the presence of scaling			
Experimental Conditions	Value	Units	Notes
Testing modes: active layer facing Feed water (AS-DI) (FO mode).			**Constant Draw Solution and Variable Feed Solution Concentration (Feed Solution is allowed to concentrate)**
Feed and Draw solution temperatures	30	˚C	
Draw solution concentration	3	M NH4HCO3	240 g/L NH4HCO3
Concentrated Draw solution concentration	4	M NH4HCO3	316 g/L NH4HCO3
Feed concentration		M NaCl	Synthetic HRP Solution (32 bar osmotic pressure)
Feed and Draw solution pH			Synthetic feed solution was corrected to pH between 5 and 6.5 before the experiment was conducted
Feed and Draw solution flow rates	1.5	L/min	
Feed Solution Starting Volume	6.9	L	
Feed and Draw solution flow direction	co-current		
Spacers	0.7874	mm	Spacers were installed in the deionised water and draw solution flow channel to promote turbulence or mixing
Feed and draw solution pressures	~0	bar	there was no pressurization of the system
Membrane Type	FO TFC		
Membrane Orientation	FO mode		
Analysis			
Feed Sample at the beginning	Draw Solution Samples at the beginning		
Feed Sample at the end of the run	Draw Solution Sample at the end of the run		
Full Analysis to quantify both reverse and forward solute diffusion			
Monitor the feed solution starting volume and end volume			
Monitor the concentrated draw solution volume (beginning, during and end of the run)			

Table 9: Descriptive Statistics for HRP run (Water Flux and Salt Flux-Deionised Water Feed)

Desciptive Statistics for HRP (High Rinse Portion)-Water Flux and Salt Flux-Deionised Water Feed												
Parameter	Valid N	mean	sd	median	trimmed	mad	min	max	range	skew	kurtosis	se
Water.Flux	49	14.18744	0.505767	14.28571	14.22626	0.374499	12.85714	14.929	2.071853	-0.79089	0.036362	0.072252
Salt.Flux	16	104919.7	1463.592	105146.2	104923.9	1284.917	102674.5	107106.9	4432.391	-0.04508	-1.16562	365.8979
DI.Tank.Cond	34	0.443512	0.145371	0.44485	0.443829	0.185028	0.2021	0.6734	0.4713	-0.01491	-1.324	0.024931
DI.Tank.pH	34	8.431765	0.031476	8.43	8.429643	0.029652	8.39	8.5	0.11	0.634492	-0.6244	0.005398
DS.Tank.Cond	33	141.3358	0.87425	141.49	141.3189	1.067472	139.99	142.94	2.95	-0.00574	-1.28231	0.152187
DS.Tank.pH	34	8.431765	0.031476	8.43	8.429643	0.029652	8.39	8.5	0.11	0.634492	-0.6244	0.005398

Table 10: Descriptive Statistics for TRO/SRO Brine run (Water Flux and Salt Flux-Deionised Water Feed)

Desciptive Statistics for TRO Brine -Water Flux and Salt Flux-Deionised Water Feed												
Parameter	Valid N	mean	sd	median	trimmed	mad	min	max	range	skew	kurtosis	se
Water.Flux	49	12.45972	0.447929	12.38095	12.4529	0.434462	11.42857	13.41191	1.983337	0.200374	-0.54219	0.06399
Salt.Flux	23	91322.41	1778.022	90843.72	91226.47	2259.211	88970.1	94585.06	5614.955	0.392524	-1.25889	370.7433
DI.Tank.Cond	34	0.3753	0.115071	0.37465	0.375314	0.145814	0.1844	0.5652	0.3808	0.002067	-1.30557	0.019734
DI.Tank.pH	34	9.076471	0.039303	9.08	9.0775	0.044478	9	9.17	0.17	-0.13891	-0.53689	0.00674
DS.Tank.Cond	34	143.275	0.812502	143.42	143.3204	0.934038	141.71	144.36	2.65	-0.42278	-1.11294	0.139343
DS.Tank.pH	34	8.545588	0.018289	8.55	8.545357	0.029652	8.52	8.58	0.06	0.038529	-1.32562	0.003137

Table 11: Descriptive Statistics for Combined Regeneration Effluent run (Water Flux and Salt Flux-Deionised Water Feed)

Desciptive Statistics for Secunda Regeneration Effluent -Water Flux and Salt Flux-Deionised Water Feed												
Parameter	Valid N	mean	sd	median	trimmed	mad	min	max	range	skew	kurtosis	se
Water.Flux	49	14.33494	0.253495	14.28571	14.33349	0.161679	13.21429	14.88399	1.669707	-1.15276	6.199077	0.036214
Salt.Flux	17	102952.9	820.987	103058.5	102987.9	888.7059	101363.5	104017.7	2654.181	-0.43031	-1.21739	199.1186
DI.Tank.Cond	32	0.450375	0.133585	0.4507	0.450931	0.170202	0.2292	0.6554	0.4262	-0.01524	-1.34287	0.023615
DI.Tank.pH	31	8.92	0.043512	8.92	8.9196	0.059304	8.85	9.02	0.17	0.112769	-0.88636	0.007815
DS.Tank.Cond	31	142.359	0.955874	142.49	142.4492	0.934038	139.97	143.74	3.77	-0.77207	-0.226	0.17168
DS.Tank.pH	31	8.53	0.027568	8.53	8.53	0.029652	8.48	8.58	0.1	0.046189	-1.20391	0.004951

Table 12: Descriptive Statistics for Mother Liquor run (Water Flux and Salt Flux-Deionised Water Feed)

Desciptive Statistics for Mother Liquor (Evaporator Blowdown-U66)-Water Flux and Salt Flux-Deionised Water Feed												
Parameter	Valid N	mean	sd	median	trimmed	mad	min	max	range	skew	kurtosis	se
Water.Flux	36	15.84934	0.619159	16.10048	15.91545	0.522623	14.43812	16.54135	2.103237	-1.02265	-0.13838	0.103193
Salt.Flux	10	95852.34	1493.931	95525.48	95690.25	1603.511	94261.43	98739.98	4478.555	0.589598	-1.10041	472.4224
DI.Tank.Cond	32	0.424688	0.127568	0.42415	0.424577	0.162271	0.2158	0.6311	0.4153	0.009279	-1.32554	0.022551
DI.Tank.pH	34	9.140588	0.029842	9.14	9.140357	0.029652	9.09	9.19	0.1	0.011213	-1.33653	0.005118
DS.Tank.Cond	34	141.8429	0.518106	141.825	141.8575	0.630105	140.83	142.85	2.02	-0.15227	-0.7359	0.088854
DS.Tank.pH	34	8.728235	0.023801	8.74	8.728929	0.029652	8.68	8.76	0.08	-0.28106	-1.34836	0.004082

Table 13: Standard relationship between measured conductivity and prepared sodium chloride salt concentration

NH_4HCO_3 (g/L)	Cond Hand (mS/cm)	Ratio (NH_4HCO_3 concentration/Conductivity)	Cond Online (mS/cm)	Ratio (NH_4HCO_3 concentration/Conductivity)
0.08	0.109	0.733945	0.117	0.683761
0.09	0.123	0.731707	0.132	0.681818
0.1	0.134	0.746269	0.144	0.694444
0.2	0.267	0.749064	0.284	0.704225
0.3	0.398	0.753769	0.424	0.707547
0.4	0.534	0.749064	0.565	0.707965
0.5	0.66	0.757576	0.699	0.715308
0.6	0.783	0.766284	0.829	0.723764
0.7	0.92	0.76087	0.97	0.721649
0.8	1.05	0.761905	1.104	0.724638
0.9	1.16	0.775862	1.222	0.736498
1	1.269	0.788022	1.336	0.748503

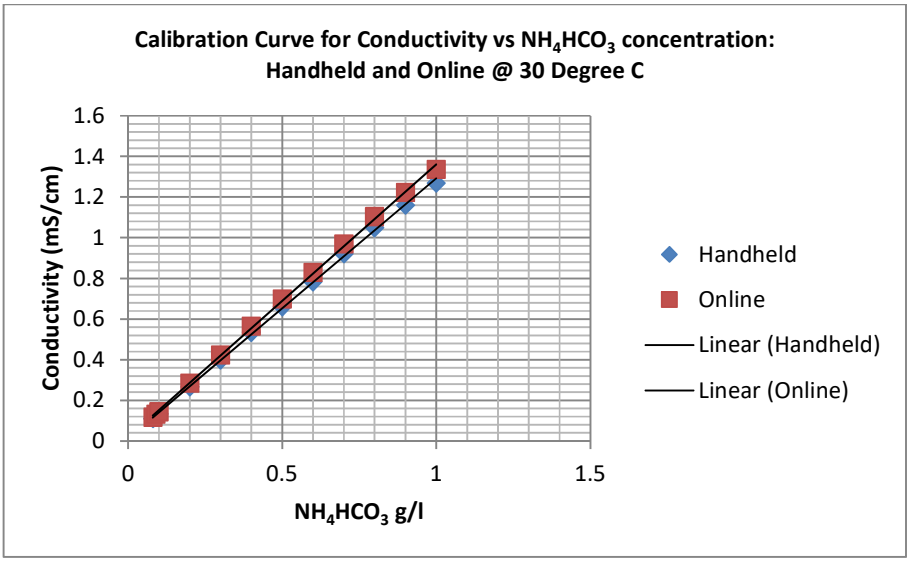

Figure 1: Calibration curve of conductivity vs sodium chloride salt concentration

Table 14: Analytical Results (Ammonium and Alkalinity) for the baseline run (NaCl) and synthetic HRP run for samples taken before and after the run

Sample	**NH_4 as NH_3 mg/L**	**M-alkalinity-mg/L as $CaCO_3$**	**P-alkalinity-mg/L as $CaCO_3$**
TK001 (NaCl) (03/07/2014)	< 0.5	5	< 0.8
TK002 (NaCl) (03/07/2014)	40000	89703	30507
TK001 (NaCl) (05/07/2014)	9 000	14058	685
TK002(NaCl) (05/07/2014)	41000	105944	24192
TK001 (HRP) (15/07/2014)	0.5	6	< 0.8
TK002 (HRP) (15/07/2014)	41500	130400	13200
TK001 (HRP) (18/07/2014)	160	56*	< 0.8
TK002(HRP) (18/07/2014)	51000	161300	36400

(*)-indicate that there could have been analytical error on the analysis

TK001-Feedtank

TK-002-Draw solution Tank

Table 15: Analytical Results (Ammonium and Alkalinity) for the baseline run (NaCl) and synthetic TRO/SRO brine run for samples taken before and after the run

Sample	NH_4 as NH_3 (mg/L)	M-Alk-mg/L as $CaCO_3$	P-Alk-mg/L as $CaCO_3$
TK001 (NaCl) (22/07/2014)	< 0.5	29	5
TK002 (NaCl) (22/07/2014)	30500*	129000	30284
TK001 (NaCl) (24/07/2014)	5450	2407	13664
TK002(NaCl) (24/07/2014)	43500	133849	31566
TK001 (TRO/SRO) (28/07/2014)	< 0.5	18	< 0.8
TK002 (TRO/SRO) (28/07/2014)	42500	133775	41951
TK001 (TRO/SRO) (31/07/2014)	365	118	< 0.8
TK002 (TRO/SRO) (31/07/2014)	37500	149715	47148

(*)-indicate that there could have been analytical error on the analysis

TK001-Feedtank

TK-002-Draw solution Tank

Table 16: Analytical Results (Ammonium and Alkalinity) for the baseline run (NaCl) and synthetic Combined Regeneration Effluent run for samples taken before and after the run

Regen Effluent (zero) (first run)		
Sample	M-alkalinity-mg/L as $CaCO_3$	P-alkalinity-mg/L as $CaCO_3$
TK001 Regen zero (11:55) 5/8/2014	6	4
TK002 Regen zero (11:55) 5/8/2014	132430	9621
TK001 Regen zero 5/8/2014	637	230
TK002 Regen zero 5/8/2014	126351	16094
Regen Effluent (NaCl) (first run)		
Sample	M-alkalinity-mg/L as $CaCO_3$	P-alkalinity-mg/L as $CaCO_3$
TK001 Regen NaCl 11/8/2014	21	< 0.8
TK002 Regen NaCl 11/8/2014	130363	11633
TK001 Regen NaCl 14/8/2014	20960	5866
TK002 Regen NaCl 14/8/2014	12561*	33806
Regen Effluent synthetic feed (first run)		
Sample	M-alkalinity-mg/L as $CaCO_3$	P-alkalinity-mg/L as $CaCO_3$
TK002 Regen 25/8/2014	135550	11354*
TK001 Regen 27/8/2014	10267	2263
TK002 Regen 27/8/2014	148637	48279
Regen Effluent (zero) (second run)		
Sample	M-alkalinity-mg/L as $CaCO_3$	P-alkalinity-mg/L as $CaCO_3$
TK001 Regen zero (12:16) 18/8/2014	12	5
TK002 Regen zero (12:16) 18/8/2014	108535	17331
TK001 Regen zero 18/8/2014	570	259
TK002 Regen zero 18/8/2015	116888	13751
Regen Effluent (NaCl) (second run)		
Sample	M-alkalinity	P-alkalinity

TK001 Regen NaCl 19/8/2014	8	< 0.8
TK002 Regen NaCl 19/8/2014	105245	27850
TK001 Regen NaCl 21/8/2014	16646	4020
TK002 Regen NaCl 21/8/2014	115490	23333
Regen Effluent synthetic feed (second run)		
Sample	M-alkalinity	P-alkalinity
TK001 Regen 27/8/2014	462*	52 (?)
TK002 Regen 27/8/2014	138512	13203*
TK001 Regen 29/8/2014	13352	2914
TK002 Regen 29/8/2014	151685	45028

(*)-indicate that there could have been analytical error on the analysis

TK001-Feedtank

TK-002-Draw solution Tank

Table 17: Analytical Results (Ammonium and Alkalinity) for the baseline run (NaCl) and synthetic Mother Liquor run for samples taken before and after the run

Mother Liquor (zero) (second run)			
Sample	NH4 as NH_3 mg/L	M-alkalinity-mg/L as CaCO3	P-alkalinity-mg/L as CaCO3
TK001 Mother Liquor zero 15/9/2014	4.7	19	< 0.8
TK002 Mother Liquor zero 15/9/2014	38373	139621	13560
TK001 Mother Liquor zero 15/9/2014 (11:40)	383	520	282
TK002 Mother Liquor zero 15/9/2014 (11:40)	40226	133884	25695
Mother liquor (NaCl) (second run)			

Sample	NH4 as NH_3 mg/L	M-alkalinity-mg/L as CaCO3	P-alkalinity-mg/L as CaCO3
TK001 NaCl 15/9/2014 (12:15)	238 *	25	10
TK002 NaCl 15/9/2014 (12:15)	N/A	N/A	N/A
TK001 NaCl 17/9/2014	12062	13074	3126
TK002 NaCl 17/9/2014	36614	147971	41205
Mother liquor synthetic feed (second run)			
Sample	NH4 as NH_3 mg/L	M-alkalinity-mg/L as CaCO3	P-alkalinity-mg/L as CaCO3
TK001 mother liquor 17/9/2014 (15:40)	128*	16	< 0.8
TK002 mother liquor 17/9/2014 (15:40)	39920	136962	17696
TK001 mother liquor (19/9/2014)	1738	595	50
TK002 mother liquor (19/9/2014)	44374	154702	46606

(*)-indicate that there could have been analytical error on the analysis

N/A-results not available

TK001-Feedtank

TK-002-Draw solution Tank

Table 18: Inorganic composition of the draw solution at the beginning and end of the experiment for synthetic solutions.

Component	Concentration (mg/L and M&P Alkalinity is mg/L as $CaCO_3$)-Draw Solution Tank							
	HRP (24/6/14)		TRO Brine (28/7/14)		Secunda Regen (27/8/14)		Mother liquor (17/9/14)	
	Before	After	Before	After	Before	After	Before	After
Cl	<1	<1	<1	<1	<1	<1	<1	<1
SO_4	<1	<1	<1	<1	<1	<1	<1	<1
F	<1	<1	<1	<1	<1	<1	<1	<1
NO_2	<1	<1	<1	<1	<1	<1	<1	<1
NO_3	<1	<1	<1	<1	<1	<1	<1	<1
NH_4 as NH3	37500	39000	42500	37500	N/A	N/A	39920	44374
M-alk	130400	161300	133775	149715	138512	151685	136962	154702
P-alk	13200	36400	12331	47148	1320	45028	17696	46606
Na	0.5	9	0.6	25	2	995*	2	280*
Ca	0.6	1	0.7	0.5	1	1	2	0.9
Mg	0.8	0.8	0.6	0.6	0.6	0.5	0.9	0.7
K	0.1	3.8	0.1	2	0.1	13	0.2	52
Al	0.1	0.2	0.1	0.08	0.1	0.1	0.1	0.1
Cd	< LOQ	0.01	< LOQ	0.002	< LOQ	0.001	< LOQ	0.002
Cr	< LOQ	0.04	< LOQ	0.02	0.004	0.01	0.003	0.01
Fe	0.1	0.6	0.2	0.4	0.1	0.1	0.07	0.3
Mn	0.003	0.02	0.002	0.01	0.002	0.004	0.004	0.01
Ni	0.004	0.2	< LOQ	0.08	0.003	0.04	< LOQ	0.08
Cu	0.01	24	0.03	13	0.01	7	0.03	12
Pb	< LOQ	2	< LOQ	0.8	< LOQ	0.4	< LOQ	0.6
Zn	0.03	24	0.04	11	0.03	4	0.004	9
Mo	< LOQ	< LOQ	< LOQ	< LOQ	< LOQ	< LOQ	< LOQ	< LOQ
Sr	< LOQ	< LOQ	< LOQ	< LOQ	< LOQ	< LOQ	< LOQ	< LOQ
V	< LOQ	< LOQ	< LOQ	< LOQ	< LOQ	< LOQ	< LOQ	< LOQ

(*)-indicate that there could have been analytical error on the analysis

N/A-results not available

LOQ-level of quantification

Table 19: Inorganic composition of the feed solution at the beginning and end of the experiment for synthetic mother liquor solutions.

Component (mg/L and M&P is mg/L as CaCO3)	Mother Liquor Zero Point (23/3/15)-Feed Tank		Mother Liqour Mid Point (27/5/15)-Feed Tank		Mother Liqour High Point (29/6/15)-Feed Tank	
	Before	After	Before	After	Before	After
Cl	12528	25438	12050	17021	12864	18571
SO_4	23918	48991	24046	34539	25141	35485
F	<1	<1	<1	<1	<1	<1
NO_2	<1	<1	<1	<1	<1	<1
NO_3	<1	<1	<1	<1	<1	<1
NH_4 as NH3	16	18097	105	6728	9	4033
M-alk	105	10547	8	4738	<1.4	491
P-alk	<0.8	280	<0.8	<0.8	<0.8	236
Na	21300	23714.29	20755	23793.33	21825	27233.33
Ca	5	14.29	263.1	9.87	467.2	179
Mg	45	57.14	75.8	113.33	75.45	116
K	2000	1573	1976.5	1937.33	2104	2385.33

Table 20: Inorganic composition of the draw solution at the beginning and end of the experiment for synthetic mother liquor solutions.

Component	Concentration (mg/L and M&P Alkalinity is mg/L as CaCO3)-Draw Solution Tank					
	Mother liquor (Zeropoint)(23/3/15)		Mother liquor (Midpoint)(27/5/15)		Mother liquor (Highpoint)(29/6/15)	
	Before	After	Before	After	Before	After
Cl	<1	<1	<1	<1	<1	<1
SO_4	<1	<1	<1	<1	<1	<1
F	<1	<1	<1	<1	<1	<1
NO_2	<1	<1	<1	<1	<1	<1
NO_3	<1	<1	<1	<1	<1	<1
NH_4 as NH_3	38237	41463	42264	45433	42407	52828
M-alk	N/A	1385	132473	141922	142163	N/A
P-alk	N/A	358	8255	39988	10647	N/A
Na	29.86	1967.38	587.00	1393.72	369.13	39.73
Ca	0.59	0.05	0.70	0.40	0.70	0.30
Mg	0.20	0.05	0.20	0.05	0.19	0.04
K	1.19	248.10	0.56	177.17	1.09	0.04
Al	1.59	0.50	3.07	0.88	3.20	1.00
Cd	0.20	0.05	0.20	0.05	0.20	0.00
Cr	0.20	0.05	0.20	0.05	0.20	0.00
Fe	0.39	0.14	0.29	0.09	0.20	0.05
Mn	0.20	0.05	0.20	0.05	0.20	0.00
Ni	0.20	0.05	0.20	0.05	0.20	0.00
Cu	4.18	4.95	2.71	5.35	2.60	0.50
Pb	0.20	0.05	0.24	0.38	0.20	0.10
Zn	1.79	3.96	1.73	4.15	1.60	0.10
Mo	0.20	0.05	0.20	0.05	0.20	0.00
Sr	0.20	0.05	0.20	0.05	0.20	0.00
V	2.59	3.96	0.20	0.05	0.20	0.00

FO Membrane Morphology Reports

MC-MEM0427.pdf

RIR2014-0026.pdf